AD-A072 080 EASTMAN KODAK CO ROCHESTER N Y APPARATUS AND OPTICAL DIV F/G 14/2
SPECTRAL RADIOMETRIC MEASUREMENT AND ANALYSIS PROGRAM. VOLUME 3--ETC(U)
APR 79 L G CHRISTENSEN, R SIMMONS, G SCHAUSS
UNCLASSIFIED AWS-TN-79/001-VOL-3 NL

1 OF 3
AD A072080

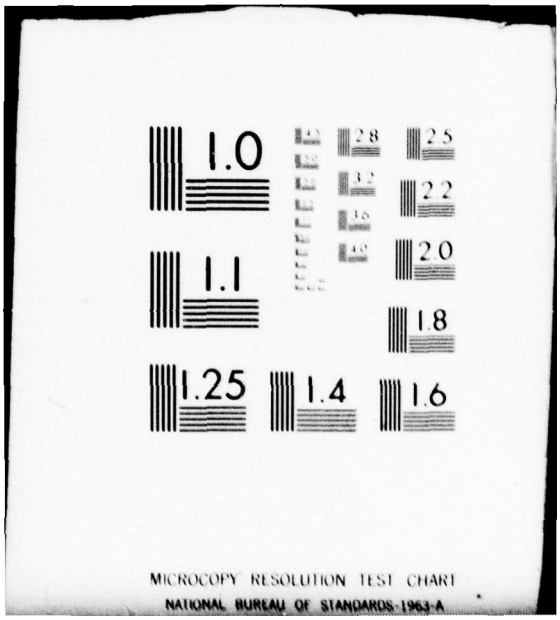
1.0
1.1
1.25
1.4
1.6
2.8
2.5
2.2
2.0
1.8
MICROCOPY RESOLUTION TEST CHART
NATIONAL BUREAU OF STANDARDS-1963-A

LEVEL II

AWS/TN-79/001
Vol. III

SPECTRAL RADIOMETRIC MEASUREMENT AND ANALYSIS PROGRAM

Data Analysis and Formulation of the Model

Lawrence G. Christensen

Eastman Kodak Co.
Kodak Apparatus Division
901 Elmgrove Road
Rochester, New York 14650

April 1979
Final Report

Prepared for
AIR WEATHER SERVICE (MAC)
Scott AFB, Illinois 62225

REVIEW AND APPROVAL STATEMENT

This report approved for public release. There is no objection to unlimited distribution of this report to the public at large, or by DDC to the National Technical Information Service (NTIS).

This technical report has been reviewed and is approved for publication.

Donald B. Hodges

DONALD B. HODGES, LtCol, USAF
Chief, Aerospace Physics and Space
Sciences Division
Directorate of Aerospace Development

FOR THE COMMANDER

Robert M Gottuso

ROBERT M. GOTTUSO, Col, USAF
DCS/Aerospace Sciences

6 Aug 79

Volumes I - IV, AD-A072 078 - AD-A072 081 were all issued without a contract per phone conversation with Shirley Wise, Eastman Kodak, Co Rochester, NY (716-726-5340)

David Mathews (TID)

SECURITY CLASSIFICATION OF THIS PAGE (When Data Entered)

(19) **REPORT DOCUMENTATION PAGE**

READ INSTRUCTIONS BEFORE COMPLETING FORM

(18) 1. REPORT NUMBER: AWS/TN-79/001-VOL-3

2. GOVT ACCESSION NO.

3. RECIPIENT'S CATALOG NUMBER

(6) 4. TITLE (and Subtitle): Spectral Radiometric Measurement and Analysis Program. Volume 3. Data Analysis and Formulation of the Model. AD A072099

(9) 5. TYPE OF REPORT & PERIOD COVERED: Final rept,

6. PERFORMING ORG. REPORT NUMBER

7. AUTHOR(s): L. Christensen et al

8. CONTRACT OR GRANT NUMBER(s)

(12) 225 p.

9. PERFORMING ORGANIZATION NAME AND ADDRESS
Eastman Kodak Co.
Kodak Apparatus Div.
901 Elmgrove Rd., Rochester, N.Y. 14624

10. PROGRAM ELEMENT, PROJECT, TASK AREA & WORK UNIT NUMBERS

11. CONTROLLING OFFICE NAME AND ADDRESS
Air Weather Service (MAC)
Scott AFB, Illinois 62225

(11) 12. REPORT DATE: April 1979

13. NUMBER OF PAGES: 225

14. MONITORING AGENCY NAME & ADDRESS(if different from Controlling Office)

(10) Lawrence G./Christensen, R./Simmons, G./Schauss, R./Norton R./Schoenfeld

15. SECURITY CLASS. (of this report): None

15a. DECLASSIFICATION DOWNGRADING SCHEDULE

16. DIS

Approved for Public Release; Distribution Unlimited

17. DISTRIBUTION STATEMENT (of the abstract entered in Block 20, if different from Report)

18. SUPPLEMENTARY NOTES

This document is Volume 3 of four volumes.

19. KEY WORDS (Continue on reverse side if necessary and identify by block number)
VISUAL & INFRARED ATMOSPHERIC TRANSMITTANCE
VISUAL & INFRARED ATMOSPHERIC SCATTERING AND ABSORPTION
SURFACE METEOROLOGY AND ATMOSPHERIC RADIOMETRIC TRANSFER
IN SITU ATMOSPHERIC MEASUREMENTS
GROUND-BASED RADIOMETRY

20. ABSTRACT (Continue on reverse side if necessary and identify by block number)

This report covers a ~~Eastman Kodak Company~~ recently completed contract with the United States Air Force Air Weather Service to conduct research into the transfer of atmospheric energy in the visible and near-infrared portions of the electromagnetic spectrum. Its objective was to produce a spectral model of path transmittance, radiance, and ground-level irradiance that could be related to meteorological observations through the use of simultaneous, in-situ data collections. For this purpose a mathematical model was developed.

CONT →

DD FORM 1 JAN 73 1473

121 220

79 07 31 116

SECURITY CLASSIFICATION OF THIS PAGE (When Data Entered)

CONT

It was based on physical equations for a homogeneous atmosphere that were modified by empirical observations made under a broad range of meteorological conditions. With the model it is possible to estimate the visible and near-infrared spectral absorption and scattering phenomena that result from atmospheric constituents, from surface synoptic weather observations.

This document presents the details of analysis used to reduce the collected radiometric and meterological data to a series of equations which became the SCAT3 model. Examples are also shown illustrating the final model's ability to match observed spectral structure based upon coefficients derived from surface meteorology.

TABLE OF CONTENTS

TABLE OF CONTENTS (CONT'D)

TABLE OF CONTENTS (CONT'D)

LIST OF ILLUSTRATIONS

LIST OF ILLUSTRATIONS (CONT'D)

LIST OF ILLUSTRATIONS (CONT'D)

LIST OF TABLES

SECTION 1
INTRODUCTION

The approach used to develop the equations of the SCAT3 atmospheric model was to start with a single linear mathematical description of the physical processes. The results of a detailed examination of changes in the spectral data were then used to introduce non-linear effects into coefficients of the various linear terms. The net effect of this approach was to create parametric spectral vectors that could be fitted by least-squares to appropriately normalized, measured spectral data. The coefficients of the vectors could then be regressed against other measurable parameters such as solar altitude, moisture scale height, and terrain reflectance. In this way, a model could be assembled that closely approximated the physics of the atmosphere, thus avoiding the equation extrapolation problems that are often encountered in a characteristic vector approach to data modeling.

This approach was used for all radiometric data, which included (1) horizontal daylight and skylight irradiance, (2) vertical front daylight and vertical back skylight irradiance, and (3) atmospheric path radiance and transmittance.* In all the cases except transmittance, the measured spectral data was normalized by the extra-terrestrial solar irradiance. The mathematical quantities representing direct beam attenuation, primary atmospheric scattering, and surface reflectance were then entered into the equation. Regression coefficients were computed by fitting, by least-squares, the spectral structure to each normalized spectral sample. The coefficients were then analyzed as functions of such measurable parameters as solar altitude, moisture scale height, and terrain reflectance.

Data was blocked in small increments of solar altitude. This was possible because of the large volume of spectral data the mobile radiometric laboratory was able to collect. The size of solar altitude cells into which the

* See Appendix A for a description of the software developed for this purpose.

data was blocked (actually interpolated to a common set of solar altitudes) varied with solar altitude; that is, between -3° and 10° the increment was 1°, between 10° and 50° it was 2°, and between 50° and 90° it was 5°.

The increment chosen was quasi-logarithmic and corresponded roughly to equal increments of change in the measured variable. The effects of the remaining parameters, moisture scale height and terrain reflectance, were determined sequentially; this was done by examining least-squares fits to the residual spectral structure that were obtained when predetermined equational shapes were regressed against the actual data. These equations were based on approximations of the integrated effects of the atmosphere without recourse to a multilayered atmosphere; in this way, the formulation of terms was an approximation of the physical equations. Several alternative equational forms were examined, but the ones used in this effort consistently resulted in the best fit to the spectral structure.

The regression coefficients corresponding to scattering and surround reflectance effects were unique for each measured spectral sample. (For an example, see the equation in para 4.2.) However, by studying first the samples for which the surround term could reasonably be expected to be zero, it was possible to determine the scattering relationship to moisture scale height. Once the scattering function was determined, the surround relationship to terrain reflectance could be found. Because these terms were not totally independent of one another in practice, some complication was introduced into the analysis.

Similar equations were built up for all four types of spectral irradiance and spectral sky radiance. The resulting formulation of each can be found in appropriate sections of this volume.*

The ability of the approach used here to separate-out effects necessitated having precise estimates of spectral extra-terrestrial irradiance, spectral transmittance, and spectral terrain reflectance. The degree of accuracy required was determined by each term's influence on calculation of the spectral

*See Appendix B for a summary of the variable names used in the equations and in the SCAT3 model.

radiometric quantity. The extra-terrestrial irradiance selected for normalization of the spectral samples was the so-called Johnson Solar Constant[1] corrected for the earth's orbital eccentricity. The solar constants discussed by Neckel[2] and Thekaekara[3] were also examined, but best agreement with measured data was generally obtained with the Johnson constant.

Estimates of the spectral transmittance due to scattering and absorption, $t_a(\lambda)$ and $t_s(\lambda)$, were obtained simultaneously from direct measurement of the solar disk radiance through the atmosphere. The procedure followed in analyzing and decomposing spectral transmittance into its component parts is described in Section 3 of this volume.

Estimates of spectral terrain reflectances for each location date were derived from color overhead photography, or in some instances, from geo-botanical maps. By means of a spectral Eigenvector technique and knowledge of the type and relative amounts of groundcover, it was possible to expand the three integrated reflectances derived from analysis of the color film dye layer into a complete spectral reflectance estimate for the general terrain reflectance corresponding to a 50- to 100-mile area surrounding the site of operation. These estimates are discussed in Section 9 of this volume.

A matrix of actual measured spectral samples was created that represented typical and extreme values of model parameters and were descriptive of the standard error of spectral reconstruction. These reconstructed samples are shown in Appendix C of this volume. Because of the importance of analysis of spectral transmittance to the results of the model's fit to data, this subject is discussed below before the topics spectral radiance and irradiance.

---

[1] F.S. Johnson, "The Solar Constant," J. Meteorology, Vol II, No. 6, December 1954.

[2] D. Neckel, "Intensity of the Center of the Solar Disk in the Spectral Region .33 to 1.25 nm Measured from High Mountain Station," Proceedings of Symposium on Solar Radiation, November 1973, Smithsonian Institute.

[3] Dr. M. P. Thekaekara, "Solar Electromagnetic Radiation," NASA Space Vehicle Design Criteria (Environment), NASA Sp. 83005,Rev May 71, Goddard Space Flight Center.

SECTION 2

ANALYSIS AND MODELING OF SPECTRAL TRANSMITTANCE

2.1 APPROACH

Atmospheric beam-path spectral transmittance was used as the basic scaling parameter of all the spectral radiometric quantities computed by SCAT3. As such, it was the single most important measurement made by the mobile laboratory and the most critical in the regression analyses that are discussed in the following sections. Spectral transmittance also provided a link between the radiometric quantities and the detailed altitude profile data on the atmosphere provided by the Rawindsonde observations made at the site of operations.

The approach taken in the regression analysis was to decompose the logarithm (base e) of the spectral transmittance into its individual spectra in the visible and near-infrared. The assumption was made that molecular scattering transmittance could be approximated by the Rayleigh equations scaled by atmospheric pressure. Aerosol scattering transmittance was estimated as the residual transmittance between the measurement and the Rayleigh equations, eliminating the absorption transmittance wavelengths. Absorption transmittance was then estimated by fitting the linear characteristic vectors to the measured data after the scattering effects were subtracted.

Meteorological data were acquired as a part of this project for the purpose of examining the correlations with atmospheric transmittance that had been discussed by Harrel and Bullrich[4] and other researchers in the field of atmospheric science. In the study, measurements were made of temperature, pressure, relative humidity, wind speed, and wind direction using an onboard weather system. In addition, Rawindsonde (RAOB) observations that

[4] G. Harrel and K. Bullrich, "On the Interpretation of Atmospheric Turbidity Measurements," Journal of the Atmospheric Sciences, Vol 33, pp 794-797 May 1975.

were made three times a day by the National Weather Service were used as the source of altitude profile data on temperature, pressure, and moisture. The NWS surface data were also collected, where available, and they were given preference over on-board weather measurements. Correlations were found to exist between meteorological data and atmospheric transmittance both in the wavelength bands corresponding to water absorption bands and in the aerosol scattering bands.

The schematic diagram in Figure 2-1 shows the physical relationship between the various data collected by the mobile laboratory.

2.2 ESTIMATION OF VERTICAL TRANSMITTANCE FROM MEASUREMENTS

Direct estimation of the solar disk radiance inside the atmosphere was possible because of the on-board, absolute calibration of the transmissometer (see Vol 1, para. 3.1 of this report). The calibration was carried out in a manner that obtained data directly from the instrument current output in units of path transmittance. After careful study, it was determined that on an absolute scale, the instrument demonstrated unacceptable non-linearities in the blue-UV spectrum that resulted in underestimation of the path transmittance in that region. The balance of the spectrum, from 0.5 μm to 1.15 μm, appeared to be in agreement with theory and with alternative methods of transmittance estimation.

The alternative method that was examined and ultimately adopted for the analysis of spectral radiometric data discussed in Section 1 of this volume was a modification of the Langley-plot method of solar disk radiance determination. This method, which was originally intended for the estimation of extra-trrestrial solar irradiance, involves plotting the logarithm of disk radiance versus the relative air mass of observation as estimated using the secant of the observation zenith angle or air mass tables developed by Bemporad[5] at low solar altitudes. The intercept of a straight line fitted

---

[5] A. Bemporad, "Search for a New Empirical Formula for the Representation of the Variation of the Intensity of Solar Radiation with Zenith Angle," Meteorologische Zeitschrift, Vol 24, July 1907.

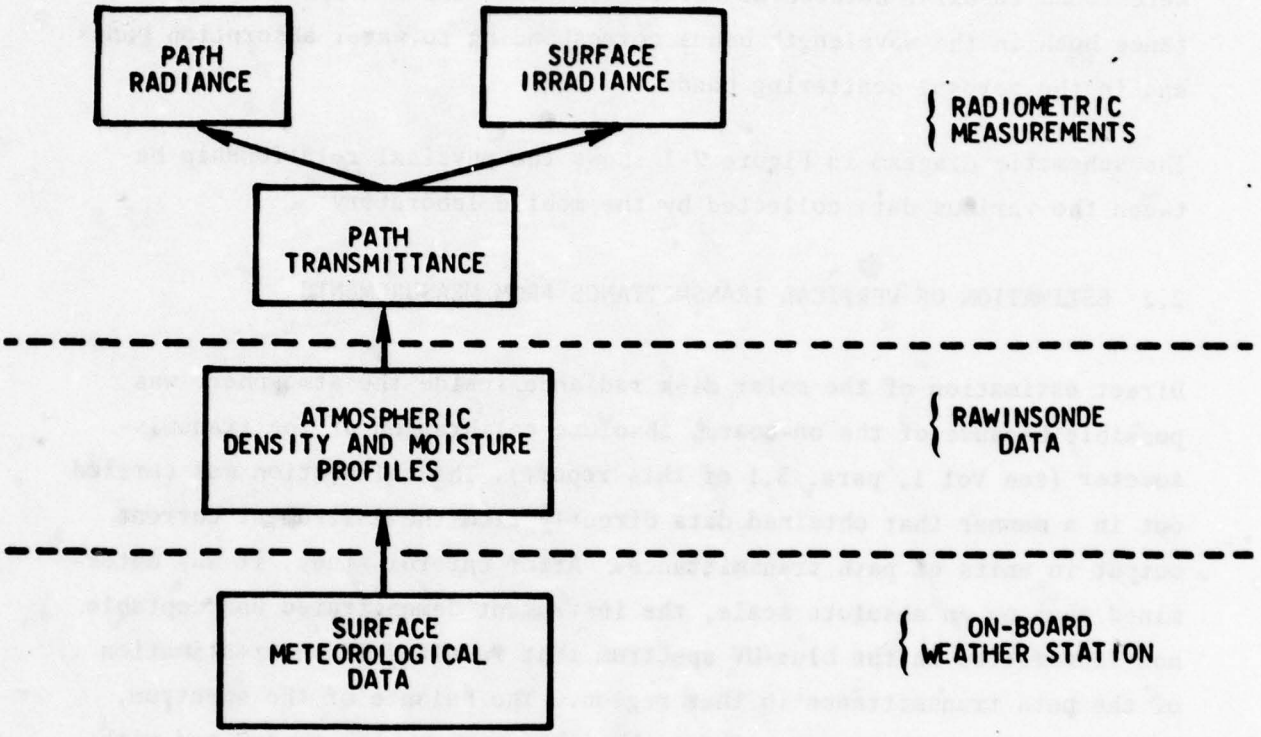

Figure 2-1. Physical Relationship Between Data Collected by Mobile Laboratory

to the radiance/air mass plot at zero air mass was the extrapolated estimate of the extra-terrestrial radiance. Normalization of the radiance scale by the solar constant resulted in a path transmittance versus air mass that was consistent with the calibrated output of the transmissometer instrument. Ideally, the linear fit to the data would result in an intercept of 0.0 (log 1.); however, the extrapolated estimation was generally less than zero, particularly below a wavelength of 500 nm.

Examination of the equation of the slope of $\log_e$ of the transmittance; that is, log $T(\lambda)$ versus the relative air mass m, if it is assumed linear, yields an instrument calibration estimate independent of the vertical atmospheric transmittance, as follows:

$$\frac{d \log T(\lambda)}{dm} = \log T_v(\lambda) \qquad \text{Equation 2-1}$$

Using a simple linear regression technique, slope estimates of the vertical transmittance were derived for every wavelength and every site both before or after true noon. A typical example of such a plot for three wavelengths at one site is shown in Figure 2-2 for Vandenberg, California, on May 12, 1976. Not all day-sites exhibited a perfectly linear relationship, but by-and-large, all scattering wavelength data could be approximated by a linear function within the standard error of the measurement (estimated to be less than 5 percent, see Vol 1, para. 3.4). Absorption transmittance measurements corresponding to the water and molecular oxygen absorption bands also exhibited non-linear variation with air mass because these absorption spectra are not strictly linear with total absorber concentration, as discussed by McClatchey.[6] The analysis proceeded linearly, however, with a correction applied in a later stage of analysis for the non-linearity of the observed data.

---

[6] R. A. McClatchey et. al., Optical Properties of the Atmosphere (Third Edition), Air Force Cambridge Research Laboratory Project 7670.

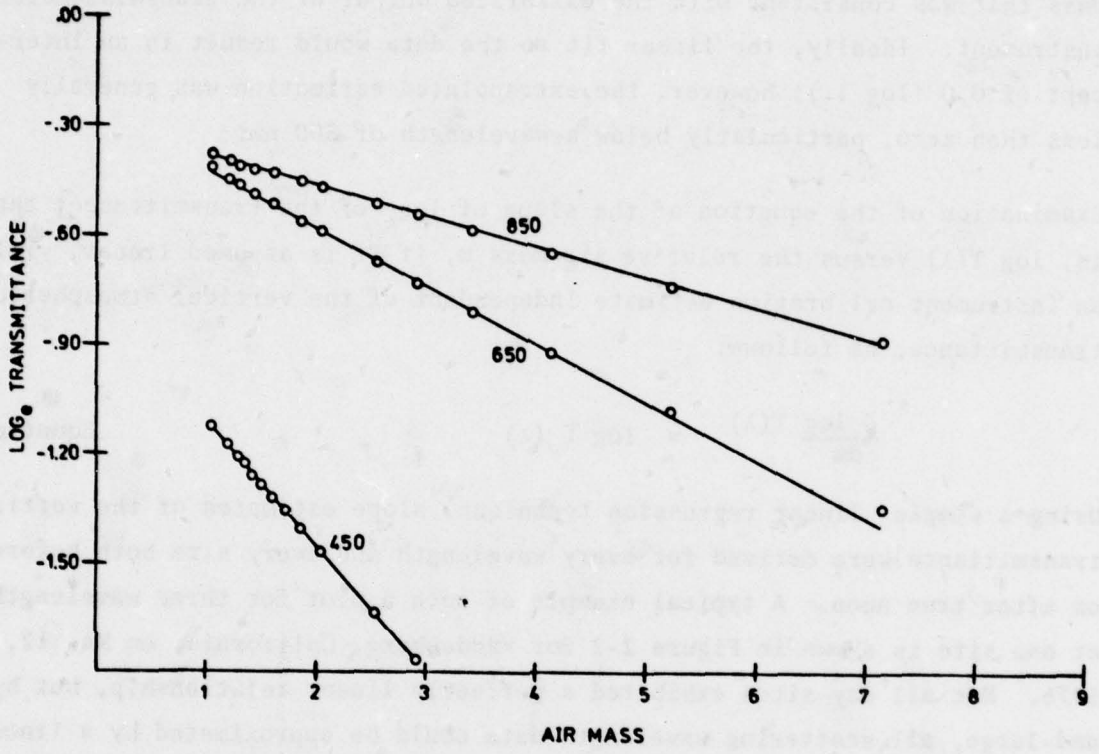

Figure 2-2. Typical Log Transmittance Versus Air Mass (Vandenberg, Ca.; May 12, 1976 P.M.)

2.3 ANALYSIS OF VERTICAL SPECTRAL TRANSMITTANCE ESTIMATES

By scaling samples linearly for air mass and correcting for the absorption nonlinearity, any individual spectral transmittance sample could be reconstructed. These reconstructed samples for each day-site were the basic spectral transmittance data used in all subsequent radiometric analysis. An example of the measured spectral transmittance showing the spectral structure and using 10-nanometer instrument sampling is shown in Figure 2-3; this measured spectral transmittance was estimated by the modified Langley-plot method.

The equivalent spectral transmittance for each day-site was then logged (to the base e) and decomposed into Rayleigh and Mie scattering terms and into molecular absorption spectra. This was done in a series of steps beginning with the removal of an assumed, fixed amount of total path transmittance due to Rayleigh scattering that was scaled for atmospheric surface pressure in millibars as described by Robinson.[7] If the absorption bands are temporarily ignored, the net spectra is that corresponding to total extinction due to large particle scattering. It was hypothesized that this scattering resulted from a combination of dust particles and water droplets that comprise the so-called atmospheric aerosols. It was further hypothesized that this would scale with the water vapor content of the atmosphere. A nonlinear function of the form suggested by Robinson[7] and shown below was fitted to the net spectra using regression techniques.

$$T_{aer} = K_a/\lambda^c$$

where K_a is the aerosol scattering coefficient and c is the aerosol scattering wavelength exponent. Figure 2-4 illustrates the fit of the function

---

[7] N. Robinson, Solar Radiation, Elsevier Publishing Co., New York, 1966, p 113.

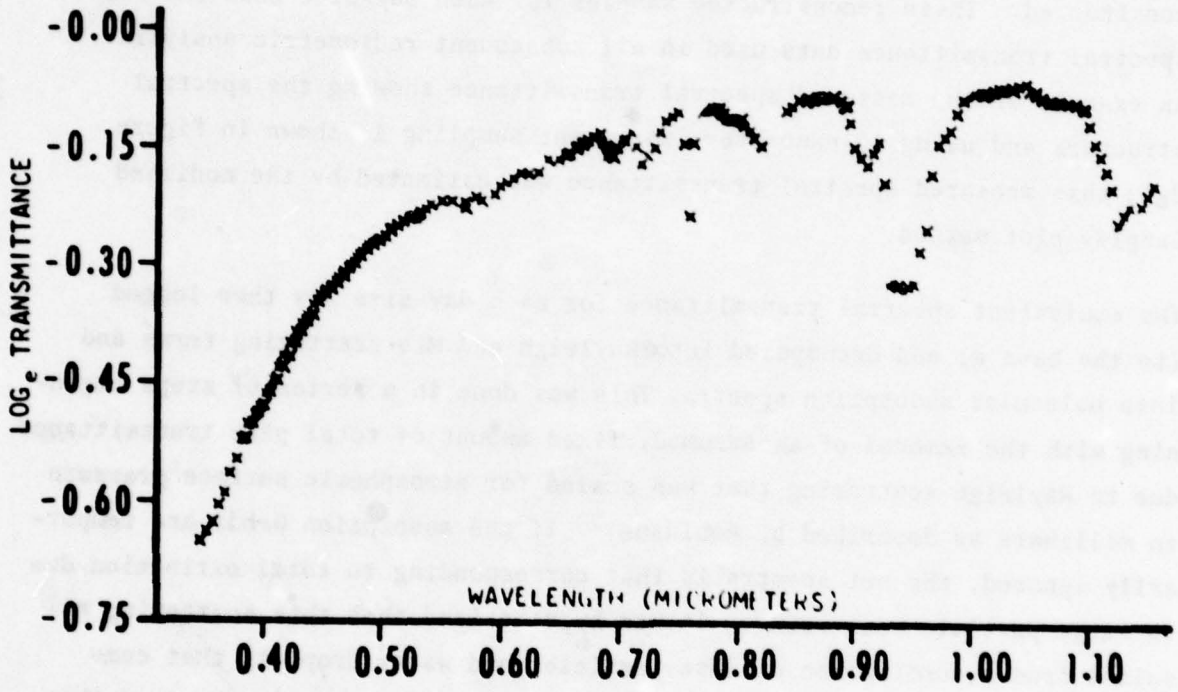

Figure 2-3. Example of Measured Spectral Vertical Atmospheric Log Transmittance (Vandenberg, Ca.; May 12, 1976 P.M.)

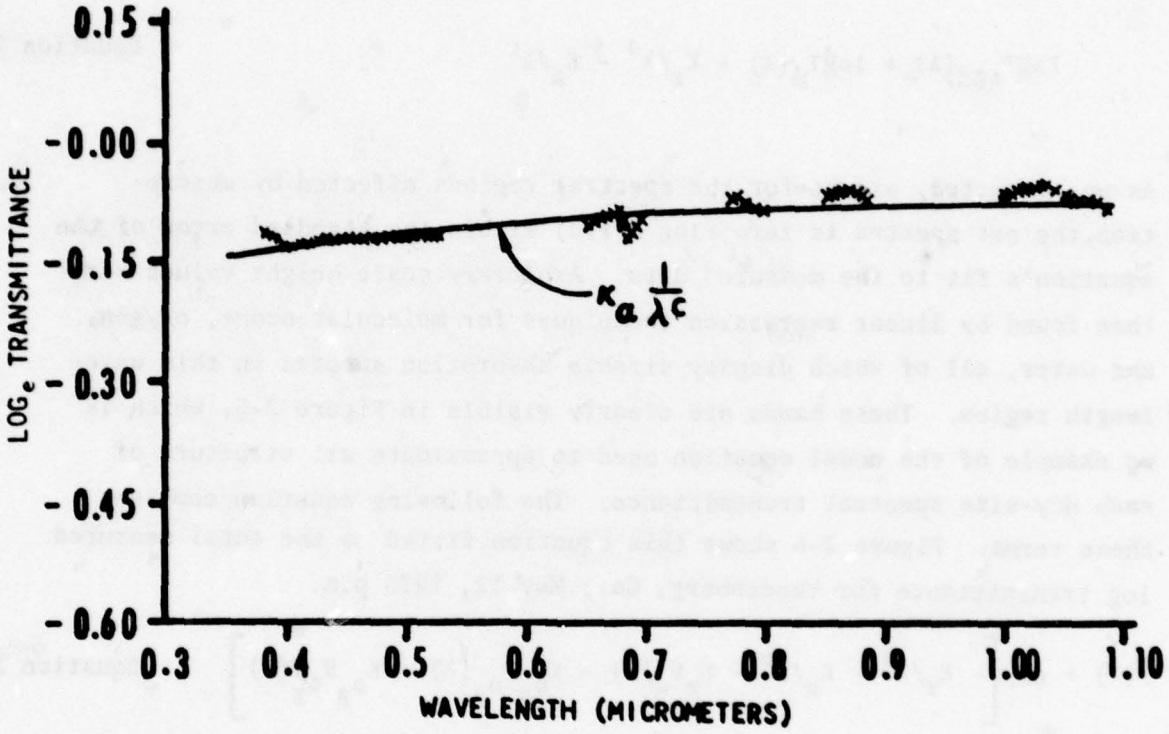

Figure 2-4. Typical Regression Model Fitted to Net Aerosol Spectral Vertical Atmospheric Log Transmittance (Vandenberg, Ca.; May 12, 1976 P.M.)

to the net log transmittance data. Recombining the scattering phenomena equations and subtracting them from the total measured log transmittance resulted in the log transmittance spectra for absorption alone. The equation for total absorption extinction was then:

$$\log T_{ABS}(\lambda) = \log T_m(\lambda) - K_r/\lambda^4 - K_a/\lambda^c \qquad \text{Equation 2-2}$$

As was expected, except for the spectral regions affected by absorption, the net spectra is zero (log E 1.0) within the standard error of the equation's fit to the measured data. Arbitrary scale height values were then found by linear regression techniques for molecular ozone, oxygen, and water, all of which display sizable absorption spectra in this wavelength region. These bands are clearly visible in Figure 2-5, which is an example of the model equation used to approximate all structure of each day-site spectral transmittance. The following equation combines these terms. Figure 2-6 shows this equation fitted to the total measured log transmittance for Vandenberg, Ca.; May 12, 1976 p.m.

$$\hat{T}(\lambda) = \text{Exp}\left[- K_r/\lambda^4 - K_a/\lambda^c - K_w V_w(\lambda) - K_{o_2} V_{o_2}(\lambda) - K_{o_3} V_{o_3}(\lambda) \right] \qquad \text{Equation 2-3}$$

Where: K_w, K_{o_2}, and K_{o_3} are the relative scale weight values corresponding to water, oxygen, and ozone absorption, and

$V_w(\lambda)$, $V_{o_2}(\lambda)$, and $V_{o_3}(\lambda)$ are the relative spectral shape vectors for water, oxygen, and ozone absorption spectra.

For the sample date used in Figures 2-2 through 2-6, the values of the constants of each term were:

$K_a = 0.0712$	$K_w = 0.100$	$K_{o_2} = 0.107$
$c = 0.685$	$k_{o_3} = 0.0157$	$K_r = 0.00884$

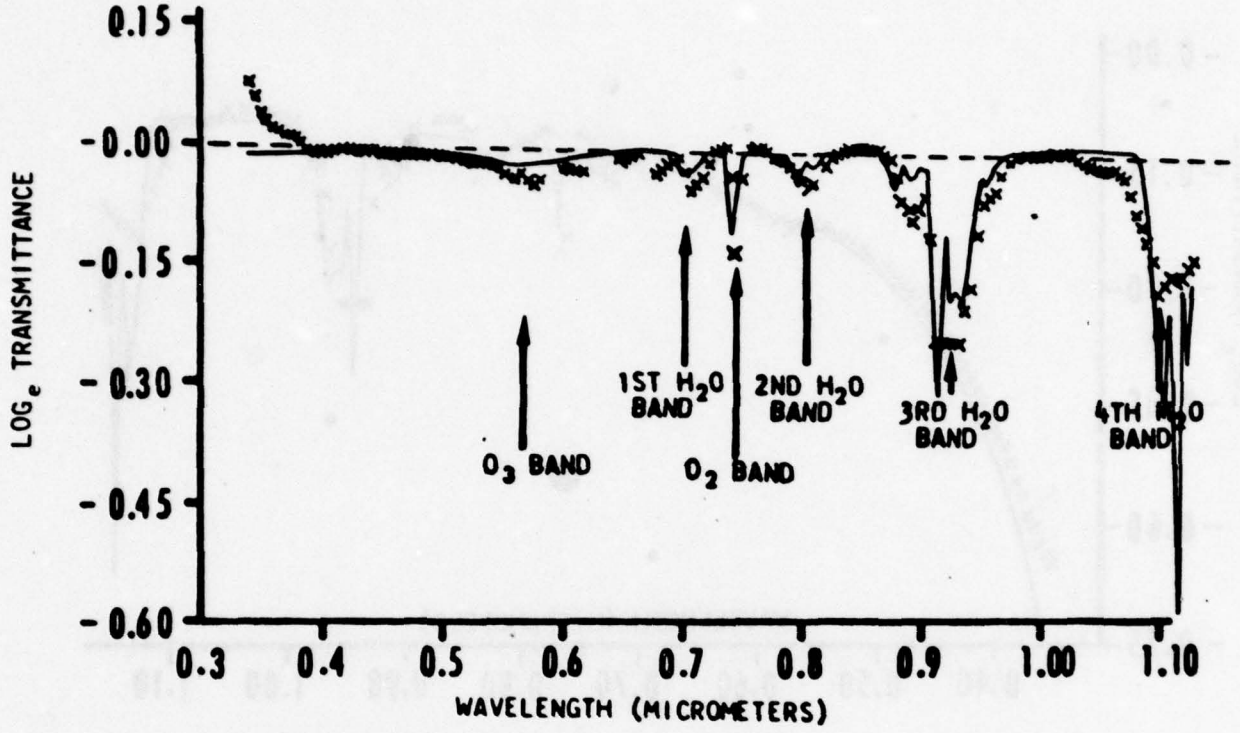

Figure 2-5. Typical Regression Model Fitted to Net Absorption Spectral Log Transmittance (Vandenberg, Ca.; May 12, 1976 P.M.)

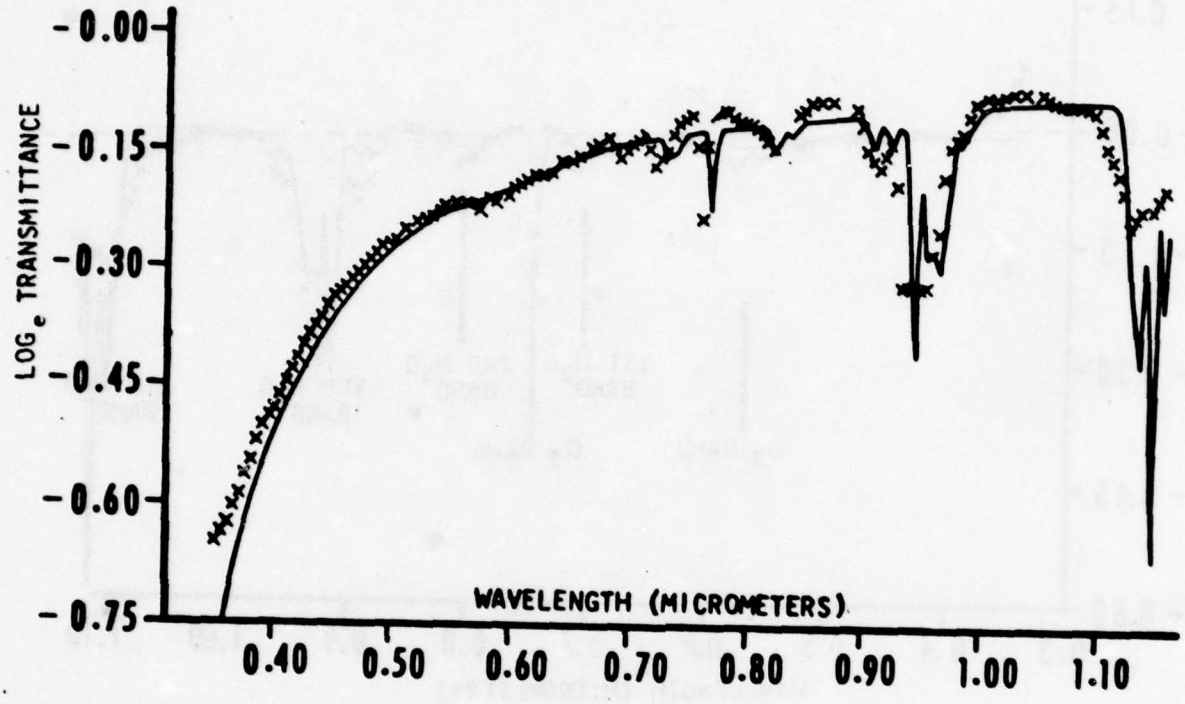

Figure 2-6. Total Regression Model Fitted to Measured Vertical Spectral Atmospheric Log Transmittance

In subsequent analyses, the relative scale heights were related to the physically measurable parameters discussed below in this section. However, for purposes of analysis of spectral sky radiance and spectral irradiance data, the exact coefficients derived from this reduction process were used. These coefficients are summarized in Table 2-1 for all day sites for which the transmittance analysis could be accomplished.

2.4 MODELING OF VERTICAL SPECTRAL TRANSMITTANCE

2.4.1 Scaling for Molecular Scattering

The molecular scattering beam alternation can be adequately described by Rayleigh scattering theory. The coefficient of the Rayleigh form has been shown to be a function of the atmospheric density and thus proportional to

$$K_r = \frac{-0.008925}{1013.25} \times \Delta P \qquad \text{Equation 2-4}$$

For the earth-to-space problem, ΔP becomes the uncorrected surface pressure in millibars. For observations from an arbitrary altitude, ΔP is the pressure difference between the observer's altitude and the terrain elevation, and it can be found by integrating the atmospheric density versus the altitude function. This density function has been modeled in SCAT3 as a closed-form, continuous function of altitude referenced to sea level. Each ROAB density profile was fit with (1) the function developed by Weibull[8] and (2) the coefficients studied as functions of surface meteorological measurements that were made concurrently. The density function and its integral between any two elevations are expressed in the following two equations:

$$D(x) = P_s \left(\frac{1.04}{b}\right)\left(\frac{x}{b}\right)^{.04} \text{Exp}\left[-\left(\frac{x}{b}\right)^{1.04}\right] \qquad \text{Equation 2-5}$$

---

[8] W. Weibull, "A Statistical Distribution Function of Wide Applicability," J. of Applied Mechanics, Vol 18, Mar 1951, pp 293-297.

TABLE 2-1

TRANSMITTANCE COEFFICIENTS SUMMARIZED BY DAY-SITE

Date	Site	Rayleigh Coefficient K_R	Aerosol Coefficient K_A	Aerosol Exponent C	Water Absorption Coefficient K_W	Ozone Absorption Coefficient K_{O3}	Oxygen Absorption Coefficient K_{O2}
8-12-75 am	Athens, Ga.	0.00872	0.176	1.385	0.097	0.095	-
8-27-75 pm	Apalachicola, Fla.	0.00899	0.199	1.486	0.173	0.163	0.0034
8-28-75 pm	Apalachicola, Fla.	0.00899	0.347	1.068	0.189	0.165	0.0108
11-9-75 pm	Vint Hill, Va.	0.00890	0.0658	1.254	0.114	0.051	-
11-11-75 pm	Vint Hill, Va.	0.00892	0.0936	0.241	0.078	0.007	-
10-21-75 pm	Denver, Col.	0.00736	0.0484	0.744	0.037	0.013	0.034
2-21-76 pm	St. Cloud, Minn.	0.00868	0.0606	0.758	0.037	0.055	0.029
2-22-76 pm	St. Cloud, Minn.	0.00870	0.0438	0.676	0.043	0.057	0.033
2-23-76 am	St. Cloud, Minn.	0.00858	0.0690	0.801	0.050	0.035	0.069
2-24-76 pm	St. Cloud, Minn.	0.00856	0.0473	0.899	0.043	0.043	0.029
3-4-76 am	Glasgow, Mont.	0.00826	0.0583	0.989	0.020	0.077	0.033
3-5-76 am	Glasgow, Mont.	0.00825	0.0408	0.752	0.012	0.061	0.056
4-26-76 am	Alameda, Cal.	00894	0.0410	0.414	0.050	0.034	0.142
4-26-76 pm	Alameda, Cal.	0.00894	0.0740	0.918	0.023	0.007	0.121
5-12-76 am	Vandenberg, Cal.	0.00884	0.0429	1.130	0.112	0.0072	0.130
5-12-76 pm	Vandenberg, Cal.	0.00884	0.0712	0.685	0.100	0.016	0.107
6-7-76 pm	Tucson, Ariz.	0.00810	0.0390	0.190	0.052	0.029	0.086
6-8-76 pm	Tucson, Ariz.	0.00811	0.0340	0.648	0.085	0.023	0.173
6-11-76 am	Tucson, Ariz.	0.00812	0.0490	0.184	0.070	0.022	0.089
6-17-76 am	Tucson, Ariz.	0.00811	0.0381	0.792	0.080	0.023	0.088
6-28-76 am	Winslow, Ariz.	0.00752	0.0639	1.192	0.083	0.043	0.157
7-19-76 am	Little Rock, Ark.	0.00889	0.0628	1.747	0.183	0.014	0.134
7-21-76 am	Little Rock, Ark.	0.00885	0.295	0.342	0.112	0.018	0.100
8-4-76 am	Athens, Ga.	0.00876	0.1311	1.263	0.119	0.078	0.083
8-6-76 am	Athens, Ga.	0.00872	0.203	0.997	0.108	0.166	0.124
8-11-76 am	Athens, Ga.	0.00877	0.153	1.257	0.091	0.081	0.094
8-12-76 am	Athens, Ga.	0.00877	0.184	1.305	0.153	0.072	0.091
8-13-76 am	Athens, Ga.	0.00871	0.209	1.125	0.148	0.122	0.110
8-22-76 pm	Apalachicola, Fla.	0.00895	0.161	1.480	0.160	0.078	0.114
8-23-76 am	Apalachicola, Fla.	0.00894	0.168	1.627	0.215	0.042	0.166
9-12-76 am	Albuquerque, N.M.	0.00739	0.025	1.780	0.111	0.008	0.100
9-13-76 am	Albuquerque, N.M.	0.00740	0.014	0.334	0.078	0.021	0.091
9-12-76 am	Albuquerque, N.M.	0.00744	0.047	-0.226	0.107	0.008	0.076
9-19-76 am	Albuquerque, N.M.	0.00737	0.027	1.732	0.107	0.011	0.127
9-28-76 am	Ogden, Utah	0.00768	0.033	1.026	0.061	0.026	0.077
9-28-76 pm	Ogden, Utah	0.00768	0.035	1.065	0.057	0.024	0.080
9-29-76 am	Ogden, Utah	0.00769	0.032	0.904	0.051	0.026	0.069
10-28-76 am	Dayton, Ohio	0.00872	0.076	0.828	0.036	0.057	0.112
10-28-76 pm	Dayton, Ohio	0.00872	0.061	1.075	0.045	0.053	0.118

$$\Delta P = \int_{x_1}^{x_2} D(x)dx = K_S \left\{ \exp\left[-\left(\frac{x_1}{b} \right)^{1.04} \right] - \exp\left[-\left(\frac{x_2}{b} \right)^{1.04} \right] \right\}$$

Equation 2-6

Where: K_s is $124.87 + 6.754 \times 10^{-6} P_s$

P_s is the station atmospheric pressure in millibars (not corrected to sea level)

b is $7.315 + .000908P + .0236T$

T is the station air temperature in degrees Celsius, and

x_1, x_2 are the elevations above sea level of the station and the observer, in kilometers.

Figure 2-7 shows a typical RAOB density profile (see x's) and the Weibull function fit. A complete table of station pressure observations for all day-sites of the project can be found in Appendix B of Volume 2 of this report.

The total vertical-beam-path transmittance due to pure Rayleigh scatter is then computed as follows:

$$t_{s_r}(\lambda) = \exp\left[-\frac{K_r}{\lambda^4} \right]$$

Equation 2-7

2.4.2 Conversion to Sea-Level Equivalent Pressure

As stated above, the SCAT3 model's algorithms were derived using station pressure. This pressure as reported by weather stations is usually the equivalent sea-level pressure obtained by reduction of the station pressure to sea level, using an inverted version of the hypsometric equation discussed by Gordon.[9]

---

[9] A. H. Gordon, Elements of Dynamic Meteorology, D. VanNostrand Company, Inc, New York, N. Y., 1962.

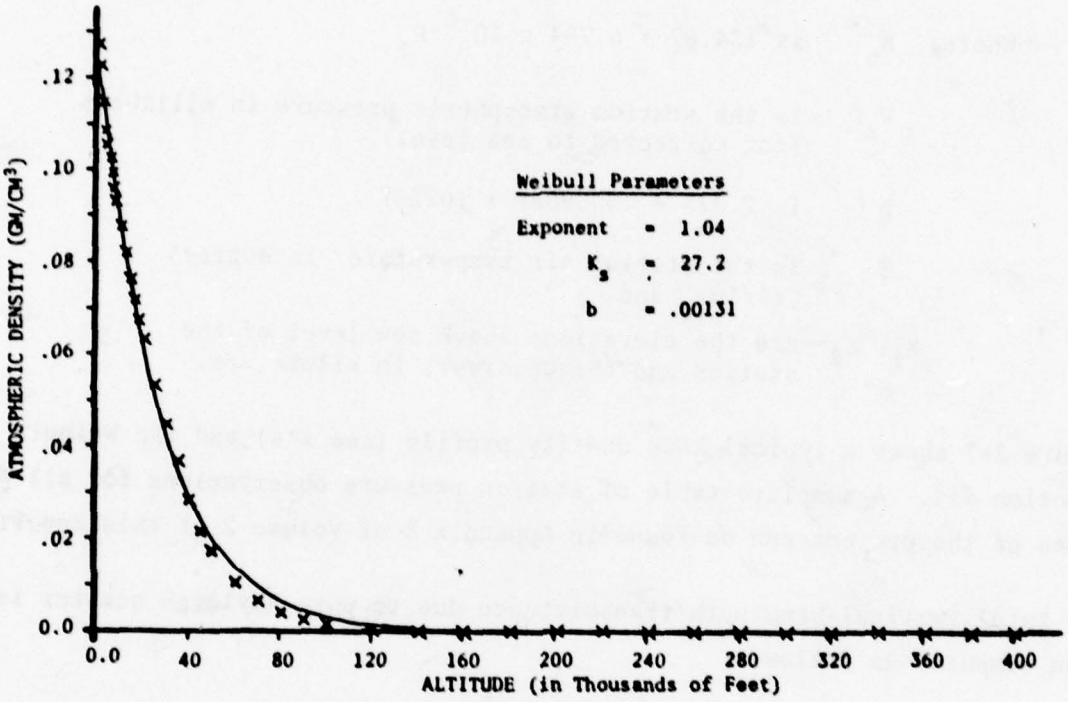

Figure 2-7. Typical Atmospheric Density Profile (23 Feb 76, 1200Z)

The sea level pressure is the input parameter for SCAT3, and the model converts the sea level pressure to station pressure by means of the following equation:

$$P_s = P_0 \times 10^{-\frac{14.825E}{273.16 + T_{mv}}} \qquad \text{Equation 2-8}$$

Where: P_0 is the sea level pressure in millibars

P_s is the station pressure in millibars

E is the station elevation in kilometers, and

T_{mv} is the mean virtual temperature in degrees Celsius.

In a system of moist air, the virtual temperature, T_{mv}, is the temperature of dry air having the same density and pressure as the moist air and is a function of station pressure, vapor pressure, and temperature. Because in most practical cases, the virtual temperature is not significantly different from the actual temperature, they were considered the same for this study. Another approximation that was made was that the station elevation in geopotential meters is equal to the elevation in meters.

2.4.3 Volumetric Scaling for Aerosol Scattering

Separation of the measured atmospheric spectral transmittance into its components permitted the aerosol extinction coefficients to be estimated for each day-site. These were then analyzed as functions of other measurable parameters, primarily moisture scale height. In addition, a joint experiment was conducted in Albuquerque, N.M., with the Atmospheric Sciences Laboratory of the U.S. Army Electronics Command, White Sands, N.M., in which measurements were made of surface dust particle concentrations. The experiment was conducted using two trailer laboratories located together in an area of sparse vegetation. Aerosol measurements were made over eight consecutive days (12-19 September 1976), and radiometric readings were made on four of these days. A description of the experiment and a summary of the data is contained in para. 5.2, Vol 2 of this report.

The Albuquerque experiment was used to refine this relationship between the aerosol extinction coefficients and moisture scale height by introducing an independent parameter for dust concentration into the coefficient equations. A complete list of aerosol extinction coefficients is contained in Table 2-1 above.

The equations, as modified by the Albuquerque experiment, were:

$$\text{Wavelength exponent, } C = 1.492 - .000424D_0 + .092MSH;\ C \geq .5 \qquad \text{Eq 2-9}$$

$$\text{Extinction Coefficient, } K_a = -.0705 + .000015D_0 + .0831MSH;\ K_a \geq .0481 \qquad \text{Eq 2-10}$$

Where: D_0 is the surface dust particle concentration in particles/cm^3 equivalent to the McClatchey mode at sea level.

$0 \leq D_0 \leq 13780$, if $1 \leq MSH \leq 2$

$D_0 = 1712$, if $MSH < 1$ or $MSH > 2$

MSH is the total moisture scale height, in centimeters ($0 \leq MSH \leq 10$)

Figure 2-8 shows the results of these equations when they are evaluated for several levels of moisture scale height and dust concentration. These parameters are used to estimate the aerosol extinction coefficient, K_a, and the vertical beam-path transmittance according to the following equation:

$$t_{s_a}(\lambda) = \exp\left[-\frac{K_a}{\lambda^c}\right] \qquad \text{Equation 2-11}$$

2.4.4 Altitude Scaling for Aerosol Scattering

Altitude scaling of the aerosol extinction coefficients was possible by using the assumption that the amount of scattering due to aerosols would be distributed vertically in the same manner as the amount of water content. Thus, the extinction coefficient would increase approximately exponentially toward the earth's surface and approach zero in space. In other models, such as the one developed by McClatchey, similar distributional shape assumptions are made, but the extinction coefficient distribution is not associated with that of moisture.

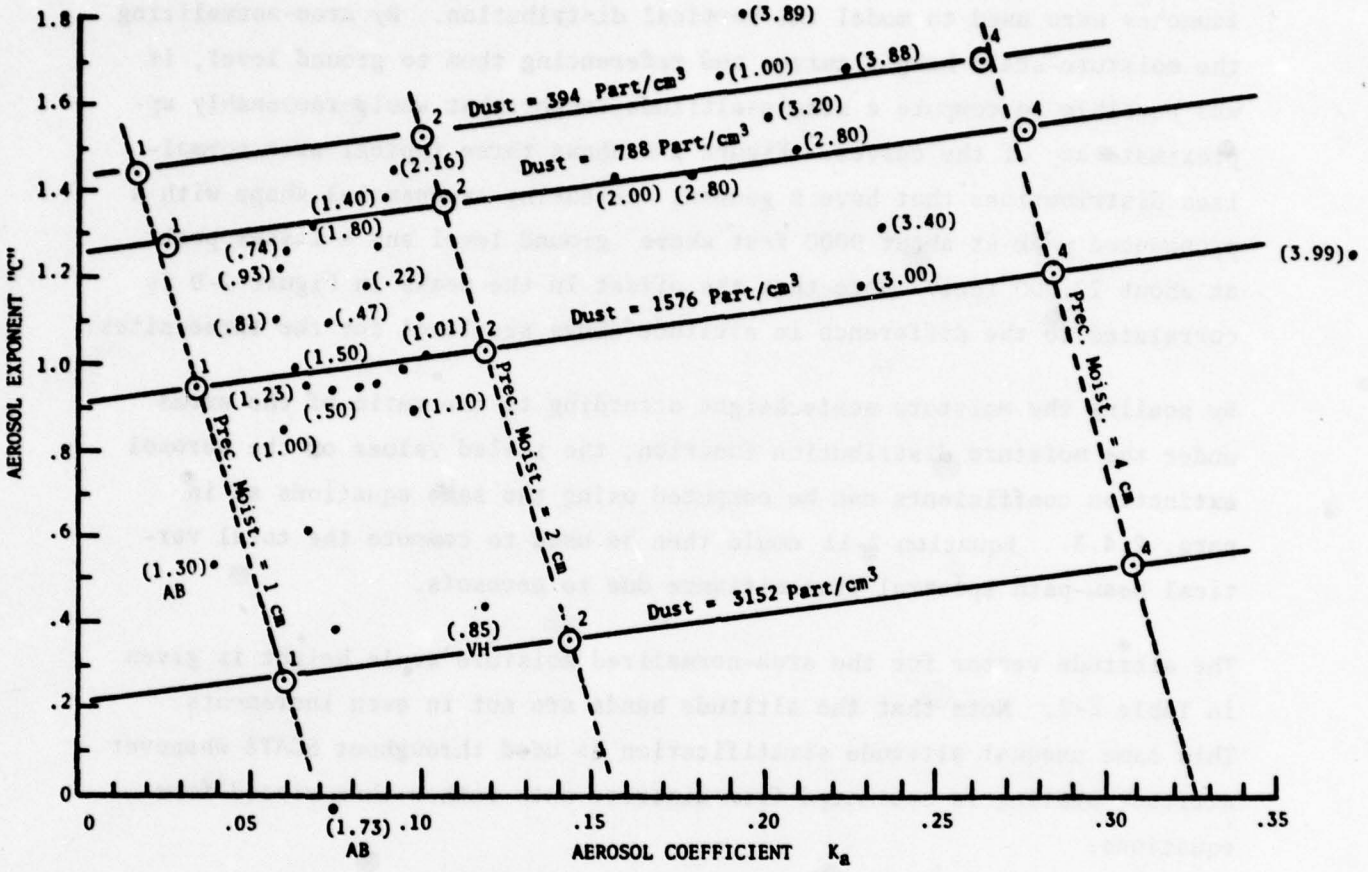

Note: Numbers given at data points are precipitable moisture in cm.

Figure 2-8. Aerosol Coefficients as a Function of Dust and Precipitable Moisture

The profiles of moisture scale height versus altitude from the RAOB launches were used to model the vertical distribution. By area-normalizing the moisture-scale-height curves and referencing them to ground level, it was possible to compute a single-altitude vector that would reasonably approximate any of the curves. Figure 2-9 shows three typical area-normalized distributions that have a general decreasing exponential shape with a pronounced peak at about 9000 feet above ground level and a lesser peak at about 22,000 feet. Note that the offset in the peaks in Figure 2-9 is correlated to the difference in altitude above sea level for the three sites.

By scaling the moisture scale height according to the ratio of the areas under the moisture distribution function, the scaled values of the aerosol extinction coefficients can be computed using the same equations as in para. 2.4.3. Equation 2-11 could then be used to compute the total vertical beam-path spectral transmittance due to aerosols.

The altitude vector for the area-normalized moisture scale height is given in Table 2-2. Note that the altitude bands are not in even increments. This same unequal altitude stratification is used throughout SCAT3 whenever altitude scaling is estimated from discrete data rather than closed-form equations.

2.4.5 Estimating Moisture Scale Height from Surface Meteorology

The on-board weather data collection system and the NWS observations permitted an examination of the relationship between surface synoptic data and detailed atmpsoheric profiles from RAOB's. Because it was anticipated that the total-column moisture scale height would be related to surface absolute humidity, a simple mathematical approximation to a psychometric chart was found useful in converting from relative humidity and temperature to absolute water vapor pressure.

A nonlinear equation was found that could be used in estimating vapor pressure from temperature (°F) along a fixed relative humidity curve. Relative humidity therefore enters the general equation for vapor pressure as a

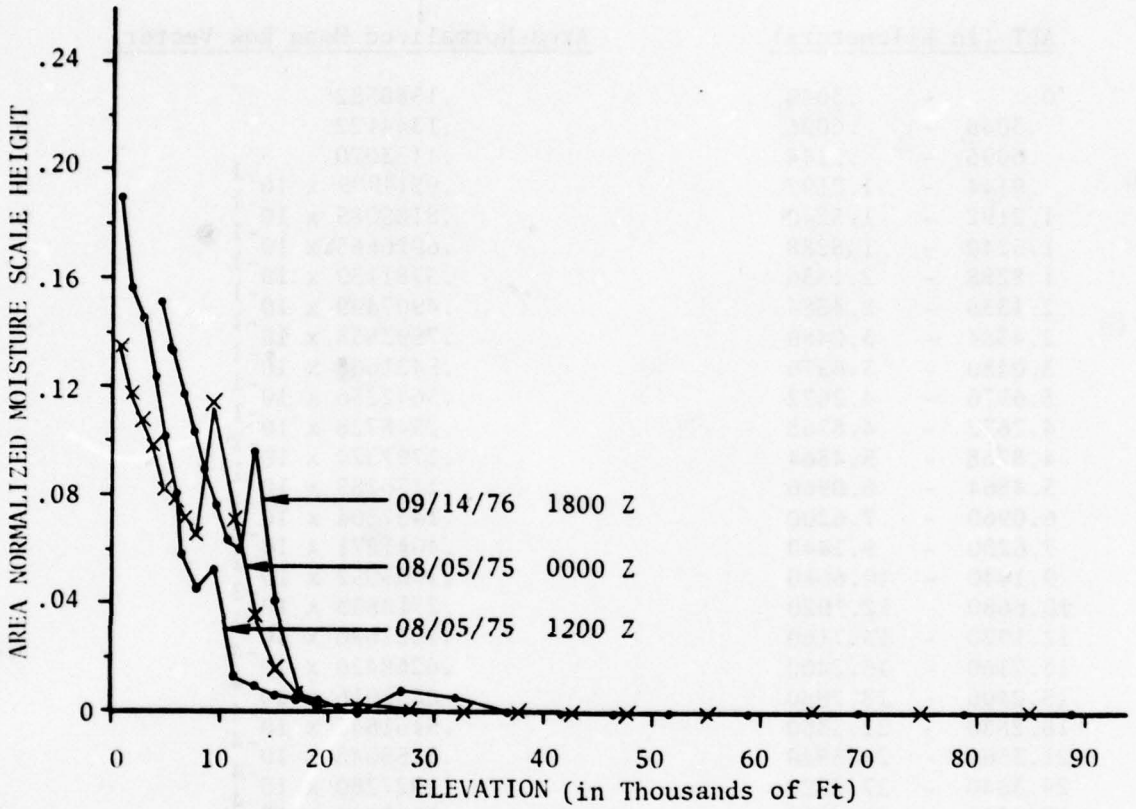

Figure 2-9. Precipitable Moisture Profile (Area Normalized)

TABLE 2-2

PRECIPITABLE MOISTURE AS A FUNCTION OF ALTITUDE

ALT (in Kilometers)			Area-Normalized Mean Row Vector
0	-	.3048	.1588552
.3048	-	.6096	.1344122
.6096	-	.9144	.1133070
.9144	-	1.2192	$.9514909 \times 10^{-1}$
1.2192	-	1.5240	$.8185085 \times 10^{-1}$
1.5240	-	1.8288	$.6916665 \times 10^{-1}$
1.8288	-	2.1336	$.5781139 \times 10^{-1}$
2.1336	-	2.4384	$.4907499 \times 10^{-1}$
2.4384	-	3.0480	$.7593858 \times 10^{-1}$
3.0480	-	3.6576	$.5431665 \times 10^{-1}$
3.6576	-	4.2672	$.3642236 \times 10^{-1}$
4.2672	-	4.8768	$.2548728 \times 10^{-1}$
4.8768	-	5.4864	$.1797324 \times 10^{-1}$
5.4864	-	6.0960	$.1170285 \times 10^{-1}$
6.0960	-	7.6200	$.1432864 \times 10^{-1}$
7.6200	-	9.1440	$.4041271 \times 10^{-2}$
9.1440	-	10.6680	$.1005052 \times 10^{-2}$
10.6680	-	12.1920	$.2710833 \times 10^{-3}$
12.1920	-	13.7160	$.1031096 \times 10^{-3}$
13.7160	-	15.2400	$.6268420 \times 10^{-4}$
15.2400	-	18.2880	$.8532016 \times 10^{-4}$
18.2880	-	21.3360	$.5161841 \times 10^{-4}$
21.3360	-	24.3840	$.3155043 \times 10^{-4}$
24.3840	-	27.4320	$.1927280 \times 10^{-4}$
27.4320	-	30.4800	$.1193245 \times 10^{-4}$

multiplying factor, resulting in:

$$VP = .805RH \times \exp\left[.183T^{.69} \right] \qquad \text{Equation 2-12}$$

where RH is the relative humidity, expressed as a decimal, and T is the temperature in degrees F.

In the above equation, the vapor pressure is given in inches of mercury, but for use in the model, the equation was converted to vapor pressure in millibars by multiplying by 33.9mb/inch Hg. In addition, the input parameters of the model are in metric units, and a temporary conversion of the input temperature from ^{o}C to ^{o}F is therefore executed internally in the SCAT3 program to make it compatible with Equation 2-12.

The vapor pressure is then converted to precipitable moisture using a linear relationship that exists between the square root of vapor pressure and the natural logarithm of the precipitable moisture. This relationship had been suggested by other experimenters[10,11], and also appeared to fit the observations made on this project although the exact coefficients deviate from the relationships in the literature. The linear fit found on this project is shown in Figure 2-10 as well as the functions suggested in the two references above.

The equation used to compute moisture scale height (MSH) is:

$$MSH = 0.134 \exp \left[.659 \cdot VP^{\frac{1}{2}} \right] \qquad \text{Equation 2-13}$$

where VP is the vapor pressure in millibars.

2.4.6 Scaling of Absorption Transmittance

Significant absorption bands are the result of water, ozone, and the oxygen molecular content of the atmosphere. The resulting absorption log transmittance can be expressed in the following vector form, as was discussed above in para. 2.3.

$$\log_e T_a(\lambda) = K_w \cdot V_w(\lambda) + K_{o_2} \cdot V_{o_2}(\lambda) + K_{o_3} \cdot V_{o_3}(\lambda) \qquad \text{Equation 2-14}$$

Vectors established for earlier atmospheric models and discussed by McClatchey[12] were used in this model with the corresponding coefficients, K_w, K_{o_2}, and K_{o_3} determined from mobile laboratory transmittance data for each day-site. The method of predicting these coefficients is discussed below.

---

[10] J.L. Montieth, "An Empirical Method of Estimating Long-Wave Radiation Exchanges in the British Isles," Quarterly Journal of the Royal Meteorological Society, 551.521.32.

[11] S.B. Idso, "Atmospheric Attenuation of Solar Radiation," Journal of Atmospheric Sciences, Vol. 26, pp 1088-1095.

[12] R.A. McClatchey et al. "Optical Properties of the Atmosphere," Air Force Cambridge Research Laboratories -72-0497, Aug 72, Environmental Research Papers #411.

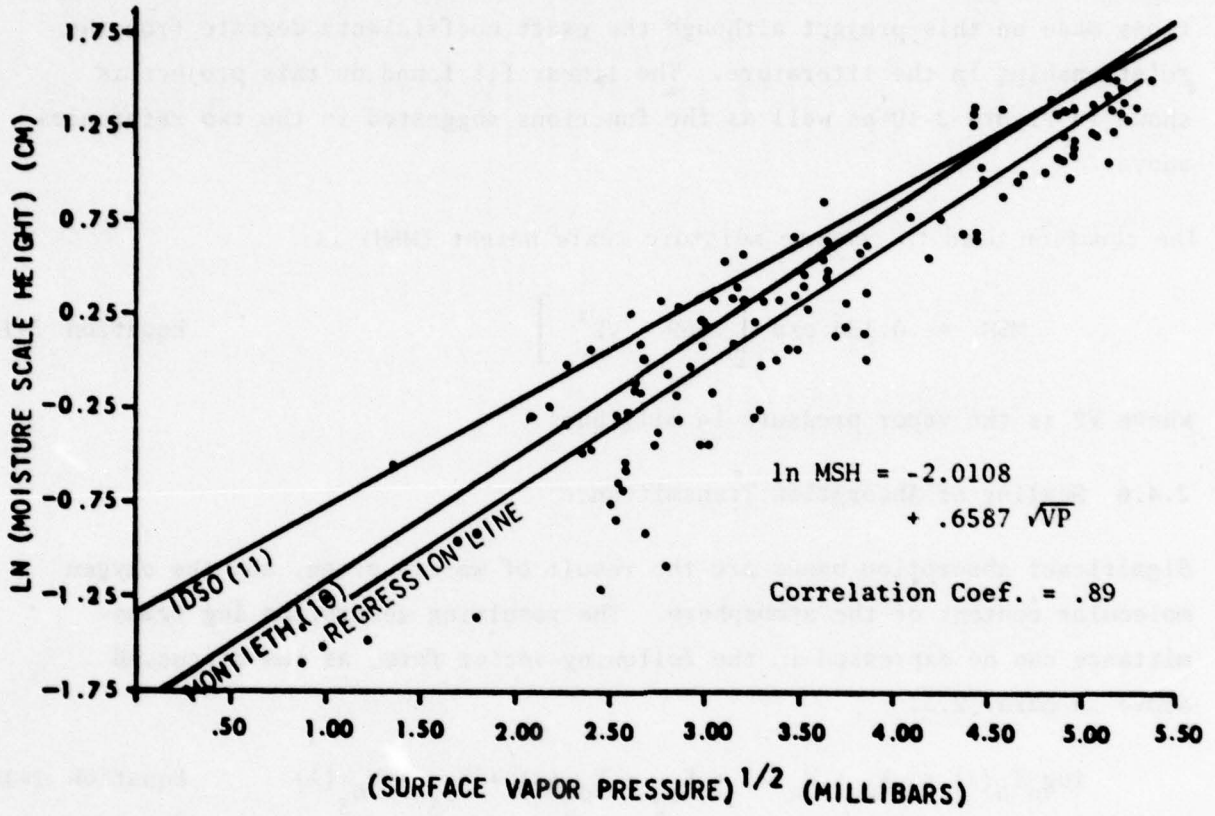

Figure 2-10. The Relationship Between Moisture Scale Height and Surface Vapor Pressure

2.4.6.1 Water Vapor Absorption

Water absorption occurs in four distinct wavelength bands: 720-735, 810-840, 895-990, and 1105-1150 nanometers. The depth of each band is given by the product of the water absorption vector, $V_w(\lambda)$, and a scaling coefficient, k_w, found to be related to moisture scale height. The water absorption vector is shown in Figure 2-11. This vector was fitted to the measured absorption log transmittance data, using the method of least squares, to determine the value of K_w for each day-site. Because instrument non-linearities were suspected beyond 1 μm, only the first three bands were used in those regressions.

As was anticipated, the relationship between the vector coefficient, K_w, and the moisture scale height was not linear. Figure 2-12 shows the regression equation fitted to the estimated coefficients as a function of moisture scale height. This regression equation is:

$$K_w = -0.0645\ MSH^{0.713} \qquad \text{Equation 2-15}$$

The model also scales the water bands as a function of the observer's altitude and the terrain altitude. This is done by ratioing the appropriate partial area, from the ground elevation to the observer's altitude, to the total area under the moisture scale height as a function of altitude (see Figure 2-9 for examples).

2.4.6.2 Oxygen Absorption Line

A molecular oxygen absorption line has been modeled in the 760-765 nm band. As was the case with other absorption transmittance data, this narrow absorption band was fitted using an arbitrary vector, $V_{o_2}(\lambda)$ and coefficient, V_{o_2}. Analysis of all day-site data resulted in an average value of 0.0905 for K_{o_2} and a standard deviation of 0.042. Since the absolute amount of oxygen is relatively constant, it was presumed that the variance about the mean K_{o_2} was the result of pure measurement error; it was therefore not modeled as

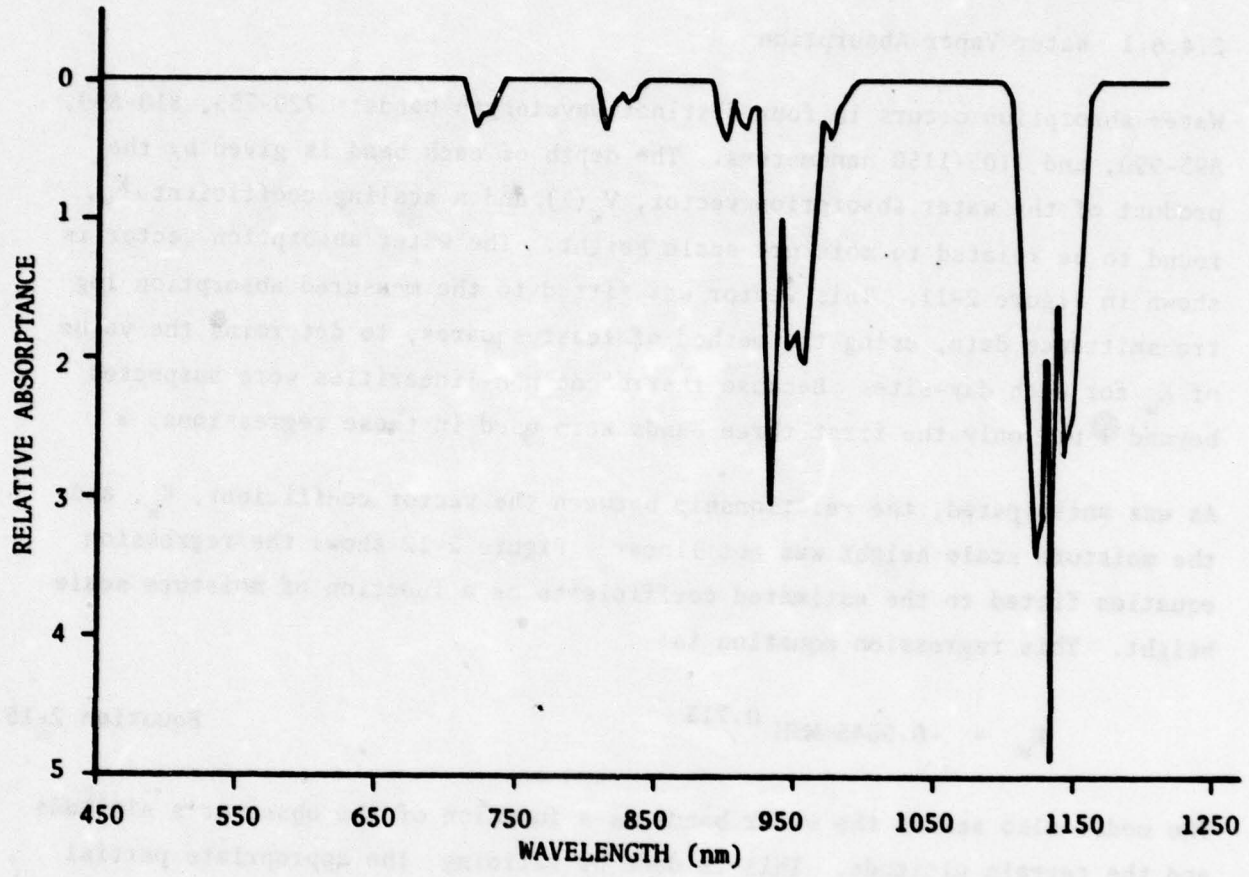

Figure 2-11. Water Vapor Absorption Vector, $V_w(\lambda)$

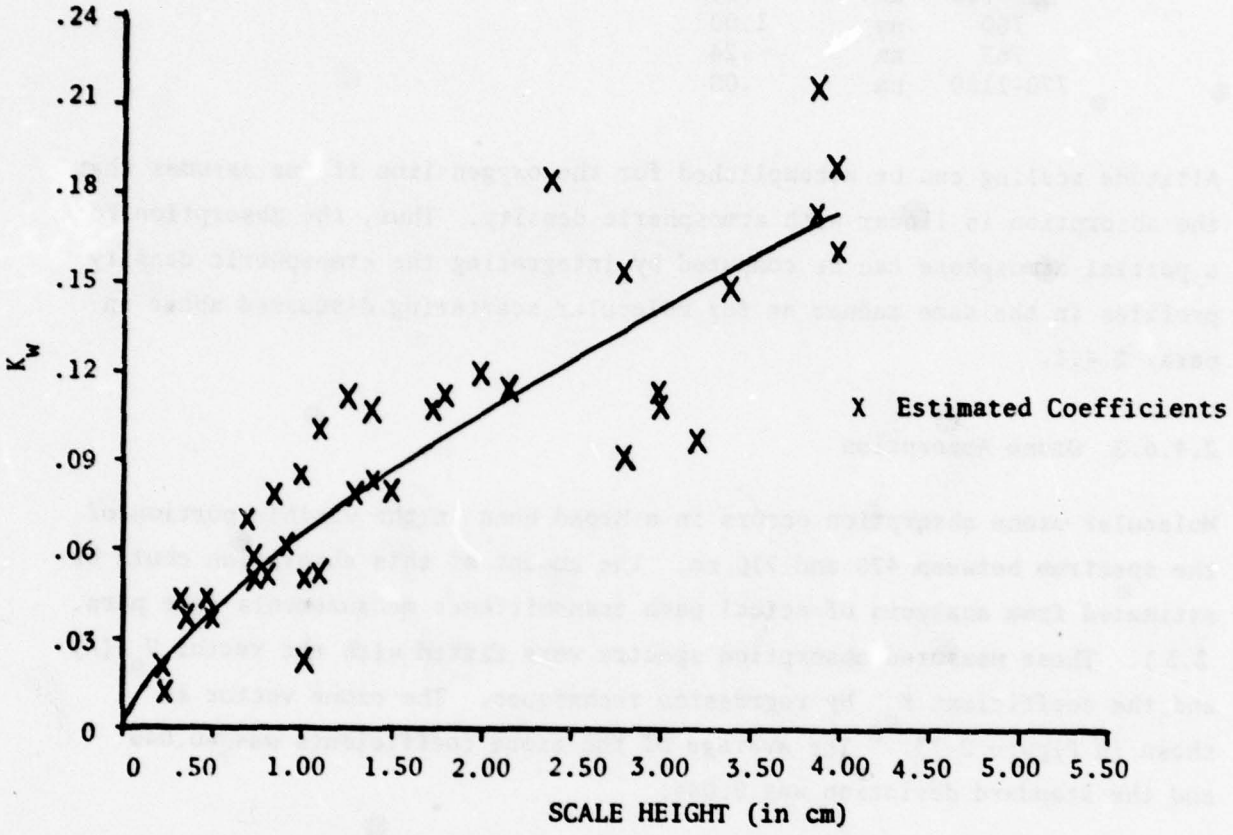

Figure 2-12. Model Equation Fitted to Water Absorption Coefficient Versus Moisture Scale Height

a function of any other measurable parameter. The vector has the following values at the wavelengths listed below.

350-755	nm	.00
760	nm	1.00
765	nm	.24
770-1150	nm	.00

Altitude scaling can be accomplished for the oxygen line if one assumes that the absorption is linear with atmospheric density. Thus, the absorption for a partial atmosphere can be computed by integrating the atmospheric density profiles in the same manner as for molecular scattering discussed above in para. 2.4.1.

2.4.6.3 Ozone Absorption

Molecular ozone absorption occurs in a broad band in the visible portion of the spectrum between 470 and 710 nm. The amount of this absorption could be estimated from analysis of actual path transmittance measurements (see para. 2.3). These measured absorption spectra were fitted with the vector $V_{O_3}(\lambda)$ and the coefficient K_{O_3} by regression techniques. The ozone vector is shown in Figure 2-13. The average of the ozone coefficients was -0.049 and the standard deviation was 0.044.

Unlike oxygen absorption, which would be expected to vary only slightly with physical changes in the atmosphere, large excursions occur seasonally and by latitude in ozone concentration. In a previous study by Craig[13], the ozone scale height (in mm) as distributed seasonally in the northern hemisphere was used to scale the absorption transmittance. The absorption was assumed to be a gaussian function having a peak value of 0.95 at 590 nm for a scale height of of 3.8 nm. When logged and peak-normalized to 1.0, this function became the ozone absorption vector used in this study as can be seen in Figure 2-13.

The scaling of ozone absorption can also be accomplished as a function of altitude according to the ozone concentration distribution from the Handbook

---

[13] R.A. Craig, "The Upper Atmosphere, Meteorology, and Physics, " Academic Press, 1965, pp 179-181.

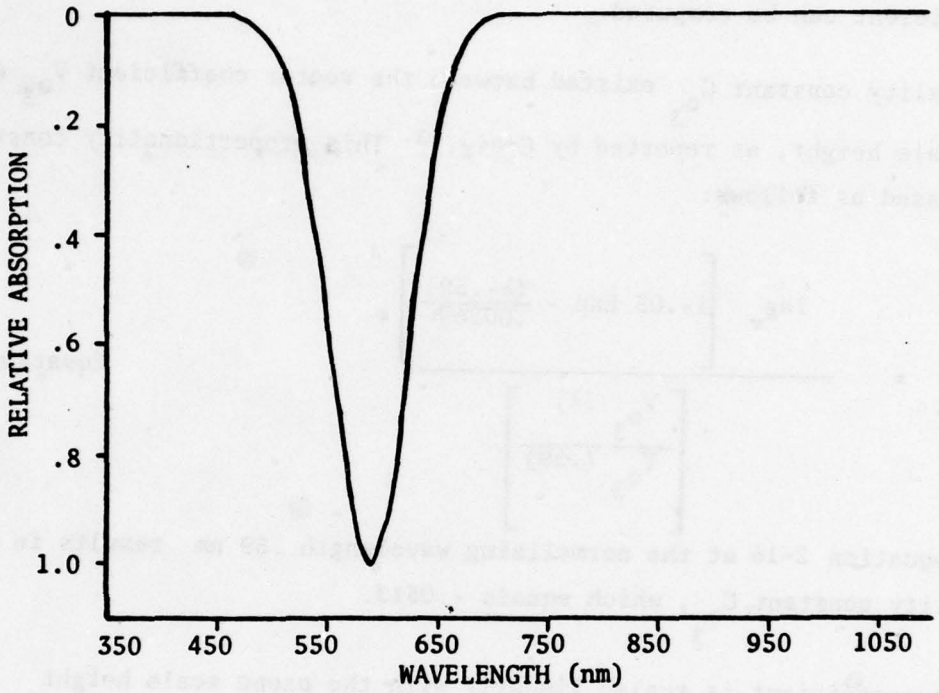

Figure 2-13. Normalized Ozone Absorption Vector

of Geophysics and Space Environments. This distribution is shown in Figure 2-14. The integral of the distribution function between the observer's altitude and the terrain altitude ratioed to the total earth-to-space scale height (3.2 mm) results in the scaled concentration from which the vector coefficient can be computed.

A proportionality constant C_{o_3} existed between the vector coefficient V_{o_3} and the ozone scale height, as reported by Craig.[13] This proportionality constant can be expressed as follows:

$$C_{o_3} = \frac{\log_e \left[1-.05 \text{ Exp} - \frac{(\lambda-.59)^2}{.00269}\right]}{\left[\frac{V_{o_3}(\lambda)}{V_{o_3}(.59)}\right]} \qquad \text{Equation 2-16}$$

Evaluating equation 2-16 at the normalizing wavelength .59 nm results in the proportionality constant C_{o_3}, which equals -.0513.

If the ozone coefficient is scaled linearly with the ozone scale height relative to the base level of 3.8mm and the constant of proportionality is introduced, the following equation results.

$$K_{o_3} = C_{o_3} \cdot \frac{OZ}{3.8} = -.0135\ OZ \qquad \text{Equation 2-17}$$

where OZ is the ozone scale height in mm, which is consistent with the data and definition discussed by Craig.[13] Scaling in the SCAT3 model is accomplished using the reference distribution of ozone concentration as a function of latitude and date. The actual distribution of the coefficient K_{o_3} as observed during this project is shown in Figure 2-15.

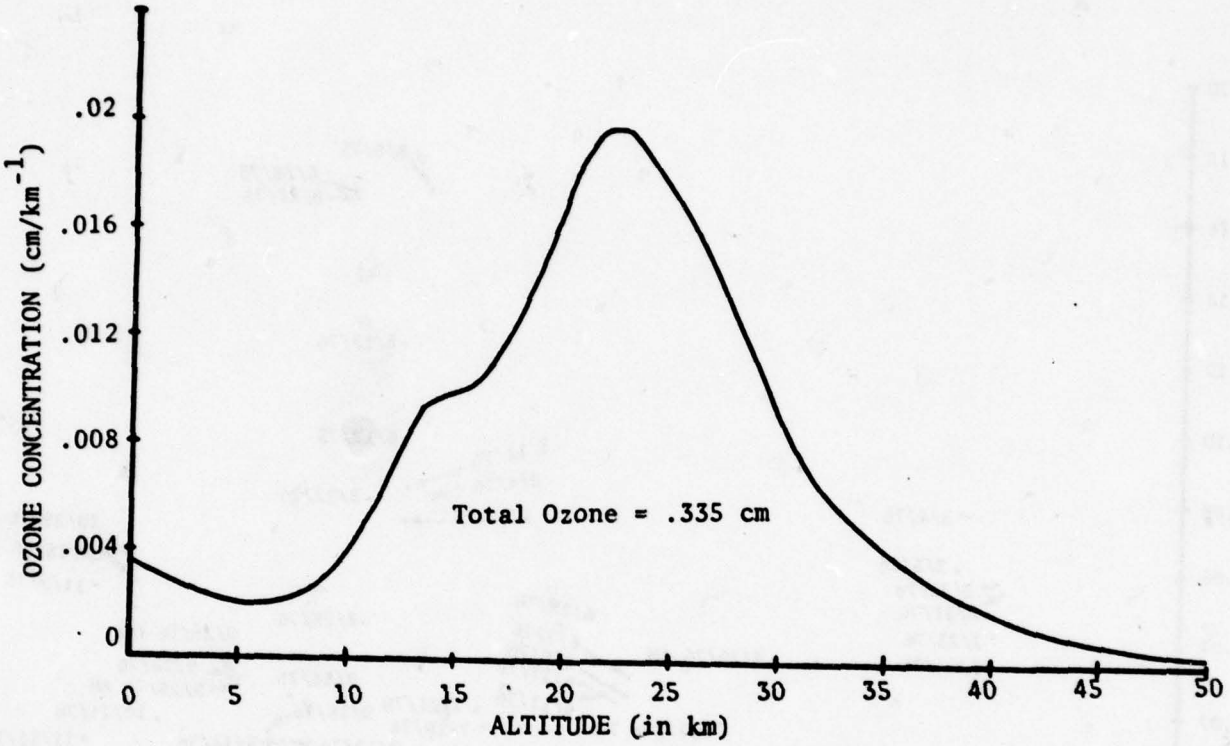

Figure 2-14. Profile of Ozone Concentration

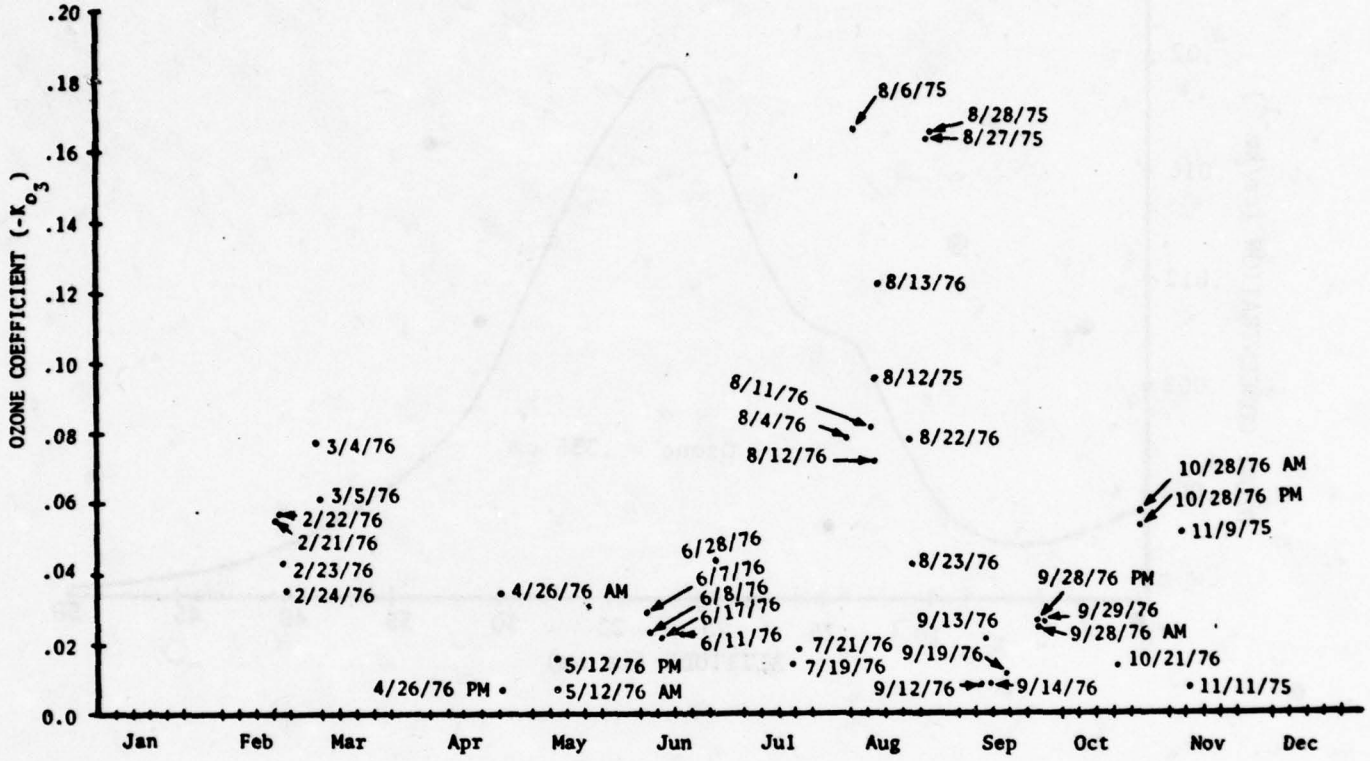

Figure 2-15. Distribution of Ozone by Date

2.4.7 Scaling for Observer's Zenith Angle

Atmospheric transmittance, of both scattering and absorption types, is assumed to vary with the observer's zenith angle according to the secant law as discussed by Robinson[14] except at low solar altitudes (below 30°) where the air mass numbers of Bemporad[15] are used. Analysis of the spectral transmittance data indicated that the total extinction coefficient was linear with air mass when computed in this manner. Water absorption level data tended to be more erratic in this relationship, probably due to diurnal variations in atmospheric moisture profiles; however, for the most part even these bands were well approximated by linear air mass scaling. SCAT3 uses the following equation for this purpose:

$$t_\theta(\lambda) = t_v(\lambda)^m$$

Where: $t_v(\lambda)$ is the total vertical spectral transmittance of the atmosphere (after scaling for altitude, moisture scale height, and dust).

$t_\theta(\lambda)$ is the total spectral transmittance of the atmosphere for the angle θ.

θ is the observer's zenith angle, and

m is the air mass $= \begin{cases} \sec\theta \text{ for the range } 0° \leq \theta \leq 60°, \\ \text{Bemporad numbers for the range } \theta > 60°. \end{cases}$

Table 2-3 lists the Bemporad air-mass numbers[15] as a function of the observer's zenith angle in 1-degree increments.

---

[14] N. Robinson, Solar Radiation, Solar Physics Laboratory, Israel Institute of Technology, Elsevier Publishing Co., 1966, p 52.

[15] A. Bemporad, "Search for a New Empirical Formula for the Representation of the Intensity of Solar Radiation with Zenith Angle," Meteorologische Zeitschrift, Vol 24, July, 1907.

TABLE 2-3

BEMPORAD AIR-MASS NUMBERS
(Observer's Zenith Angle > 60°)

Zenith Angle (in degrees)	Air Mass	Zenith Angle (in degrees)	Air Mass
61	2.06	76°	4.07
62	2.12	77	4.37
63	2.19	78	4.72
64	2.27	79	5.12
65	2.36	80	5.60
66	2.45	81	6.18
67	2.55	82	6.88
68	2.65	83	7.77
69	2.77	84	8.90
70	2.90	85	10.39
71	3.05	86	12.44
72	3.21	87	15.36
73	3.39	88	19.79
74	3.59	89	26.96
75	3.82	90	39.65

2.5 THE RELATIONSHIP BETWEEN METEOROLOGICAL/CLIMATOLOGICAL DATA AND T550

As stated above, the atmospheric model was designed to use temperature, pressure, and relative humidity as basic input parameters. Situations may occur, however, where it would be desirable not to use the surface meteorology data and key the model to a given transmittance value. For this purpose, the transmittance at 550 nm was arbitrarily selected as the alternative input parameter. Provision was therefore made in the SCAT3 model to input a T550 value instead of the meteorological parameters. When the T550 input option is used, the model creates a set of meteorological parameters that will give the specified transmittance value at 550 nanometers. When the created values of temperature, pressure, and relative humidity, are used, the model continues its calculation of the spectral transmittance in the usual manner.

To create the meteorological parameters, the model assumes a standard pressure of 1013.25 millibars and a standard temperature of 20°C unless they are specified otherwise by the program user. SCAT3 then solves the equations in reverse order to calculate the corresponding relative humidity. This is done by first calculating the Rayleigh coefficient, K_r, using the following equation:

$$K_r = \frac{.008925}{1013.25} \times \Delta P \qquad \text{Equation 2-18}$$

In this calculation, the aerosol coefficient C is taken to be the overall project average value of 1.1014 and if the values of K_r, C, t_s are combined, Equation 2-3 can be solved for the aerosol coefficient K_a after dividing out an assumed amount of ozone absorption transmittance that is derived from an input or default value for ozone scale height.

To compute the equivalent aerosol scattering coefficient, the following equation is used:

$$K_a = - 0.545 \cdot \ln T550 + 5.960\ K_r + .296\ K_{o_3} \qquad \text{Equation 2-19}$$

Given K_a and C, the moisture scale height can be computed using the inversion of equation 2-10, as follows:

$$MSH = - 11.57\ K_a + .420C + .189 \qquad \text{Equation 2-20}$$

The vapor pressure in millibars can then be computed using the inversion of equation 2-13, as shown below.

$$VP = \left(\frac{\ln(MSH) + 2.011}{.659}\right)^2 \qquad \text{Equation 2-21}$$

As a final step, the relative humidity is computed using the assumed temperature of 20°C and VP in inverted equation 2-12.

$$RH = 1.242\ VP \exp\left[-.183T^{.69}\right] \qquad \text{Equation 2-22}$$

If the relative humidity when computed is greater than 1.0, then the program will increase T in one-degree increments until a relative humidity of less than 1.0 is achieved. The algorithm then satisfies the requirement of T550 while physically possible surface meteorological conditions are selected.

As can be seen in the description above, when T550 is specified, average values of the two meteorological parameters temperature and pressure are assumed when the third, relative humidity, is calculated. This approach is based on the assumption that relative humidity changes through a wide range of values in a way that is harder to approximate accurately than by using values of temperature or pressure. In addition, pressure variations affect the transmittance less than changes in temperature and relative humidity do (see Figures D-1 to D-3 in Appendix D). If it is known that for a particular case the temperature will be significantly different from 20°C, the user may choose to input T.

For comparison purposes, measured temperature, pressure, and relative humidity were used along with transmittance values at 550 nm to reconstruct the spectral transmittances in Figures 2-16 and 2-17. Figure 2-16 shows the comparison for a clear day having a low moisture scale height; Figure 2-17, on the other hand, shows a similar comparison for a high-moisture, hazy day. Figure 2-16 shows practically no difference in the transmittance generated by either method for low-moisture days. A slightly larger but still small difference in transmittance across the spectrum is evident in Figure 2-17 for high-moisture days. Because these differences are small, it was concluded that the model can be used successfully in either the T550 or the meteorological mode.

To make the relationship between relative humidity, temperature, and T550 easier to understand, Figure 2-18 was prepared by operating the program over a large range of parameter values. In the figure, lines of constant T550 were interpolated to show the trade-offs in selection of temperature and relative humidity.

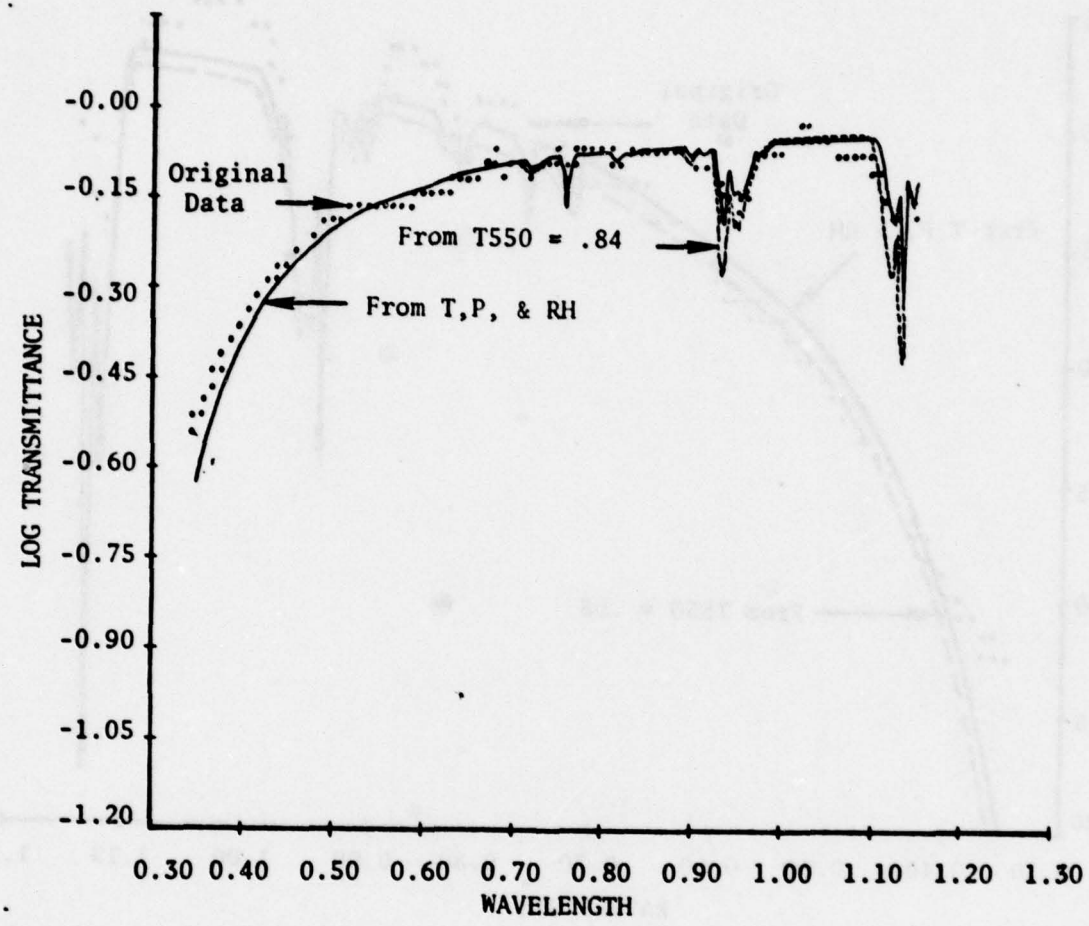

Figure 2-16. Comparison of T550 and Meterologically Generated Spectral Log Transmittance for a Low-Moisture Day

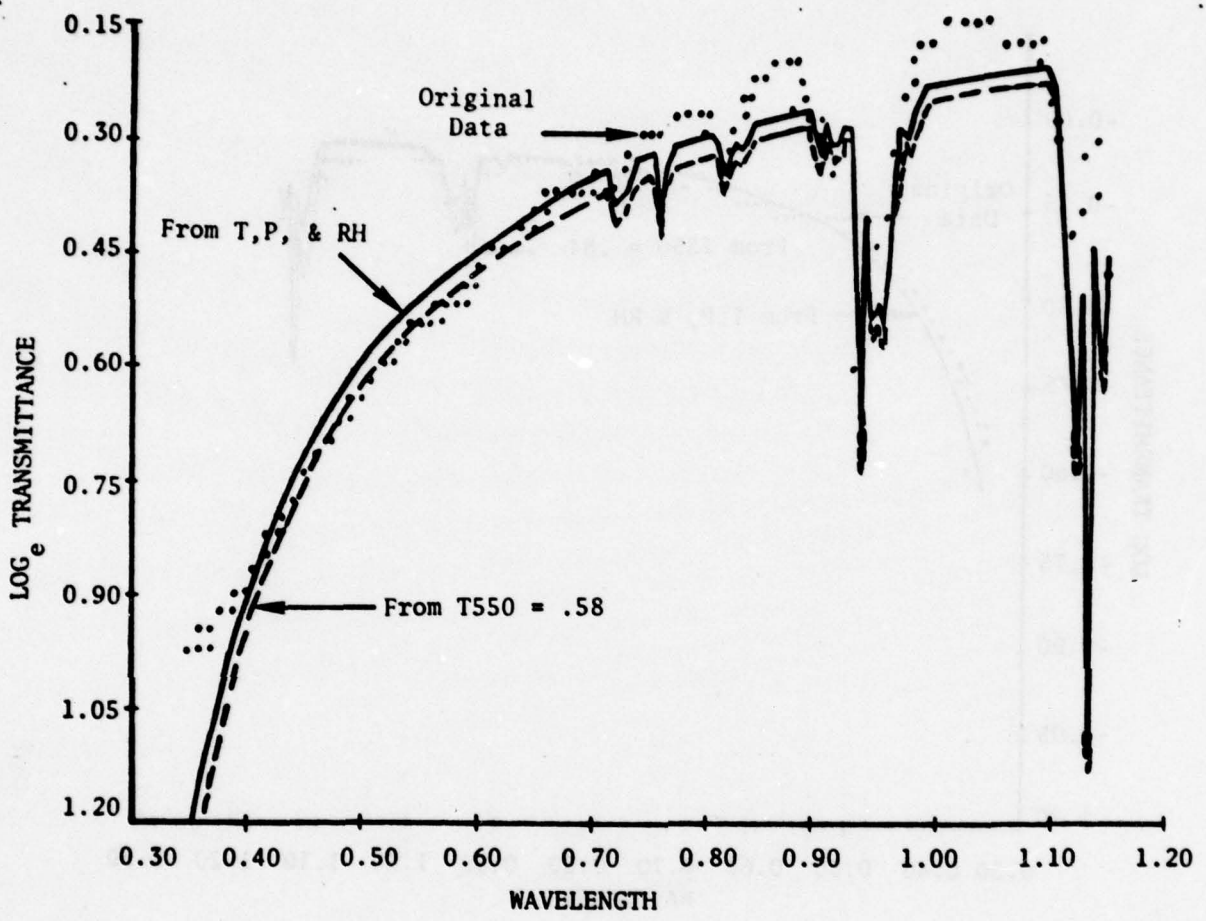

Figure 2-17. Comparison of T550 and Meterologically Generated Spectral Log Transmittance for a High-Moisture Day

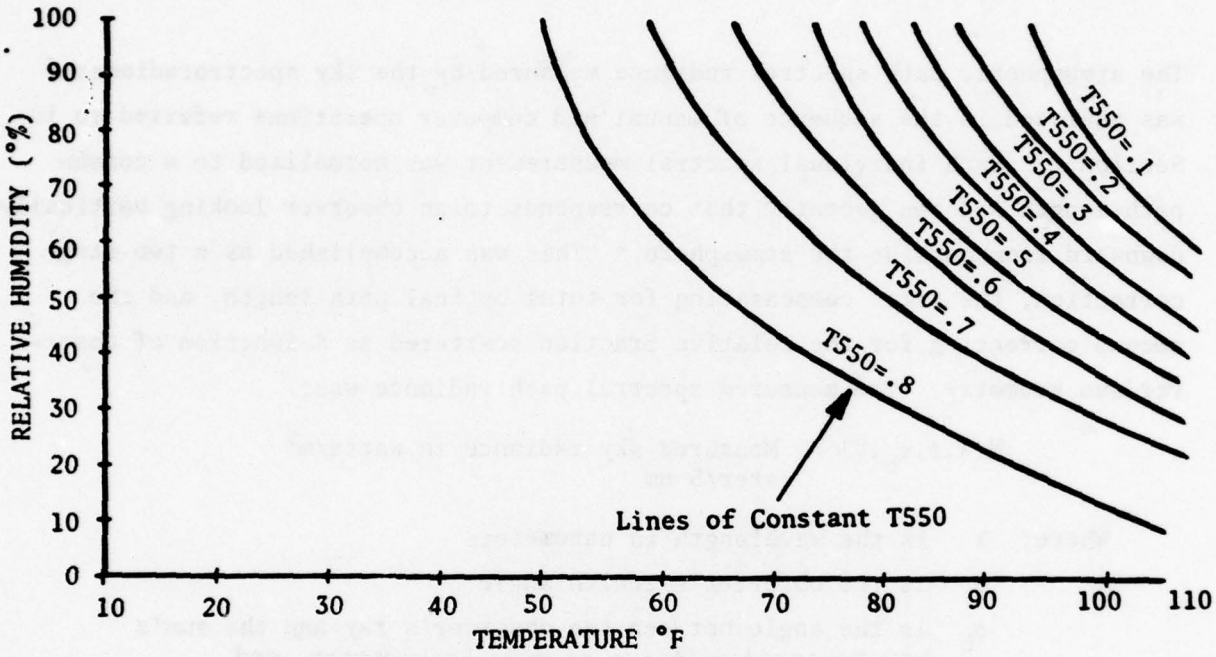

Figure 2-18. The Relationship Between Surface Meteorology and T550

SECTION 3

ANALYSIS AND MODELING OF THE ATMOSPHERIC PATH RADIANCE

3.1 NORMALIZATION OF MEASURED DATA

The atmospheric path spectral radiance measured by the sky spectroradiometer was analyzed in the sequence of manual and computer operations referred to in Section 1. Each individual spectral measurement was normalized to a common path-length and the geometry that corresponds to an observer looking vertically downward from outside the atmosphere.* This was accomplished as a two-stage correction, the first compensating for total optical path length, and the second correcting for the relative fraction scattered as a function of observer/sun geometry. The measured spectral path radiance was:

$N(\lambda,\phi,\phi_b,\theta)$ = Measured sky radiance in watts/m^2 ster/5 nm

Where: λ is the wavelength in nanometers

ϕ is the observer's zenith angle

ϕ_b is the angle between the observer's ray and the sun's ray measured relative to pure backscatter, and

θ is the solar zenith angle (90° minus solar altitude).

The sky spectroradiometer telescope was always pointed at a specific point in the sky, the azimuth (AZ) and elevation (EL) of which maintained a precise relationship to the sun's position as discussed by Edgerton.[16] For positions above and below 35° solar altitude, the relationship was different and resulted in the following equations:

$$\text{Measurement angle } \phi = \begin{cases} 180°-2\theta;\ 55° \leq \theta \leq 90° \\ 90°-\theta;\ \theta \leq 55° \end{cases} \qquad \text{Equation 3-1}$$

---

* Another correction was required at extreme low solar altitudes to compensate for the non-instantaneous nature of the spectral radiometric measurements referred to in Appendix E.

[16] C.F. Edgerton, Relationship Between Meteorological Conditions and Optical Properties of the Atmosphere, U. of Cal. Scripps Inst. of Oceonography and Visibility Lab, May 1967.

$$\text{Measurement angle } \phi_b = \begin{cases} \theta \ ; \ 55^\circ \leq \theta \leq 90^\circ \\ 90^\circ \ ; \ \theta < 55^\circ \end{cases} \qquad \text{Equation 3-2}$$

Measurement azimuth AZ = 180° - Solar Azimuth

The above restrictions in collection geometry significantly simplified normalization of the spectral sky radiance data by eliminating the requirement for scatter-angle correction for most of the measurements. Figure 3-1 shows the geometry used to normalize measurements to the vertical look.

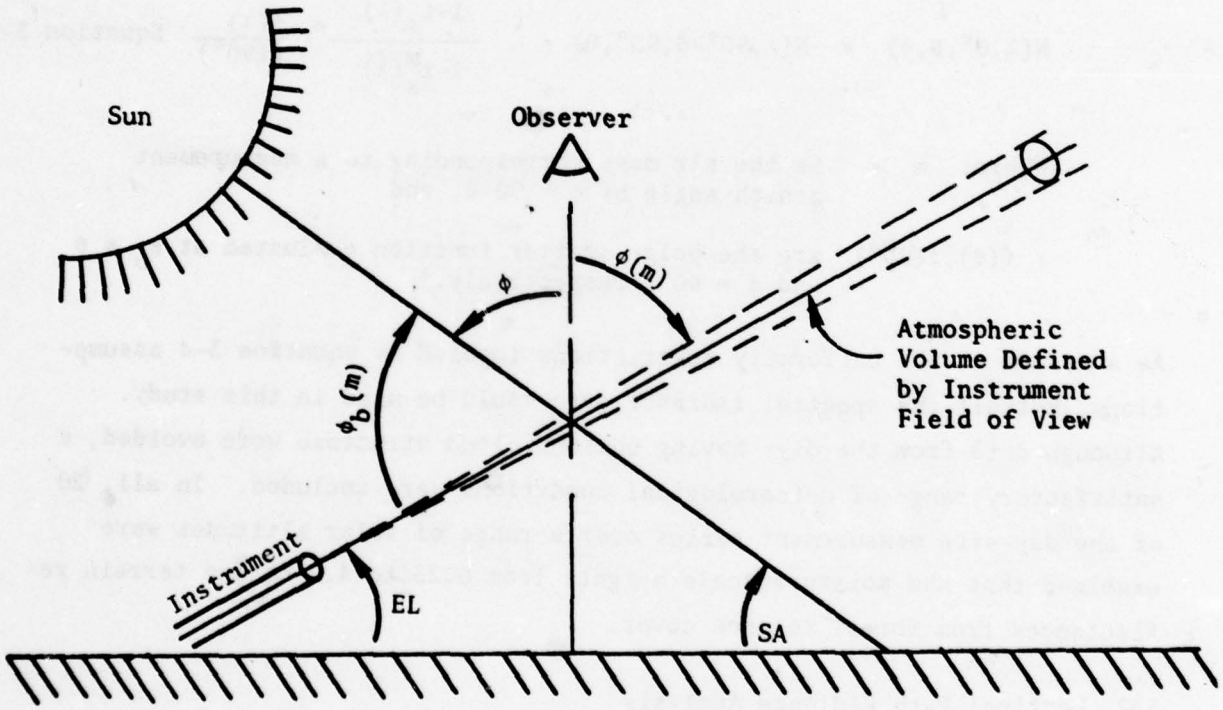

Figure 3-1. Measurement of Sky Radiance
(Sun's and Observer's Rays are Coplanar)

The two equations of normalization are shown below. For solar zenith angles between 55° and 90°:

$$N(\lambda,0°,\theta,\theta) = N(\lambda, 180°-2\theta,\theta,\theta) \cdot \left(\frac{1-t_s(\lambda)}{1-t_s^m(\lambda)} \right) \quad \text{Equation 3-3}$$

Where: $t_s(\lambda)$ is the vertical atmospheric path transmittance due to scattering, and

m is the air mass corresponding to a measurement zenith angle of $\phi = 180-2\theta$

For solar zenith angles less than 55°:

$$N(\lambda,0°,\theta,\theta) = N(\lambda,90°-\theta,90°,\theta) \cdot \frac{1-t_s(\lambda)}{1-t_s^m(\lambda)} \cdot \frac{f(\lambda)}{f(90°)} \quad \text{Equation 3-4}$$

Where: m is the air mass corresponding to a measurement zenith angle of $\phi = 90-\theta$, and

$f(\theta), f(90°)$ are the polar scatter function evaluated at $\phi_b = \theta$ and $\phi = 90°$, respectively.*

As a result of the uniformity restrictions imposed by Equation 3-4 assumptions, not all the spectral radiance data could be used in this study. Although data from the days having obvious cloud structure were avoided, a satisfactory range of meteorological conditions were included. In all, 20 of the day-site measurement series over a range of solar altitudes were examined that had moisture scale heights from 0.23 to 4.2 cm and terrain reflectances from forest to snow cover.

3.2 Vertical Path Radiance Analysis

As is shown in Equations 3-3 and 3-4, once the path radiance was normalized, it was strictly a function of wavelength and solar zenith angle, θ. Normalization of these data in turn by the extraterrestrial irradiance and vertical

* For the derivation of the polar scatter function, see Section 5 of this report.

path absorption transmittance permitted the examination of vertical path radiance as a function of the total fraction scattered, as estimated by $1 - t_s(\lambda)$. The mathematical model below for path radiance was hypothesized and then regressed against all available spectral vertical path radiance data.

$$N(\lambda,\theta) = b_1 H_{sc}(\lambda)\left[1-t_s(\lambda)\right]^{b_2} t_a(\lambda) \qquad \text{Equation 3-5}$$

Where: $H_{sc}(\lambda)$ is the spectral extraterrestrial irradiance in watts/m^2,

$t_s(\lambda), t_a(\lambda)$ is the vertical path transmittance due to scattering and absorption, and

b_1, b_2 are regression-determined parameters.

Dividing Equations 3-5 through by the solar constant, $H_{sc}(\lambda)$, and the absorption transmittance, $t_a(\lambda)$, creates a normalized radiance variable as a function of soatter fraction.

$$\frac{N(\lambda,\theta)}{H_{sc}(\lambda)\, t_a(\lambda)} = b_1\left[1 - t_s(\lambda)\right]^{b_2} \qquad \text{Equation 3-6}$$

3.2.1 The Shape Parameter, b_2

Through study of the log of Equation 3-6, the relationship of the shape parameter b_2 to solar altitude and/or moisture scale height was determined. A typical example of this relationship is solar altitude shown in Figures 3-2 and 3-3. On the basis of examination of all data, a two-piece linear model was fitted to these data as shown in Figures 3-2 and 3-3. In addition, a slight correlation was apparent with moisture scale height as can be seen in Figures 3-4 and 3-5, and the equations were modified to incorporate this minor effect. The resulting equation used to compute the shape parameter was:

$$b_2 \text{ (shape parameter)} = 1.037 + .015\,SA + .0030\,SA\,(MSH - 1.0) \qquad \text{Equation 3-7}$$

Where: SA = Solar Altitude (°) $= \begin{cases} SA, & SA \le 40° \\ 40°, & SA > 40° \end{cases}$ and

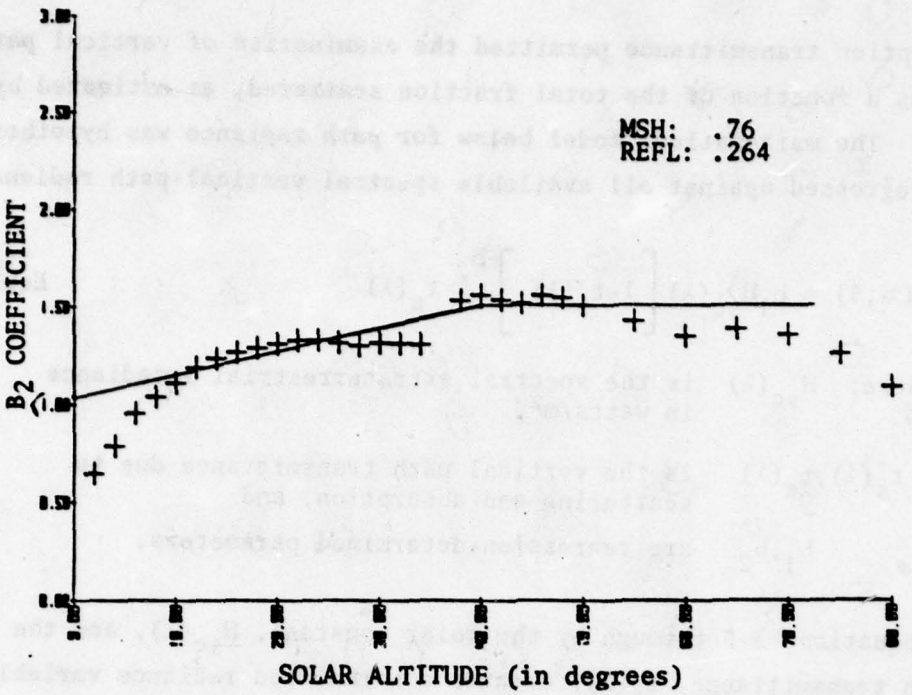

Figure 3-2. B_2 Coefficient as a Function of Solar Altitude for June 11, 1976 Data

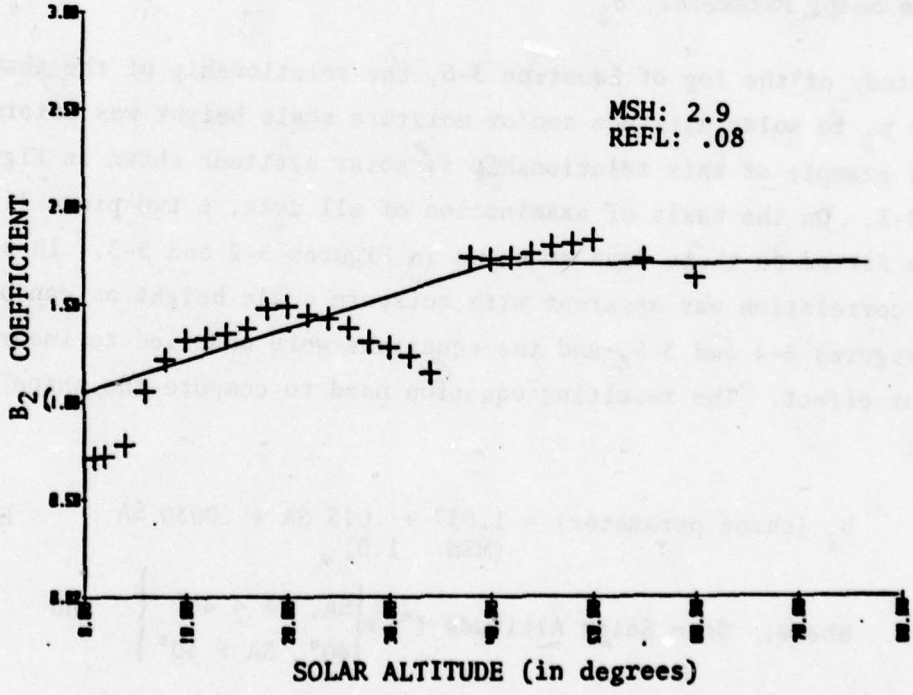

Figure 3-3. B_2 Coefficient as a Function of Solar Altitude for August 11, 1976 Data

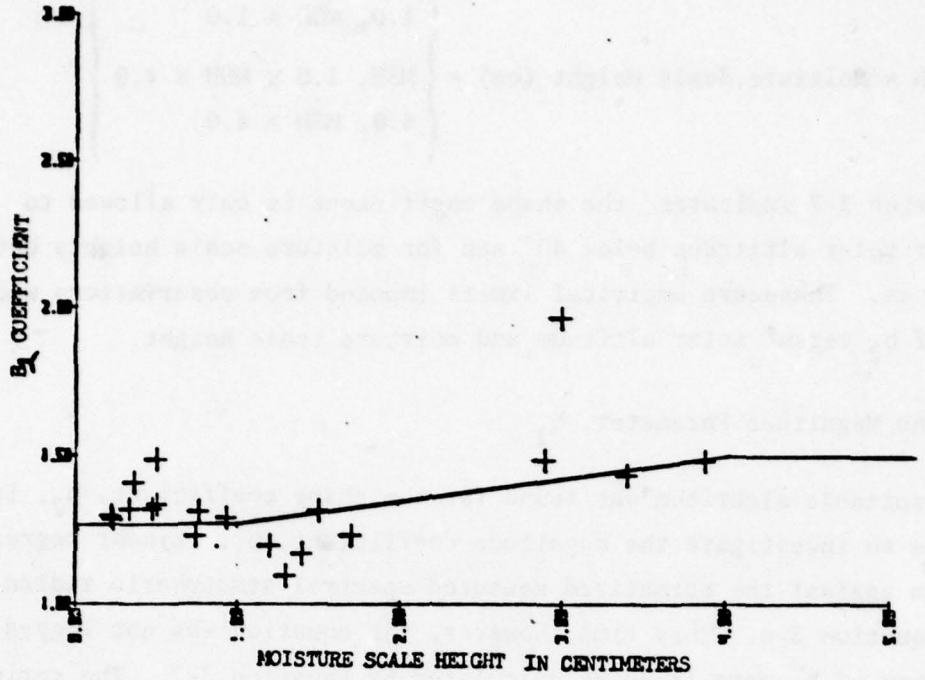

Figure 3-4. B_2 Coefficient As a Function of Moisture Scale Height for All Day-Site Data (SA = 20°)

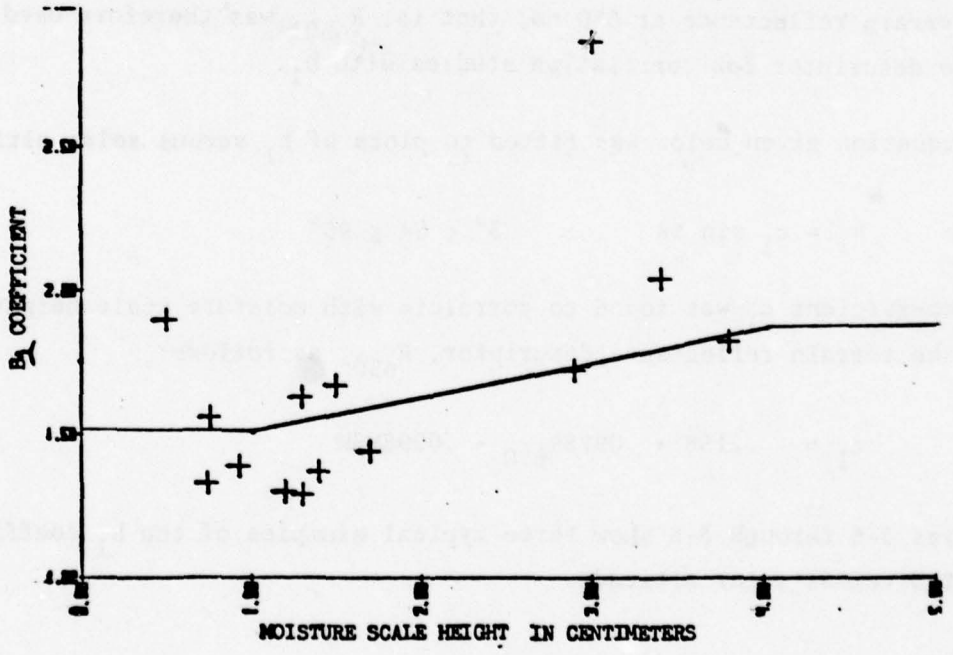

Figure 3-5. B_2 Coefficient As a Function of Moisture Scale Height for All Day-Site Data (SA = 40°)

$$\text{MSH} = \text{Moisture Scale Height (cm)} = \left\{ \begin{array}{l} 1.0, \text{ MSH} < 1.0 \\ \text{MSH}, \ 1.0 \leq \text{MSH} \leq 4.0 \\ 4.0, \text{ MSH} > 4.0 \end{array} \right\}$$

As Equation 3-7 indicates, the shape coefficient is only allowed to vary for solar altitudes below 40° and for moisture scale heights between 1 and 4 cm. These are empirical limits imposed from observations made from plots of b_2 versus solar altitude and moisture scale height.

3.2.2 The Magnitude Parameter, b_1

Once a suitable algorithm was found for the shape coefficient, b_2, it was possible to investigate the magnitude coefficient, b_1. Linear regressions were run against the normalized measured spectral atmospheric radiance data using Equation 3-6. This time, however, the equation was not logged and the values of b_2 were fixed as calculated by Equation 3-7. The series of scalars, b_1, developed for the normalized data for each day were then studied as functions of solar altitude, moisture scale height, and terrain reflectance. No spectral shaping could be observed in the normalized path radiance data that could be correlated to terrain spectral reflectance. The terrain reflectance at 650 nm; that is, R_{650}, was therefore used as a single descriptor for correlation studies with b_1.

The equation given below was fitted to plots of b_1 versus solar altitude:

$$b_1 = c_1 \sin \text{SA} \qquad 3° \leq \text{SA} \leq 90° \qquad \text{Equation 3-8}$$

The coefficient c_1 was found to correlate with moisture scale height, MSH, and the terrain reflectance descriptor, R_{650}, as follows:

$$c_1 = .2158 + .0978R_{650} - .0298\text{MSH} \qquad \text{Equation 3-9}$$

Figures 3-6 through 3-8 show three typical examples of the b_1 coefficient plotted versus solar altitude.

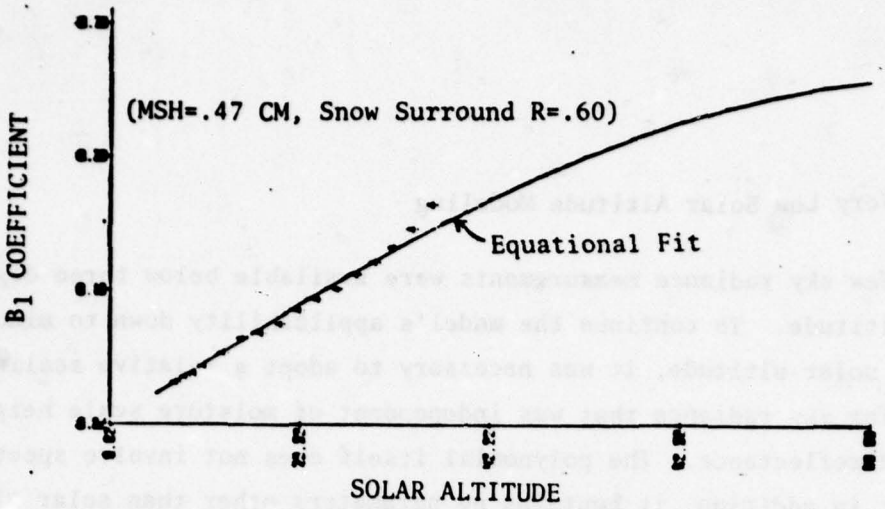

Figure 3-6. Dependence of the B_1 Coefficient for Feb 24, 1976

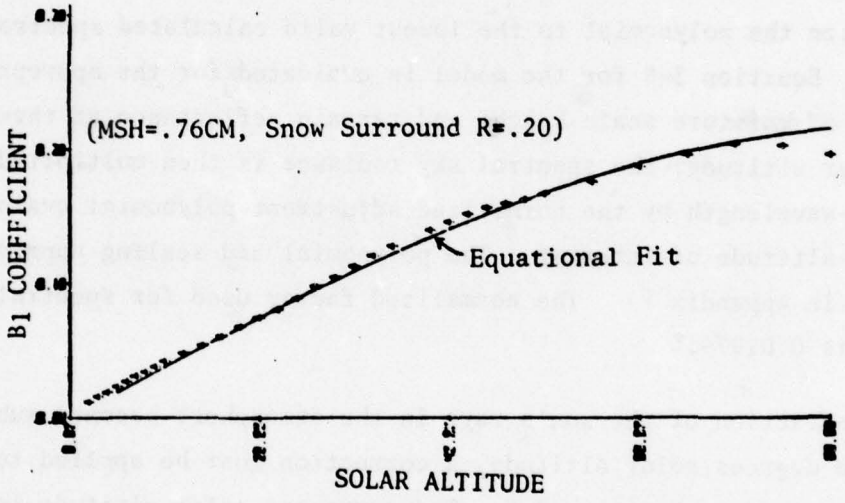

Figure 3-7. Dependence of the B_1 Coefficient for Jan 11, 1976

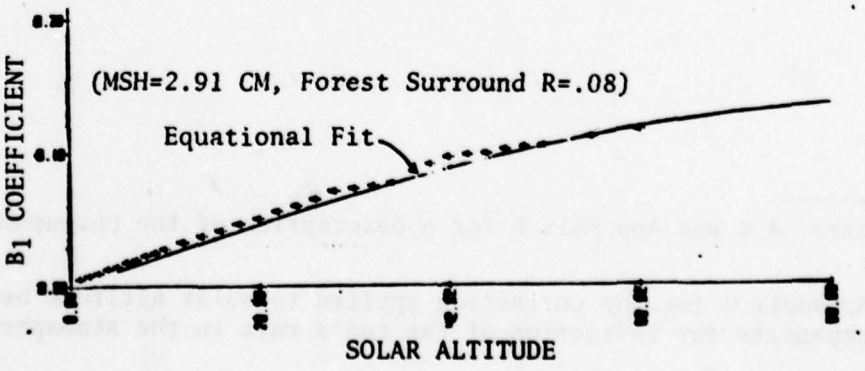

Figure 3-8. Dependence of the B_1 Coefficient for Aug 11, 1976

3.2.3 Very Low Solar Altitude Modeling

Only a few sky radiance measurements were available below three degrees solar altitude. To continue the model's applicability down to minus five degrees solar altitude, it was necessary to adopt a relative scaling polynomial for sky radiance that was independent of moisture scale height or surround reflectance. The polynomial itself does not involve spectral shaping; in addition, it contains no parameters other than solar altitude and is used strictly as a relative magnitude adjustment for the sky radiance term. The adjustment polynomial P(SA)* had been evaluated at three degrees solar altitude, and this value was divided into the coefficients to normalize the polynomial to the lowest valid calculated spectral sky radiance. Equation 3-5 for the model is evaluated for the appropriate condition of moisture scale height and terrain reflectance at three degrees solar altitude; the spectral sky radiance is then multiplied wavelength-by-wavelength by the normalized adjustment polynomial evaluated at the solar altitude of interest. The polynomial and scaling approach are explained in Appendix F. The normalized factor used for spectral sky radiance is 0.01975.

Because refraction of the sun's rays in the atmosphere becomes substantial below five degrees solar altitude, a correction must be applied to solar altitude as used in Equation 3-8. The corrected solar altitude is referred to as the "apparent" solar altitude and is described mathematically in Appendix G.**

---

* See para. 4.4 and Appendix F for a description of the polynomial p(SA).

** See Appendix G for the correction applied to solar altitude below 5° to compensate for refraction of the sun's rays in the atmosphere.

3.3 ATMOSPHERIC PATH RADIANCE MODEL IN SCAT3

Starting with the three parameters solar altitude, moisture scale height, and the terrain reflectance at 650 nm, the vertical atmospheric path radiance can be computed as follows from Equation 3-5 if the scattering and absorption transmittance ts(λ) and ta(λ) are first computed using the equations discussed in Section 2 of this report.

$$N(\lambda,0°,\theta,\theta) = b_1 H_{sc}(\lambda)\ [1 - t_s(\lambda)]^{b_2}\ t_a(\lambda) \qquad \text{Equation 3-10}$$

Where θ is 90° minus the solar altitude.

Scaling for the path length and relative angle from back scatter results in the following general expression for any path through the atmosphere:

$$N(\lambda,\phi,\phi_b,\theta) = K_s \cdot b_1(\theta,MSH,R_{650}) \cdot H_{sc}(\lambda) \cdot [1 - t_s(\lambda)]^{b_2(\theta,MSH)} \cdot t_a(\lambda) \cdot \frac{1 - t_s^{m(\phi)}(\lambda)}{1 - t_s(\lambda)} \cdot \frac{f(\phi,\lambda)}{f(\phi_b,\lambda)} \qquad \text{Equation 3-11}$$

Where:

- λ is the wavelength in nanometers
- θ is the solar zenith angle
- ϕ is the observer's zenith angle
- ϕ_b is the relative angle between direct backscatter and the observer's line-of-sight
- MSH is the moisture scale height in cm
- $M(\phi)$ is air mass corresponding to the observer's zenith angle
- $f(\phi,\lambda)$ is the polar scatter function evaluated at the observer's zenith angle
- $f(\phi_b,\lambda)$ is the polar scatter function evaluated at the relative angle from backscatter, and
- K_s is 1.0 when SA>3°, or is p(SA) when SK<3°.

3.4 ANALYSIS OF THE VOLUMETRIC SCATTERING FUNCTION, $f(\phi,\lambda)$*

3.4.1 Data Base

An estimate of the volumetric scattering function (the relative intensity of scattered light as a function of the angle around a volume of atmosphere illuminated by a collimated source) was sought that could be made to vary spectrally and according to atmospheric optical conditions. For this purpose, sky spectral radiance measurements were made during the data collection program in 15-degree increments of azimuth between 0 and 360 degrees, and at an elevation of 7 degrees above the horizon**. Although the complete hemisphere of downward radiance was actually mapped at 15-degree increments of elevation from 7 degrees to 83 degrees above the horizon, only the 7 degree ring was used in this analysis because this elevation ring measured nearest the true profile of the scattering function when the sun was near the horizon.The data base was also culled by eliminating all measurements made above 10 degrees solar altitude. The spectral dependence was evaluated by making measurements at the following three wavelengths: 450 nanometers, 650 nanometers, and 850 nanometers.

Because the measurements were made over a finite time and from the ground looking out toward space, corrections had to be applied to the measurements to convert them into equivalent, instantaneous, gonioradiometric measurements of an equivalent volume of atmosphere. The method of correcting the data and its subsequent reduction to equational form is the subject of this section and Appendix H of this volume.

3.4.2 Time Correction

At the same time data was being collected by the sky radiometer at different instrument azimuths and elevations, data was collected for horizontal sky irradiance by one of the two irradiometers. Since this irradiometer was oriented in the same position for all readings and at the same wavelength as

---

* See para. 3.3 for explanation of the use of this function.

** See Section 3, Vol 2 for an explanation of the polar scattering measurements.

the sky radiometer, any changes in this measurement were changes corresponding to changes in sky conditions. The simultaneous sky irradiance data, taken at a specific azimuth, were divided into the sky irradiance data corresponding to the time of the sky radiometer direct backscatter measurements made at zero degrees azimuth from the sun. This fraction was then multiplied by the sky radiance at the corresponding azimuth to give the following time-corrected radiance.

$$N'(AZ) = N(AZ) \cdot \frac{H(0)}{H(AZ)}$$

Where: $N'(AZ)$ is the time-corrected sky radiance at azimuth angle AZ

$N(AZ)$ is the sky radiance at angle AZ before time correction.

$H(0)$ is the sky irradiance data recorded at the same time as the sky radiance for pure backscatter, made at zero degrees azimuth from the sun.

$H(AZ)$ is the sky irradiance data recorded at the same time as the sky radiance at angle AZ, and

AZ is the instrument azimuth angle measured relative to the solar azimuth (zero degrees is directly away from sun).

3.4.3 Path Length Correction

As stated above, only solar altitude data less than 10 degrees and at a 7-degree instrument elevation were chosen for use. In the 15-degree azimuth increments, there are 24 points in the 7 degree ring, each of which is illuminated differently, due to its atmospheric path length relative to the sun. Since the atmosphere absorbs and scatters a fraction of the incident light, the longer the path the light must travel, the smaller the amount of light that reaches a particular point. The amount of light reaching its destination depends on the length of the path that the light must travel and the extinction coefficient that determines the amount of light the atmosphere absorbs or scatters.

Similarly, the total energy reaching the sky radiometer is the integration of scattering gains and losses along the path toward the radiometer and along its line of sight. The double integration, sun-to-volume and volume-to-radiometer, was digitally approximated using a Hewlett-Packard 9830 program, the arguments for which were the measurement's starting solar geometry and the vertical air-path transmittance as determined from the day-site measurements.* In the program, an azimuth-angle-dependent correction was computed that was applied to the sky radiometer measurements. Details about the deviation of this correction are discussed in Appendix H of this volume.

Correction of the path length was made relative to the solar azimuth, as was the time correction. Twenty-four correction values were computed and divided into the value for the azimuth that corresponded to backscatter. These in turn were multiplied by the data already corrected for time as indicated in the equation above, resulting in the following:

$$N''(AZ) = N'(AZ) \cdot \frac{PL(0)}{PL(AZ)} \qquad \text{Equation 3-12}$$

Where: $N''(AZ)$ is the path-length and time-corrected sky radiance at azimuth angle AZ

$N'(AZ)$ is the sky radiance at azimuth angle AZ before path length correction

$PL(0)$ is the relative amount of light reaching the observer at the azimuth, corresponding to backscatter

$PL(AZ)$ is the relative amount of light reaching the observer at azimuth AZ, and

AZ is the instrument azimuth angle relative to solar azimuth (defined as zero when it is directly away from the sun).

3.4.4 Equational Form of Scattering Function

After the data were corrected for path length and time, the azimuth dependent radiance data were normalized by the data point nearest to pure

* See Section 2 of this volume, where normalization of this measurement is discussed.

backscatter and the relative azimuth was redefined as the angle from backscatter, ϕ. The model, fitted to this normalized data was:

$$f(\phi) = A_0 + A_1(1 + \cos^2\phi) + A_2 \cos^2 \frac{3\phi}{2} + A_3 e^{-3(\phi-\pi)^2} \qquad \text{Equation 3-13}$$

where A_0, A_1, A_2, A_3 are the weighting coefficients.

The terms of this equation were arrived at by examination of the normalized polar scatter function measurements. It involved adding the classical Rayleigh term to an empirical approximation of the aggregate scatter profile of atmospheric particles on the range of Mie theory sizes.

The data for each of the three wavelengths was analyzed separately for the four coefficients. Data points within 7 degrees of the point 180 degrees from backscatter, where the instrument is pointed directly toward the sun, were eliminated because of the influence of direct sunlight on the instrument measurement.

For each data set, the four coefficients (A_0, A_1, A_2, A_3) were found by use of nonlinear regression routines. For each wavelength, the coefficients were further analyzed as functions of moisture scale height and the A_1 coefficient. The wavelength dependency was then incorporated by finding the coefficients for the moisture scale height and the A_{0-3} terms as log-linear fits to the 450-nanometer, 650-nanometer, and 850-nanometer wavelength measurements. The final equations for computing the A_0, A_1, A_2, and A_3 coefficients of Equation 3-13 were:

$$A_0 = 0.765 - 1.412A_1 \qquad \text{Equation 3-14}$$

$$A_1 = 0.947e^{-2.13\lambda} - (0.258 + 0.243 \log_{10}\lambda)\ \text{MSH} \qquad \text{Equation 3-15}$$

$$A_2 = 0.288 - 0.813A_1\text{, and} \qquad \text{Equation 3-16}$$

$$A_3 = 8.083 + 7.076 \log_{10}\lambda - (10.37 + 7.836 \log_{10}\lambda) A_1 \qquad \text{Equation 3-17}$$

where λ is the wavelength in nanometers and MSH is the moisture scale height in centimeters.

3.4.5 Volumetric Normalization

The function in Equation 3-13 was then volumetrically normalized to correspond with the definition of the scattering extinction coefficient. To accomplish this, it was necessary to find the scattering volume by integrating the scattering profile over all solid angles:

$$\int_{\Omega} f(\phi)\, d\Omega = \int_0^{2\pi}\int_0^{\pi} f(\phi)\, \sin\phi\, d\phi\, d\theta \qquad \text{Equation 3-18}$$

Where: ϕ is the angle from backscatter in the plane of the sun's rays and

θ is the angle of rotation about the sun's ray.

Substitution of Equation 3-13 into Equation 3-18 results in the following equation:

$$\int_{\Omega} f(\phi)\, d\Omega = 4\pi A_0 \int_0^{\pi/2} \sin\phi\, d\phi + 4\pi A_1 \int_0^{\pi/2} (1 + \cos^2\phi) \sin\phi\, d\phi$$

$$+ 4\pi A_2 \int_0^{\pi/3} \cos^2\left(\frac{3\phi}{2}\right) \sin\phi\, d\phi \qquad \text{Equation 3-19}$$

$$+ 4\pi A_3 \int_0^{\pi} e^{-3(\phi-\pi)^2} \sin\phi\, d\phi$$

Because the terms of Equation 3-19 could not all be solved in closed form, numerical integration techniques were used. The resulting integral was a function of the coefficients $A_{0,1,2,3}$*.

$$\int_{\Omega} f(\phi)d\Omega = 4\pi A_0 + 5.33\pi A_1 + .938\pi A_2 + .315\pi A_3 \qquad \text{Equation 3-20}$$

Dividing Equation 3-13 through by the normalizing integral of Equation 3-20 results in polor scatter function** that was coded into the program SCAT3, as follows:

$$\int_{\Omega} f(\phi) = B_0 + B_1(1 + \cos^2\phi) + B_2\cos^2\left(\frac{3\phi}{2}\right) + B_3 e^{-3(\phi-\pi)^2} \qquad \text{Equation 3-21}$$

Where: $B_0 = \frac{1}{4\pi}\left(1 + 1.333\,\frac{A_1}{A_0} + .235\,\frac{A_2}{A_0} + .079\,\frac{A_3}{A_0}\right)^{-1}$

$B_1 = \frac{1}{4\pi}\left(\frac{A_0}{A_1} + 1.333 + .235\,\frac{A_2}{A_1} + .079\,\frac{A_3}{A_1}\right)^{-1}$

$B_2 = \frac{1}{4\pi}\left(\frac{A_0}{A_2} + 1.333\,\frac{A_1}{A_2} + .235 + .079\,\frac{A_3}{A_2}\right)^{-1}$

$B_3 = \frac{1}{4\pi}\left(\frac{A_0}{A_3} + 1.333\,\frac{A_1}{A_3} + .235\,\frac{A_2}{A_3} + .079\right)^{-1}$, and

A_0, A_1, A_2, and A_3 are computed from Equations 3-14 through 3-17.

Equation 3-21 is useful because it always integrates, over all solid angles, to a unit volume regardless of the estimates of A_0, A_1, A_2, and A_3.

* The A_1 coefficient is exactly equal to the $\frac{16}{3}\pi$ integral for pure Rayleigh scatter.

** Definition of this function was also necessary in the analysis of atmospheric path spectral radiance as discussed above in para. 3.1.

3.4.6 Examples of Scatter Function Fit to Data

Figure 3-9 shows typical examples of the model expressed in Equation 3-21, fitted to typical examples of the original polar scatter data corrected for time and path length.

3.5 SCAT3 MODEL FITTED TO MEASURED DATA

Equation 3-12 was used to generate spectral atmospheric path radiance functions corresponding to specific measurements on days typical of the collection program. The actual measured data and the model fit are shown in Appendix C, Figures C-1 through C-29.

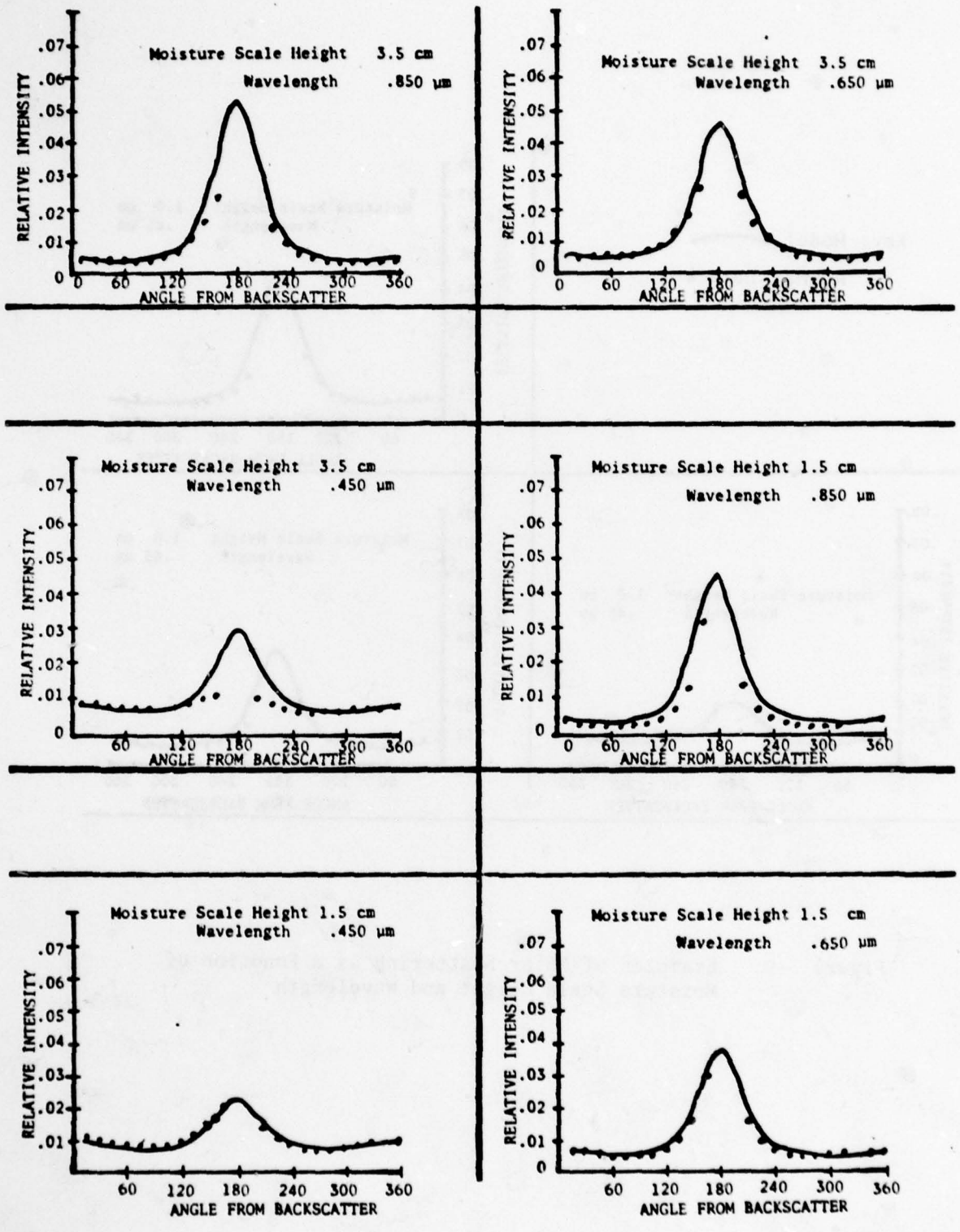
Moisture Scale Height 3.5 cm
Wavelength .850 µm
RELATIVE INTENSITY
ANGLE FROM BACKSCATTER
Moisture Scale Height 3.5 cm
Wavelength .650 µm
Moisture Scale Height 3.5 cm
Wavelength .450 µm
Moisture Scale Height 1.5 cm
Wavelength .850 µm
Moisture Scale Height 1.5 cm
Wavelength .450 µm
Moisture Scale Height 1.5 cm
Wavelength .650 µm

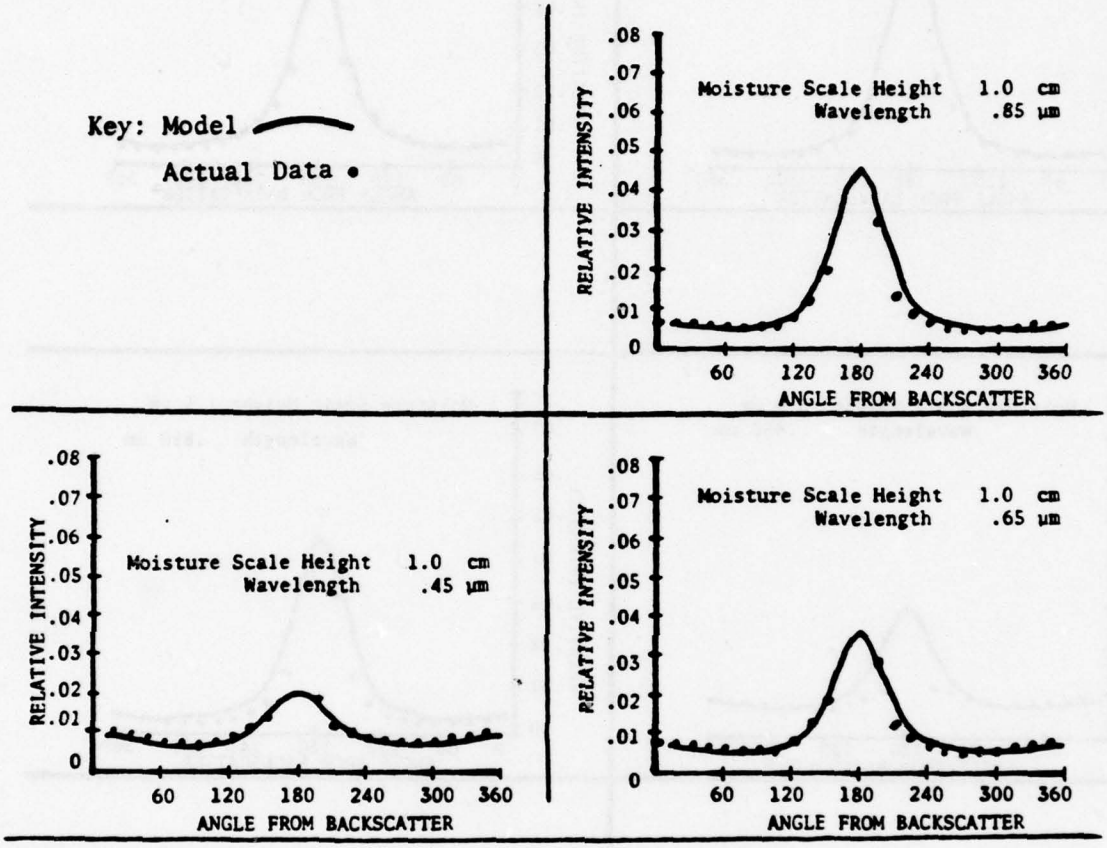

Figure 3-9. Examples of Polar Scattering as a Function of Moisture Scale Height and Wavelength

SECTION 4

ANALYSIS AND MODELING OF HORIZONTAL DAYLIGHT IRRADIANCE

4.1 APPROACH

The total irradiance incident upon a horizontal surface can be considered to be the sum of three distinct irradiance forms: (1) direct solar irradiation, (2) indirect atmospheric downward scatter, and (3) indirect reflected irradiance from the earth's surface rescattered downward by the atmosphere. To create the spectral model described below, each individual horizontal daylight irradiance measurement made by the radiometric trailer was separated into these three components. The coefficients derived from regressing the model against each individual spectral sample were studied as functions of measurable parameters such as solar altitude and moisture scale height. Figure 4-1 illustrates the three-component model.

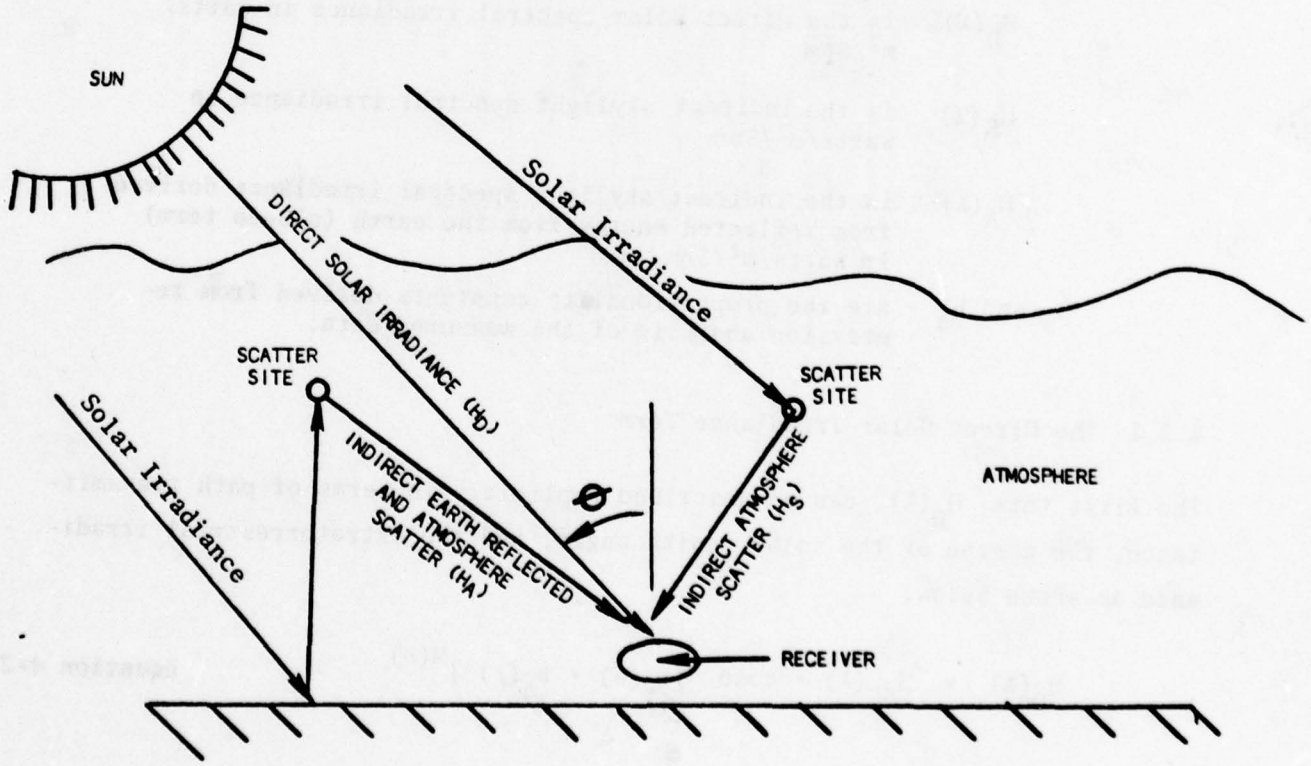

Figure 4-1. Model Used for Horizontal Daylight Irradiance

In preparing the data set for analysis, only those day-sites having estimates of the spectral transmittance parameter (see Section 2 of this volume) were used. This eliminated most of the days having obvious cloud structure and permitted the analysis to be devoted to modeling of uniform but optically varying cloud-free atmospheric conditions. Data from days having cloud cover observable from the ground were only included if there was no indication of sun obscuration.

4.2 REGRESSION ANALYSIS

Expressed mathematically, the component sum equivalent to total horizontal daylight irradiance according to Robinson[17] is:

$$H_{DH}(\lambda) = H_D(\lambda) + b_s H_S(\lambda) + b_a H_A(\lambda) \qquad \text{Equation 4-1}$$

Where: $H_{DH}(\lambda)$ is the total measured horizontal daylight spectral irradiance in watts/m^2/5nm

$H_D(\lambda)$ is the direct solar spectral irradiance in watts/m^2/5nm

$H_S(\lambda)$ is the indirect skylight spectral irradiance in watts/m^2/5nm

$H_A(\lambda)$ is the indirect skylight spectral irradiance derived from reflected energy from the earth (albedo term) in watts/m^2/5nm, and

b_s and b_a are the proportionality constants derived from regression analysis of the measured data.

4.2.1 The Direct Solar Irradiance Term

The first term, $H_D(\lambda)$, can be described explicitly in terms of path transmittance, the cosine of the solar zenith angle, and the extraterrestrial irradiance as shown below.

$$H_D(\lambda) = H_{SC}(\lambda) \cdot \cos\theta \ [t_s(\lambda) \cdot t_a(\lambda)]^{M(\theta)} \qquad \text{Equation 4-2}$$

---

[17] N. Robinson, Solar Radiation, Solar Physics Laboratory, Haifa, Israel, 1966, pp 118-120.

Where: $H_{SC}(\lambda)$ is the extraterrestrial spectral irradiance (solar constant) in watts/m^2/5 nm

θ is the solar zenith angle

$t_s(\lambda)$ is the vertical spectral transmittance due to scattering phenomena

$t_a(\lambda)$ is the vertical spectral transmittance due to absorption phenomena, and

$M(\theta)$ is the air mass corresponding to zenith angle θ.

4.2.2 The Indirect Skylight Irradiance Term

The definitions of the second two terms of Equation 4-1, $H_S(\lambda)$ and $H_A(\lambda)$, are less easy to derive because they involve the integration of the non-uniform downward sky hemisphere irradiance, and in the case of $H_A(\lambda)$, the non-uniform surround reflectance of the terrain. The equational forms chosen for use in the model were:

$$H_S(\lambda) = H_{SC}(\lambda) \cdot \cos\theta \quad [1 - t_s^{M(\theta)}(\lambda)] \cdot t_a(\lambda) \qquad \text{Equation 4-3}$$

and

$$H_A(\lambda) = H_{SC}(\lambda) \cdot \cos \quad [t_a(\lambda) \cdot t_s(\lambda)]^{M(\lambda)} R(\lambda) \cdot \qquad \text{Equation 4-4}$$

$$[1 - t_s(\lambda)] \cdot t_a(\lambda)$$

where $R(\lambda)$ is the spectral reflectance of the general surround terrain.*

Substituting Equations 4-2, 4-3, and 4-4 into Equation 4-1, dividing through by common terms, and subtracting 1.0 from both sides results in:

---

* See Volume 2, Section 5.1 of this report for the derivation of these reflectance data.

$$\frac{H_{DH}(\lambda)}{H_{SC}(\lambda) \cdot \cos\theta \, [t_s(\lambda)t_a(\lambda)]^{m(\theta)}} - 1 = b_s \frac{[1-t_s(\lambda)]^{m(\theta)} t_a(\theta)}{[t_a(\lambda)t_s(\lambda)]^{m(\theta)}}$$

Equation 4-5

$$+ b_a R(\lambda) \, [1-t_s(\lambda)] \, t_a(\lambda)$$

Examination of the measured spectral irradiance data showed that the terrain term did not noticeably affect the irradiance data except under extreme conditions of snow cover. By disregarding the day-site measurements where snow was present, the b_s coefficient was found by linear regression techniques for all other spectral samples. The spectral transmittance values $t_s(\lambda)$ and $t_a(\lambda)$ were derived from the scattering and absorption coefficients estimated for each day of measurement*.

Within the random error of estimation, the daily plots of b_s versus solar altitude could be estimated from linear equations. Figure 4-2 shows two typical examples of the b_s coefficient versus solar altitude. The slope and intercept of the daily plots of b_s were regressed against moisture scale height and found to correlate. Figures 4-3 and 4-4 show the slope and intercept terms versus moisture scale height and fitted with the regression equations. The complete equation for the indirect skylight irradiance coefficient b_s in terms of solar altitude and moisture scale height is:

$$b_s = .387 - .0131MSH - (.00392 - .00221MSH) \, SA \qquad \text{Equation 4-6}$$

Where: MSH is moisture scale height (cm), and
SA is solar altitude (degrees)

---

* See Section 2, Table 2-1, of this volume for the list of coefficients.

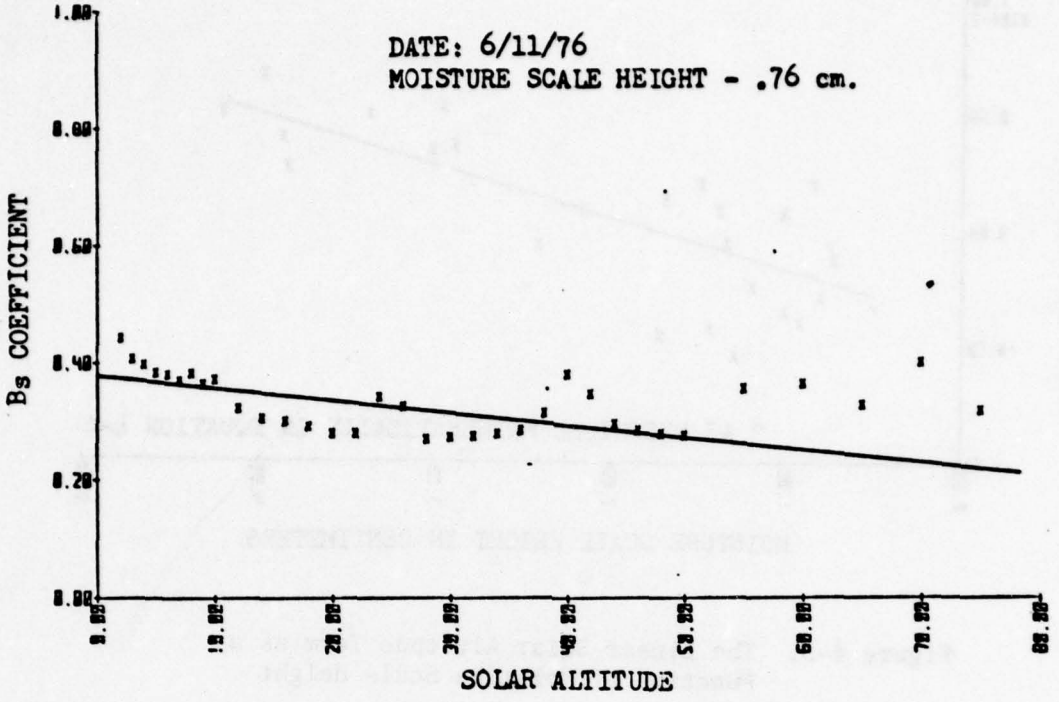

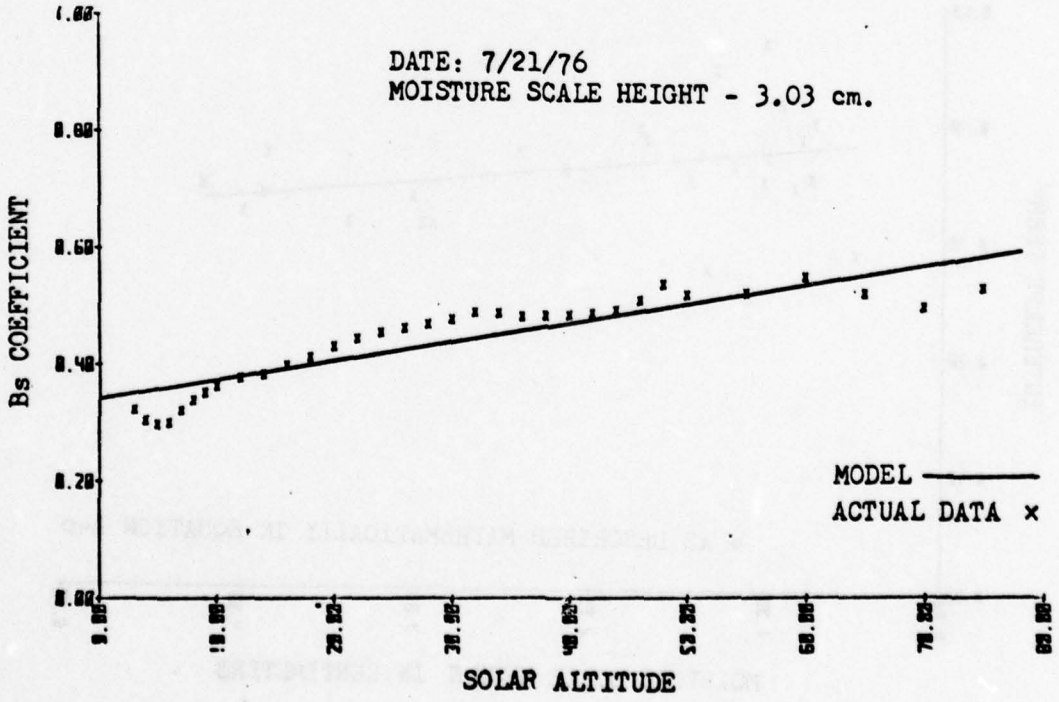

Figure 4-2. Two Typical Plots Showing the B_s Coefficient as a Function of Solar Altitude

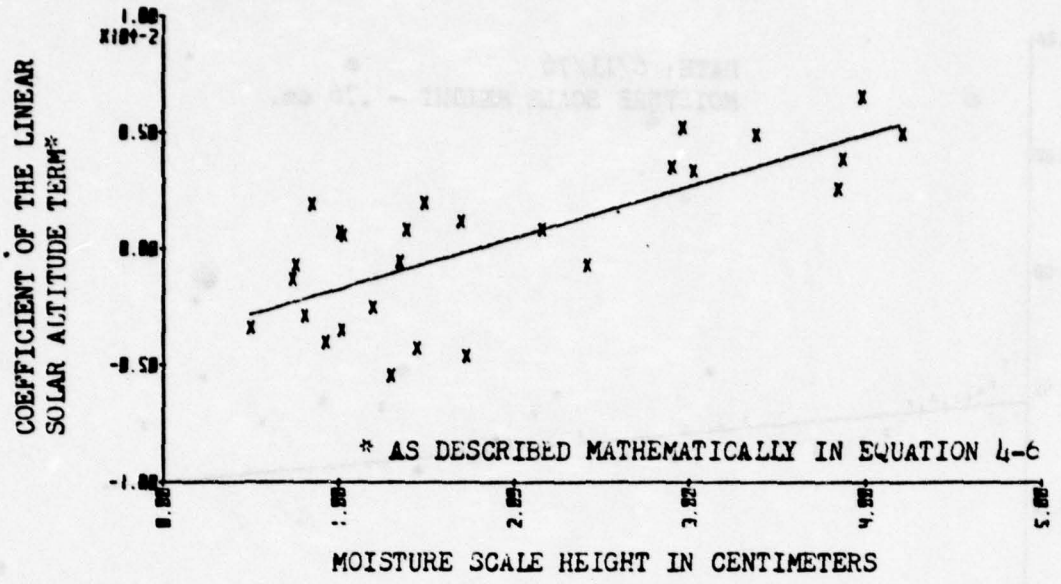

Figure 4-3. The Linear Solar Altitude Term as a Function of Moisture Scale Height

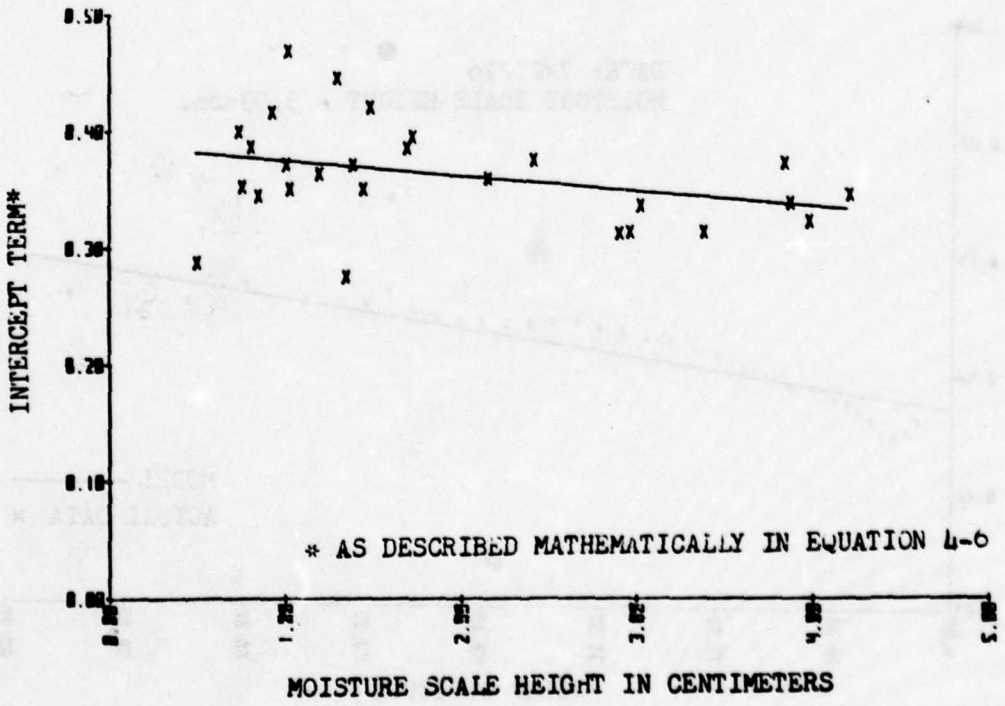

Figure 4-4. The B_s Intercept Term as a Function of Moisture Scale Height

where the equation limits are: $0 \leq MSH \leq 3.5$ cm

$-5° \leq SA < 90°$

4.2.3 Terrain Reflectance Term

The day-site data collections in which there was extensive snow cover were used to estimate the coefficient of the terrain reflectance term. By evaluating the b_s coefficient for the appropriate solar altitude and moisture scale height, the skylight term could be effectively subtracted from the measurement in the same manor as the direct solar irradiance term and resulted in the following equation:

$$\frac{H_{DH}(\lambda)}{H_{SC}(\lambda) \cdot \cos\theta [t_s(\lambda) t_a(\lambda)^{m(\theta)}} - 1 - b_s(SA, MSH) \frac{[1-t_s(\lambda)^{m(\theta)}]\ t_a(\lambda)}{[t_s(\lambda)\ t_a(\lambda)]^{m(\theta)}}$$

Equation 4-7

$$= b_a R(\lambda)\ [1-t_s(\lambda)]\ t_a(\lambda)$$

By following the same regression procedure used for b_s, b_a coefficients for each solar altitude and each day-site could be estimated. A solar altitude plot of the average b_a coefficient for all snow sites is shown in Figure 4-5. The upward curvature of b_a at low solar altitude was considered to be more an artifact of the analysis than a physical condition and was therefore not modeled. No attempt to correlate the b_a coefficient with moisture scale height was, or could be, made. The resulting equation for b_a was therefore:

$$b_a = 3.908 - 0.0739\ SA \qquad \text{Equation 4-8}$$

The value of b_a is limited to a minimum value of 0.5 corresponding approximately to the highest solar altitude observed with snow surround.

4.3 MODEL EQUATIONS IN SCAT3

The mathematical model for horizontal daylight irradiance discussed in this section is a mixture of physical and empirical equations. It has the dis-

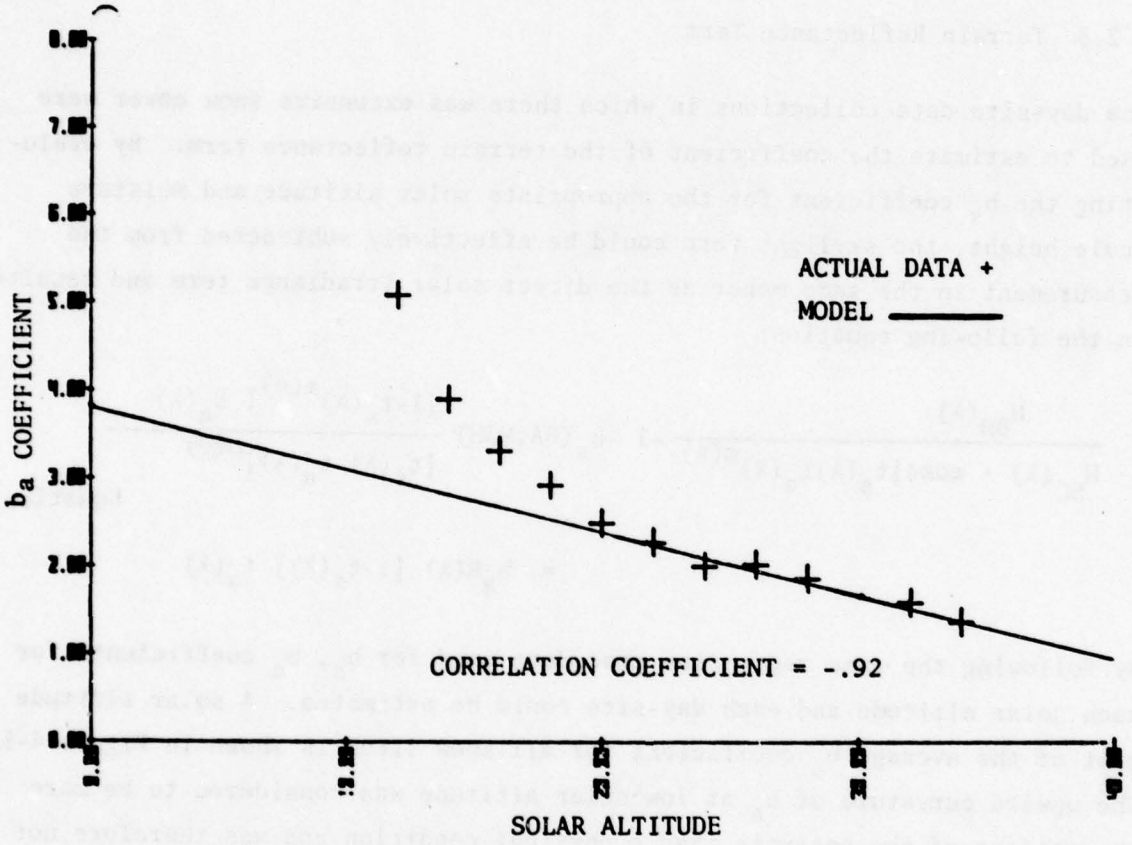

Figure 4-5. Average Terrain Term Coefficient as a Function of Solar Altitude

tinct advantage of satisfying both the requirements of atmospheric physics and observed spectral data. In the final form of the SCAT3 equation, the spectral reconstruction of horizontal daylight is accomplished as follows:

$$H_{DH}(\lambda) = H_{SC}(\lambda)\cos\theta\,[t_s(\lambda)t_a(\lambda)]^{m(\theta)} \cdot k_D + k_s \cdot b_s(SA,MSH) \cdot H_{sc}(\lambda)\cos\theta\left[1-t_s(\lambda)^{m(\theta)}\right]t_a(\lambda) + b_a(SA) \cdot H_{sc}(\lambda) \cdot \cos\theta \cdot [t_s(\lambda)t_a(\lambda)]^{m(\theta)} \cdot R(\lambda)\,[1-t_s(\lambda)]\,t_a(\lambda) \qquad \text{Equation 4-9}$$

Where: $H_{SC}(\lambda)$ is the mean extraterrestrial spectral solar irradiance corrected for seasonal variation* (watts/m^2/5nm),

θ is the solar zenith angle between 0° and 87°,

$t_s(\lambda), t_a(\lambda)$ are the spectral vertical atmospheric scattering and absorption transmittances,

$M(\theta)$ is the relative air mass corresponding to solar zenith angle θ,

$R(\lambda)$ is the spectral reflectance of the general terrain,

$b_s(SA,MSH)$ is the skylight irradiance proportionality constant evaluated for a specific solar altitude and moisture scale height (as calculated in Equation 4-6),

$b_a(SA)$ is terrain/skylight irradiance proportionality constant evaluated for a specific solar altitude (Equation 4-8), and

* See Appendix D for a description of this correction which adjusts the solar constant for the orbital eccentricity of the earth about the sun.

$$k_D = \begin{cases} 1, & SA > 0° \\ 0, & SA < 0° \end{cases}$$

$$k_s = \begin{cases} 0, & SA \geq 3° \\ p(SA) & SA < 3°* \end{cases}$$

SA = Apparent solar altitude**

4.4 VERY LOW SOLAR ALTITUDE MODELING

Only a few daylight irradiance measurements were available below three degrees solar altitude. To continue the model's applicability down to minus five degrees solar altitude, it was necessary to adopt a relative scaling polynomial for daylight that was derived from separate data. The polynomial itself does not involve spectral shaping; in addition, it contains no parameters other than solar altitude and is used strictly as a relative magnitude adjustment for the skylight irradiance term, $H_S(\lambda)$. The adjustment polynomial p(SA) had been evaluated at three degrees solar altitude, and this value was divided into the coefficients to normalize the polynomial to the lowest valid calculated daylight spectral irradiance. Equations 4-1 through 4-4 for the model are evaluated for the appropriate condition of moisture scale height and terrain reflectance at three degrees solar altitude; they are then multiplied wavelength-by-wavelength by the normalized adjustment polynomial evaluated at the solar altitude of interest. The polynomial and scaling approach are explained in Appendix F. The normalized factor used for horizontal daylight spectral irradiance is 0.037440.

Because refraction of the sun's rays in the atmosphere becomes substantial below five degrees solar altitude, a correction must be applied to solar altitude as was used in Equation 4-10. The corrected solar altitude is referred to as the "apparent" solar altitude and is described mathematically in Appendix G.

---

* See para. 4.4 and Appendix F for a description of the polynomial p(SA).

** See Appendix G for the correction applied to solar altitude below 5° to compensate for refraction of the sun's rays in the atmosphere.

4.5 SPECTRAL RECONSTRUCTION OF MEASURED DATA

Equation 4-10 for the model was used to reconstruct a series of actual spectral daylight irradiance measurements that typify the overall collection program. These data and the model fits are shown in Appendix C.

SECTION 5

ANALYSIS AND MODELING OF HORIZONTAL SKYLIGHT IRRADIANCE

5.1 INTRODUCTION

For the purposes of this study, horizontal skylight irradiance is defined as the total irradiance on a horizontal surface with the direct rays of the sun blocked. The horizontal surface in this case can be considered to be irradiated by light from the sun that is both (1) scattered downward by the atmosphere on the horizontal surface and (2) reflected from the surrounding terrain and scattered by the atmosphere downward to the horizontal surface.

To create the model for horizontal skylight irradiance, the following were used in the analysis: irradiometer data recorded by the mobile radiometric trailer, estimates of the vertical transmittance based on the analysis in Section 2, and meteorological data collected concurrent with the radiometric data. The data had a solar altitude range of 0.73 to 80.95 degrees and a moisture scale height range of 0.23 to 4.2 centimeters. Figure 5-1 illustrates the geometry of the model used in this analysis. Each of the additive terms has a coefficient associated with it that was estimated by linear regression of the model equational terms to the measured skylight irradiance.

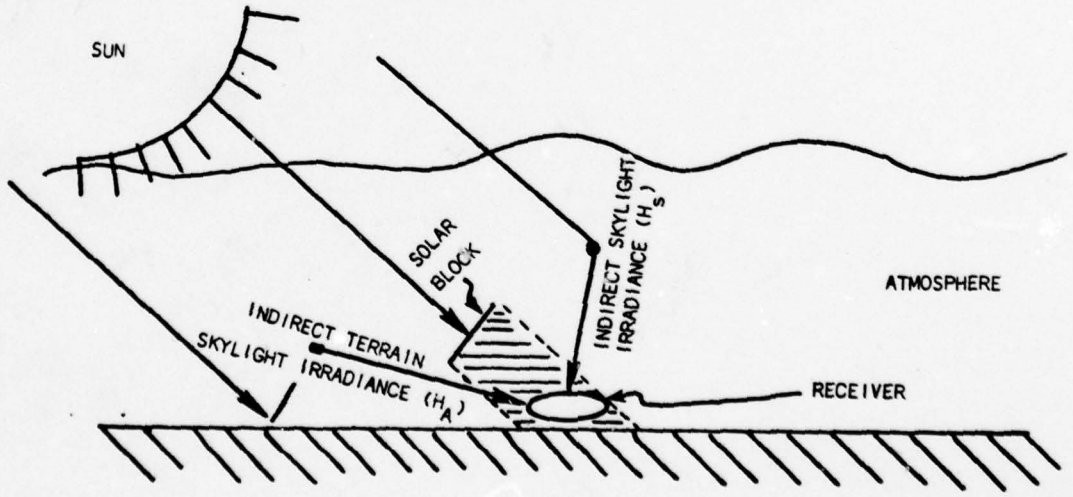

Figure 5-1. Geometry Model for Horizontal Skylight Irradiance

The skylight irradiance model is illustrated in Figure 5-1 and shown mathematically below.

$$H_{SH}(\lambda) = b_S H_S(\lambda) + b_A H_A(\lambda) \qquad \text{Equation 5-1}$$

Where: $H_{SH}(\lambda)$ is the total horizontal skylight spectral irradiance, in watts/m^2/5nm

$H_S(\lambda)$ is the spectral irradiance from the atmospheric scatter of direct solar rays, in watts/m^2/5nm

$H_A(\lambda)$ is the spectral irradiance from atmospheric scatter of reflected daylight from the surround terrain reflectance, in watts/m^2/5nm.

b_S, b_A are the proportionality constants determined from regression analysis.

Derivation of the above terms and their coefficients is explained below.

5.2 ANALYSIS OF COMPONENTS

As was the case for other forms of ground-level irradiance, the equation terms were taken sequentially in the regression analysis.

5.2.1 Direct Atmospheric Scatter Term

The first component of skylight irradiance is the direct solar irradiance scattered downward. This term represents a fraction of the total irradiance outside the atmosphere that is not transmitted but scattered by the atmosphere, and is represented by the equation:

$$H_S(\lambda) = H_{SC}(\lambda)\cos\theta \cdot \left[1 - T_S^{m(\theta)}(\lambda)\right] \cdot T_A(\lambda) \qquad \text{Equation 5-2}$$

Where: $H_{SC}(\lambda)$ is the extraterrestrial spectral irradiance, in watts/m^2/5nm,

$T_S(\lambda)$ is the vertical spectral transmittance due to scattering.

$T_A(\lambda)$ is the vertical spectral transmittance due to absorption, and

$m(\theta)$ is the air mass at solar zenith angle θ.

It was assumed that the terrain reflectance term of Equation 5-1, $H_A(\lambda)$, was negligible for all day-sites except those with snow surround, and all non-snow day-site data was regressed according to the following equation:

$$H_{SH}(\lambda) = b_S \cdot H_{SC}(\lambda)\cos\theta \left[1 - T_S(\lambda)^{m(\theta)}\right] T_A(\lambda) \qquad \text{Equation 5-3}$$

The regression-determined value for b_S was then studied as a function of solar altitude and moisture scale height. Each day-site b_S value set was fitted with a linear regression, and the slope and intercept were determined. Figures 5-2 and 5-3 are two typical plots of the b_S coefficient versus solar altitude.

No relationship with moisture scale height could be found for the intercept of the linear equations; however, as Figure 5-4 illustrates, the slope term correlated with moisture scale height to a slight degree. The final equation for the b_S coefficient was therefore:

$$b_S(SA,MSH) = 0.348 + (-0.000326 + 0.001318\ MSH)\ SA \qquad \text{Equation 5-4}$$

Where: MSH is the moisture scale height, between 0 and 3.5cm, and

SA is solar altitude ($SA = 90° - \theta$).

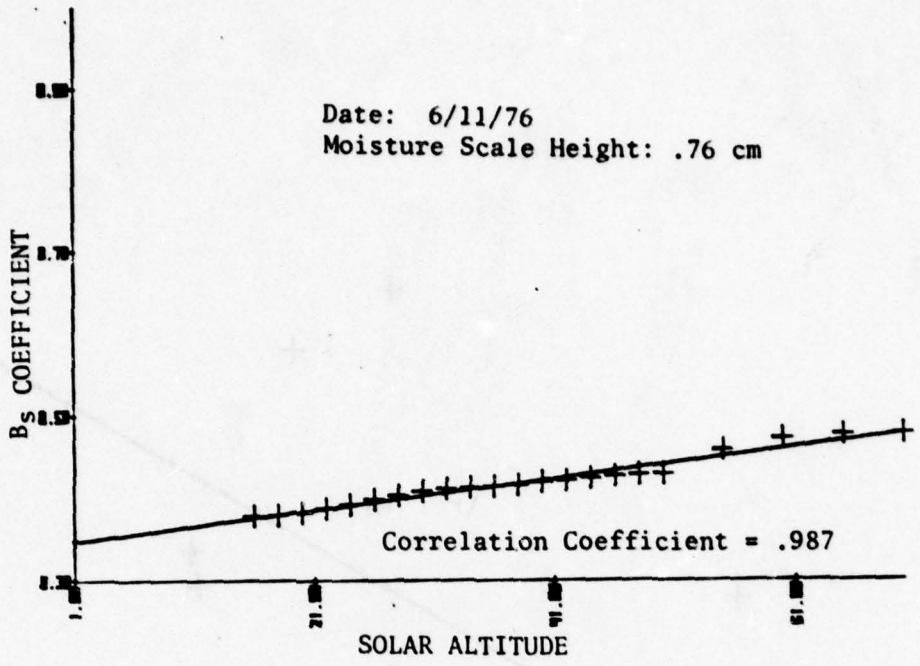

Figure 5-2. Typical Example of the b_s Coefficient Relationship to Solar Altitude for Low Moisture Scale Height

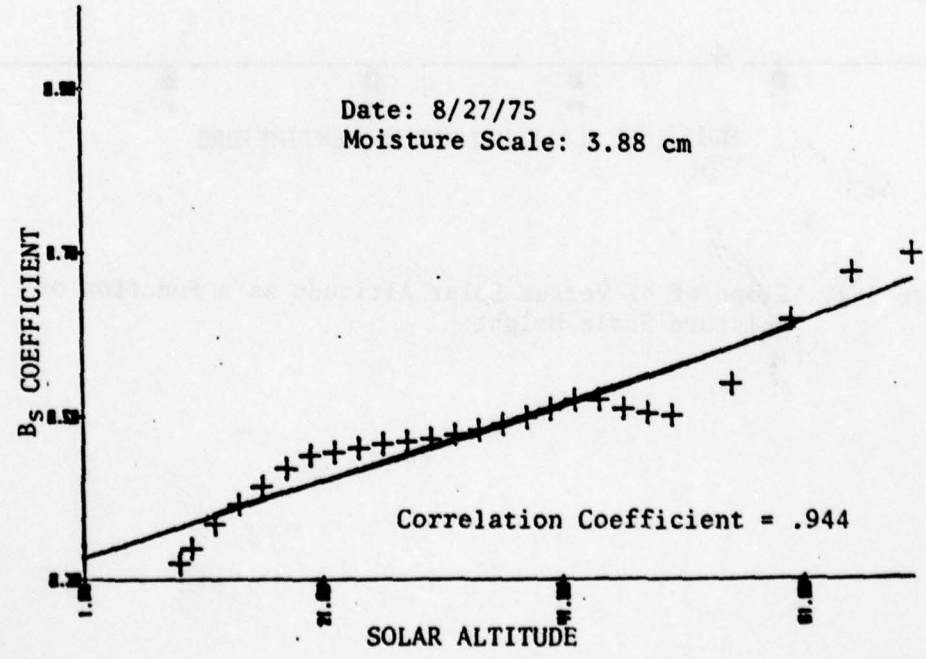

Figure 5-3. Typical Example of the b_s Coefficient Relationship to Solar Altitude for High Moisture Scale Height

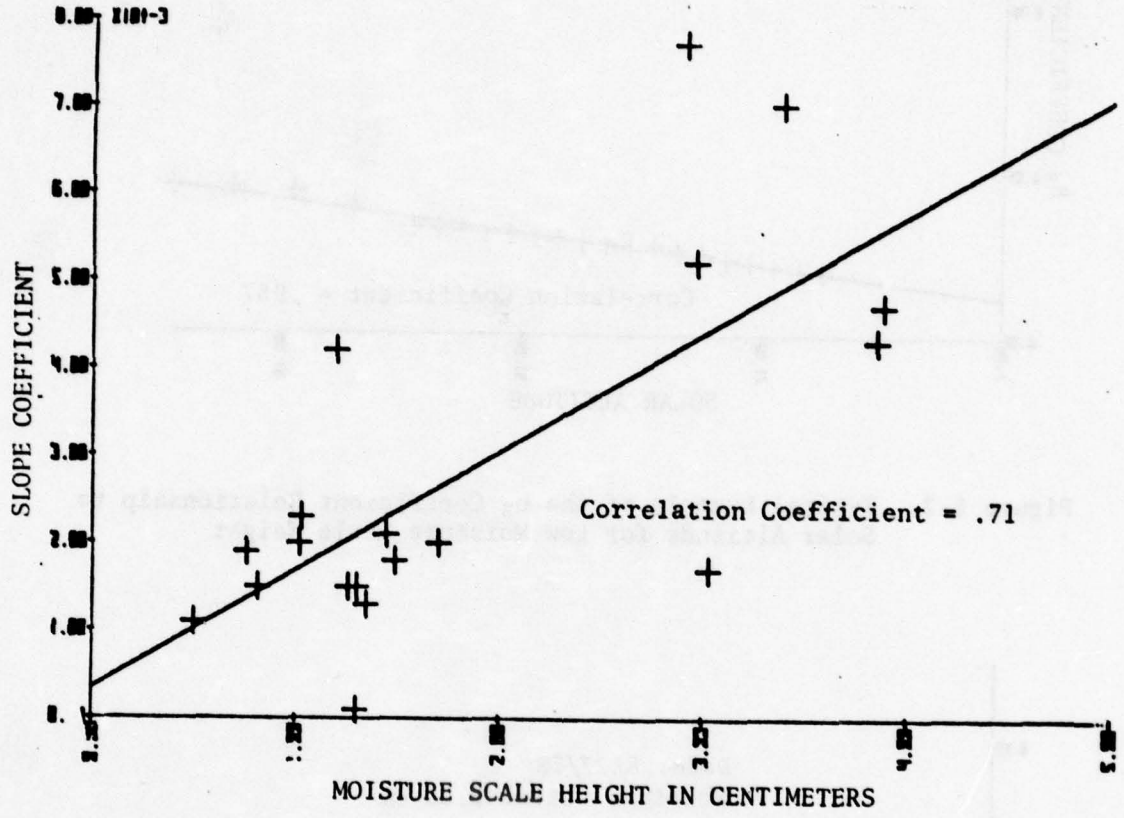

Figure 5-4. Slope of b_s Versus Solar Altitude as a Function of Moisture Scale Height

5.2.2 Terrain Reflectance Term

The coefficient for the terrain term, b_A, was investigated using day-site measurements acquired while snow was present on the ground around the measurement site. An equational form identical with that for horizontal daylight irradiance was chosen for use and regressed against the measured data as follows:

$$\frac{H_{SH}(\lambda)}{H_{sc}(\lambda)\cos\theta\,[1-t_s^{m(\theta)}(\lambda)]\,t_a(\lambda)} - b_s = b_A \cdot \frac{[1-t_s(\lambda)]}{[1-t_s^{m(\theta)}(\lambda)]}$$

$$[t_a(\lambda)\cdot t_s(\lambda)]^{m(\theta)}\cdot R(\lambda) \quad \text{Equation 5-5}$$

where $R(\lambda)$ is the spectral reflectance of the surrounding terrain.

The terrain coefficient, b_A, was found to operate in a manner similar to that for horizontal daylight irradiance (see para. 4.2 of this volume). The horizontal daylight functions for b_A below were therefore used for the skylight irradiance model.

Equation 5-6

$$b_A(SA) = 3.908 - 0.0739 \cdot SA$$

where SA is the solar altitude ($SA = 90° - \theta$).

5.3 VERY LOW SOLAR ALTITUDE MODELING

The model described in Section 5 was considered to be valid to a solar altitude as low as 3 degrees. Extension of the model to -5 degrees solar altitude was accomplished using the scaling function described for the horizontal daylight irradiance model, in Section 4, and Appendix F of this volume.

The scaling factor is applied to the skylight term and operates only below 3 degrees solar altitude. The factor is not a function of wavelength and atmospheric condition.

5.4 MODEL EQUATIONS IN SCAT3

The following equation is used in the program to model horizontal skylight irradiance:

$$H_{SH}(\lambda) = k_s \cdot b_S(SA,MSH) \cdot H_{SC}(\lambda) \cos\theta \left[1-t_s^{m(\theta)}(\lambda)\right] \cdot t_a(\lambda) \quad \text{Equation 5-7}$$

$$+ b_A H_{SC}(\lambda) \cos\theta \left[t_a(\lambda) t_s(\lambda)\right]^{m(\theta)} \cdot R(\lambda)$$

$$\left[1-t_s(\lambda)\right] \cdot t_a(\lambda)$$

Where: $H_{SC}(\lambda)$ is the mean extraterrestrial spectral solar irradiance corrected for seasonal variation* (watts/m^2/5nm).

$t_s(\lambda), t_a(\lambda)$ are the vertical spectral transmittances due to scattering and absorption.

$R(\lambda)$ is spectral reflectance of terrain.

$M(\theta)$ is the relative air mass corresponding to the solar zenith angle θ.

θ is the solar zenith angle, between 0° and 87°.

$b_S(SA,MSH)$ is the skylight irradiance proportionality constant evaluated for a specific solar altitude and moisture scale height (as computed in Equation 5-4).

$b_A(SA)$ is the terrain/skylight irradiance proportionality constant evaluated for a specific solar altitude (as computed in Equation 5-6).

SA is the apparent solar altitude,** and

k_s $= \begin{cases} 1, & SA \geq 3° \\ p(SA), & SA < 3°*** \end{cases}$.

---

* See Appendix I

** See Appendix G

*** See Appendix F

5.5 SPECTRAL RECONSTRUCTION OF MEASURED DATA

Equations 5-4, 5-6, and 5-7 were used to re-create spectral skylight irradiance data corresponding to a typical set of measured data. Graphs of these data are shown in Appendix C.

SECTION 6

ANALYSIS AND MODELING OF VERTICAL DAYLIGHT IRRADIANCE

6.1 INTRODUCTION

The vertical surface irradiance measurements made by the mobile radiometric trailer and described in Volume 2 of this report were all made with the sampling aperture axis co-planar with the sun's azimuth. These measurements were of two types: (1) looking directly toward the sun, and (2) looking directly away from the sun. The analysis of data from the first type, vertical daylight irradiance, is described in this section. The second type is described in Section 7 of this volume.

Although the terms are similar, the model for vertical front daylight irradiance differs in several respects from that for horizontal daylight as shown below.

$$H_{DV}(\lambda) = H'_D(\lambda) + b'_s \cdot H'_S(\lambda) + b'_a \cdot H'_a(\lambda) \qquad \text{Equation 6-1}$$

Where: $H_{DV}(\lambda)$ is the spectral vertical daylight irradiance (front-lighted), in watts/m^2/5nm,

$H'_D(\lambda)$ is the direct solar spectral irradiance, in watts/m^2/5nm,

$H'_s(\lambda)$ is the indirect skylight irradiance, in watts/m^2/5nm).

$H'_a(\lambda)$ is the indirect reflected irradiance from the nearby terrain, in watts/m^2/5nm, and

b'_s, b'_a are the proportionality constants determined from regression analysis.

Figure 6-1 shows the geometry that is assumed in the basic model of Equation 6-1.

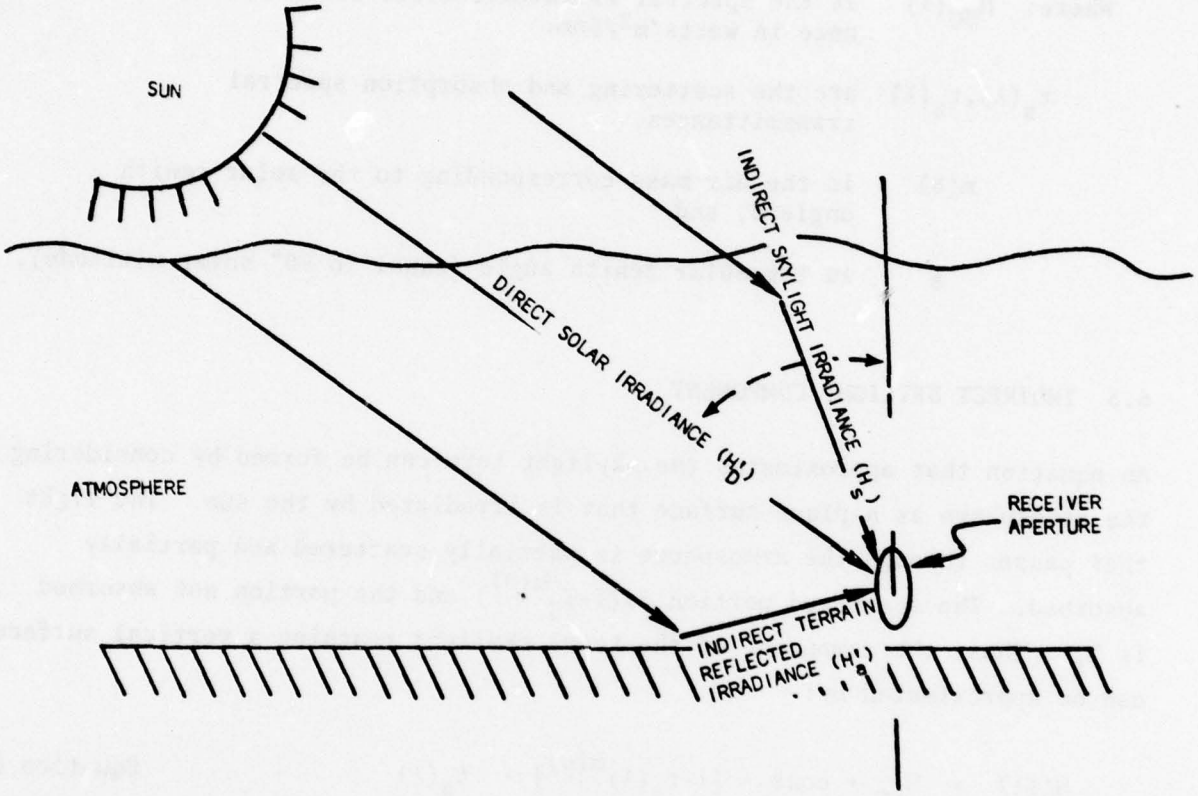

Figure 6-1. Geometry Model Used for Vertical Daylight Irradiance

6.2 DIRECT SOLAR IRRADIANCE COMPONENT

The direct sunlight component can be expressed as a product of four items: the solar constant $H_{SC}(\lambda)$ times the scattering transmittance $t_s(\lambda)^{m(\theta)}$ times the absorption transmittance $t_a(\lambda)^{m(\theta)}$ times a sine of the solar zenith angle ϕ, which is in conformity with Lambert's law of illumination. Thus,

the irradiance of the direct component can be written as:

$$H'_D(\lambda) = H_{SC}(\lambda) \sin\theta \cdot [t_s(\lambda) \cdot t_a(\lambda)]^{m(\theta)} \qquad \text{Equation 6-2}$$

Where: $H_{SC}(\lambda)$ is the spectral extraterrestrial solar irradiance in watts/m^2/5nm.

$t_s(\lambda), t_a(\lambda)$ are the scattering and absorption spectral transmittances.

$m(\theta)$ is the air mass corresponding to the solar zenith angle θ, and

θ is the solar zenith angle (equal to 90° solar altitude).

6.3 INDIRECT SKYLIGHT COMPONENT

An equation that approximates the skylight term can be formed by considering the atmosphere as a plane surface that is irradiated by the sun. The light that passes through the atmosphere is partially scattered and partially absorbed. The scattered portion is $(1-T_S^{m(\theta)})$ and the portion not absorbed is T_A. Thus, the component of the total skylight reaching a vertical surface can be approximated by:

$$H'_S(\lambda) = H_{SC} \cdot \cos\theta \cdot [1-t_s(\lambda)^{m(\theta)}] \cdot t_a(\lambda) \qquad \text{Equation 6-3}$$

6.4 INDIRECT SURROUND REFLECTANCE COMPONENT

Since any plane orientation other than horizontal receives some irradiance from the terrain within the field of view, a third term is necessary that involves the reflectance of the instrument surround. The mathematical approximation for this term is:

$$H'_a(\lambda) = H_{SC}(\lambda) \cdot \cos\theta \cdot [t_s(\lambda) \cdot t_a(\lambda)]^{m(\lambda)} \cdot R(\lambda) \qquad \text{Equation 6-4}$$

where $R(\lambda)$ is the spectral reflectance of the terrain surrounding the instrument.*

6.5 REGRESSION ANALYSIS FOR PROPORTIONALITY CONSTANTS

The three terms described in Equations 6-2, 6-3, and 6-4 were substituted into Equation 6-1 and algebraicly manipulated as follows:

$$\frac{H_{DV}(\lambda)}{H_{sc}(\lambda)\cos\theta\,[t_a(\lambda)\cdot t_s(\lambda)]^{m(\theta)}} - \tan\theta = b'_s \frac{[1-t_s(\lambda)^{m(\theta)}]\,t_a(\lambda)}{[t_a(\lambda)\cdot t_s(\lambda)]^{m(\theta)}} + b'_a\,R(\lambda)[1-t_s(\lambda)]\cdot t_a(\lambda) \qquad \text{Equation 6-5}$$

Observations that had been made from the measured data indicated that, as in the case of horizontal daylight irradiance, the indirect skylight component coefficient b'_s could be determined from regression analysis of the data from all days not having snow surround so that the terrain reflectance term could be assumed to be zero. The b'_s coefficient was then studied as a function of solar altitude and moisture scale height. The coefficient did not show strong correlation with either solar altitude or moisture scale height. However, a linear model was regressed and fitted because of a weak dependence upon these parameters.

The assumption that the terrain reflectance term is small compared to the skylight contribution for low and medium surround reflectances was verified by experiment. Vertical daylight irradiance measurements were made in the normal manner that were followed immediately by similar measurements made with a black cloth positioned so that it eliminated direct reflections from the

---

* Section 5.1, Volume 2, for a description of these data.

terrain into the irradiometer. These measurements, when compared with the direct component calculated from the measured transmittance, showed the skylight contribution to be considerably greater than that from the terrain reflectance.

6.5.1 Skylight Coefficient

The b_s coefficient that corresponds to the proportion of skylight irradiance, is shown in Figure 6-2 as a function of the moisture scale height. The plotted b_s coefficient, which is the average coefficient determined for all solar altitudes of a given day-site, shows a tendency to increase with moisture scale height. A slight solar altitude dependence of b_s can be seen in Figure 6-3, which is a graph of all the values of b_s for each day-site plotted versus their respective solar altitudes. The regression equation shown in Figure 6-2 for b_s versus moisture scale height was determined first. A multiplying factor was then determined that was based on the solar altitude versus b_s regression, and it was used to modify the b_s moisture scale height relationship.

The multiplying factor is the value of b_s at a given solar altitude as determined by the regression equation shown in Figure 6-3 divided by the regression value of b_s at 28 degrees solar altitude (the median solar altitude of the data forming the relationship of Figure 6-2). Thus, the multiplying factor is normalized so that it does not change b_s at 28 degrees solar altitude, but makes a change at all other solar altitudes equal to the fractional change of b_s in the solar-altitude-dependent regression of Figure 6-3. The equation for b_s in terms of both the solar altitude factor and the moisture scale height becomes:

$$b_s = (0.3355 + 0.0428 \times MSH) \times (0.848 + 0.00544 \times SA) \qquad \text{Equation 6-6}$$

where MSH is the moisture scale height between 0 and 4.2cm, and
SA is the solar altitude, in degrees.

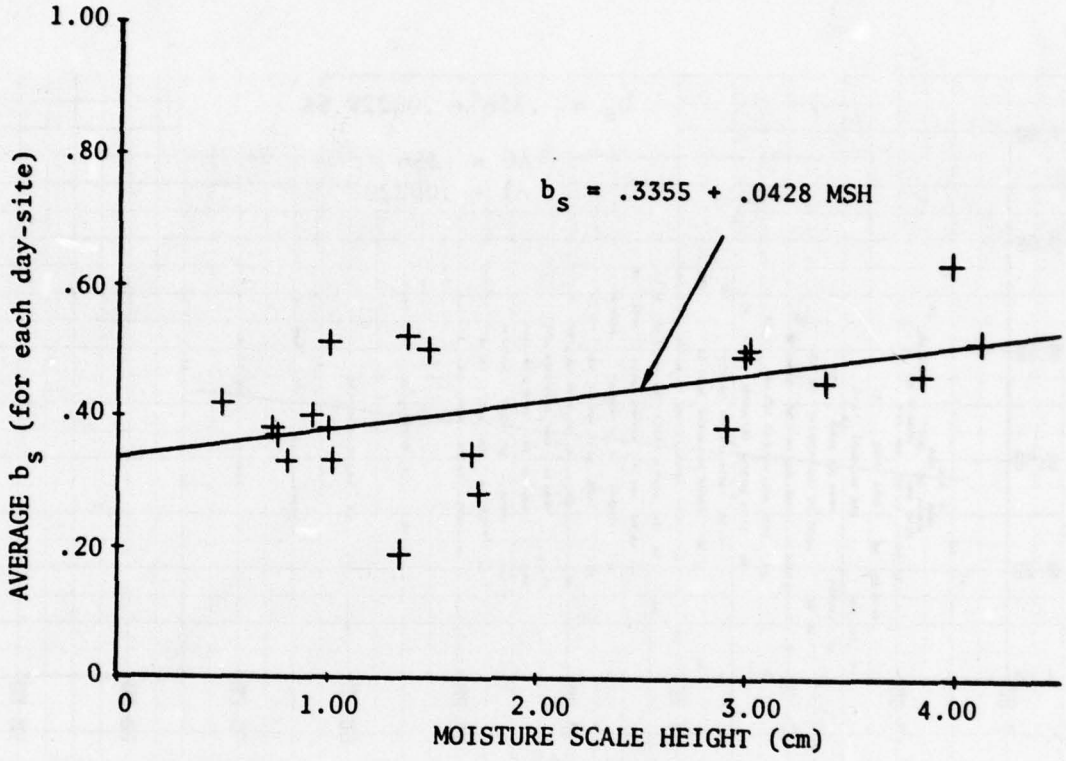

Figure 6-2. Vertical Front-Lit Skylight Coefficient as a Function of Moisture Scale Height

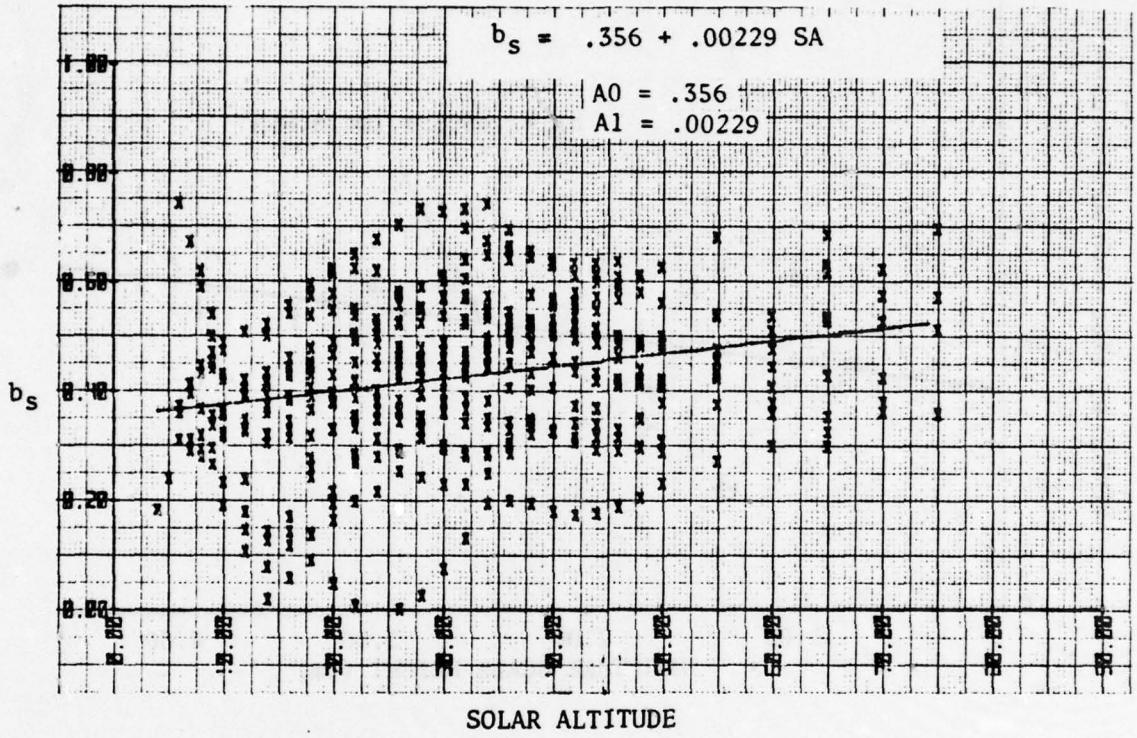

Figure 6-3. Vertical Front-Lit Skylight Coefficient as a Function of Solar Altitude

AD-A072 080 EASTMAN KODAK CO ROCHESTER N Y APPARATUS AND OPTICAL DIV F/G 14/2
SPECTRAL RADIOMETRIC MEASUREMENT AND ANALYSIS PROGRAM. VOLUME 3--ETC(U)
APR 79 L G CHRISTENSEN, R SIMMONS, G SCHAUSS

UNCLASSIFIED AWS-TN-79/001-VOL-3 NL

2 OF 3
AD A072080

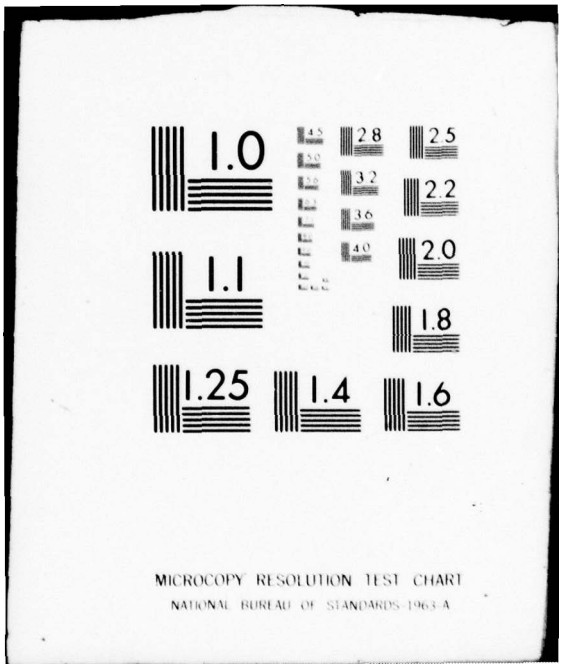
1.0
1.1
1.25
1.4
1.6
1.8
2.0
2.2
2.5
2.8
3.2
3.6
4.0
MICROCOPY RESOLUTION TEST CHART
NATIONAL BUREAU OF STANDARDS 1963-A

6.5.2 Terrain Reflectance Coefficient

A scaling coefficient, b_A, that was based on acquired data was calculated for the term expressed in Equation 6-4. Because only the days with snow surround were considered to have sufficient reflectance to exceed the noise level of the measurements, only these data were considered in forming the b_A coefficient. In Figure 6-4, it can be seen that b_A is a function of solar altitude. At about 10 degrees solar altitude, specular reflections caused a large increase in the b_A coefficient, making it necessary to model the b_A coefficient in two parts (below 10° SA and above 10° SA). Both solar altitude ranges were fitted separately with straight lines determined by least squares regressions. The two line segments were then modified so that they would be without discontinuity at 10 degrees solar altitude. The final equation for b_A was then:

$$b_A = \begin{cases} 2.50 - 0.1945\ SA, & SA < 10° \\ 0.5927 - 0.003769\ SA, & SA \geq 10° \end{cases} \qquad \text{Equation 6-7}$$

The terrain term above is allowed to go to zero at zero degrees solar altitude in accordance with the cosine term in Equation 6-4. It is set to zero for solar altitudes less than zero degrees.

6.6 MODIFICATION OF THE DIRECT AND SKYLIGHT COMPONENTS FOR IMPROVED FITTING TO EMPIRICAL DATA

The sum of the direct, skylight, and terrain terms as calculated in the model slightly underestimated the vertical daylight irradiance compared to a cross-section of actual measured data. To make them fit the model better, the first two terms (direct and skylight) were increased by a factor calculated to correct for the average offset. The necessary multiplying factor was found to be 1.14. The factor was not applied to the albedo term, however, since the offset was needed even in cases where the terrain contribution could be considered negligible.

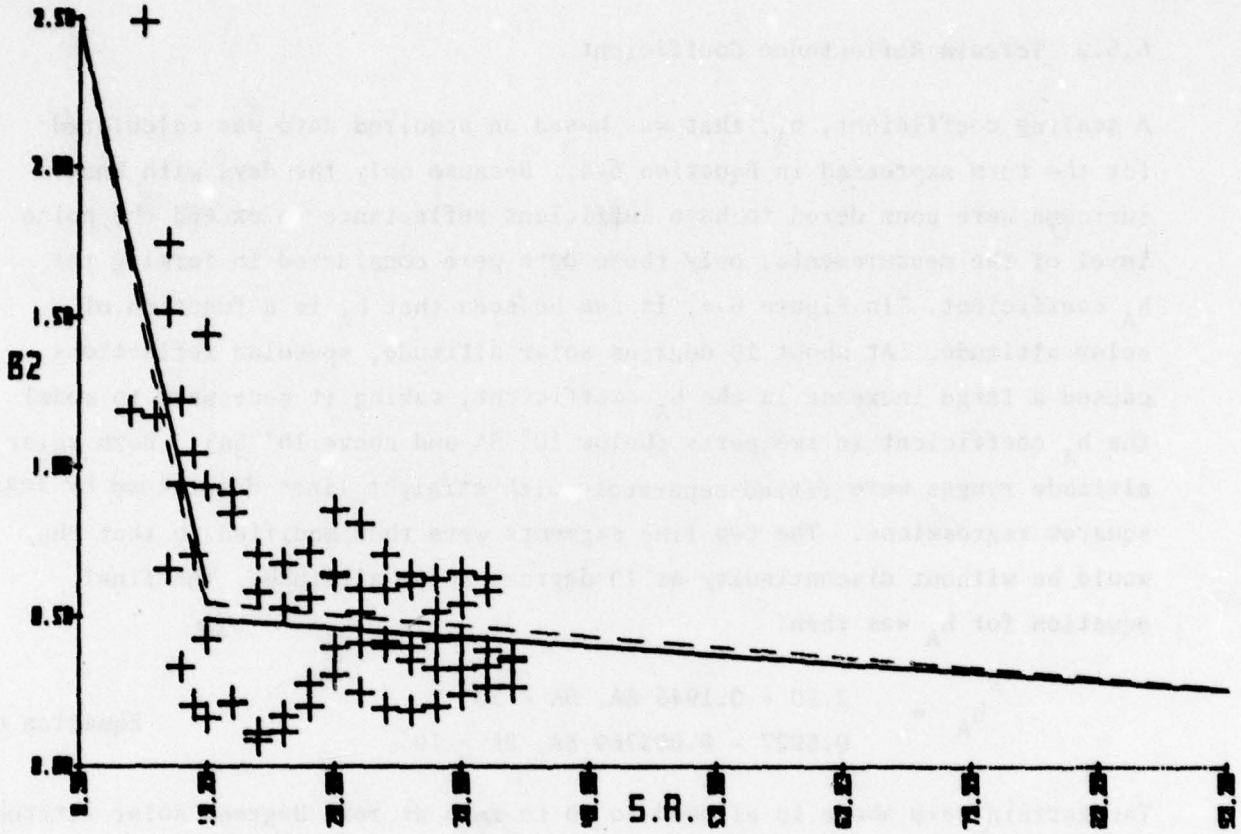

Figure 6-4. A Plot of the Vertical Front-Lit Albedo Coefficient Versus Solar Altitude

6.7 VERY LOW SOLAR ALTITUDE MODELING

Although the model's equations were shown to be valid for solar altitudes down to and including 6 degrees, below 6 degrees, there was insufficient data to verify the model. Equation 6-2 continues to be used as the model for the direct component down to zero degrees, below which it is set to zero. However, Equation 6-3 for the skylight component is not suitable down to zero degrees because the term goes to zero even though skylight is physically present below zero degrees. Modeling of skylight below 6 degrees is accomplished by applying the adjustment polynomial P(SA) given in Appendix F. The model-predicted skylight values at 6 degrees solar altitude then define the shape of the function with the skylight irradiance decreasing in proportion to the decrease in the irradiance scaling polynomial p(SA).

6.8 EQUATIONS USED IN SCAT3

The derivation of each of the terms making up the vertical daylight irradiance were discussed above. In its complete form, the daylight irradiance is represented by:

$$H_{DV}(\lambda) = k'_D \cdot H_{SC}(\lambda) \sin\theta \cdot [t_s(\lambda)\, t_a(\lambda)]^{m(\theta)}$$

Equation 6-8

$$+ 1.14\, K'_s \cdot b'_s\,(SA, MSH) \cdot H_{SC} \cos\theta\, [1 - t_s(\lambda)^{m(\theta)}] \cdot t_a(\lambda)$$

$$+ b'_a\,(SA) \cdot H_{SC} \cos\theta\, [t_s(\lambda)\, t_a(\lambda)]^{m(\theta)} \cdot R(\lambda)$$

Where: $H_{SC}(\lambda)$ is the spectral extraterrestrial solar irradiance, in watts/m^2/5nm, corrected for seasonal variation*.

θ is the solar zenith angle (equal to 90° solar altitude).

$t_s(\lambda), t_a(\lambda)$ are the scattering and absorption spectral transmittance.

* See Appendix I for a description of this correction.

$m(\lambda)$ is the air mass corresponding to the solar zenith angle θ.

$R(\theta)$ is the spectral reflectance of the terrain surrounding the instrument.

$b_s'(SA,MSH)$ is the skylight irradiance proportionality constant evaluated for a specific solar altitude and moisture scale height computed in Equation 6-6.

$b_a'(SA)$ is the terrain/skylight irradiance proportionality constant evaluated for a specific solar altitude computed in Equation 6-7.

SA is the apparent solar altitude*

K_D' $\begin{cases} 1, & SA \geq 0^\circ \\ 0, & SA < 0^\circ \end{cases}$

K_S' $\begin{cases} 1, & SA \geq 6^\circ \\ P(SA), & SA < 6^\circ ** \end{cases}$

---

* See Appendix G for the correction applied to solar altitude below 5° to compensate for refraction of the sun's rays in the atmosphere.

** See Section 4.4 and Appendix F for a description of the polynomial P(SA).

SECTION 7

VERTICAL SKYLIGHT IRRADIANCE

7.1 INTRODUCTION

Vertical skylight irradiance is defined for this study as the indirect irradiance from atmospheric scatter and terrain reflectance on a vertical plane oriented 180 degrees away from the solar azimuth. This measurement is the sum of contributions from the skylight half-hemisphere and the horizontal surfaces surrounding the instrument, that define the terrain half-hemisphere. Special experiments were conducted to remove the effect of surround so that the skylight term could be studied independently. The surround term was later re-introduced into the final equations. Figure 7-1 shows the model assumed in the analysis.

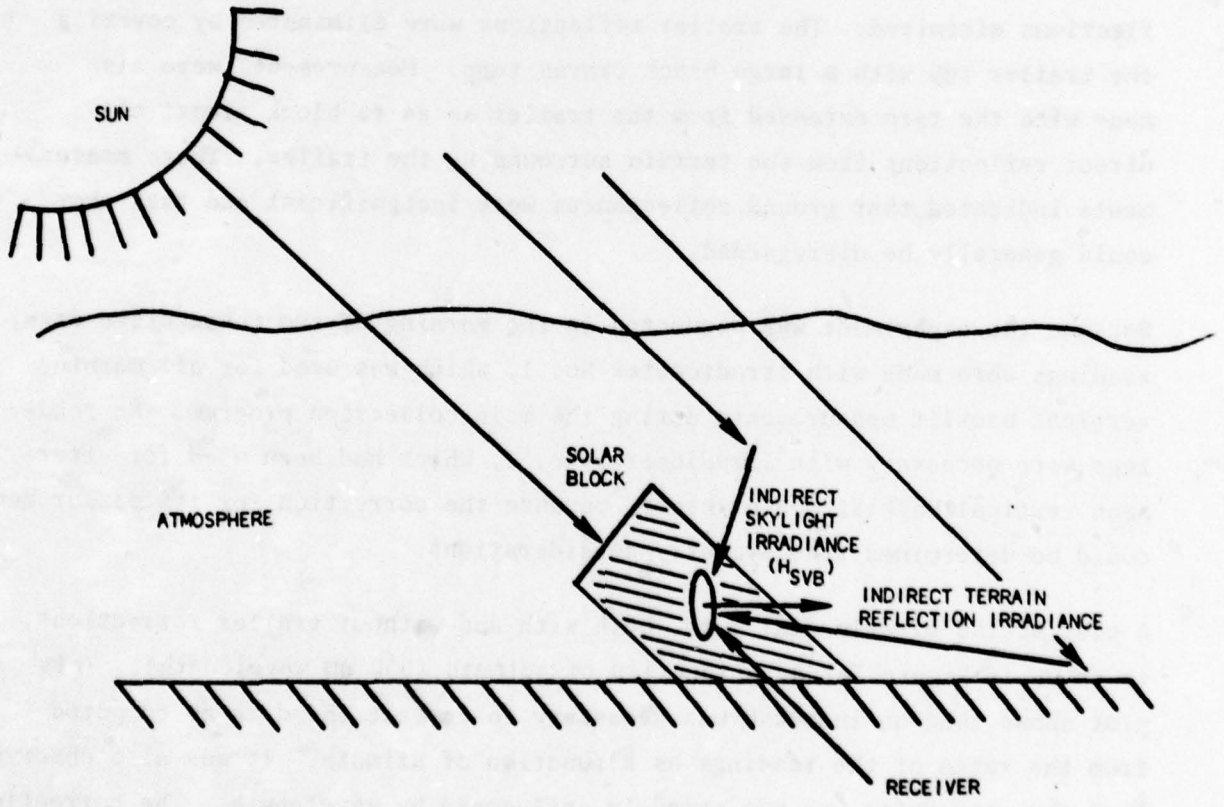

Figure 7-1. Geometry Model Used for Vertical Skylight Irradiance

7.2 ELIMINATION OF NEAR-FIELD SURROUND EFFECTS

The vertical backlit measurements were found to contain a significant amount of trailer reflection irradiance along with the skylight irradiance. The amount of reflection is substantially influenced by the azimuth of the instrument because a variety of reflecting surfaces are present near the irradiometers on the trailer roof. As an irradiometer changes azimuth, it sees various portions of the ground, the trailer top, and the other instruments. Furthermore, the white styrofoam hatch covers that are also visible to the irradiometers were surfaces of higher reflectance than the rest of the gray trailer roof.

In order to back the unwanted trailer reflections out from this data, an experiment was conducted to measure vertical backlit skylight at various azimuths, both under normal operating conditions and also with trailer reflections minimized. The trailer reflections were eliminated by covering the trailer top with a large black canvas tarp. Measurements were also made with the tarp extended from the trailer so as to block almost all direct reflections from the terrain surrounding the trailer. These measurements indicated that ground reflectances were insignificant and that they could generally be disregarded.

Because the experiment was conducted in the morning of two consecutive days, readings were made with Irradiometer No. 1, which was used for all morning vertical backlit measurements during the main collection program. No readings were necessary with Irradiometer No. 2, which had been used for afternoon vertical backlit measurements, because the correction for its measurements could be determined from symmetry considerations.

A plot of the experimental data, both with and without trailer reflections, is shown in Figure 7-2 as a function of azimuth (550 nm wavelength). This plot shows that an increase was necessary to correct the data as computed from the ratio of the readings as a function of azimuth. It was also observed that the correction was not strongly influenced by wavelength. The correction

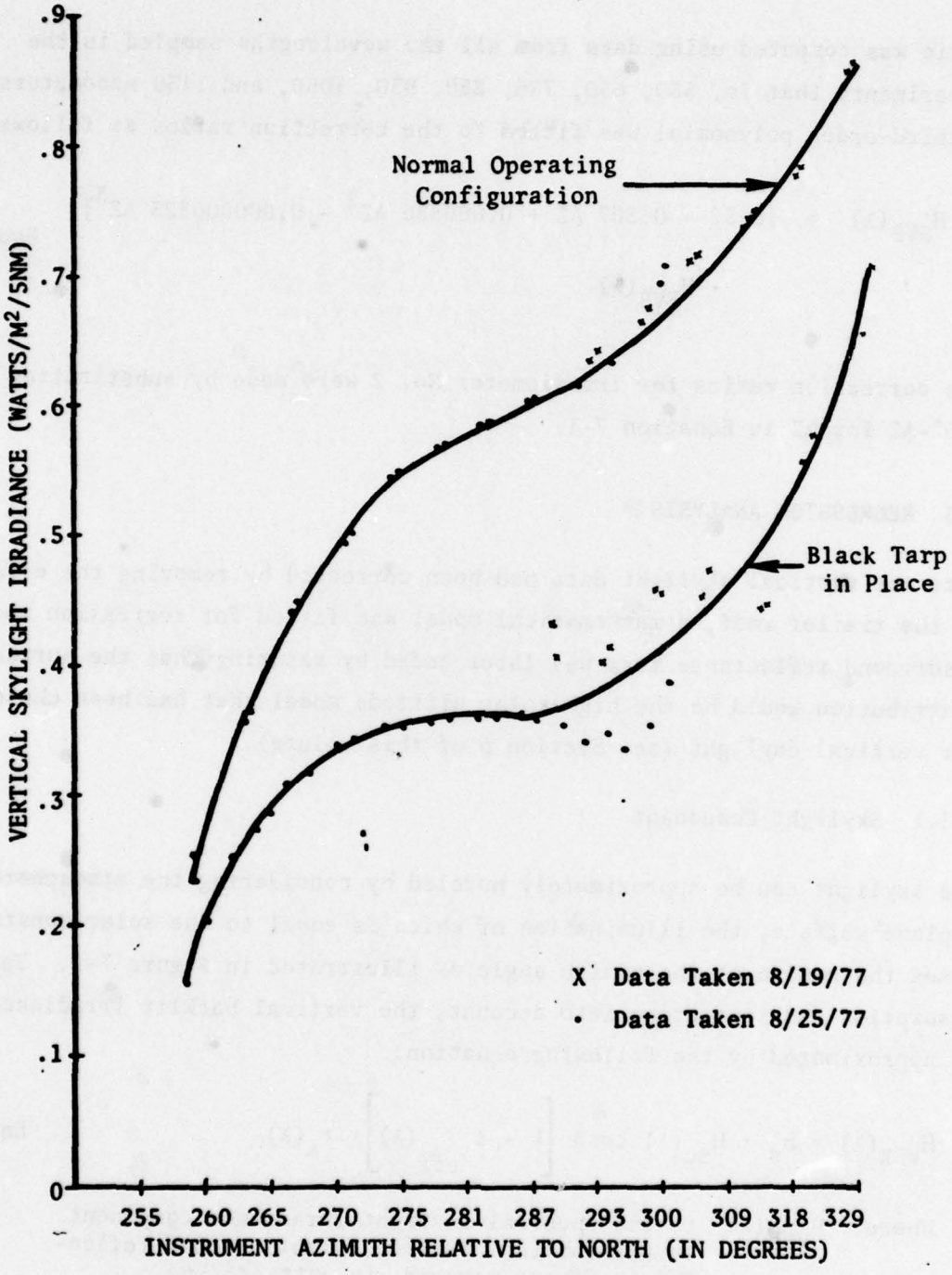

Figure 7-2. Comparison of Vertical Skylight Irradiance Data With and Without Trailer Reflections (Values at 550nm)

ratio was computed using data from all the wavelengths sampled in the experiment; that is, 550, 650, 750, 850, 950, 1050, and 1150 nanometers. A third-order polynomial was fitted to the correction ratios as follows:

$$H'_{SVB}(\lambda) = [3.52 - 0.307\ AZ + 0.000886\ AZ^2 - 0.000000823\ AZ^3] \cdot H_{SVB}(\lambda) \qquad \text{Equation 7-1}$$

The correction ratios for Irradiometer No. 2 were made by substituting 360°-AZ for AZ in Equation 7-1.

7.3 REGRESSION ANALYSIS

Once the vertical skylight data had been corrected by removing the effects of the trailer roof, a mathematical model was fitted for regression analysis. A surround reflectance term was later added by assuming that the surround contribution would be the high solar altitude model that had been chosen for vertical daylight (see Section 6 of this volume).

7.3.1 Skylight Component

The skylight can be approximately modeled by considering the atmosphere as a plane surface, the illumination of which is equal to the solar constant times the cosine of the zenith angle as illustrated in Figure 7-1. Taking absorption and scattering into account, the vertical backlit irradiance can be approximated by the following equation:

$$H_{VSK}(\lambda) = b_s \cdot H_{sc}(\lambda) \cos\theta \left[1 - t_{s_{eff}}(\lambda)\right] \cdot t_a(\lambda) \qquad \text{Equation 7-2}$$

Where: $H_{VSK}(\lambda)$ is the spectral skylight irradiance component on the vertical surface, with surround reflectance effects removed, in watts/m^2/5nm.

$H_{sc}(\lambda)$ is the mean spectral extraterrestrial irradiance, in watts/m^2/5nm.

θ is the solar zenith angle

$t_a(\lambda)$ is the vertical spectral transmittance due to absorption

$t_{s_{eff}}(\lambda)$ is the effective vertical spectral transmittance due to scattering, and

b_s is the regression-determined proportionality constant.

Unlike the other regressions discussed above, the model had to be modified to better approximate the spectral shape of the data. The correct description for $t_{s_{eff}}(\lambda)$ was determined by trial and error, first by trying $t_{s_{eff}}(\lambda) = t_s(\lambda)^{m(\theta)}$. This equation produced skylight values that were too high in the blue end of the spectrum and too low in the IR end of the spectrum. A tailoring of the shape of this function was achieved by letting $t_{s_{eff}}(\lambda)$ equal a fraction of $t_s(\lambda)^{m(\theta)}$ as in the following equation:

$$T_{s_{eff}}(\lambda) = 0.3\ t_s(\lambda)^{m(\theta)} \qquad \text{Equation 7-3}$$

Once the shape had been defined, the scaling coefficient b_s could be computed to make the skylight model fit the data. This scaling coefficient, as determined by the regression of Equation 7-2, is a function of solar altitude expressed by:

$$b_s = 0.217 - 0.00199\ SA \qquad \text{Equation 7-4}$$

The fitting of this regression to the skylight data is shown in Figure 7-3. No attempt to correlate b_s to moisture scale height was made because of statistical errors associated with normalization of the data to an equivalent no-surround condition.

7.3.2 Terrain Reflectance Component

Because the vertical skylight data was altered specifically to eliminate surround reflection effects, it therefore could not be used to formulate a model of this effect. After reconstructions of the vertical spectral skylight

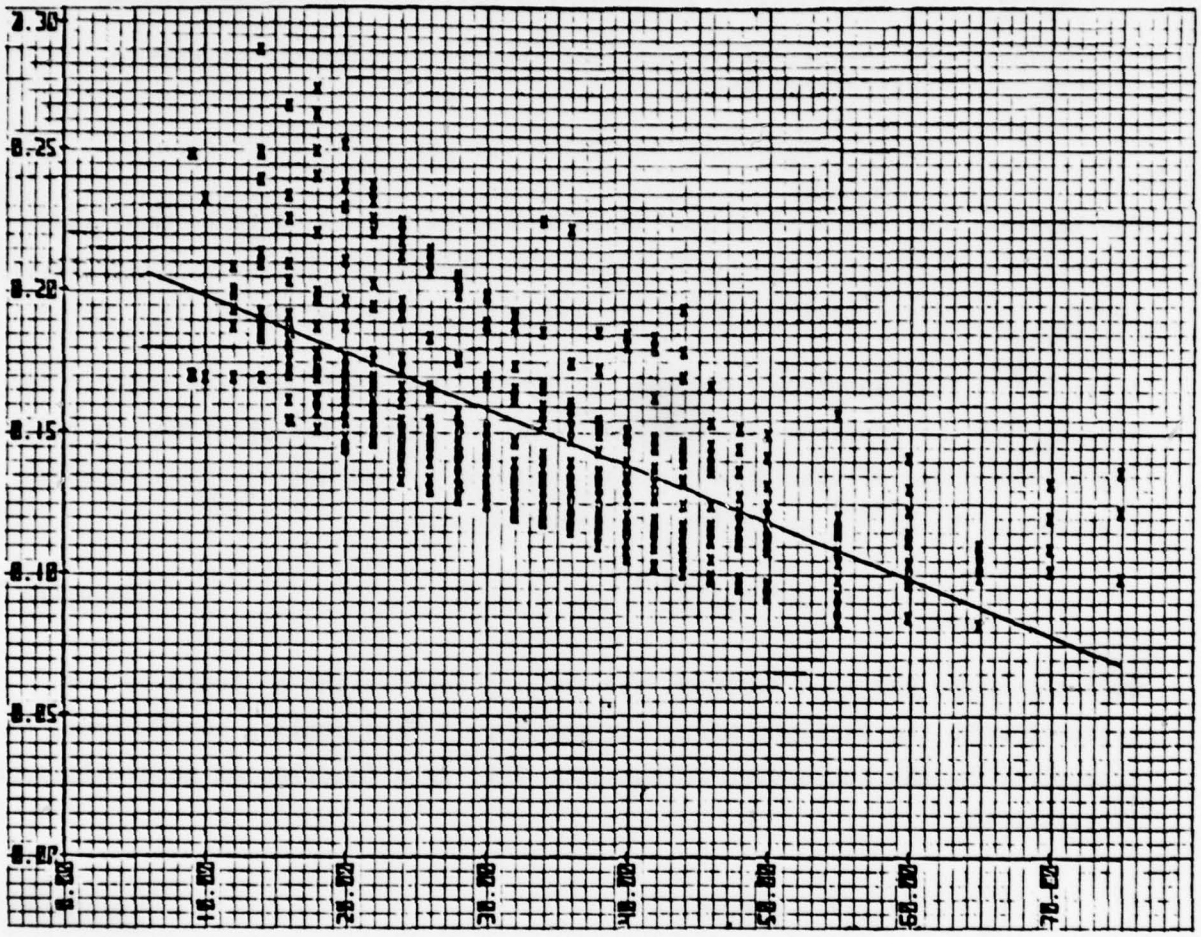

Figure 7-3. Vertical Back-Lit Skylight Coefficient Versus Solar Altitude

samples were examined, it was decided that this term could satisfactorily be approximated by the one for vertical daylight irradiance by eliminating the equation change associated with specular reflection at low solar altitude (see Section 6 of this volume).

7.4 VERY LOW SOLAR ALTITUDE MODELING

Solar altitude data as low as 8 degrees was used in developing the vertical backlit irradiance model. In addition, a scaling coefficient was applied to the 8-degree spectral curve to extend the model from 8 degrees to minus 5 degrees solar altitude. The scaling function was again necessary as with the other irradiance conditions already described because the skylight does not physically go to zero when the equations do. The terrain reflectance term is allowed to go to zero at zero degrees solar altitude as required by Equation 6-4, and it is set to zero for solar altitudes less than zero degrees.

7.5 MODEL EQUATIONS IN SCAT3

The equation in final form as modeled for use in SCAT3 is:

$$H_{VSB}(\lambda) = K_S \cdot b_S(SA)\, H_{SC}(\lambda) \cos\theta \,[1-.3\, t_s(\lambda)^{m(\theta)}]\, t_a(\lambda$$

$$+ K_A \cdot b_A(SA)\, H_{SC}(\lambda) \cos\theta \,[t_s(\lambda)t_a(\lambda)]^{m(\theta)} \cdot R(\lambda) \qquad \text{Equation 7-5}$$

Where: $H_{VSB}(\lambda)$ is the vertical spectral skylight irradiance, in watts/m^2/5 nm.

$H_{SC}(\lambda)$ is the mean spectral extraterrestrial irradiance, in watts/m^2/5nm.

θ is the solar zenith angle (θ also equals 90° minus the solar altitude).

$t_s(\lambda), t_a(\lambda)$ is the vertical spectral transmittance due to scattering and absorption.

$m(\theta)$ is the relative air mass corresponding to solar zenith angle θ.

$R(\lambda)$ is the spectral reflectance of the surrounding surface near the receiver.

$b_{A(SA)}$ is the surround reflectance proportionality constant evaluated for a specific solar altitude, as computed in Equation 6-7.

$b_S(SA)$ is the skylight proportionality constant evaluated for a specific solar altitude, as computed in Equation 7-4, and

$$K_S = \begin{cases} 1.0 \text{ for } SA \geq 6^\circ \text{ or,} \\ p(SA)^* \text{ for } SA < 6^\circ \end{cases}$$

$$K_A = \begin{cases} 1.0, \; SA \geq 0^\circ \\ 0, \; SA < 0^\circ . \end{cases}$$

Typical vertical spectral skylight irradiance curves reconstructed from Equation 7-5 are contained in Appendix C along with the actual measured data.

---

* For a description of the polynomial p(SA), see para. 4.4 and Appendix F.

APPENDIX A
ABSTRACT DESCRIPTION OF ANALYTICAL SOFTWARE

A.1 INTRODUCTION

The software needed to analyze the radiometric van data was a combination of package programs for the IBM 370 and Hewlett Packard 9830, and software written in-house for the IBM 370, Hewlett Packard 9830, and Data General Nova.

In general, three different types of analytical software were used for the analysis: (1) the transmittance analysis, which used the nonlinear and linear regression programs previously developed for the IBM 370 and Hewlett Packard 9830; (2) the analysis of the scattering function, which used programs developed for the Data General Nova and a nonlinear regression program on the IBM 370; and (3) the daylight horizontal, skylight horizontal, daylight vertical, skylight vertical, and sky radiance analysis, which used linear regressions on the IBM 370 and the Hewlett Packard 9830.

The equipment required in the analysis was: (1) an IBM 370 with a 3330 disk pack, card reader, printer, an Eastman Kodak Komstar microfiche generator, and a 936 Calcomp plotter; (2) a Hewlett Packard 9830 with a cassette unit and plotter; and (3) a Data General Nova with a nine-track tape drive and a teletypewriter.

The three different types of analytical software involved are described below, and a flowchart that illustrates each one is included. All of the flowcharts contain the EXTRACT Program, which is used to transfer data from the direct access files to the sequential access files. (See Section 7, Vol 2, for a description of the EXTRACT Program.)

A.2 ANALYTICAL SOFTWARE FOR ANALYSIS OF THE TRANSMITTANCE

Figure A-1 is a flowchart that shows the programs used for transmittance analysis. Seven programs were involved in its analysis. The first program,

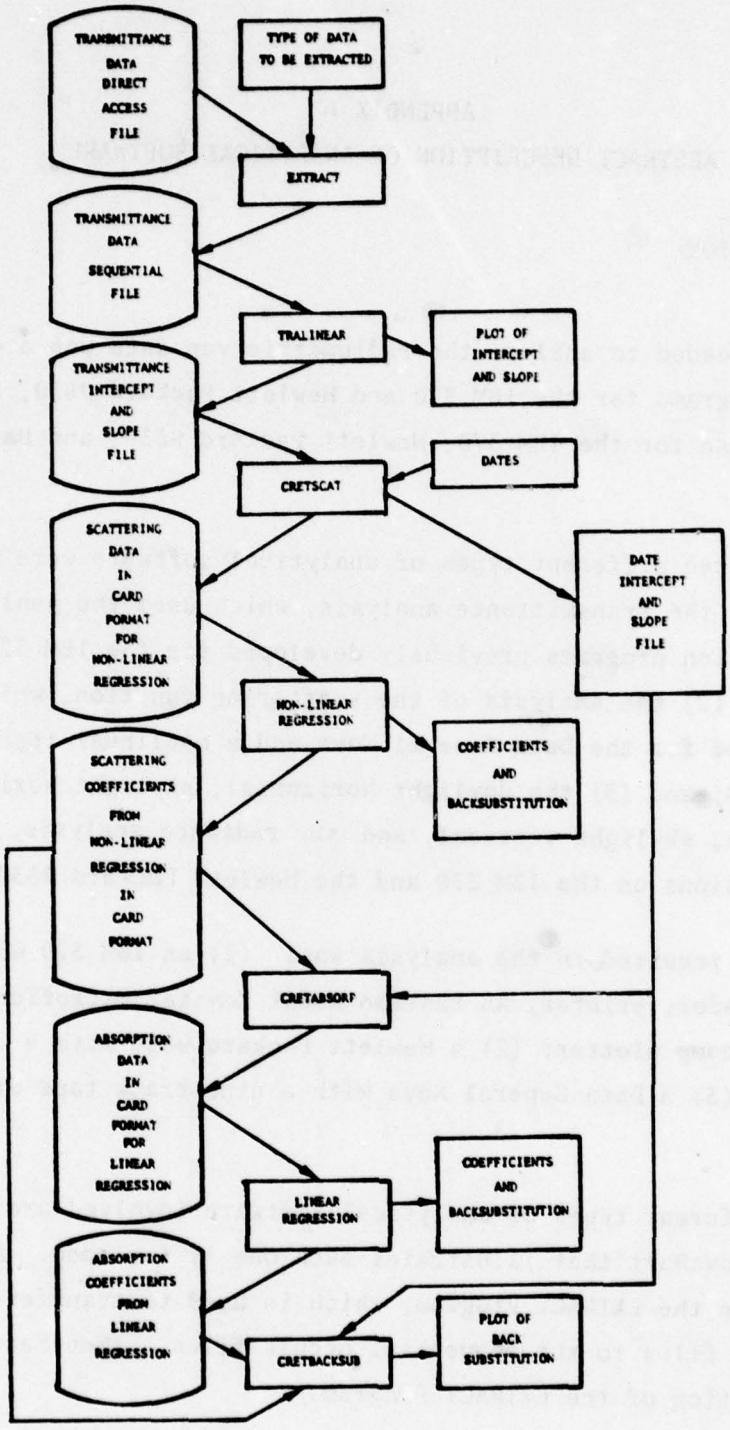

Figure A-1. Analytical Software for Transmittance Analysis; IBM 370

EXTRACT, has already been mentioned.

The second program, TRALINEAR, computed the coefficients of the linear relationship of airmass and log transmittance for each half day in which data was collected. The coefficients, slope and intercept, were then stored in a disk file for further processing.

The third program, CRETSCAT, has two inputs: (1) a card input that specifies the 1/2 day for which the analysis is to be performed, and (2) the file that was created by TRALINEAR that contained the coefficients. The two functions of CRETSCAT are: (a) to eliminate absorption and Rayleigh scattering from the slope-estimated transmittance so that it has only aerosol scattering transmittance (the slope term from TRALINEAR was used to estimate the transmittance as described in Section 2), and (b) to put the data created above in the card format which is needed to run an in-house non-linear regression program. The output from CRETSCAT is a card-formatted disk file of aerosol scattering log transmittance, and a disk file containing the data sets chosen for the analysis.

The fourth program, TREGANA, is a standardized in-house nonlinear regression program that solves for the coefficients C and K_a referred to in Section 2. The output from this program consists of (1) the coefficients C and K_a written on a disk file in card format, (2) a printout of the estimated value of the aerosol scattering log transmittance, and (3) a printout and plot of the residuals; that is, the actual aerosol scattering minus the estimated.

The fifth program CRETABSORP has two functions: (1) to isolate the absorption component of the slope-estimated transmittance, and (2) to create a card-formatted disk file that is passed to a multiple linear-regression program. The absorption component is isolated by subtracting the Rayleigh scattering and estimated aerosol scattering from the original slope-estimated transmittance that was contained in the file from CRETSCAT. The disk file contains the absorption component of the transmittance analysis plus data for the water, ozone, and oxygen bands. This data is regressed against the absorption component.

The sixth program is again TREGANA, an in-house multiple linear regression in which coefficients are calculated for the water, ozone, and oxygen bands to predict the absorption component. The input file is from the program CRETABSORP, and the output files consist of (1) the coefficients from the regression which are on a disk file that is in card format, and (2) a print-out of the estimated value of absorption, the residuals (the actual absorption minus the estimated), and the statistics associated with the regression.

The last program for the transmittance analysis is CRETBACKSUB, which uses (1) the coefficients from the non-linear regression, (2) the coefficients from the linear regression, and (3) the data and atmospheric pressure that were written on the intercept and slope file by CRETSCAT to recreate the total log transmittance.

The final regressions between the nonlinear and linear coefficients and the meteorological parameters was done on a Hewlett Packard 9830 calculator. These results are discussed in Section 2.

A.3 ANALYTICAL SOFTWARE FOR THE SCATTERING FUNCTION

The software for this function necessitated use of the Data General Nova, the IBM 370, and the Hewlett Packard 9830. A flowchart of the Data General and IBM 370 programs needed for the analysis is shown in Figure A-2.

The Data General software was used in creating the correction factors for time and path length. The inputs for the Data General program included: (1) a back-up, nine-track magnetic tape that contained irradiance measurements necessary for the time correction; and (2) the date, time, solar altitude, solar azimuth, and transmittance that were input manually at run time. The date and time were used to locate the data set of interest on the magnetic tape; and the solar altitude, solar azimuth, and transmittance were needed to compute the path length correction. When the correction factors were calculated, they were printed out on the teletype. After these factors were checked manually for validity, they were then punched on cards for input into an IBM 370 program.

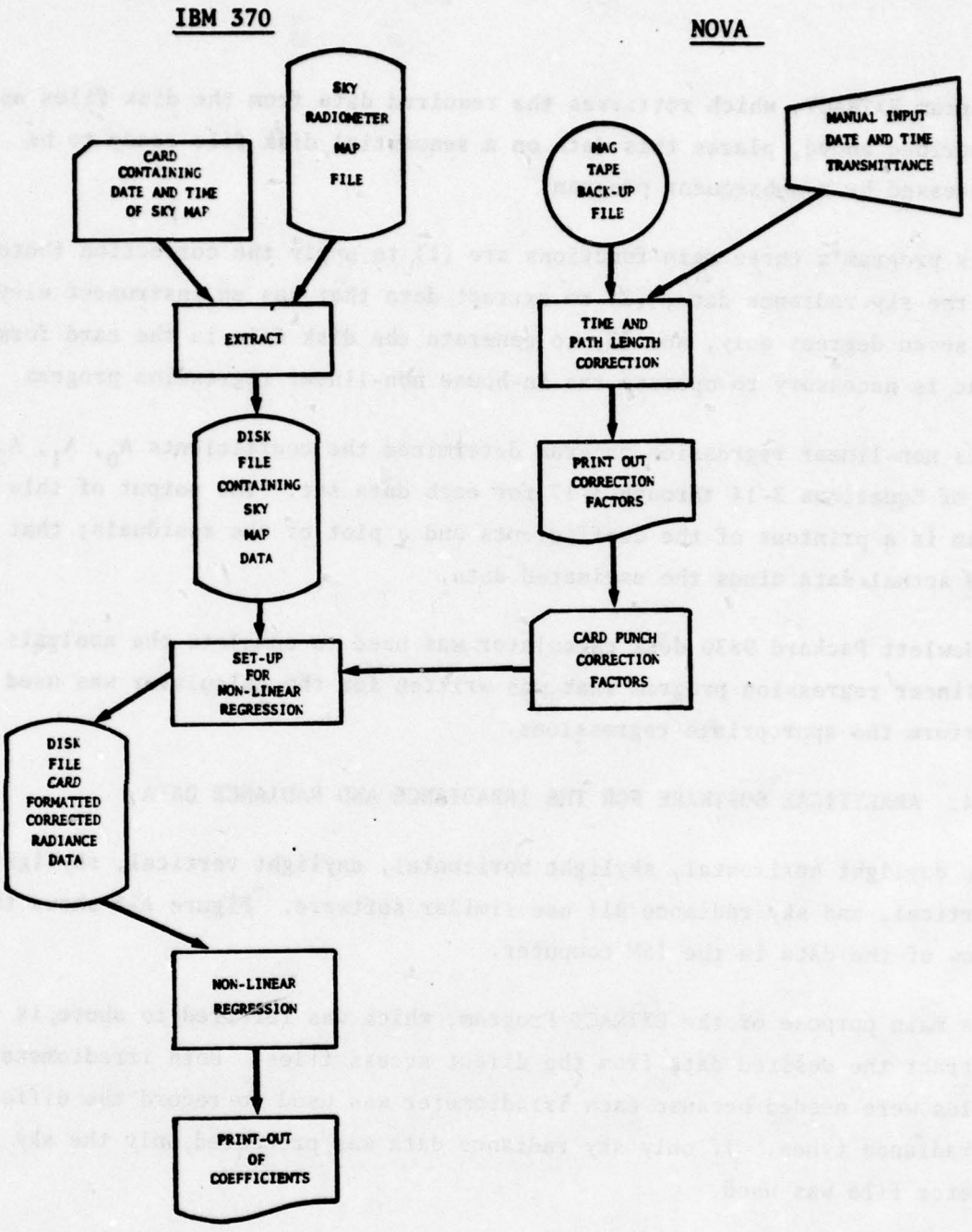

Figure A-2. Analytical Software for the Scattering Function

Program EXTRACT, which retrieves the required data from the disk files as described above, places this data on a sequential disk file ready to be processed by a subsequent program.

This program's three main functions are (1) to apply the correction factor to the sky radiance data, (2) to extract data that has an instrument elevation of seven degrees only, and (3) to generate the disk file in the card format that is necessary to operate the in-house non-linear regression program.

This non-linear regression program determined the coefficients A_0, A_1, A_2, and A_3 of Equations 3-14 through 3-17 for each data set. The output of this program is a printout of the coefficients and a plot of the residuals; that is, the actual data minus the estimated data.

A Hewlett Packard 9830 desk calculator was used to complete the analysis. A linear regression program that was written for the calculator was used to perform the appropriate regressions.

A-4. ANALYTICAL SOFTWARE FOR THE IRRADIANCE AND RADIANCE DATA

The daylight horizontal, skylight horizontal, daylight vertical, skylight vertical, and sky radiance all use similar software. Figure A-3 shows the flow of the data in the IBM computer.

The main purpose of the EXTRACT Program, which was referred to above, is to extract the desired data from the direct access files. Both irradiometer files were needed because each irradiometer was used to record the different irradiance types. If only sky radiance data was processed, only the sky radiometer file was used.

The file was then sorted by year, month, day, hour, and minute by an IBM System sort routine and sent to a program that converts the data to even increments of solar altitude. To accomplish this, a method of linear interpolation was used. The same program also provides a time correction for low-solar-altitude data.

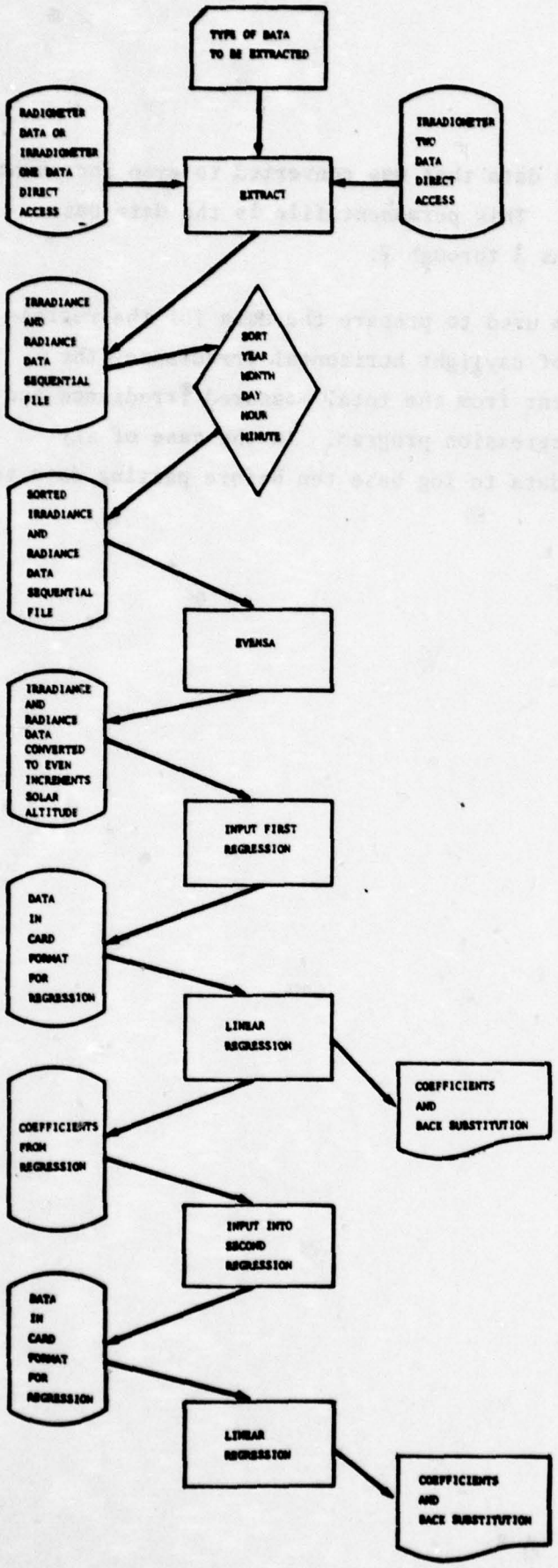

Figure A-3. Analytical Software for Irradiance and Radiance Data; IBM 370

A permanent file is used to store the data that was converted to even increments of solar altitude and time-corrected. This permanent file is the data base for the analyses described in Sections 3 through 7.

This file was then input to a program used to prepare the data for the regression program, TREGANA. In the case of daylight horizontal irradiance, the program subtracted the direct component from the total measured irradiance and then passed the data to the linear regression program. In the case of sky radiance, the program converted the data to log base ten before passing data to the regression program.

APPENDIX B

GLOSSARY OF VARIABLE NAMES IN SCAT3

ABBREVIATIONS	DEFINITION
$AM(\theta)$	Airmass as a function of solar zenith angle θ.
AZ	Solar azimuth angle in degrees.
CATS	Angle between observer's ray and sun's ray.
DUST	Atmospheric dry aerosol content in parts per milliliter.
EL	Terrain elevation above sea level in kilometers.
$H_2O(\lambda)$	Spectral structure for the water absorption bands.
$H_D \cdot [\lambda, T_A(\lambda), T_S(\lambda), SA, AM(ZEN)]$	Direct Solar Irradiance Component*
H_{DH} $[\lambda, SA, MSH, R(\lambda), T_A(\lambda), T_S(\lambda), AM(ZEN)]$	Daylight irradiance on a horizontal surface.*
H_{DV} $[\lambda, SA, MSH, R(\lambda), T_A(\lambda), T_S(\lambda), AM(ZEN)]$	Daylight irradiance on a vertical surface perpendicular to the sun's azimuth.*
H_{PS} $[\lambda, SA, MSH, T_A(\lambda). T_S(\lambda), AM(ZEN)]$	Indirect downward scattered skylight irradiance on a horizontal surface.*
H_R $[\lambda, SA, MSH, R(\lambda), T_A(\lambda), T_S(\lambda) AM(ZEN)]$	Indirect downward scattered skylight reflected from the terrain.
$H_{SC}(\lambda)$	Johnson's extraterrestrial spectral irradiance outside the atmosphere.*
H_{SH} $[\lambda, SA, MSH, R(\lambda), T_A(\lambda), T_S(\lambda), AM(ZEN)]$	Skylight irradiance on a horizontal surface.*
H_{SVB} $[\lambda, SA, MSH, R(\lambda), T_A(\lambda), T_S(\lambda), AM(ZEN)]$	Skylight irradiance on a vertical surface perpendicular to the sun's azimuth and pointed away from the sun.
IEL	Instrument elevation above the horizon in degrees.
λ	Wavelength in nanometers.
MSH	Moisture scale height in centimeters.

* All irradiances have the units: watts/meter^2/5 nanometers.

ABBREVIATIONS	DEFINITION
$N[\lambda, OBS, CATS, ZEN, AM(OBS), T_A(\lambda), T_S(\lambda) MSH, R(650)]$	Atmospheric path radiance in watts/meter^2/steradian/5 nanometers.
$O_2(\lambda)$	Spectral structure for the oxygen absorption band.
$O_3(\lambda)$	Spectral structure for the ozone absorption band.
OBS	Angle between observer's line-of-sight and local zenith.
P	Pressure in millibars.
$R(\lambda)$	Spectral reflectance.
RH	Relative humidity in percent.
SA	Solar altitude in degrees.
TC	Temperature in degrees centigrade.
TF	Temperature in degrees Fahrenheit
$T_A [\lambda, O_3(\lambda), H_2O(\lambda), O_2(\lambda)]$	Spectral transmittance due to absorption.
$T_S [\lambda, P, MSH, DUST]$	Spectral transmittance due to scattering
ZEN or ϕ	Solar zenith angle in degrees

This program also created the control cards necessary to run the in-house, multiple-linear-regression program TREGANA. This program then: (1) computed the appropriate coefficients, (2) printed and card punched the coefficients, and (3) printed the statistics of the regression.

A subsequent program then performed the calculations needed to run a second regression, which included calculating the residuals between the results of the first regression and the data that went into the first regression. For the irradiance data, only the days with snow albedo were passed to the second regression; this program therefore extracted only those days with this type of albedo. The coefficients from the linear regressions where then regressed against solar altitude and/or moisture scale height. For this purpose, a Hewlett Packard 9830 calculator multiple linear regression program was used.

Several computers were used for different purposes; for example, the IBM 370 was used for large-scale data analysis, the Hewlett Packard 9830 was used for small-scale data analysis and testing, and the Data General was used to re-format data to make them compatible with the IBM 370 system. Because of the large volume of printout from the IBM most of it was written to microfiche to provide easy accessibility.

APPENDIX C

EXAMPLES OF SCAT3 RECONSTRUCTION OF ACTUAL DATA

Estimates of actual measured data for a selected cross section of meteorological and solar altitude conditions are shown in Figures C-1 through C-84. Reconstruction was accomplished using the surface meteorology algorithms of SCAT3, substituting in the exact measured pressure temperature, relative humidity, and geometry given in Table C-1 below.

Figure C-1

INSTR SKY

DATA 6/11/76 TIME 16:40: 0 SA 76.97 SAZ 131.25 T650 0.69 LATITUDE 32.19 LONGITUDE -110.87
INSTR AZ 311 INSTR ELEV 13

WIND SPEED 23 WIND DIRECTION 0 HUMID 239 TEMPERATURE 81 PRESSURE 922 ELEV ABOVE SEA 2705

COMMENTS 3,IR1=DV,IR2=SH

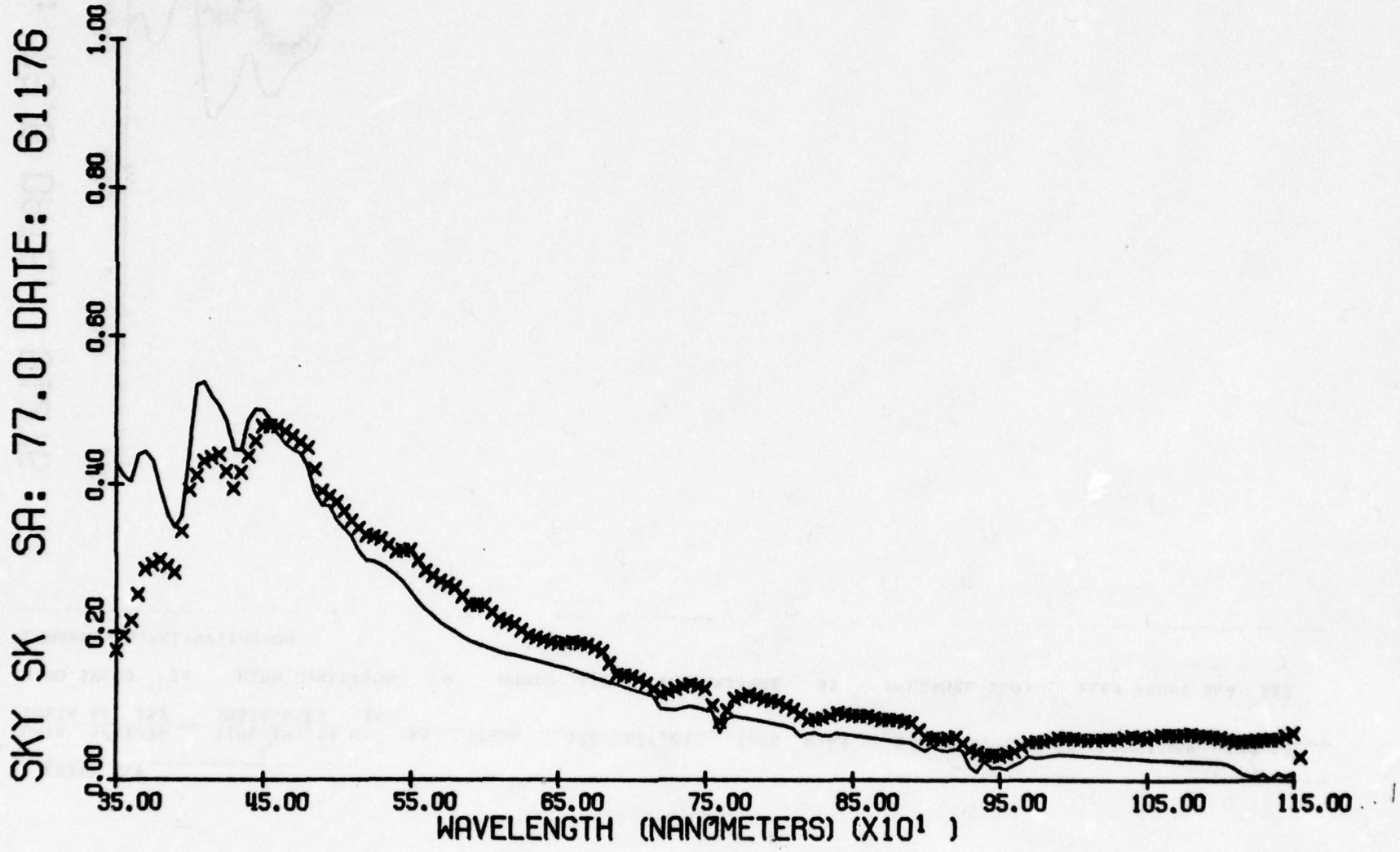

Figure C-2

INSTR SKY

DATA 5/12/76 TIME 19:55:1 U SA 73.29 SAZ 177.26 1050 0.87 LATITUDE 34.75 LONGITUDE -120.57
INSTR AZ 357 INSTR ELEV 16

WIND SPEED 26 WIND DIRECTION 0 HUMID 428 TEMPERATURE 81 PRESSURE 1003 ELEV ABOVE SEA 327

COMMENTS 3,IN1=UV,IN2=OM

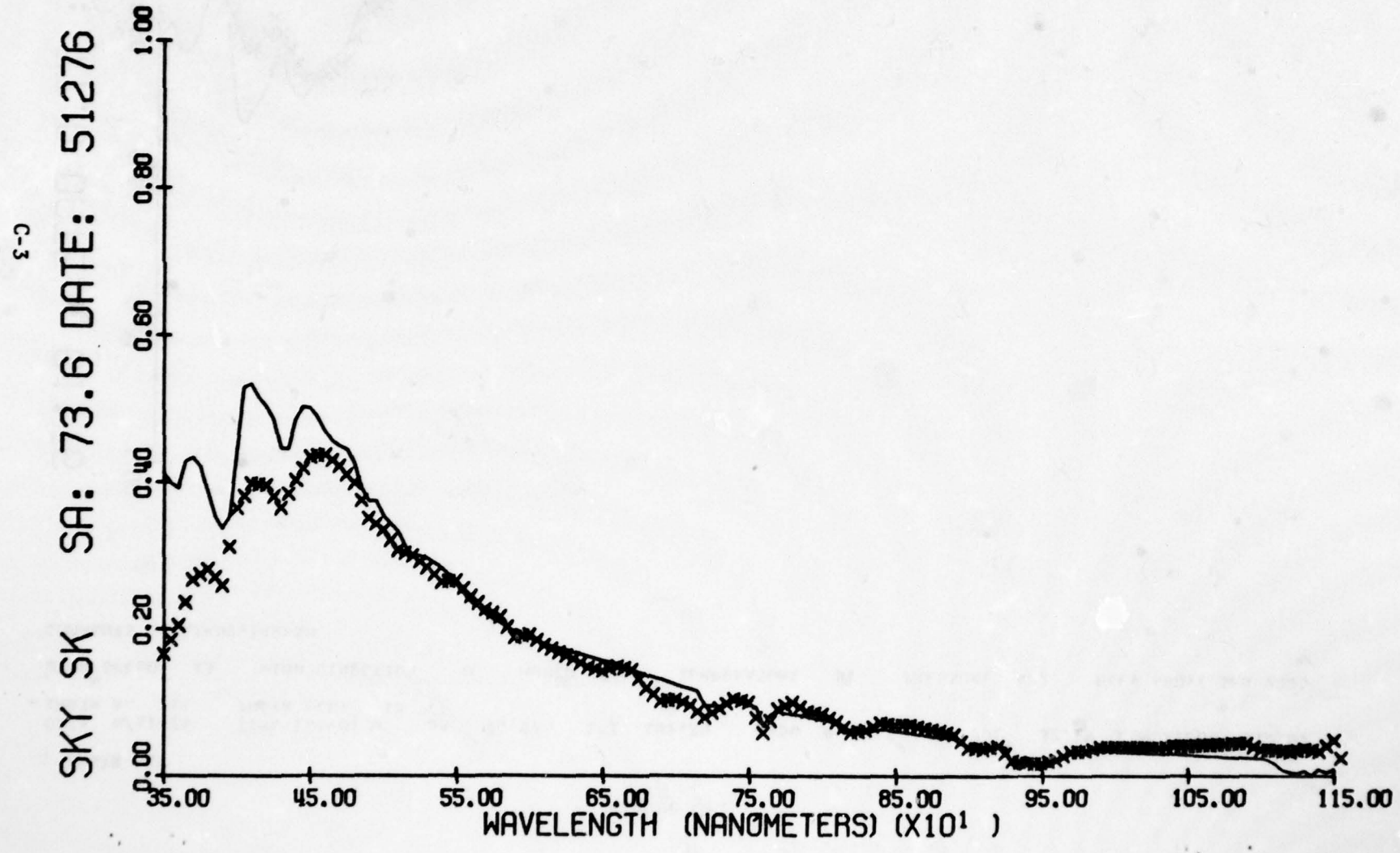

Figure C-3

INSTR SKY

DATA 5/12/76 TIME 20:25: 0 SA 72.54 SAZ 201.60 T650 0.07 LATITUDE 34.75 LONGITUDE -120.57
INSTR AZ 22 INSTR ELEV 17

WIND SPEED 36 WIND DIRECTION 0 HUMID 424 TEMPERATURE 80 PRESSURE 1003 ELEV ABOVE SEA 327

COMMENTS 3,IR1=SV0,IR2=SH

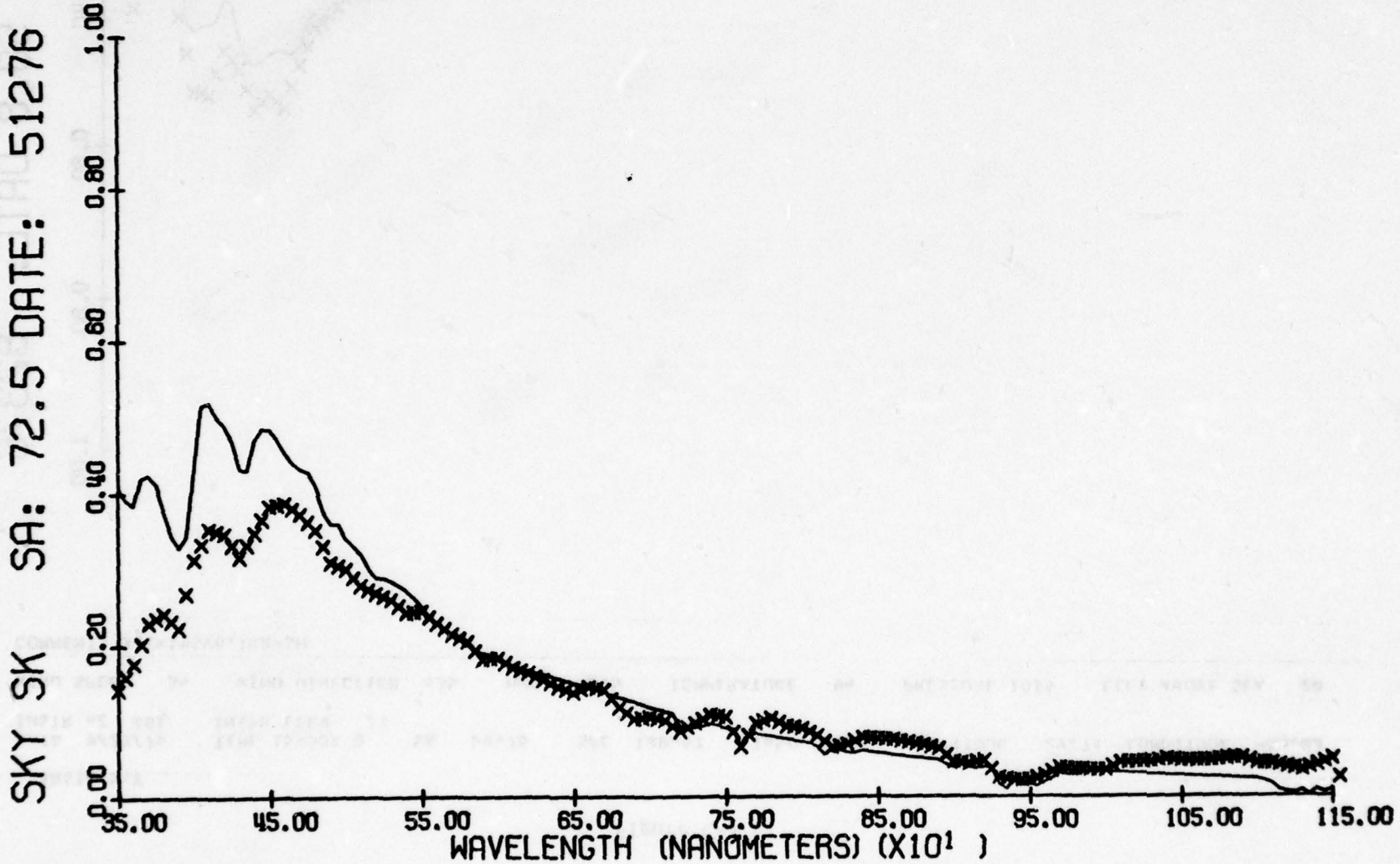

Figure C-4

INSTR SKY

DATA 8/23/76 TIME 15:55: 0 SA 58.76 SAZ 120.67 T650 0.57 LATITUDE 29.73 LONGITUDE -95.03
INSTR AZ 301 INSTR ELEV 31

WIND SPEED 34 WIND DIRECTION 335 HUMID 375 TEMPERATURE 94 PRESSURE 1015 ELEV ABOVE SEA 20

COMMENTS 3,IR1=SV8,IR2=SH

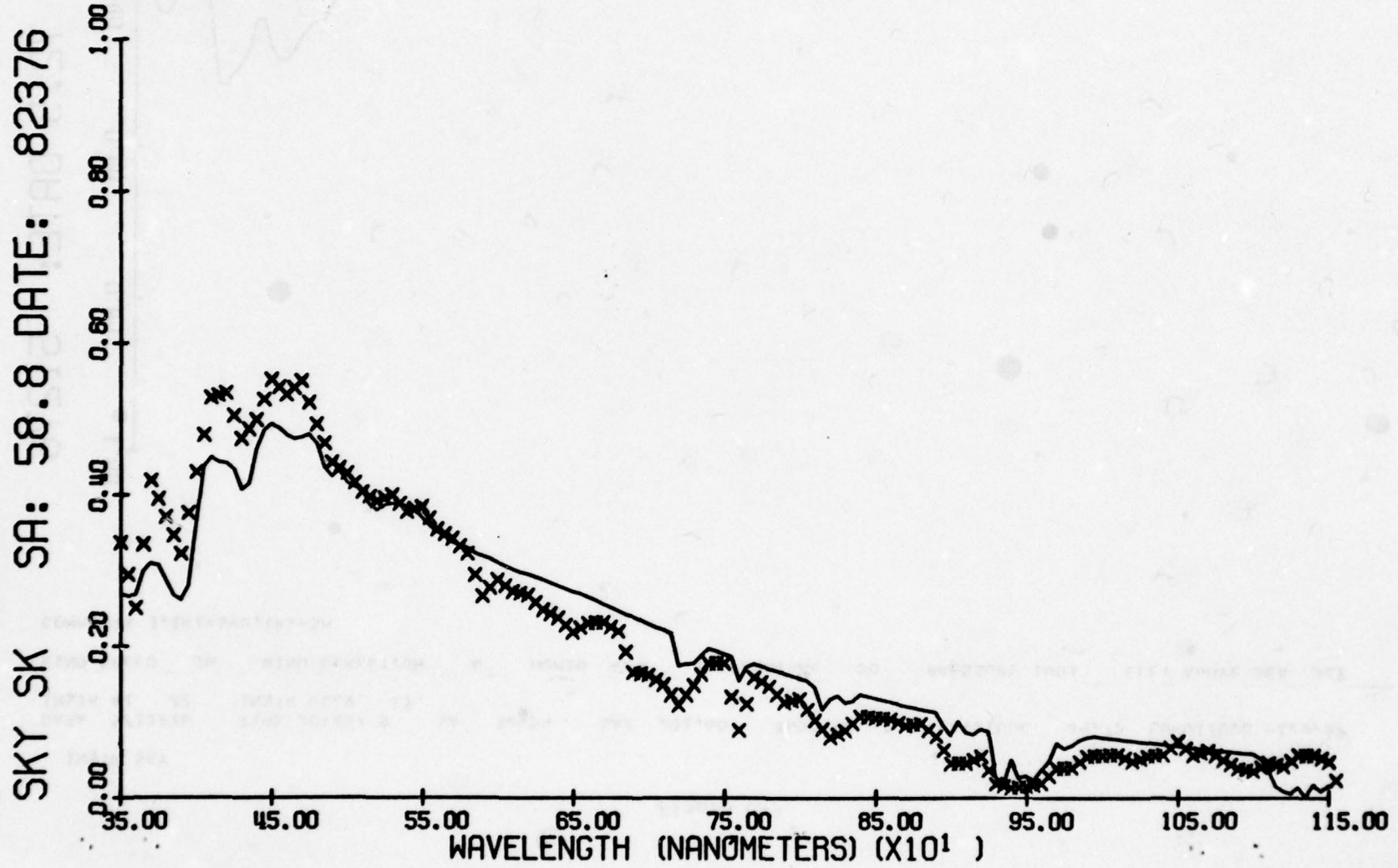

Figure C-5

INSTR SKY

DATA 8/23/76 TIME 12:25: 0 SA 52.94 SAZ 112.62 TAU 0.60 LATITUDE 29.73 LONGITUDE -95.03
INSTR AZ 293 INSTR ELEV 37

WIND SPEED 50 WIND DIRECTION 308 HUMID 403 TEMPERATURE 93 PRESSURE 1015 ELEV ABOVE SEA 40

COMMENTS 3,IR1=DV,IR2=UH

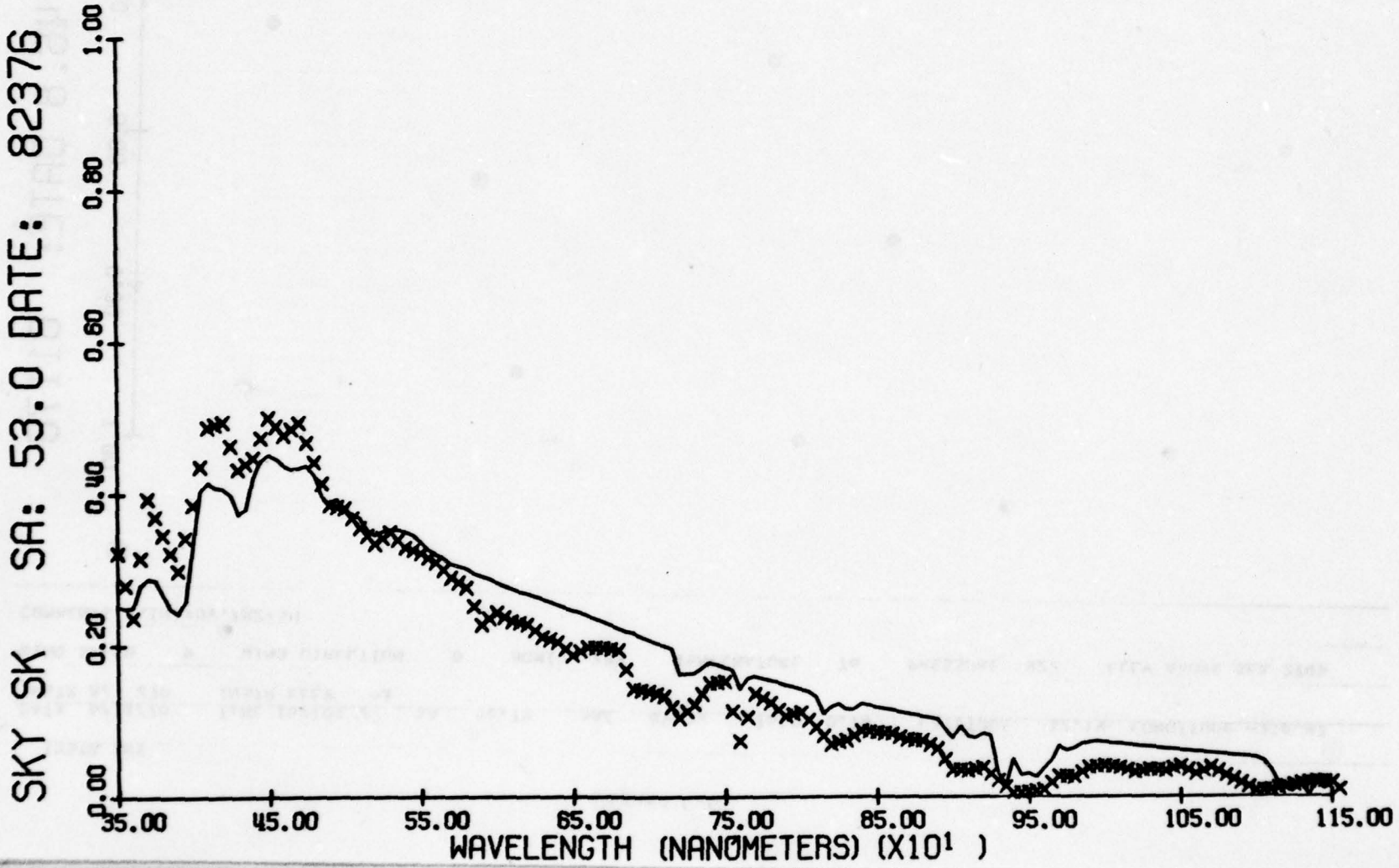

Figure C-6

INSTR SKY

DATA 6/11/76 TIME 10:10: 0 SA 46.79 AMZ 84.34 I650 0.74 LATITUDE 32.19 LONGITUDE -110.87
INSTR AZ 270 INSTR ELEV 43

WIND SPEED 9 WIND DIRECTION 0 HUMID 283 TEMPERATURE 76 PRESSURE 922 ELEV ABOVE SEA 2705

COMMENTS 3,IR1=DV,IR2=SH

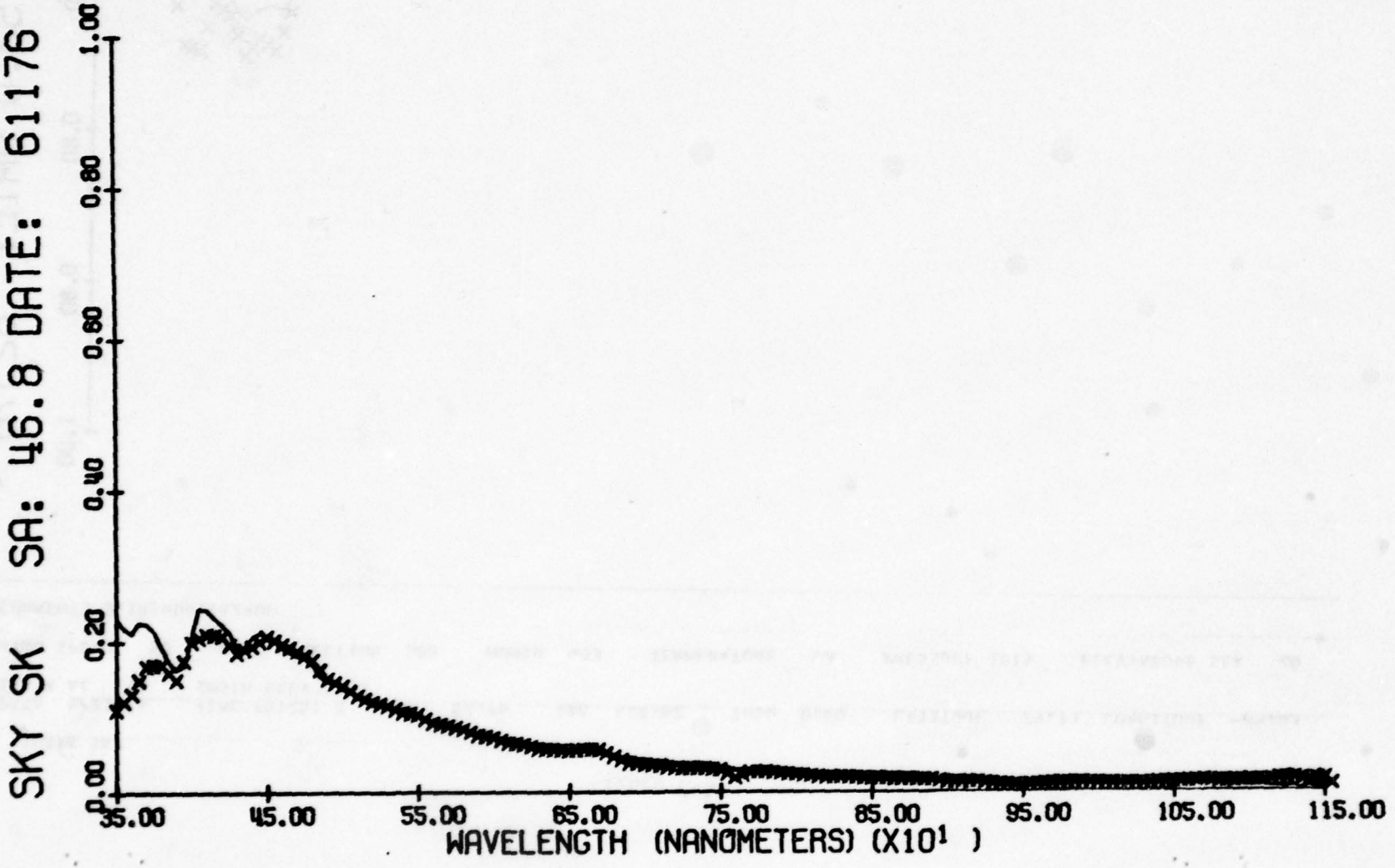

Figure C-7

INSTR SKY

DATA 7/21/76 TIME 13: 0: 0 SA 45.00 SAZ 92.01 TAU 0.27 LATITUDE 34.92 LONGITUDE -92.15
INSTR AZ 270 INSTR ELEV 45

WIND SPEED 50 WIND DIRECTION 252 HUMID 580 TEMPERATURE 89 PRESSURE 1005 ELEV ABOVE SEA 311

COMMENTS 3,IR1=SVB,IR2=DH

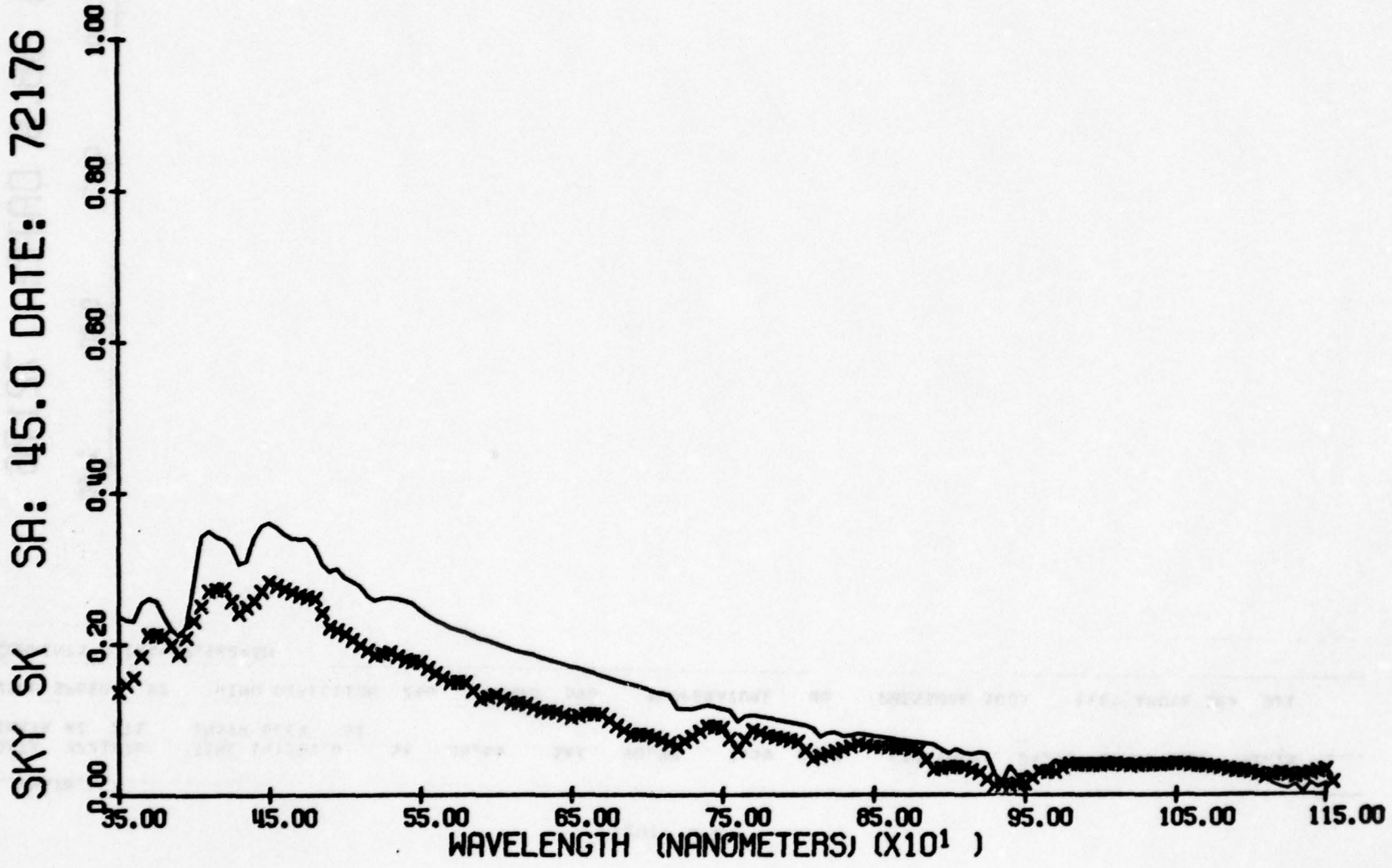

Figure C-8

INSTR SKY

DATA 7/21/76 TIME 14:30:0 6 SA 38.66 SAZ 90.99 T650 0.58 LATITUDE 34.92 LONGITUDE -92.15
INSTR AZ 271 INSTR ELEV 51

WIND SPEED 52 WIND DIRECTION 248 HUMID 59% TEMPERATURE 88 PRESSURE 1005 ELEV ABOVE SEA 311

COMMENTS 3,IR1=UV,IR2=SW

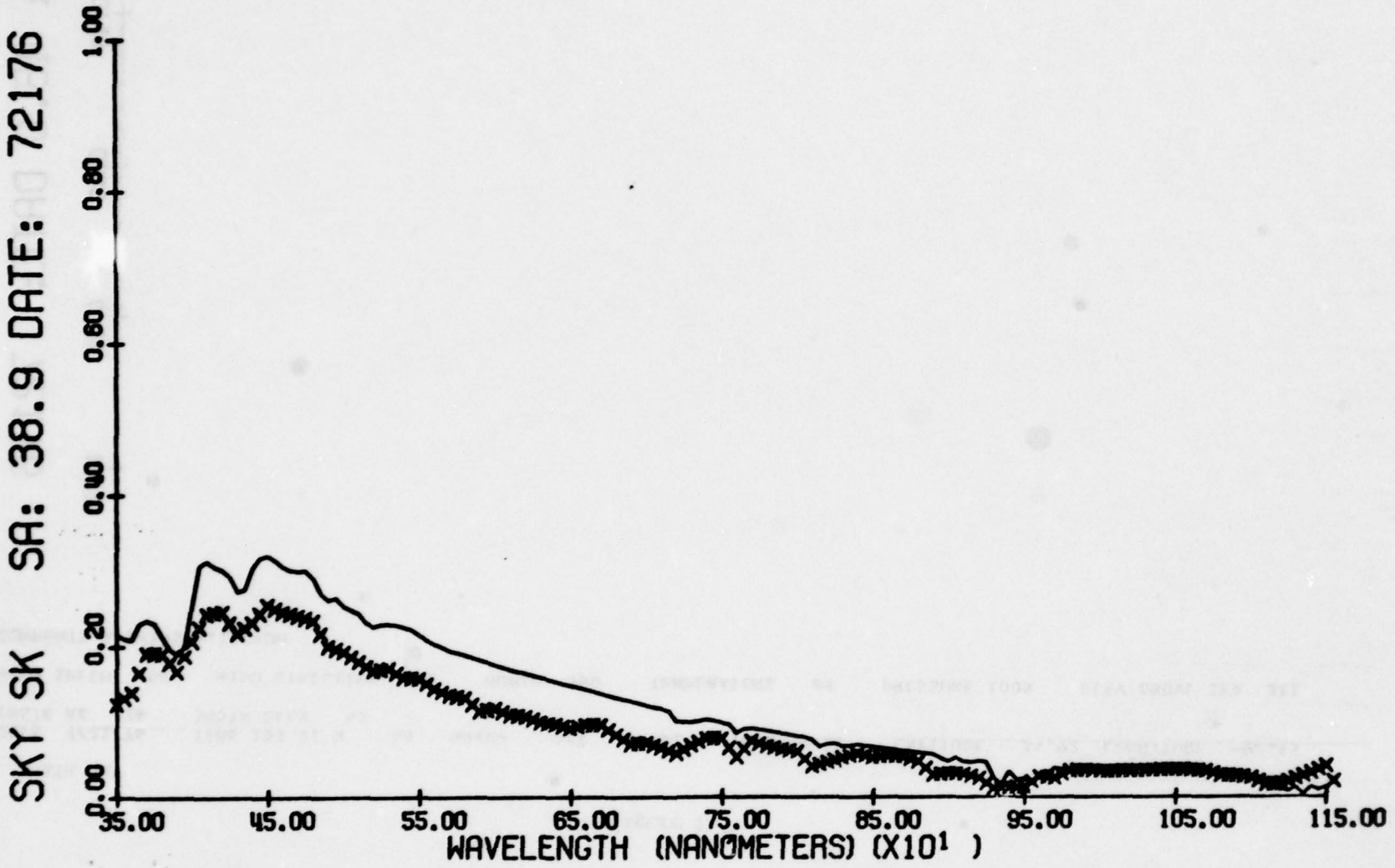

Figure C-9

INSTR SKY

DATA 5/12/76 TIME 23:46: 0 SA 36.46 SAZ 266.48 To50 0.73 LATITUDE 34.75 LONGITUDE =120.57
INSTR AZ 86 INSTR ELEV 52

WIND SPEED 20 WIND DIRECTION 0 HUMID 40% TEMPERATURE 81 PRESSURE 1003 ELEV ABOVE SEA 327

COMMENTS 3,IR1=UM,IR2=DV

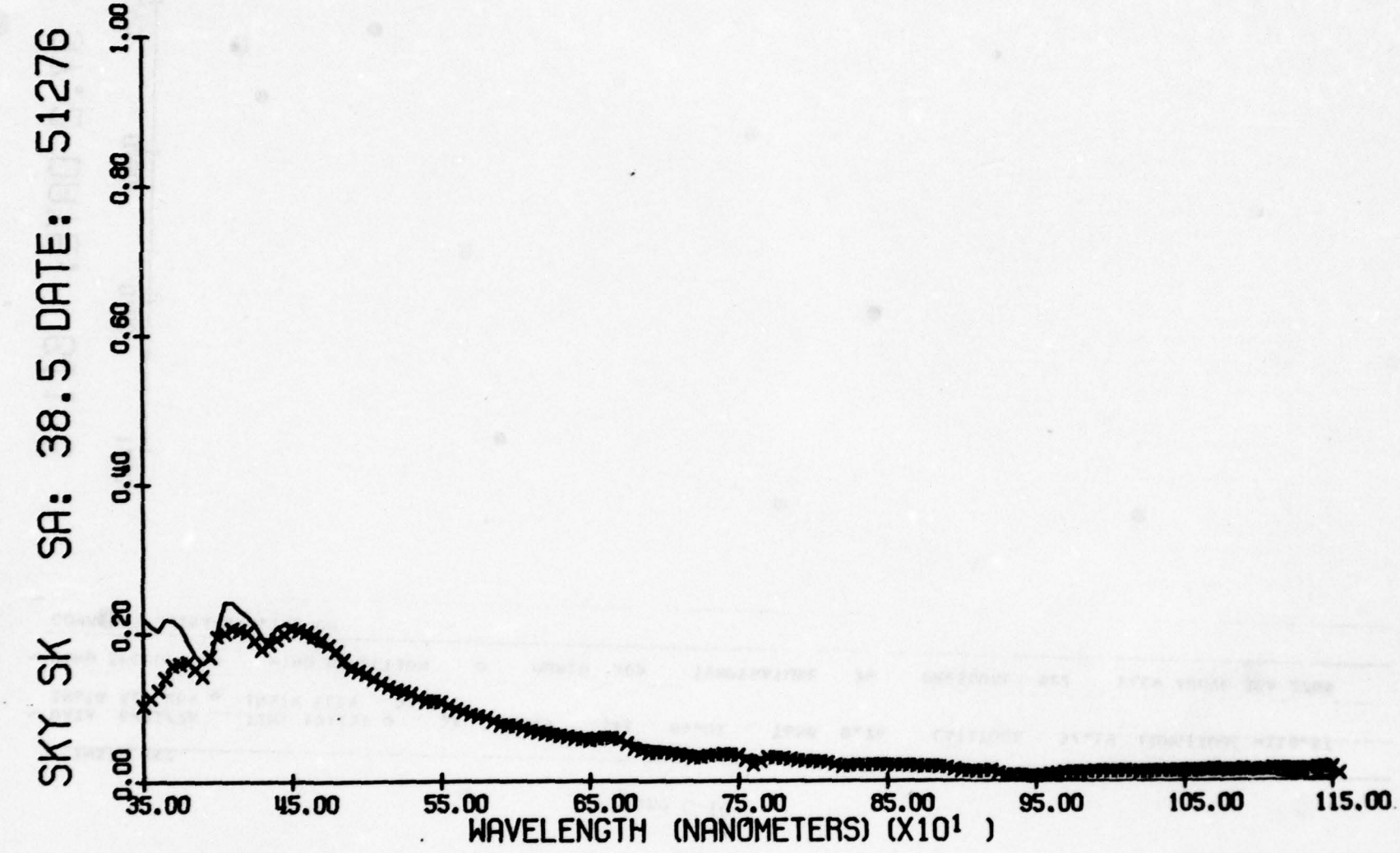

Figure C-10

INSTR SKY

DATA 6/11/76 TIME 15:25: 0 SA 37.29 SAZ 84.01 T650 0.76 LATITUDE 32.19 LONGITUDE =110.87
INSTR AZ 264 INSTR ELEV 53

WIND SPEED 0 WIND DIRECTION 0 HUMID 305 TEMPERATURE 74 PRESSURE 922 ELEV ABOVE SEA 2705

COMMENTS 3,IR1=SVB,IR2=DM

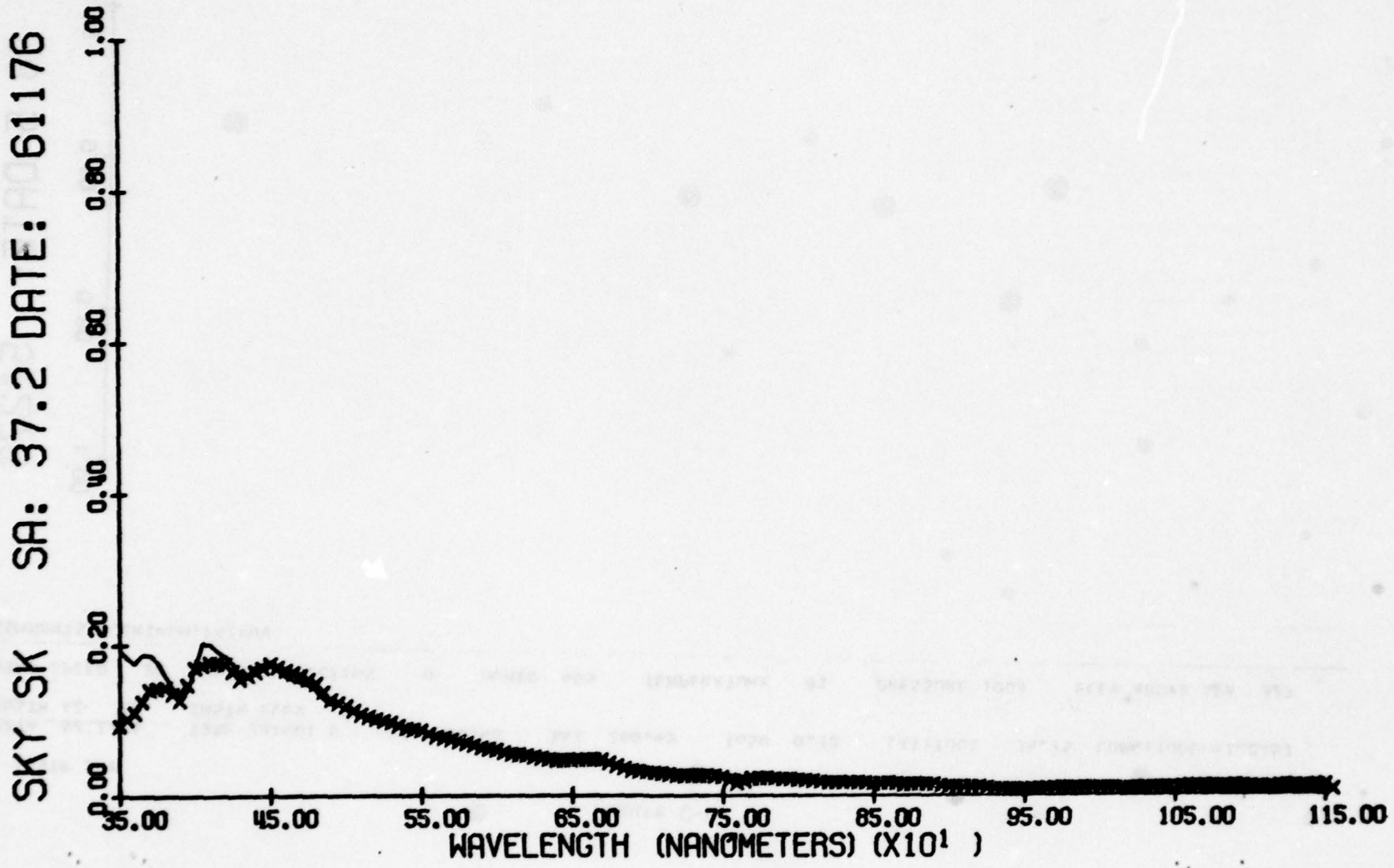

Figure C-11

INSTR SKY

DATA 5/13/76 TIME 0:10: 6 SA 32.30 SAZ 270.87 T650 0.74 LATITUDE 34.75 LONGITUDE =120.57
INSTR AZ 91 INSTR ELEV 25

WIND SPEED 22 WIND DIRECTION 0 HUMID 403 TEMPERATURE 82 PRESSURE 1003 ELEV ABOVE SEA 327

COMMENTS 3,IR1=SM,IR2=SVB

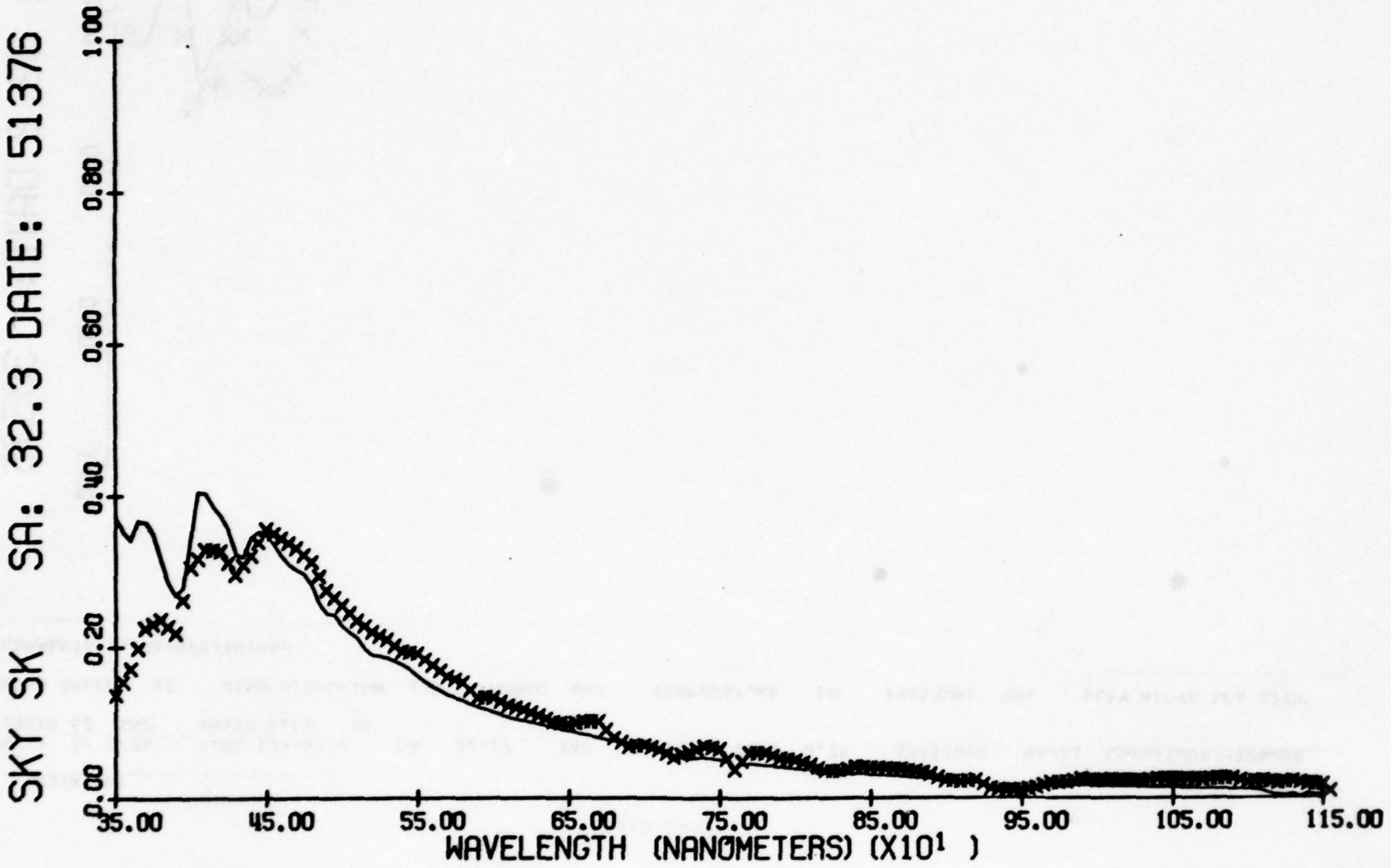

Figure C-12

INSTR SKY

DATA 3/ 5/76 TIME 17:45: 0 SA 32.17 SAZ 152.22 T450 0.75 LATITUDE 90.22 LUNGITUDE -104.02
INSTR AZ 332 INSTR ELEV 26

WIND SPEED 21 WIND DIRECTION 135 HUMID 662 TEMPERATURE 10 PRESSURE 936 ELEV ABOVE SEA 2279

COMMENTS 3,IR1=SVB,IR2=SH

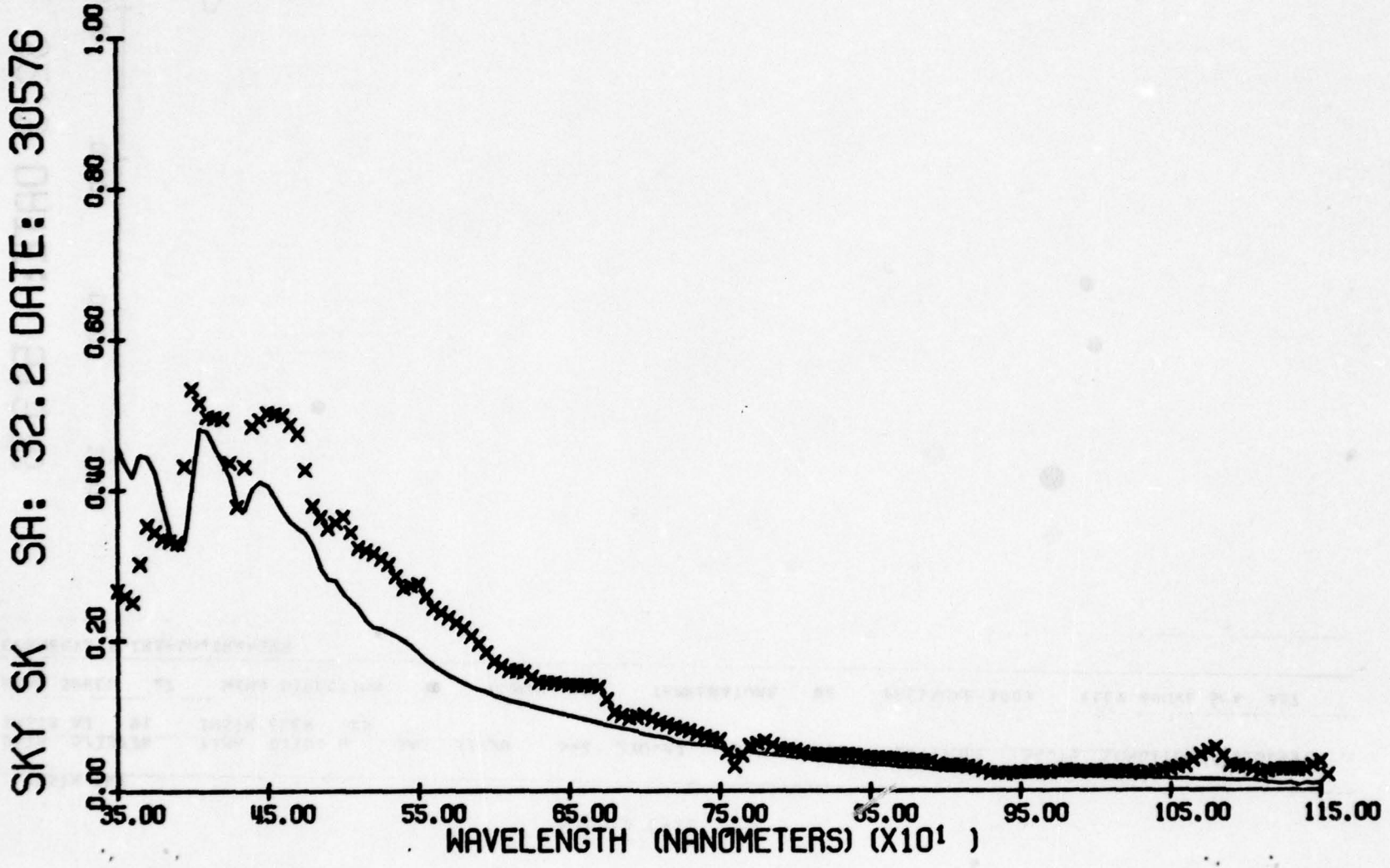

Figure C-13

INSTR SKY

DATA 3/ 5/76 TIME 17:15: 0 SA 69.23 SAZ 144.09 To>0 0.77 LATITUDE 46.22 LONGITUDE -104.62
INSTR AZ 324 INSTR ELEV 31

WIND SPEED 5 WIND DIRECTION 157 HUMID 66% TEMPERATURE 9 PRESSURE 936 ELEV ABOVE SEA 2279

COMMENTS 3,IR1=UV,IR2=UM

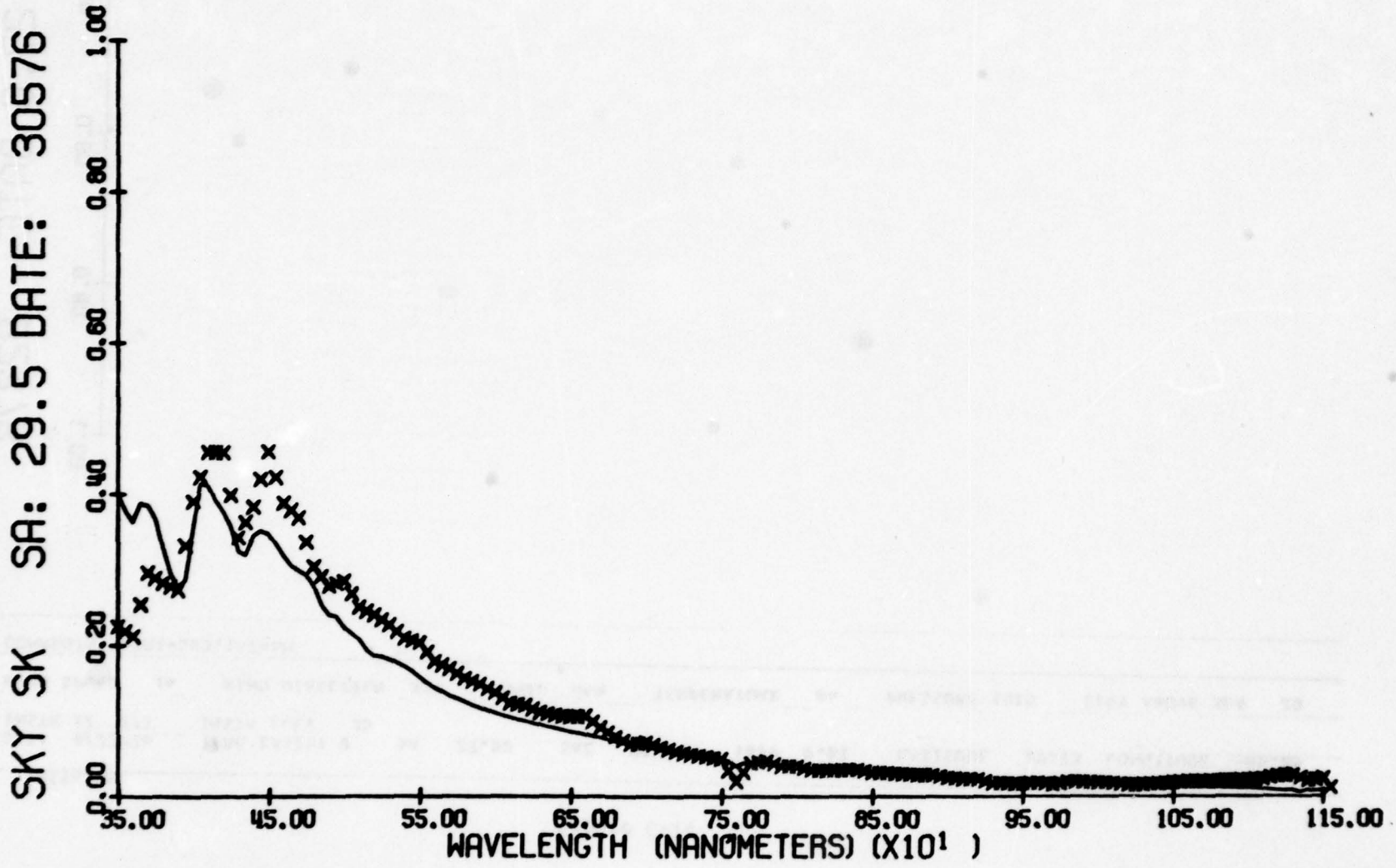

Figure C-14

INSTR SKY

DATA 8/23/7e TIME 13:25: 0 SA 27.58 SAZ 92.57 Tau50 0.61 LATITUDE 29.73 LONGITUDE -95.83
INSTR AZ 273 INSTR ELEV 35

WIND SPEED 16 WIND DIRECTION 334 HUMID 644 TEMPERATURE 84 PRESSURE 1015 ELEV ABOVE SEA 20

COMMENTS 3,IR1=SVB,IR2=SH

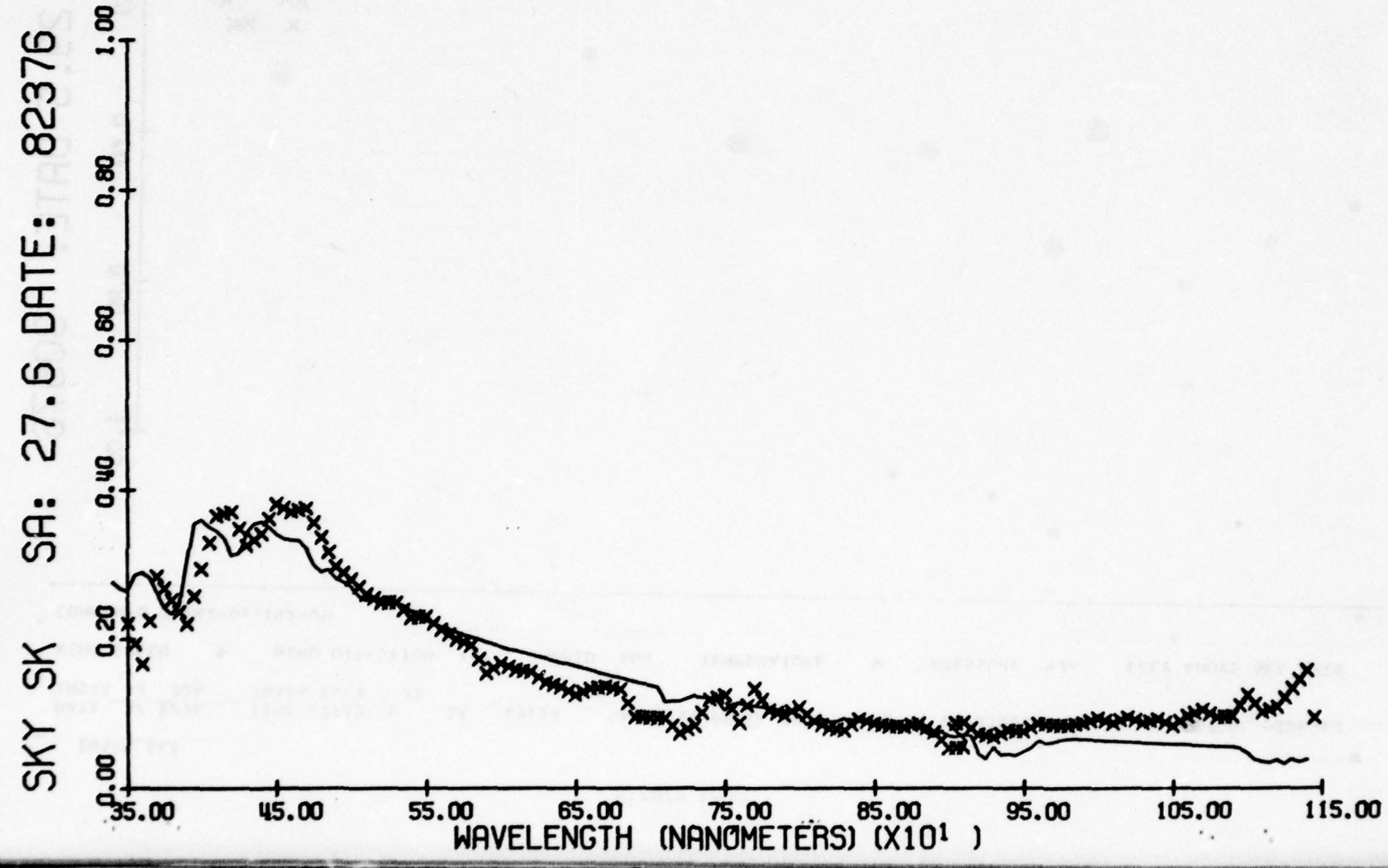

Figure C-15

INSTR SKY

DATA 8/23/76 TIME 12:55: 0 SA 21.07 SAZ 88.80 TAU 0.59 LATITUDE 29.73 LONGITUDE -85.03
INSTR AZ 269 INSTR ELEV 48

WIND SPEED 24 WIND DIRECTION 339 HUMID 706 TEMPERATURE 81 PRESSURE 1015 ELEV ABOVE SEA 20

COMMENTS 3,IR1=DV,IR2=DH

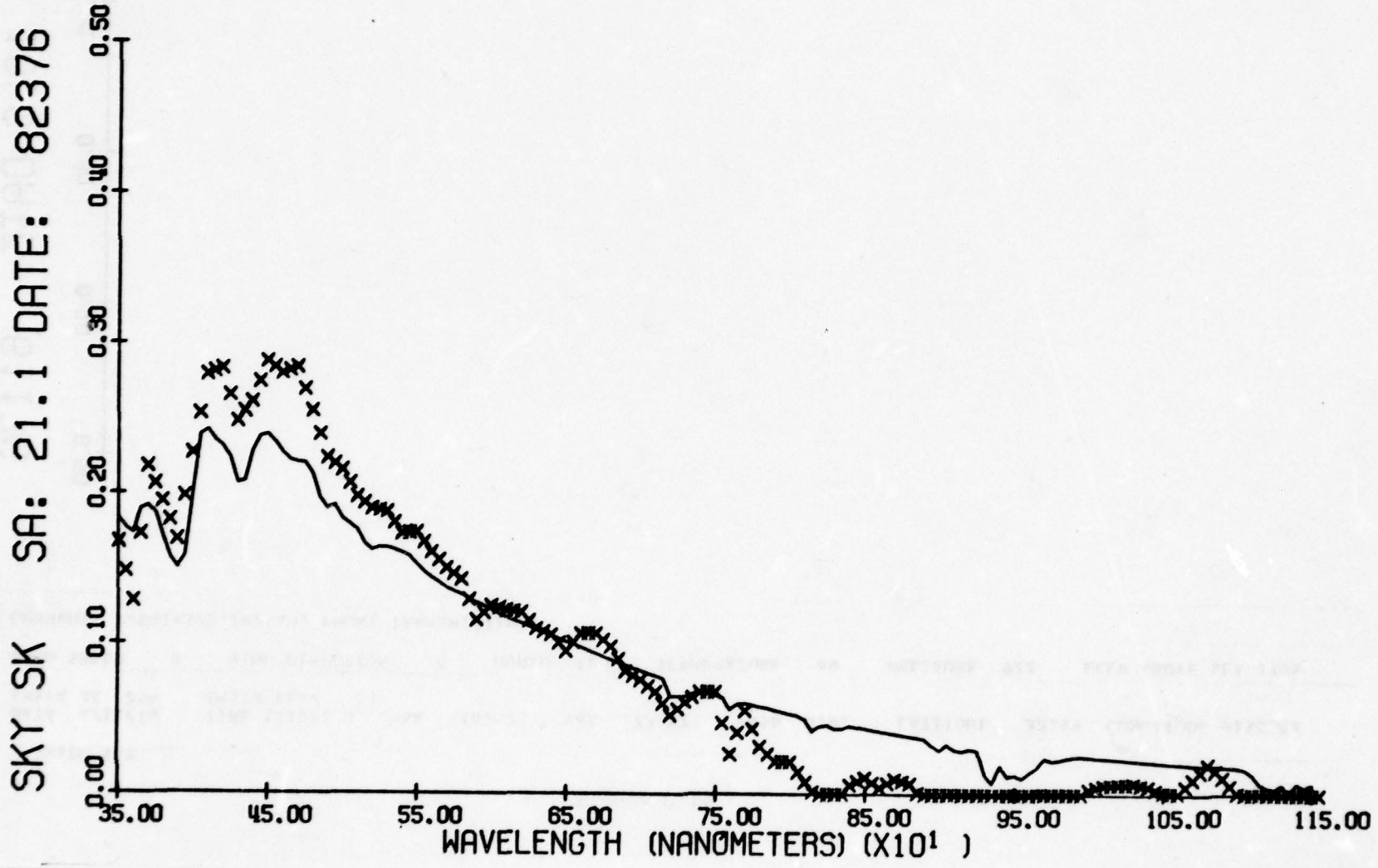

Figure C-16

INSTR SKY

DATA 6/11/76 TIME 13:55:0.0 SA 18.62 SAZ 73.87 1650 0.82 LATITUDE 32.19 LONGITUDE =110.87
INSTR AZ 254 INSTR ELEV 53

WIND SPEED 0 WIND DIRECTION 0 HUMID 310 TEMPERATURE 69 PRESSURE 922 ELEV ABOVE SEA 2705

COMMENTS 2,1R1=SVB,1R2=SH, PHONE TRANSMITTANCE

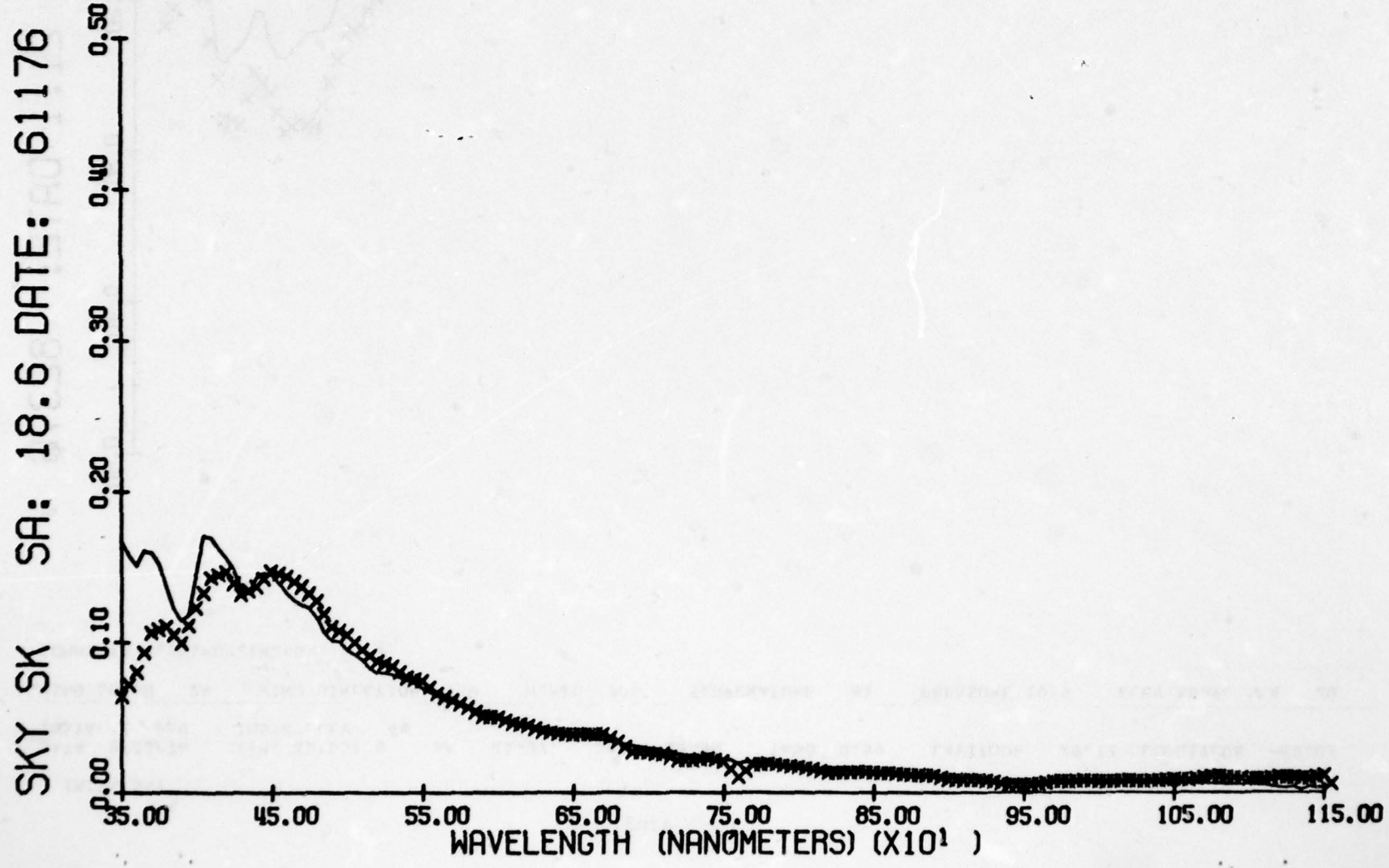

Figure C-17

INSTR SKY

DATA 7/21/76 TIME 12:30: 0 SA 14.54 SAZ 75.05 To50 0.62 LATITUDE 34.92 LONGITUDE -92.15
INSTR AZ 255 INSTR ELEV 61

WIND SPEED 16 WIND DIRECTION 245 HUMID 28 TEMPERATURE 81 PRESSURE 1005 ELEV ABOVE SEA 311

COMMENTS 3,IR1=SVB,IR2=DH

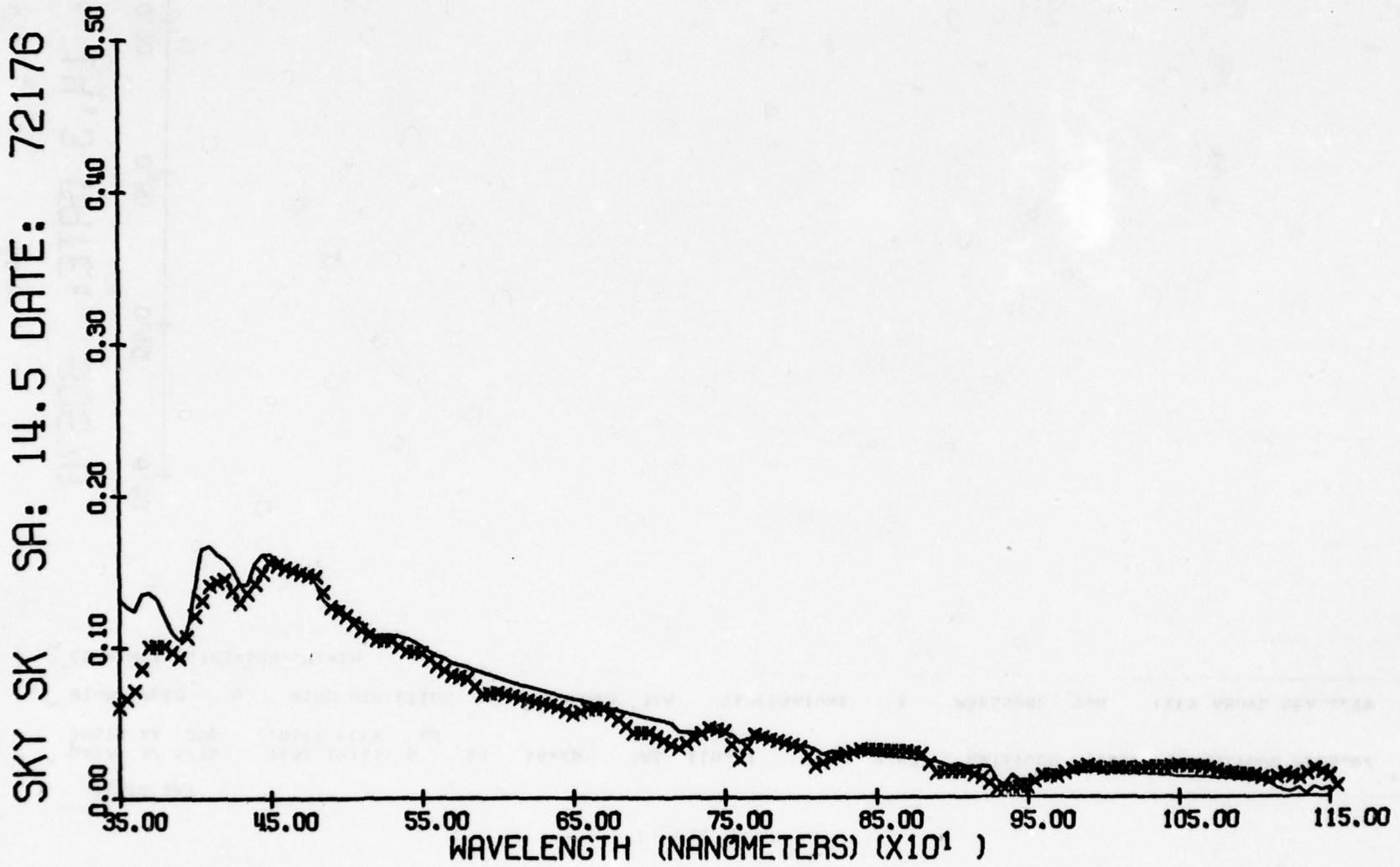

Figure C-18

INSTR SAT

DATA 3/ 5/76 TIME 15:15: 0 SA 14.25 SAZ 110.31 TAU 0.02 LATITUDE 48.22 LONGITUDE -100.62
INSTR AZ 296 INSTR ELEV 62

WIND SPEED 0 WIND DIRECTION 152 HUMID 72% TEMPERATURE 1 PRESSURE 930 ELEV ABOVE SEA 2279

COMMENTS 3,IR1=SVB,IR2=SH

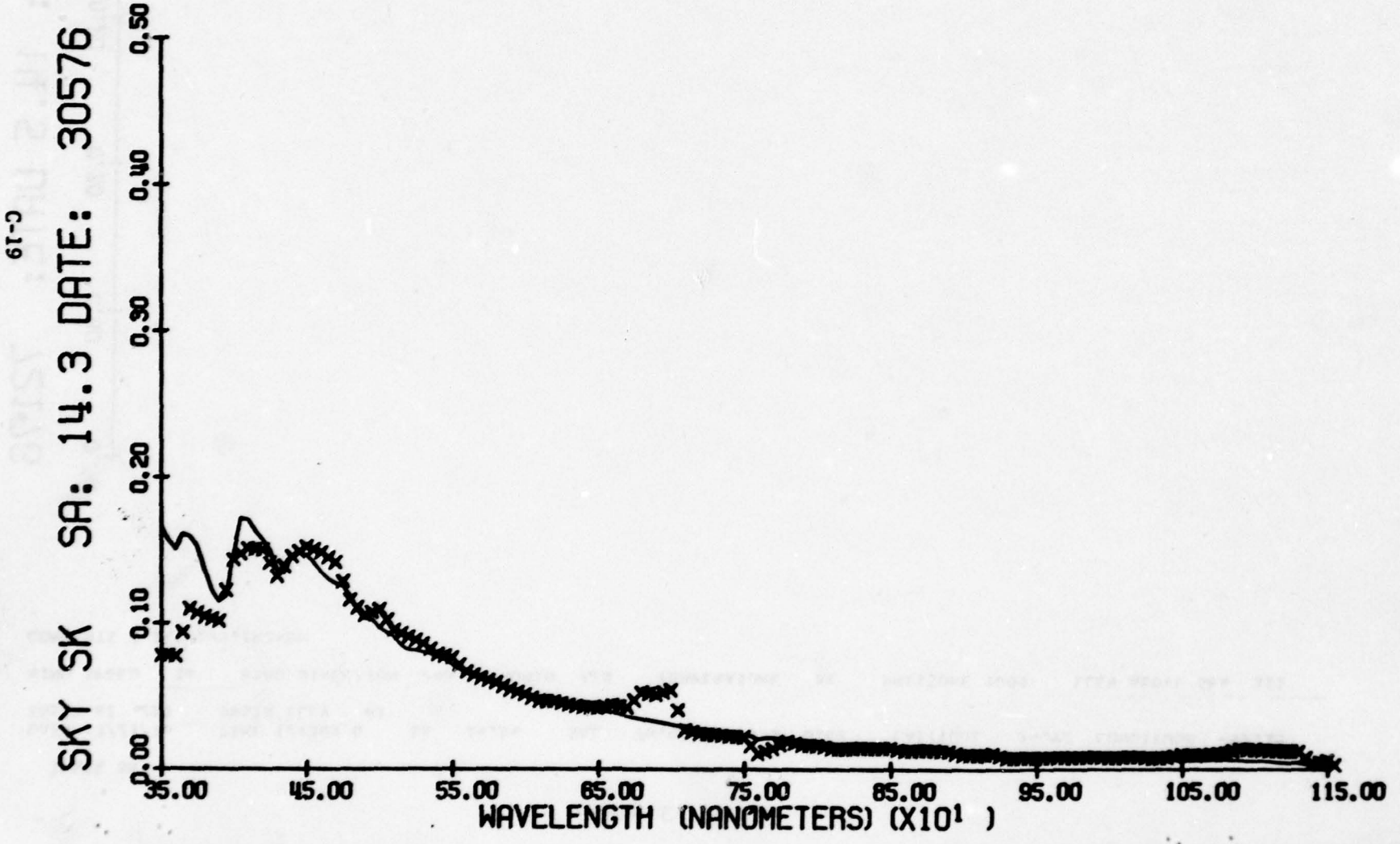

Figure C-19

INSIR SKY

DATA 5/13/76 TIME 1340: 0 SA 13.99 SAZ 282.87 1650 0.80 LATITUDE 34.75 LONGITUDE -120.57
INSTR AZ 103 INSTR ELEV 62

WIND SPEED 0 WIND DIRECTION 0 HUMID 425 TEMPERATURE 80 PRESSURE 1003 ELEV ABOVE SEA 327

COMMENTS 3,IR1=OH,IR2=SVB

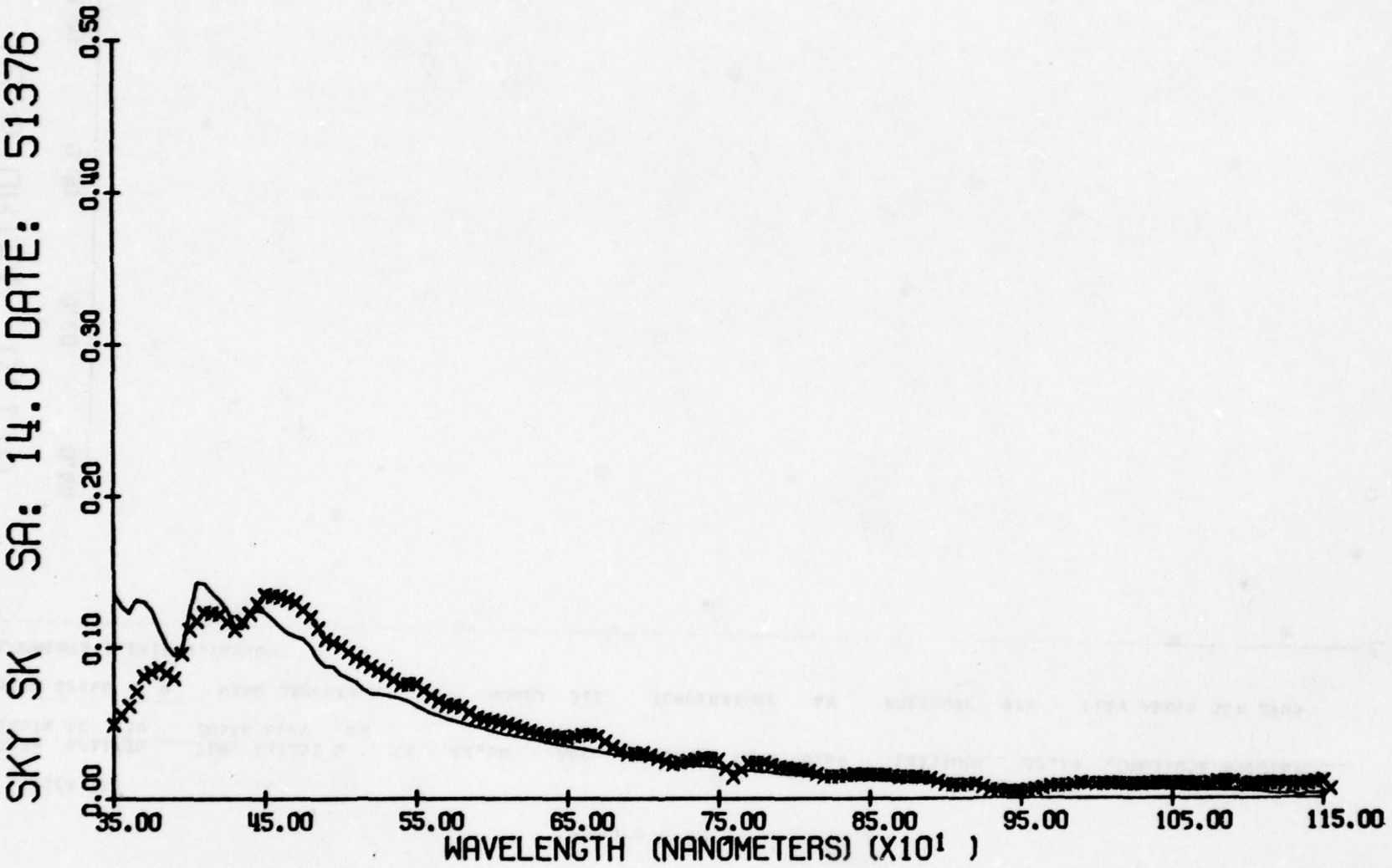

Figure C-20

INSTR SKY

DATA 6/11/76 TIME 13:25:6 SA 12.56 SAZ 70.41 1650 0.84 LATITUDE 32.12 LONGITUDE =110.87
INSTR AZ 250 INSTR ELEV 65

WIND SPEED 0 WIND DIRECTION 0 HUMID 311 TEMPERATURE 68 PRESSURE 922 ELEV ABOVE SEA 2705

COMMENTS 3,IR1=0V,IR2=0M

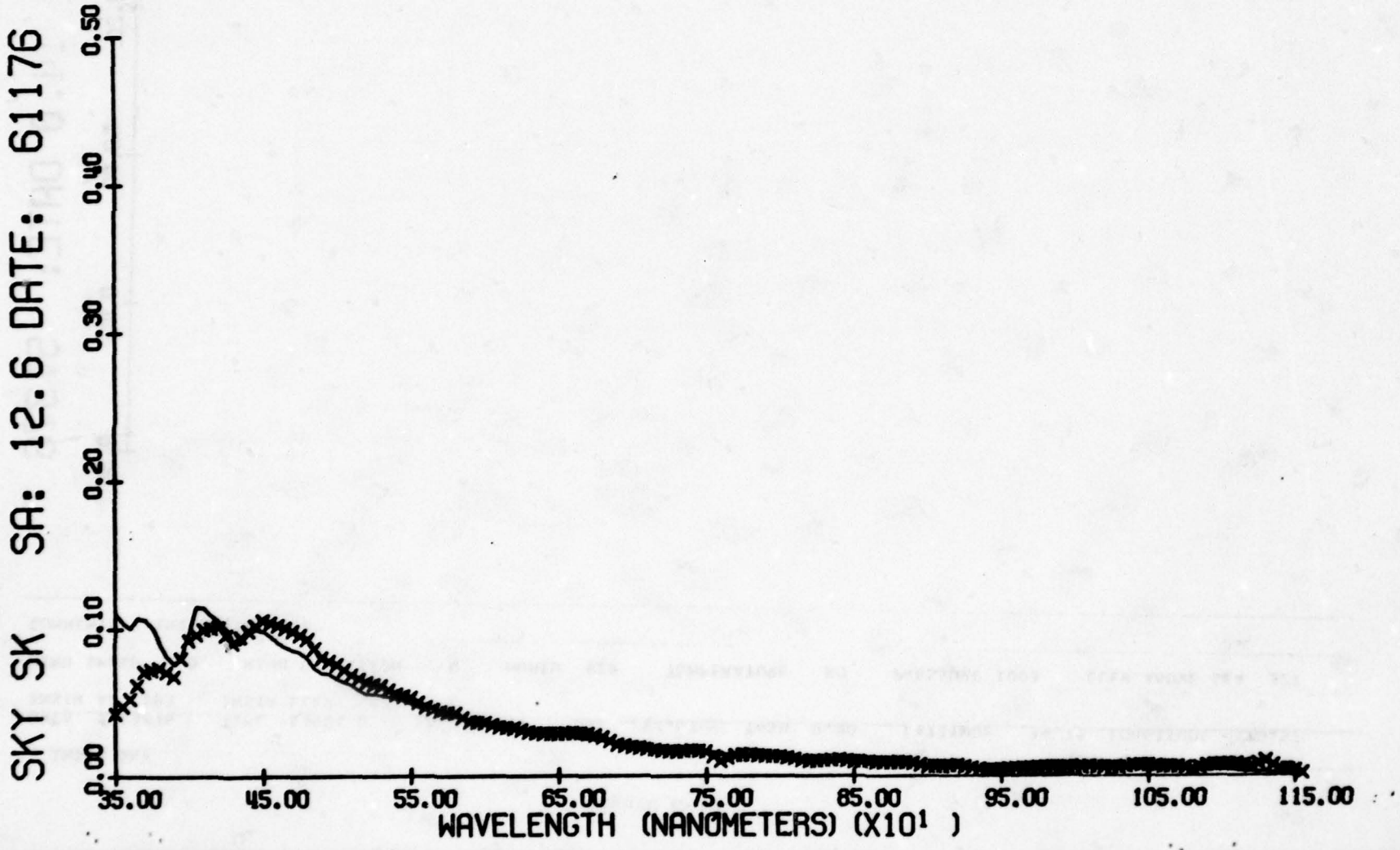

Figure C-21

INSTR SAV

DATA 5/13/76 TIME 18553 0 SA 11.00 SAZ 284.05 T650 0.81 LATITUDE 34.75 LONGITUDE -120.57
INSTR AZ 105 INSTR ELEV 68

WIND SPEED 0 WIND DIRECTION 0 HUMID 41% TEMPERATURE 79 PRESSURE 1003 ELEV ABOVE SEA 327

COMMENTS 3,IR1=SH,IR2=DH

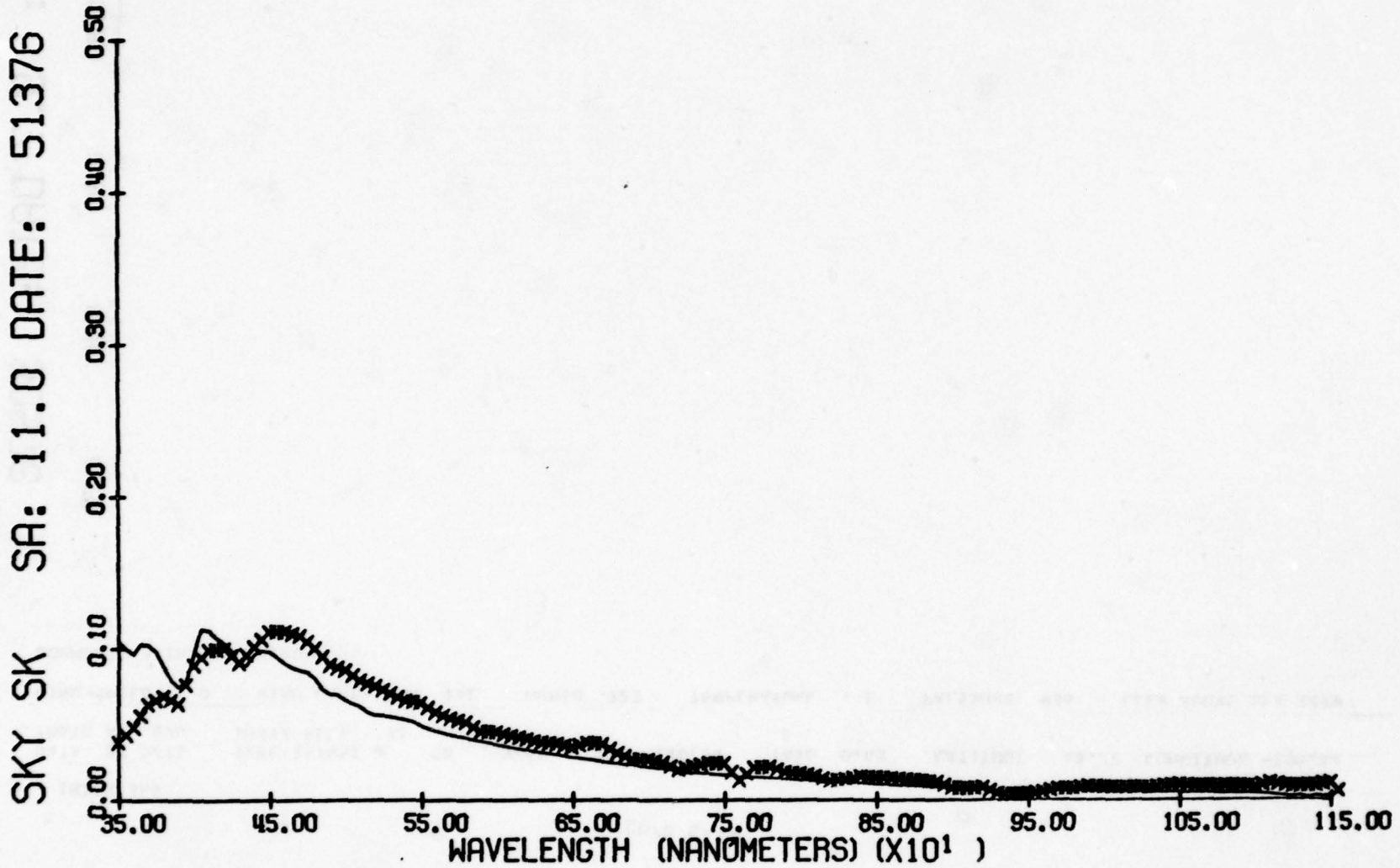

Figure C-22

INSTR SKY

DATA 3/ 5/76 TIME 14:45:0 0 SA 9.65 SAZ 110.30 T650 0.63 LATITUDE 48.22 LONGITUDE -106.62
INSTR AZ 290 INSTR ELEV 71

WIND SPEED 0 WIND DIRECTION 162 HUMID 727 TEMPERATURE 1 PRESSURE 936 ELEV ABOVE SEA 2279

COMMENTS 3,IR1=DV,IR2=DH

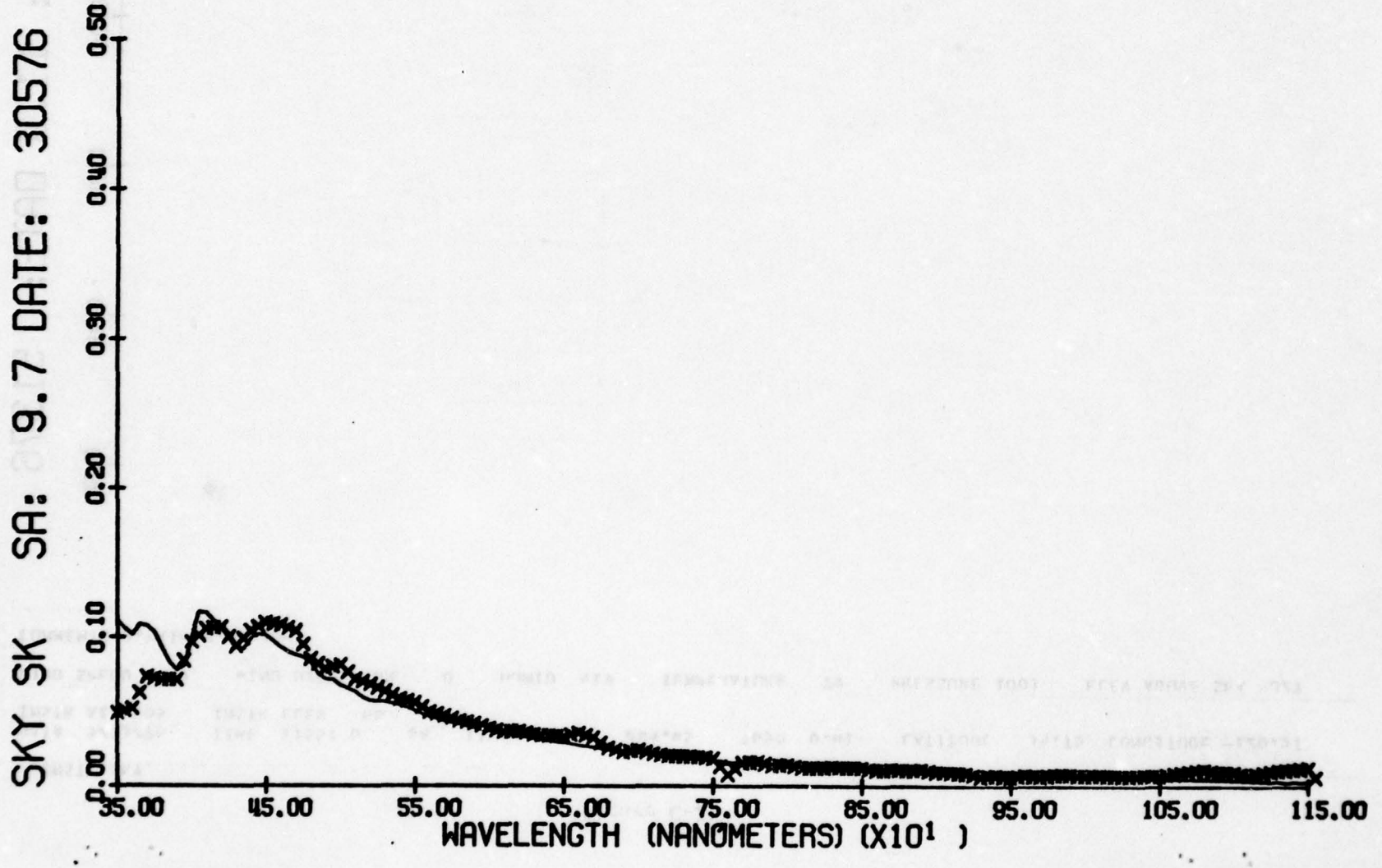

Figure C-23

INSTR SKY

DATA 7/21/76 TIME 12: 0: 9 SA 8.00 SAZ 71.12 To50 0.64 LATITUDE 34.92 LONGITUDE -92.15
INSTR AZ 251 INSTR ELEV 73

WIND SPEED 0 WIND DIRECTION 222 HUMID 76% TEMPERATURE 79 PRESSURE 1005 ELEV ABOVE SEA 311

COMMENTS 3,IR1=DV,IR2=SH

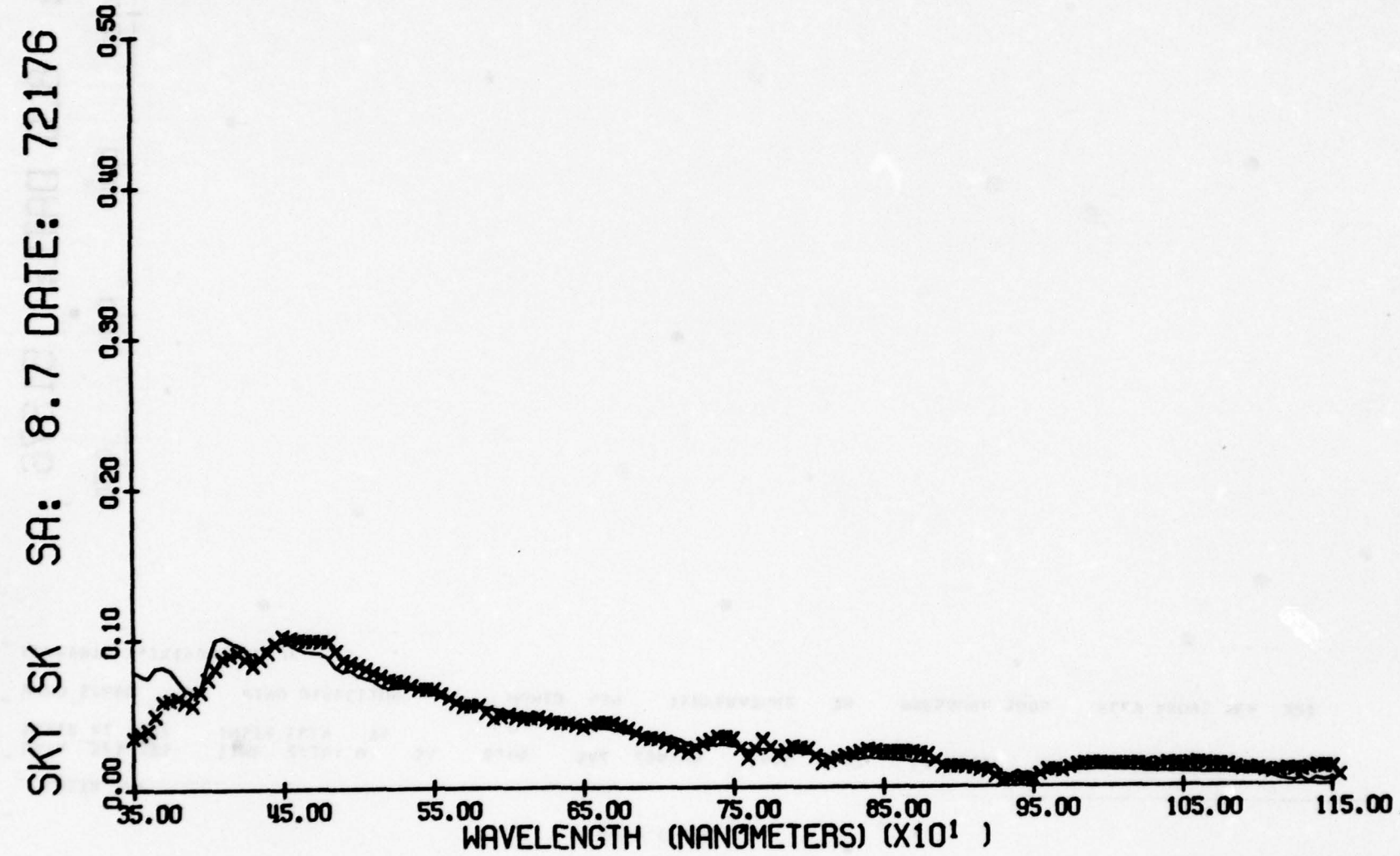

Figure C-24

INSTR SKY

DATA 5/13/76 TIME 2:10: 0 SA 8.04 SAZ 280.04 1050 0.82 LATITUDE 34.75 LONGITUDE -120.57
INSTR AZ 107 INSTR ELEV 74

WIND SPEED 0 WIND DIRECTION 0 HUMID 439 TEMPERATURE 78 PRESSURE 1003 ELEV ABOVE SEA 327

COMMENTS 3,IR1=DM,IR2=DV

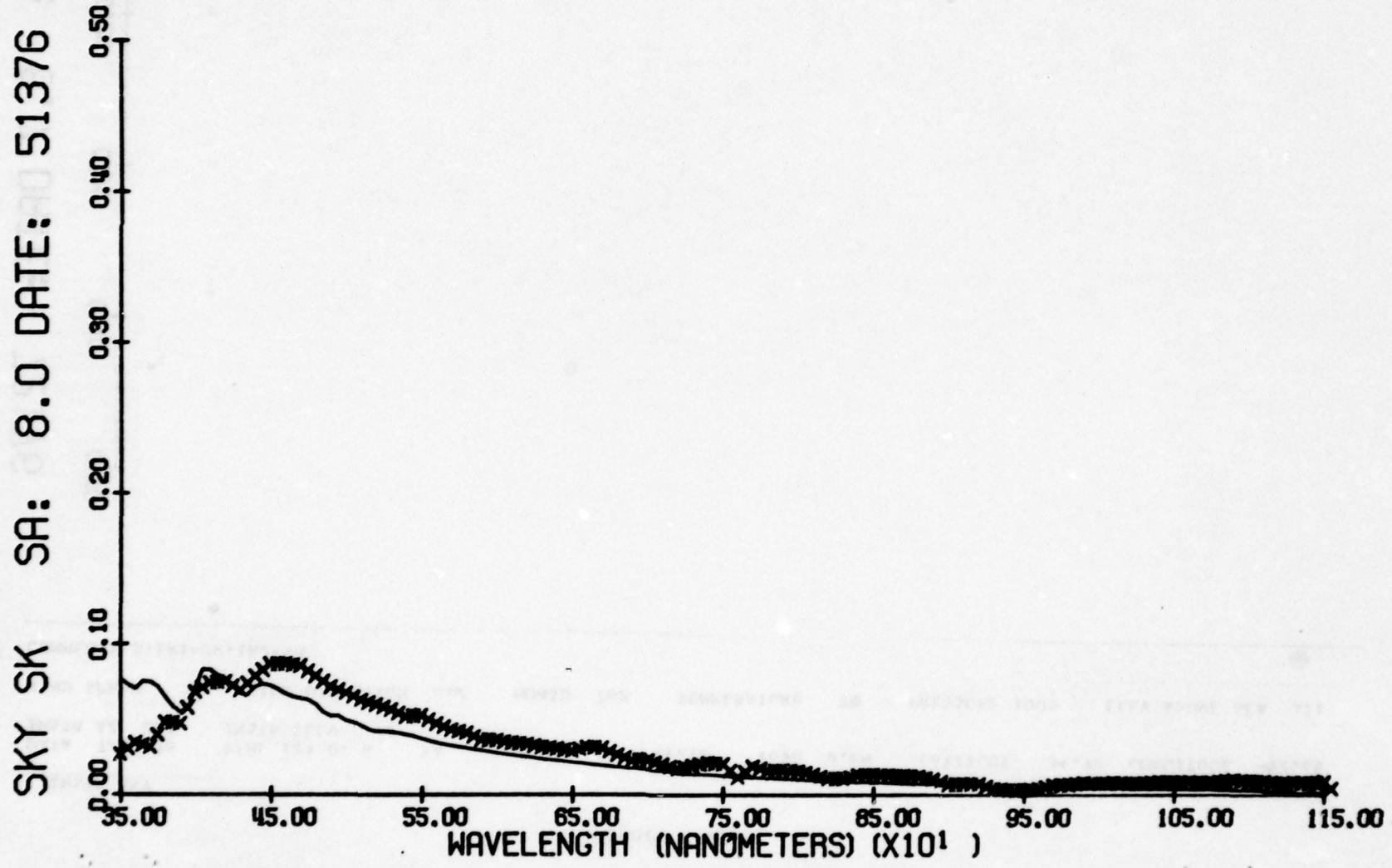

Figure C-25

INSTR SKY

DATA 4/27/76 TIME 21:20:0.0 SA 2.96 SAZ 282.90 TAU50 0.83 LATITUDE 37.78 LONGITUDE -122.42
INSTR AZ 103 INSTR ELEV 70

WIND SPEED 53 WIND DIRECTION 289 HUMID 37% TEMPERATURE 69 PRESSURE 888 ELEV ABOVE SEA 15

COMMENTS 3,IR1=SH,IR2=DV

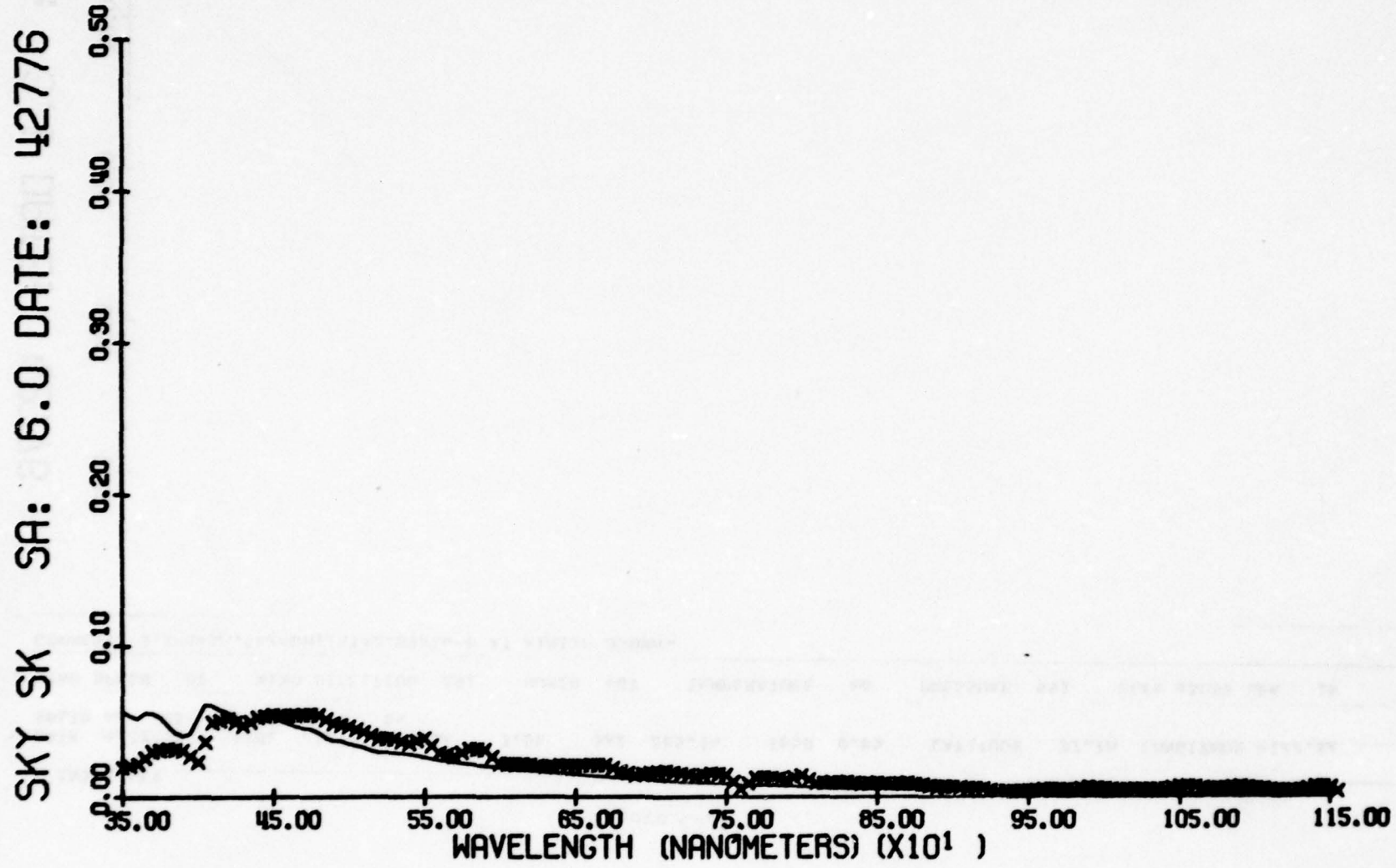

Figure C-28

INSTR SKY

DATA 4/27/76 TIME 21358 0 SA 3.08 SAZ 285.14 T650 0.85 LATITUDE 37.78 LONGITUDE =122.34
INSTR AZ 105 INSTR ELEV 84

WIND SPEED 08 WIND DIRECTION 291 HUMID 407 TEMPERATURE 66 PRESSURE 891 ELEV ABOVE SEA 15

COMMENTS 3,IR1=SH,IR2=OH,IR1=2.09X10-8 AT FINISH 350NM.

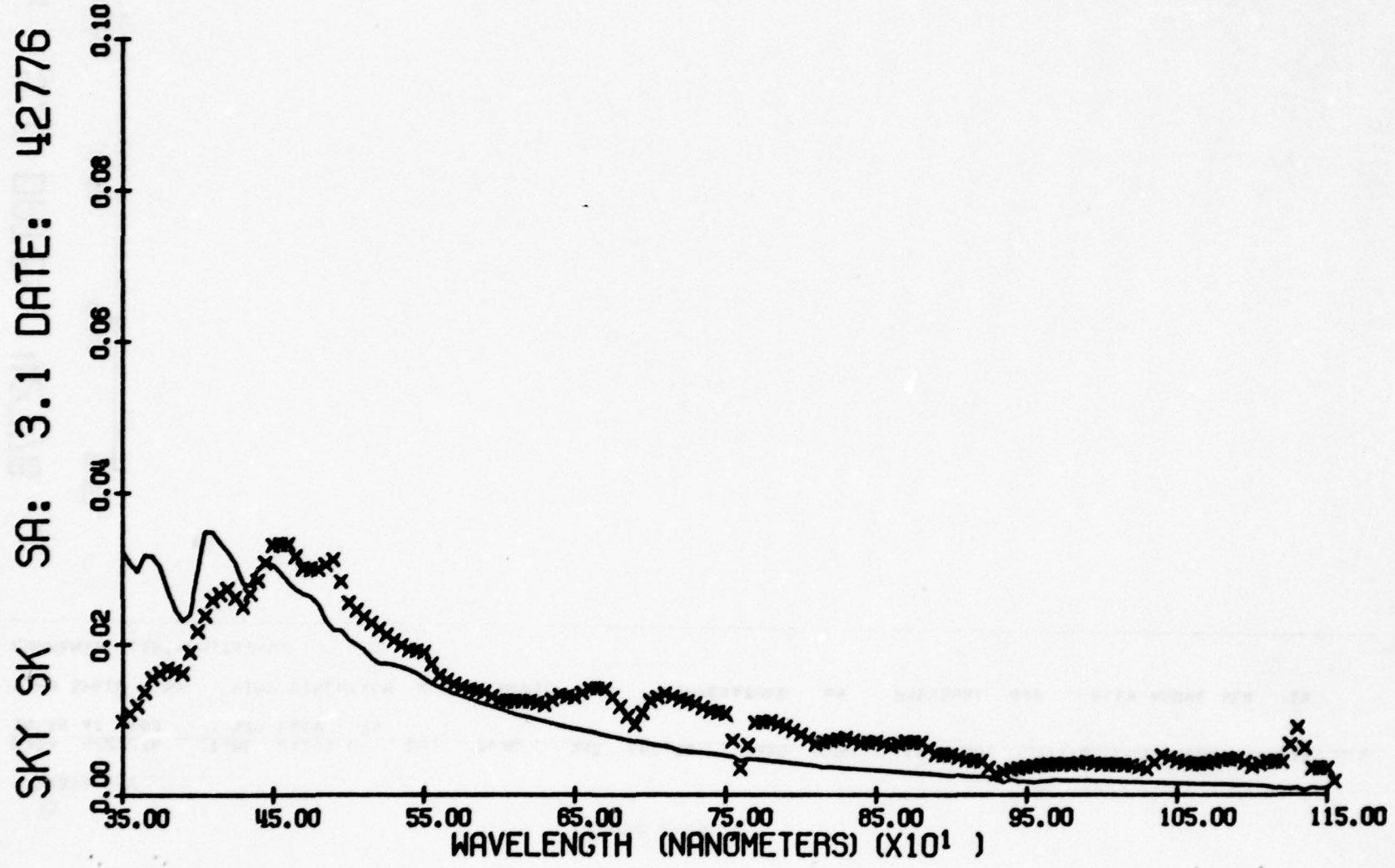

Figure C-27

INSTR SKY

DATA 9/24/76 TIME 13:45:1.0 SA 3.16 SAZ 26.11 To50 0.56 LATITUDE 41.12 LONGITUDE -111.97
INSTR AZ 276 INSTR ELEV 84

WIND SPEED 127 WIND DIRECTION 97 HUMID 481 TEMPERATURE 54 PRESSURE 873 ELEV ABOVE SEA 4766

COMMENTS 3,IR1=DV,IR2=SH, IR1(350)=1.44-8 IR2(350)=1.07-7

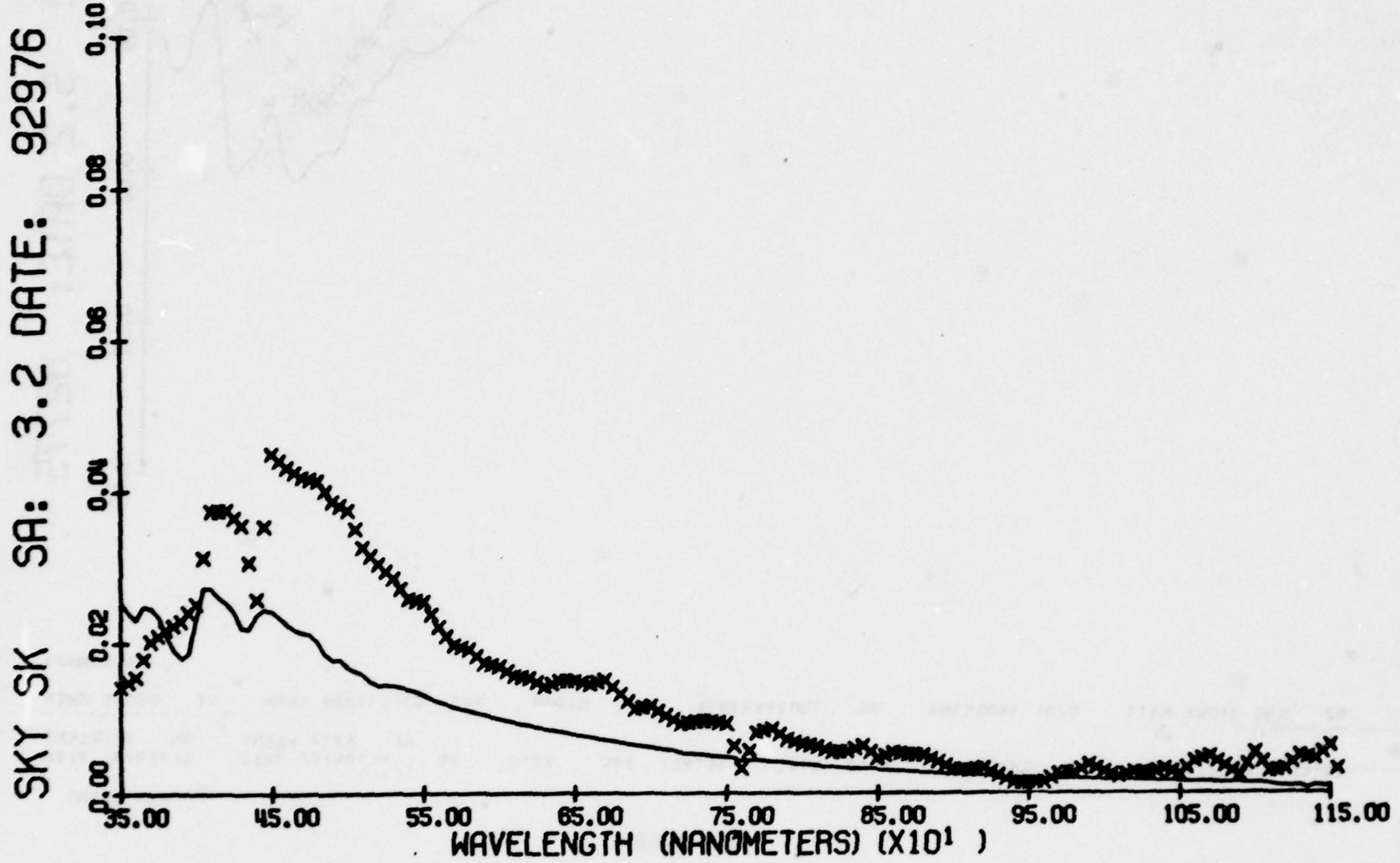

Figure C-26

INSTR SKY

DATA 6/27/75 TIME 23:40:54 SA 5.22 SAZ 278.54 T650 0.47 LATITUDE 29.73 LONGITUDE -85.05
INSTR AZ 98 INSTR ELEV 79

WIND SPEED 18 WIND DIRECTION 150 HUMID 56% TEMPERATURE 90 PRESSURE 1020 ELEV ABOVE SEA 20

COMMENTS

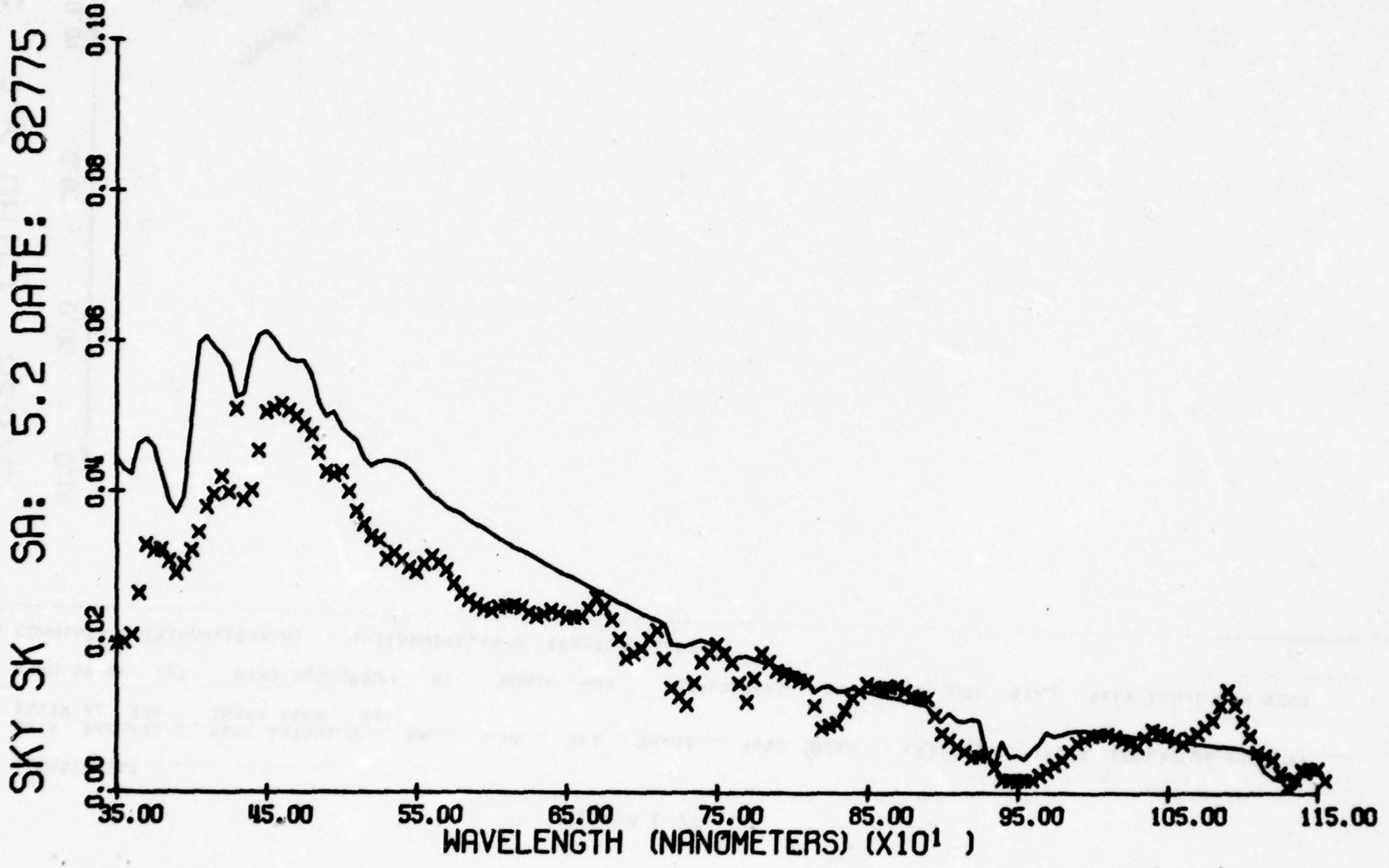

Figure C-29

INSTR SKY

DATA 9/29/76 TIME 13:30: 0 SA 0.35 SAZ 93.83 T650 0.78 LATITUDE 41.12 LONGITUDE -111.97
INSTR AZ 274 INSTR ELEV 89

WIND SPEED 113 WIND DIRECTION 114 HUMID 486 TEMPERATURE 53 PRESSURE 873 ELEV ABOVE SEA 4788

COMMENTS 3,IR1=DV,IR2=SH, IR1(350)=6.57-9 IR2(350)=4.77-8

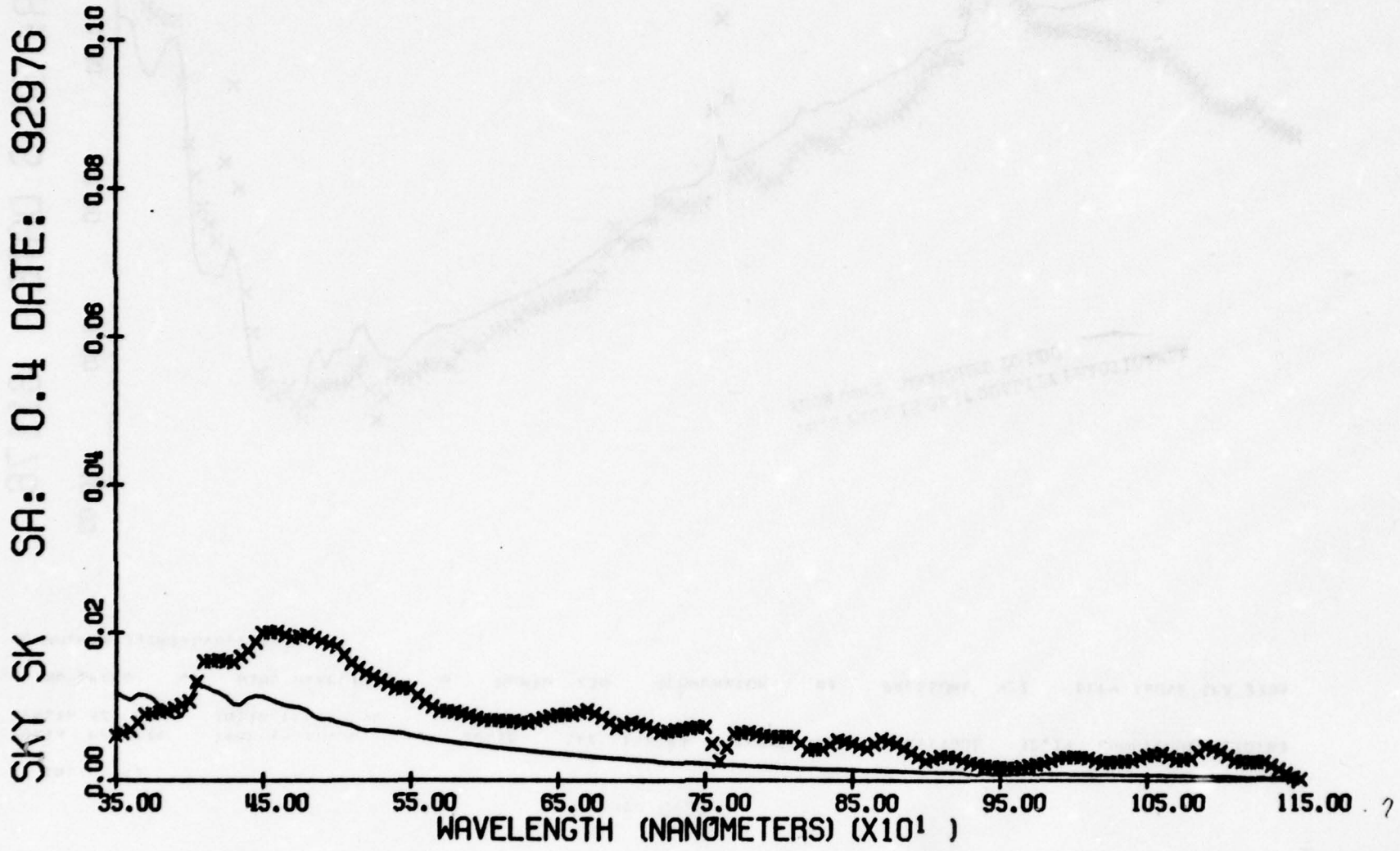

Figure C-30

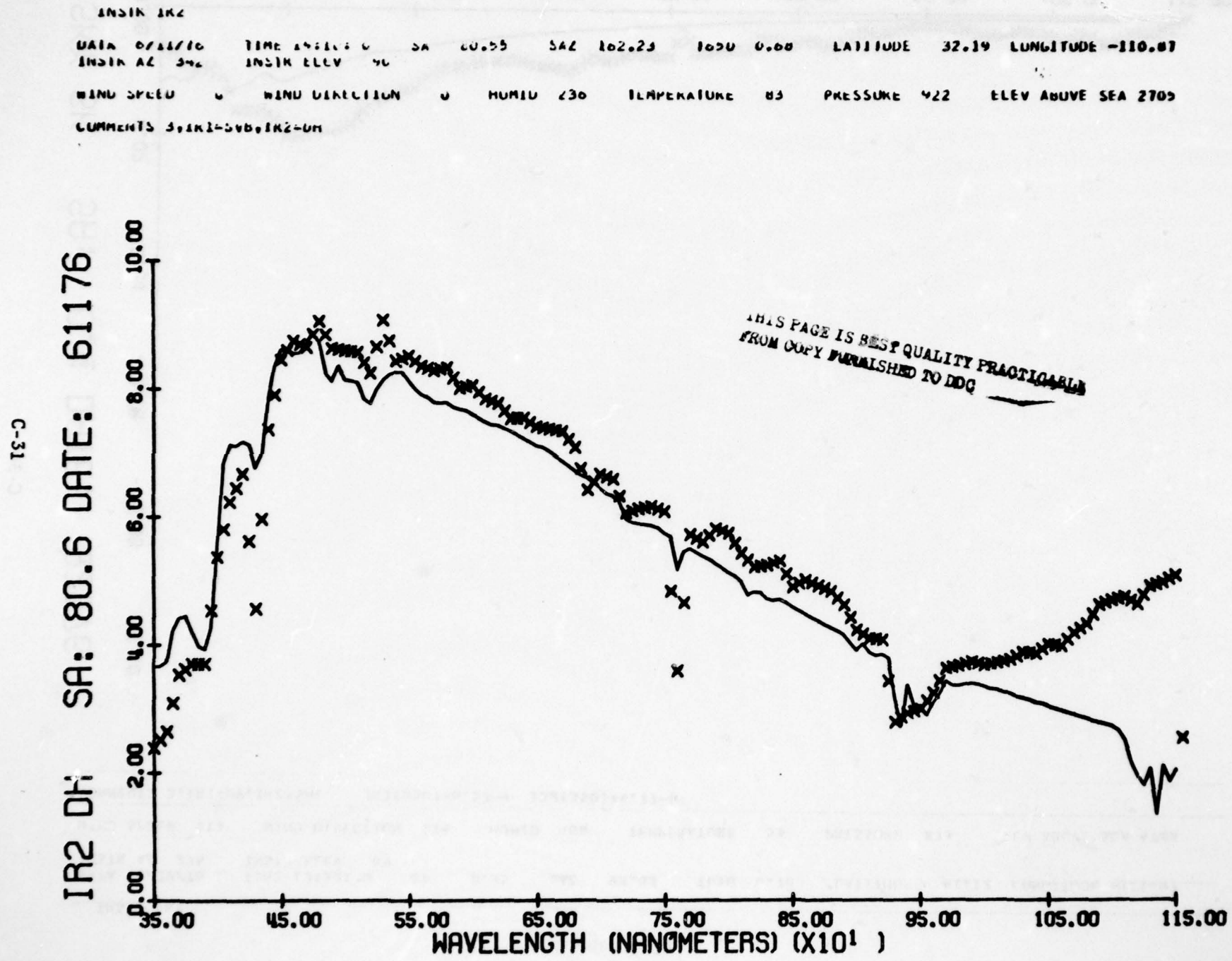

Figure C-31

INSTR IR2

DATA 5/12/76 TIME 14:55: U SA 73.56 SAZ 177.26 1650 0.67 LATITUDE 34.75 LONGITUDE -120.57
INSTR AZ 357 INSTR ELEV 50

WIND SPEED 20 WIND DIRECTION 0 HUMID 428 TEMPERATURE 81 PRESSURE 1003 ELEV ABOVE SEA 327

COMMENTS 3,IR1=DV,IR2=UH

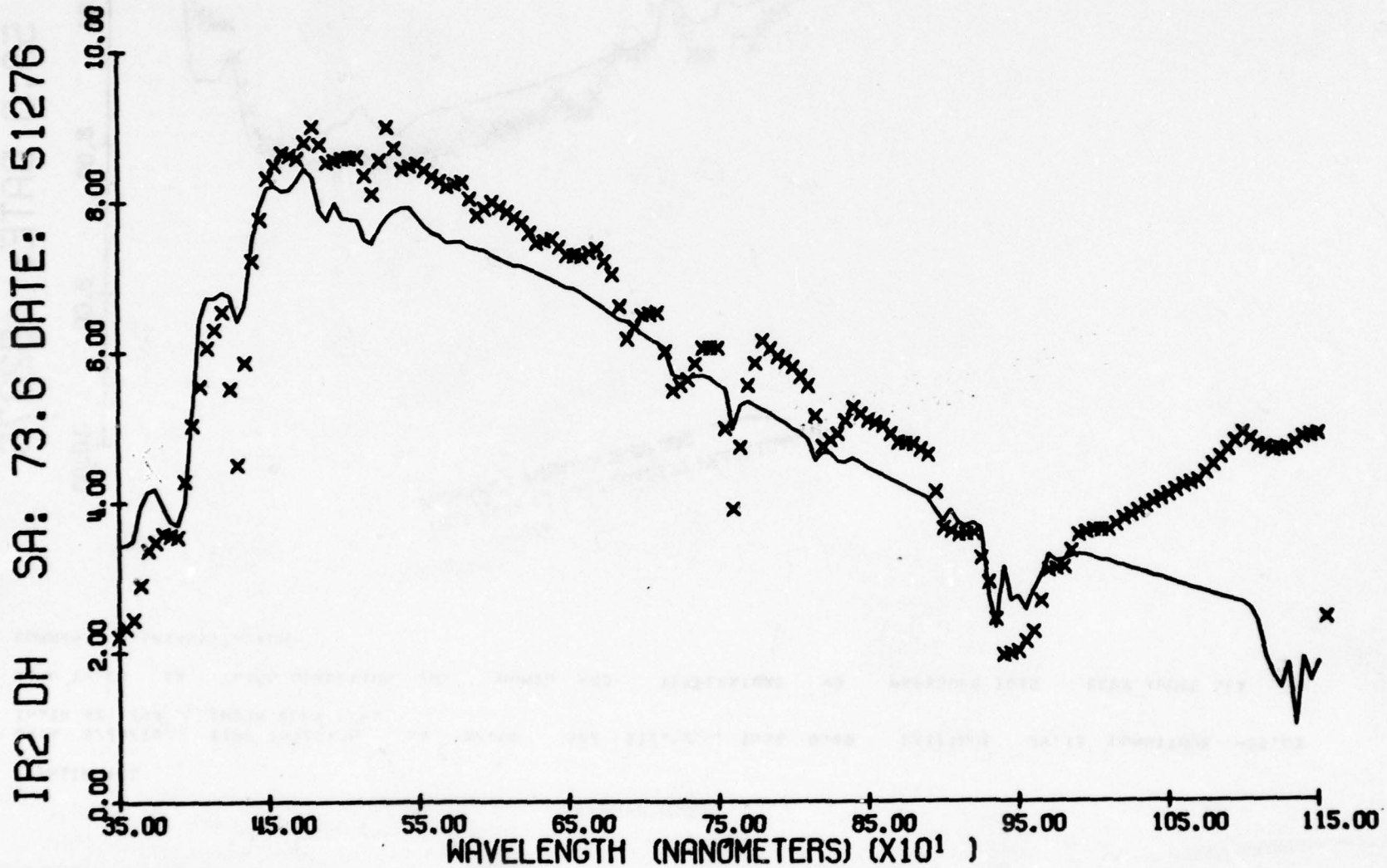

Figure C-32

INSTR IR2

DATA 8/23/76 TIME 15:23:0 0 SA 52.96 SAZ 112.62 TOSO 0.00 LATITUDE 24.73 LONGITUDE -85.03
INSTR AZ 293 . INSTR ELEV 46

WIND SPEED 20 WIND DIRECTION 300 HUMID 403 TEMPERATURE 93 PRESSURE 1015 ELEV ABOVE SEA 20

COMMENTS 3:IR1=UV,IR2=DH

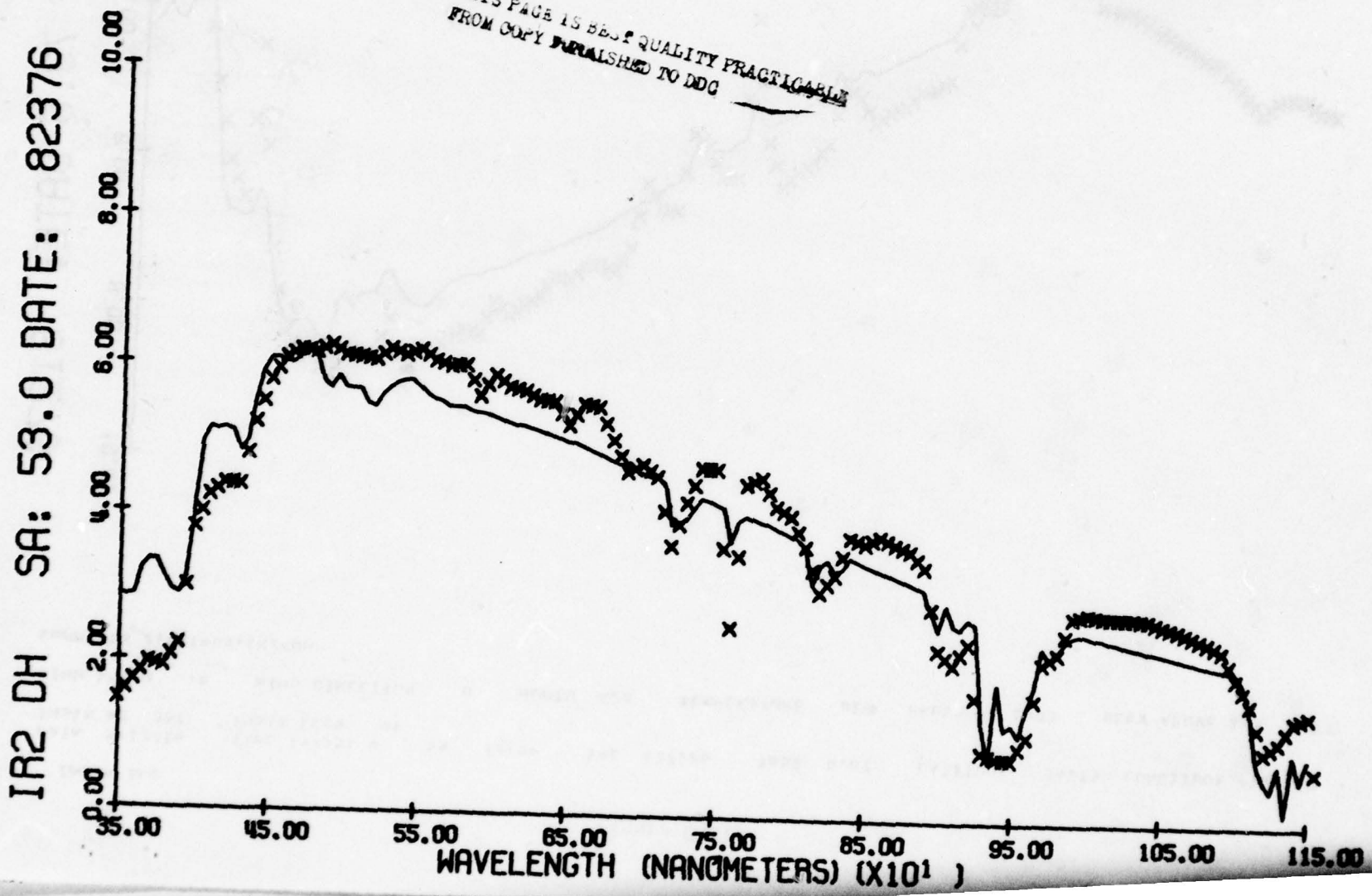

Figure C-33

INSTR IR2

DATA 7/21/76 TIME 15: 01: 0 SA 45.00 SAZ 45.61 1650 0.57 LATITUDE 34.92 LONGITUDE -92.15
INSTR AZ 270 INSTR ELEV 90

WIND SPEED 50 WIND DIRECTION 252 HUMID 580 TEMPERATURE 84 PRESSURE 1005 ELEV ABOVE SEA 311

COMMENTS 3,IR1=SVB,IR2=UM

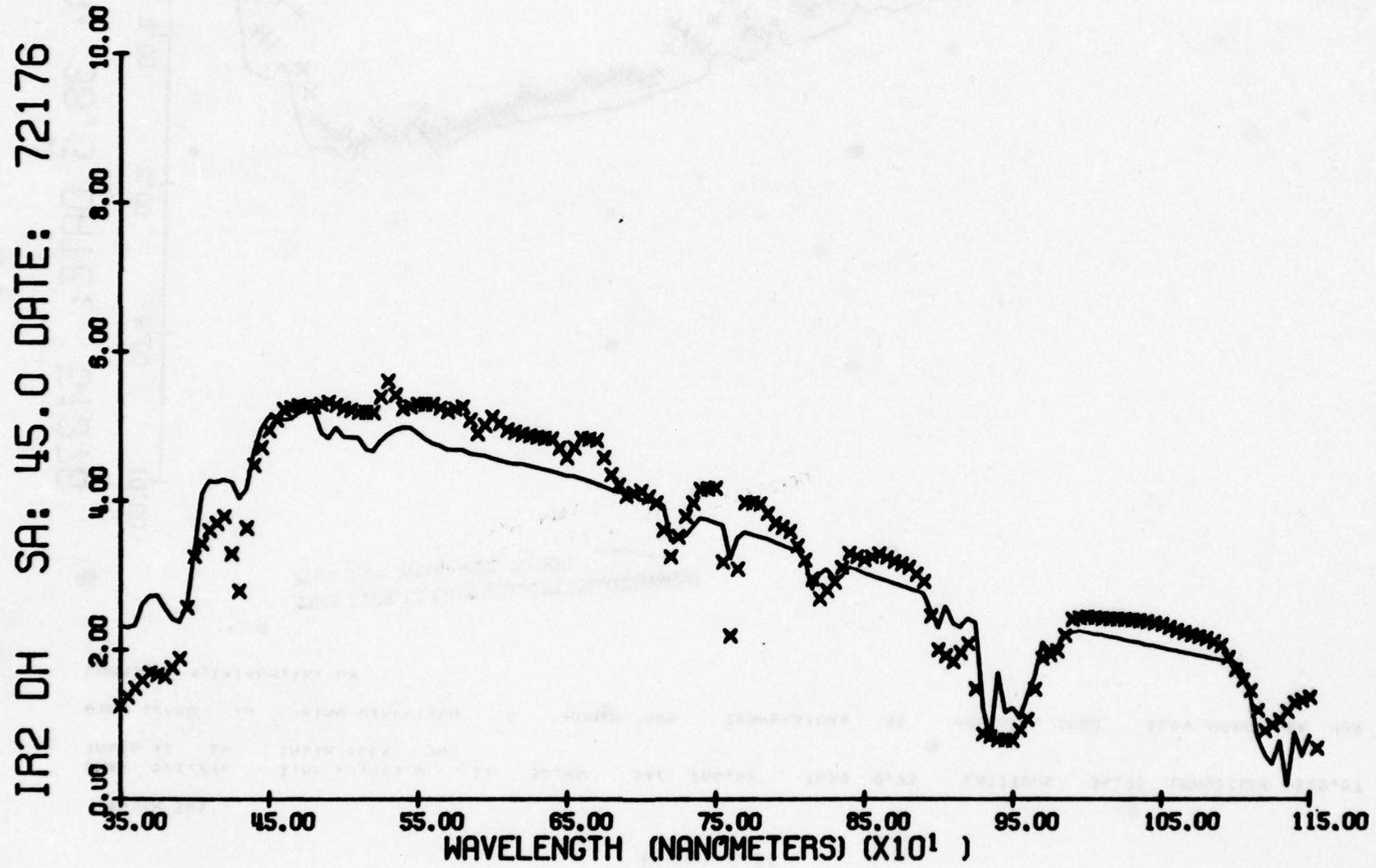

Figure C-34

INSTR IR1

DATA 3/12/80 TIME 23:40:0 U SA 38.46 SAZ 266.48 T650 0.73 LATITUDE 34.75 LONGITUDE -120.57
INSTR AZ 66 INSTR ELEV 90

WIND SPEED 20 WIND DIRECTION 0 HUMID 40% TEMPERATURE 81 PRESSURE 1003 ELEV ABOVE SEA 327

COMMENTS 3,IR1=DH,IR2=DV

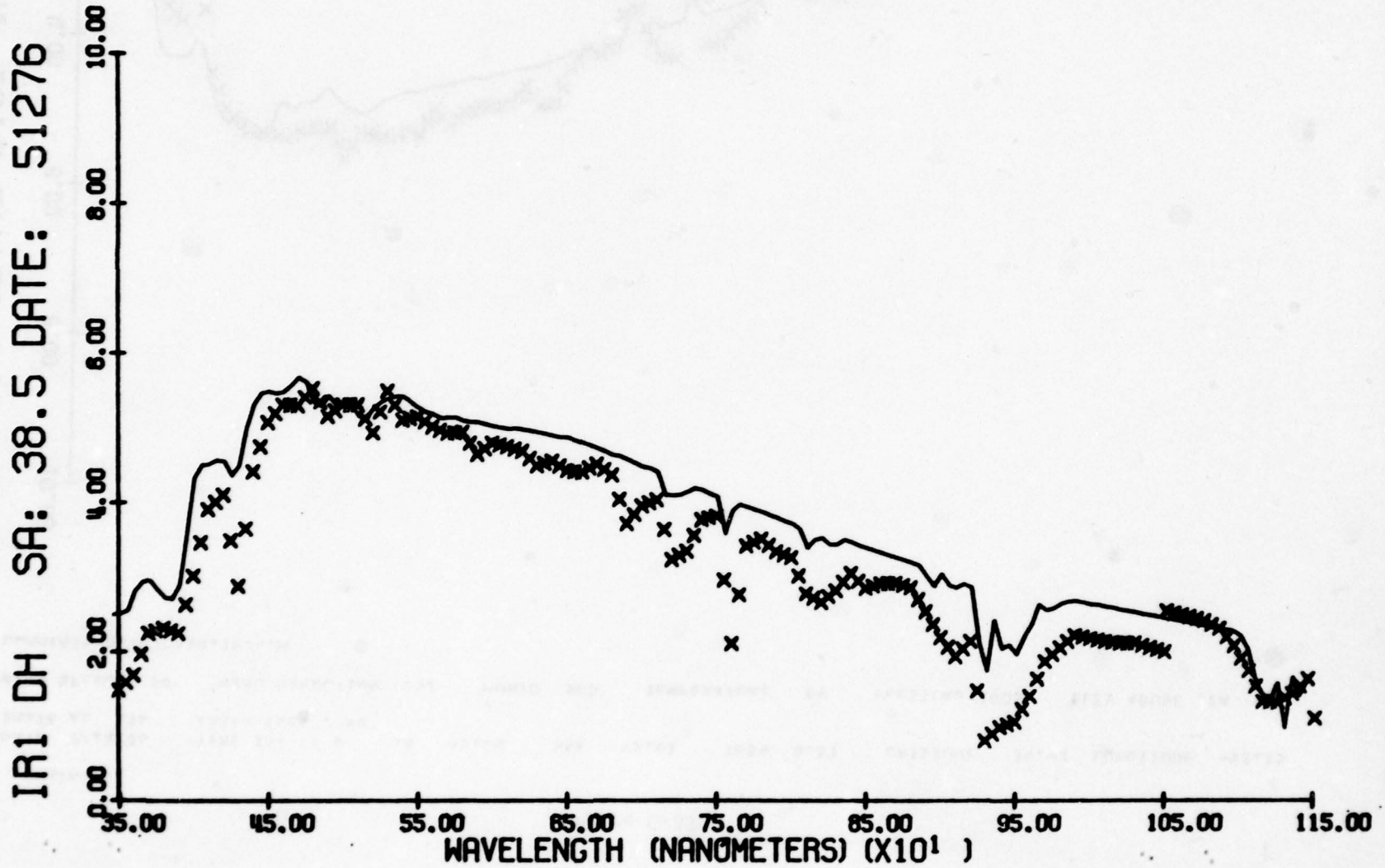

Figure C-35

INSTR IR2

DATA 6/11/80 TIME 23:23:23 G SA 37.29 SAZ 84.01 TAU6 0.76 LATITUDE 32.19 LONGITUDE -110.87
INSTR AZ 264 INSTR ELEV 90

WIND SPEED 0 WIND DIRECTION 0 HUMID 305 TEMPERATURE 74 PRESSURE 922 ELEV ABOVE SEA 2765

COMMENTS S,IR1=SVB,IR2=UM

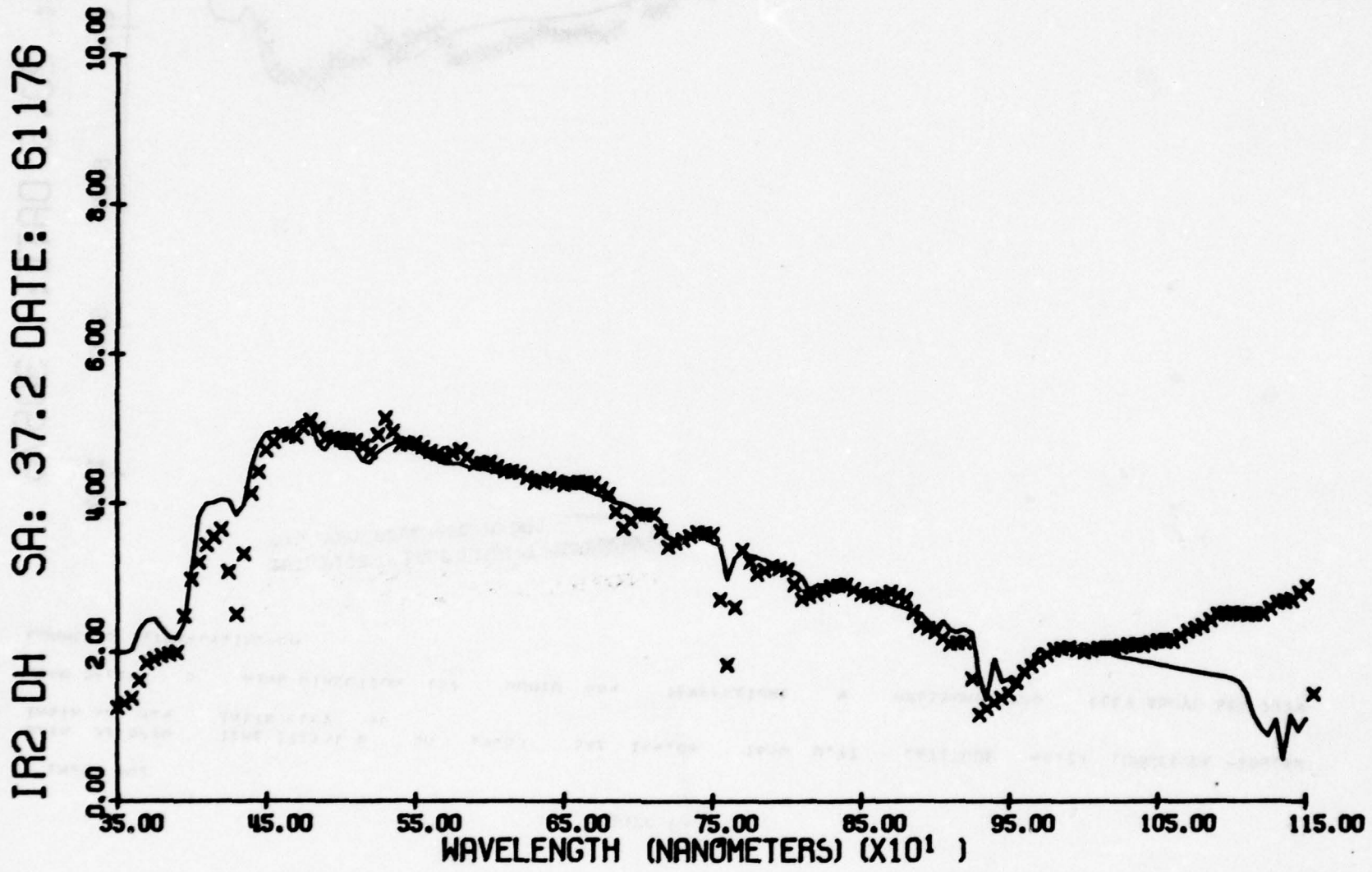

Figure C-36

INSTR IR2

DATA 3/ 5/10 TIME 17:15: 0 SA 29.53 SAZ 144.09 TOSO 0.77 LATITUDE 48.22 LONGITUDE -106.62
INSTR AZ 324 INSTR ELEV 90

WIND SPEED 5 WIND DIRECTION 157 HUMID 064 TEMPERATURE 9 PRESSURE 936 ELEV ABOVE SEA 2279

COMMENTS 5,IR1=DV,IR2=DH

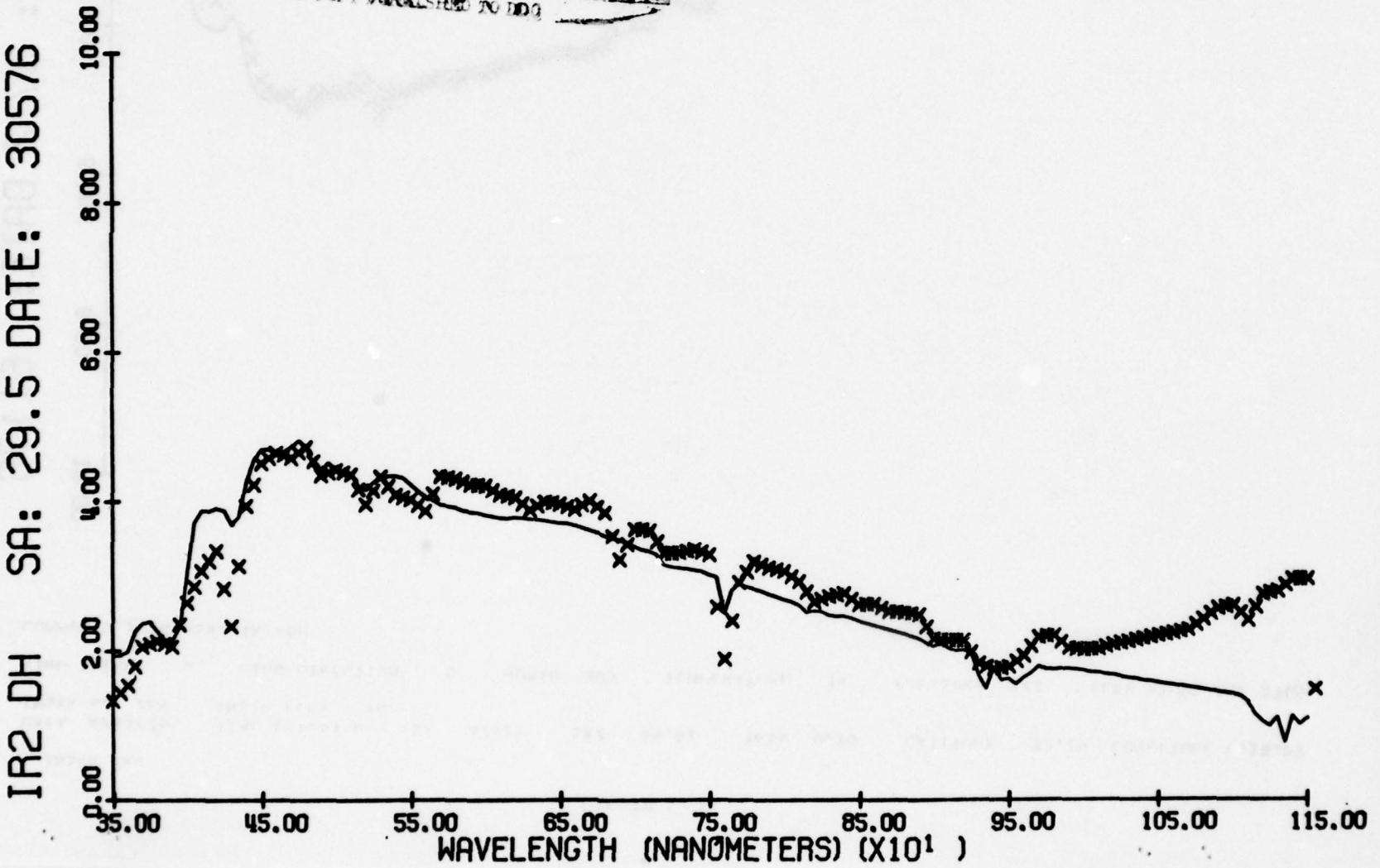

Figure C-37

INSTR IR2

DATA 8/23/76 TIME 12:53: 0 SA 21.07 SAZ 88.80 1o50 0.59 LATITUDE 29.73 LONGITUDE -85.03
INSTR AZ 269 INSTR ELEV 90

WIND SPEED 24 WIND DIRECTION 339 HUMID 706 TEMPERATURE 81 PRESSURE 1015 ELEV ABOVE SEA 20

COMMENTS 3,IR1=DV,IR2=UH

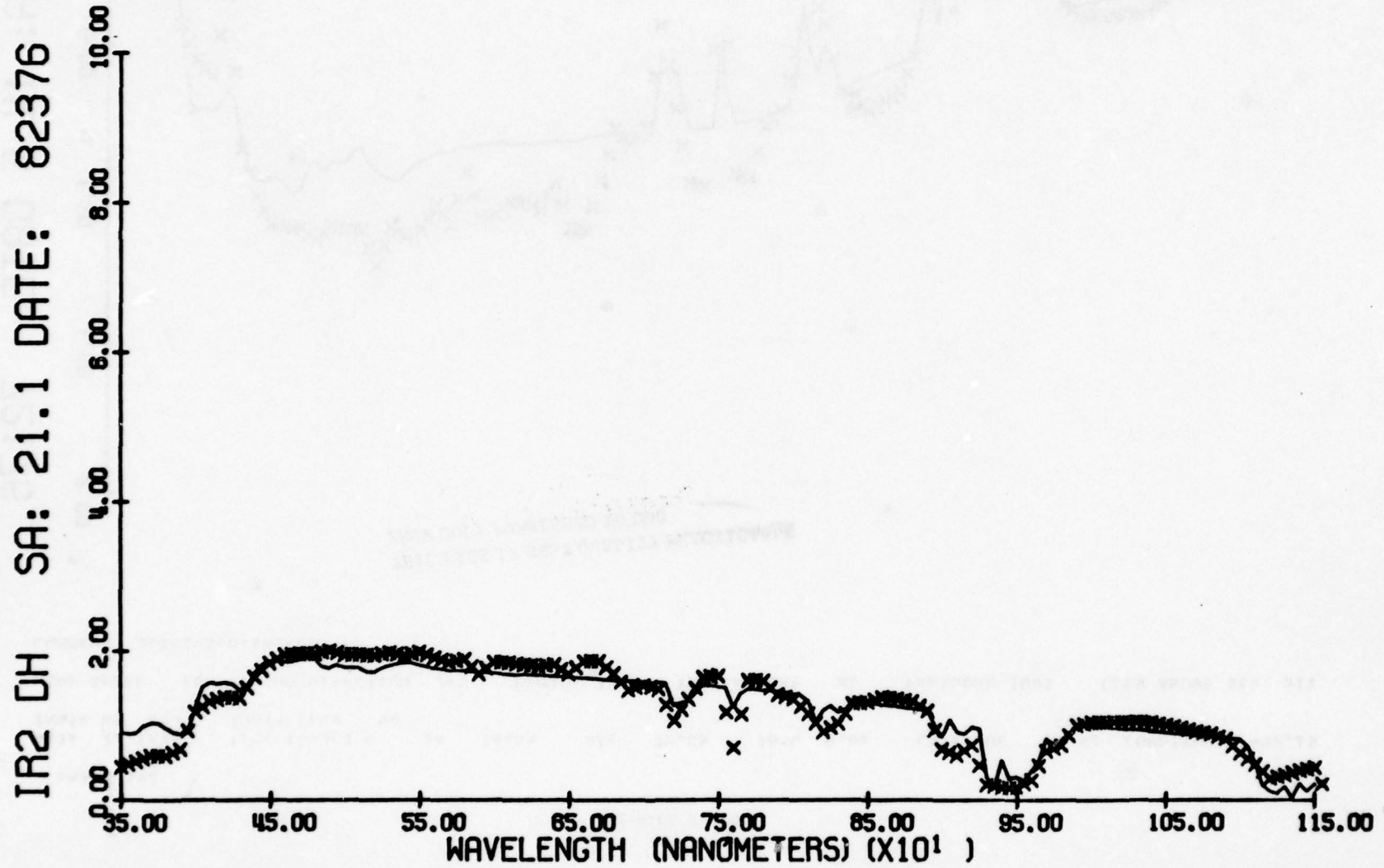

Figure C-38

INSTR IR2

DATA 7/21/76 TIME 12:30:0 SA 14.54 SAZ 75.05 1650 0.02 LATITUDE 34.92 LONGITUDE -92.15
INSTR AZ 253 INSTR ELEV 90

WIND SPEED 16 WIND DIRECTION 245 HUMID 728 TEMPERATURE 81 PRESSURE 1005 ELEV ABOVE SEA 311

COMMENTS S,IR1=SVB,IR2=DH

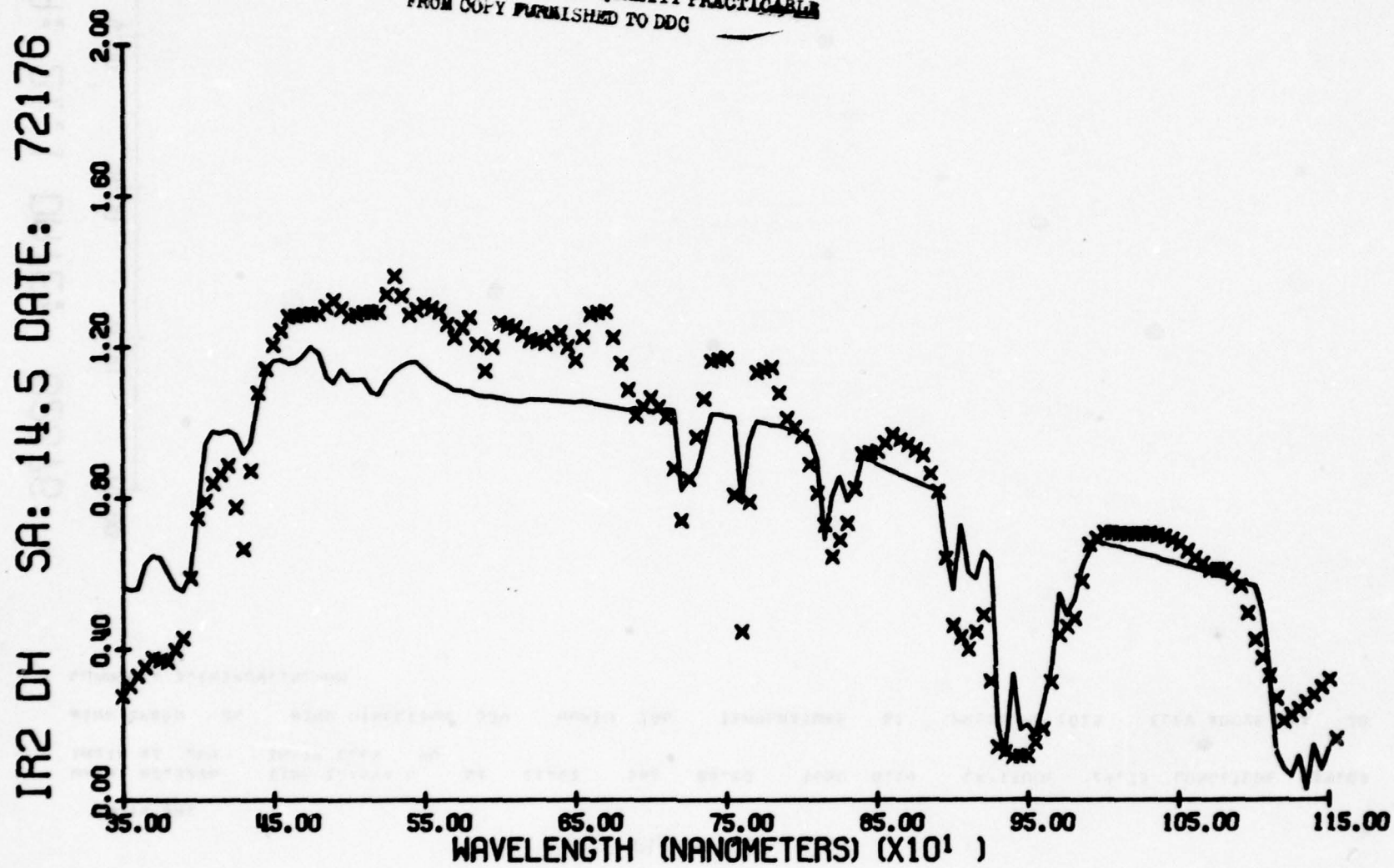

Figure C-39

INSTR IR1

DATA 5/13/76 TIME 1:46:0 SA 13.99 SAZ 282.87 1650 0.86 LATITUDE 34.75 LONGITUDE -120.57
INSTR AZ 103 INSTR ELEV 90

WIND SPEED 0 WIND DIRECTION 0 HUMID 425 TEMPERATURE 80 PRESSURE 1003 ELEV ABOVE SEA 327

COMMENTS 3,IR1-DH,IR2=SVB

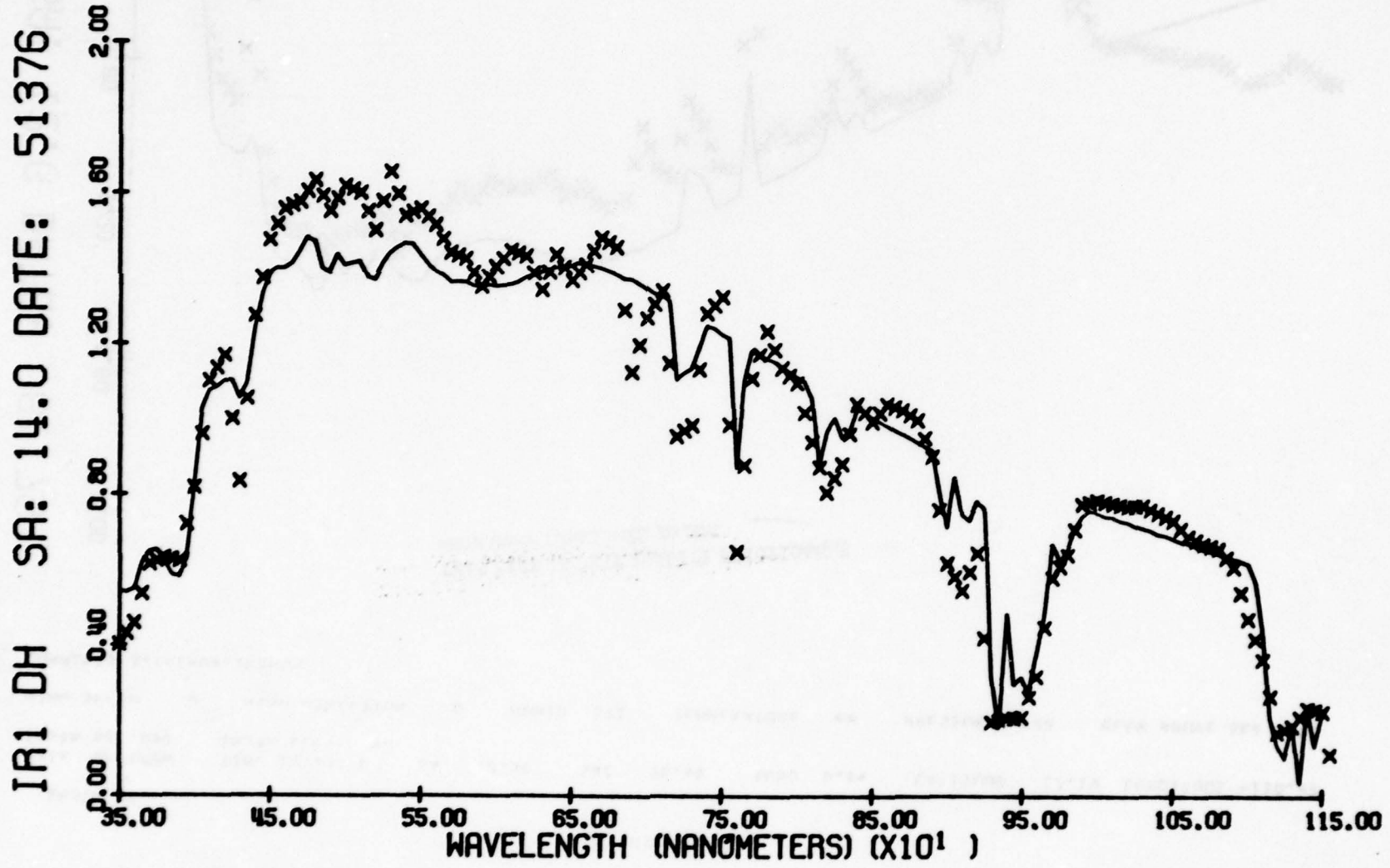

Figure C-40

INSTR IR2

DATA 6/11/76 TIME 13:25: 0 SA 12.58 SAZ 76.41 1650 0.84 LATITUDE 32.19 LONGITUDE -110.87
INSTR AZ 250 INSTR ELEV 90

WIND SPEED 0 WIND DIRECTION 0 HUMID 311 TEMPERATURE 68 PRESSURE 922 ELEV ABOVE SEA 2705

COMMENTS 3,IR1=UV,IR2=DH

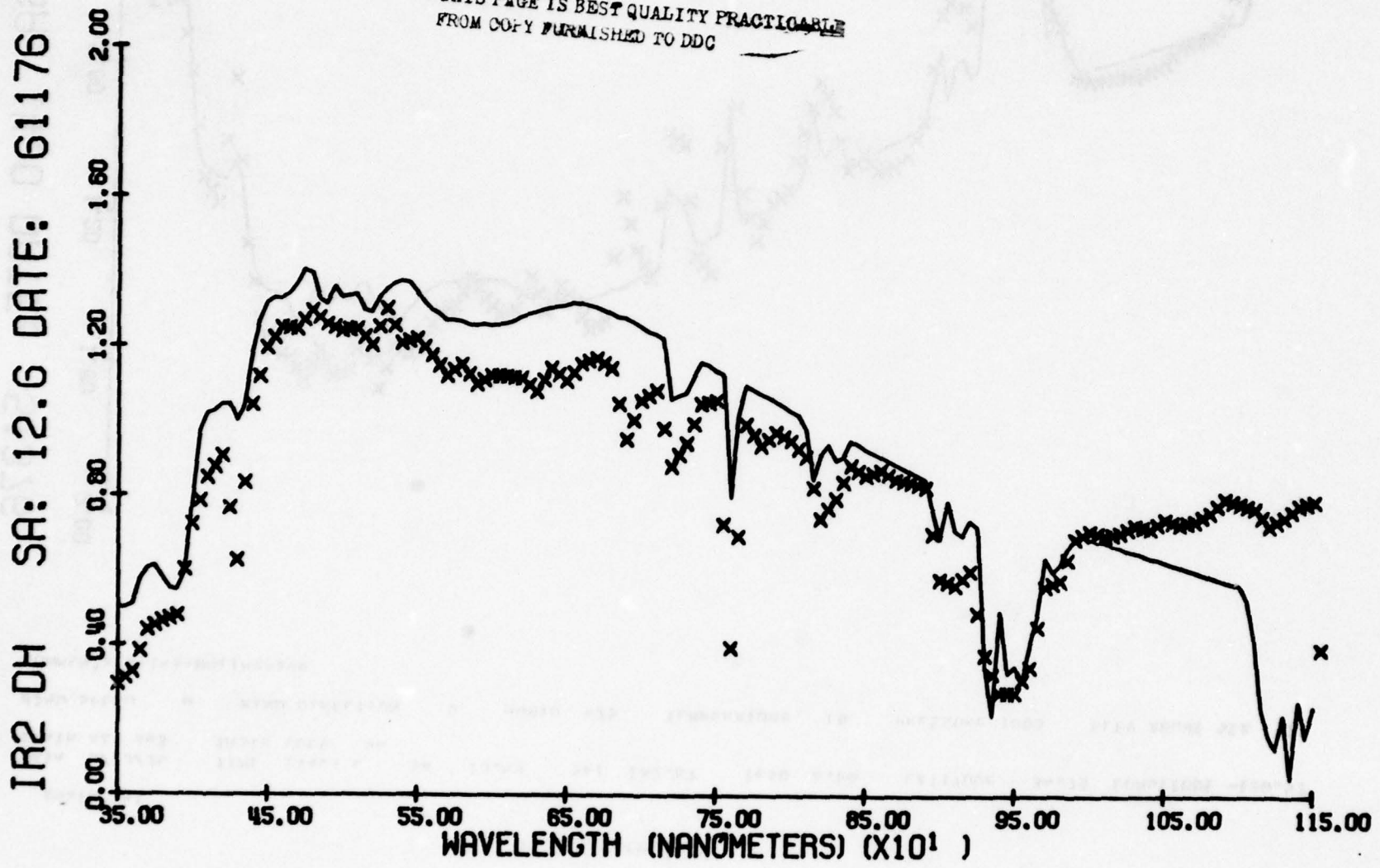

Figure C-41

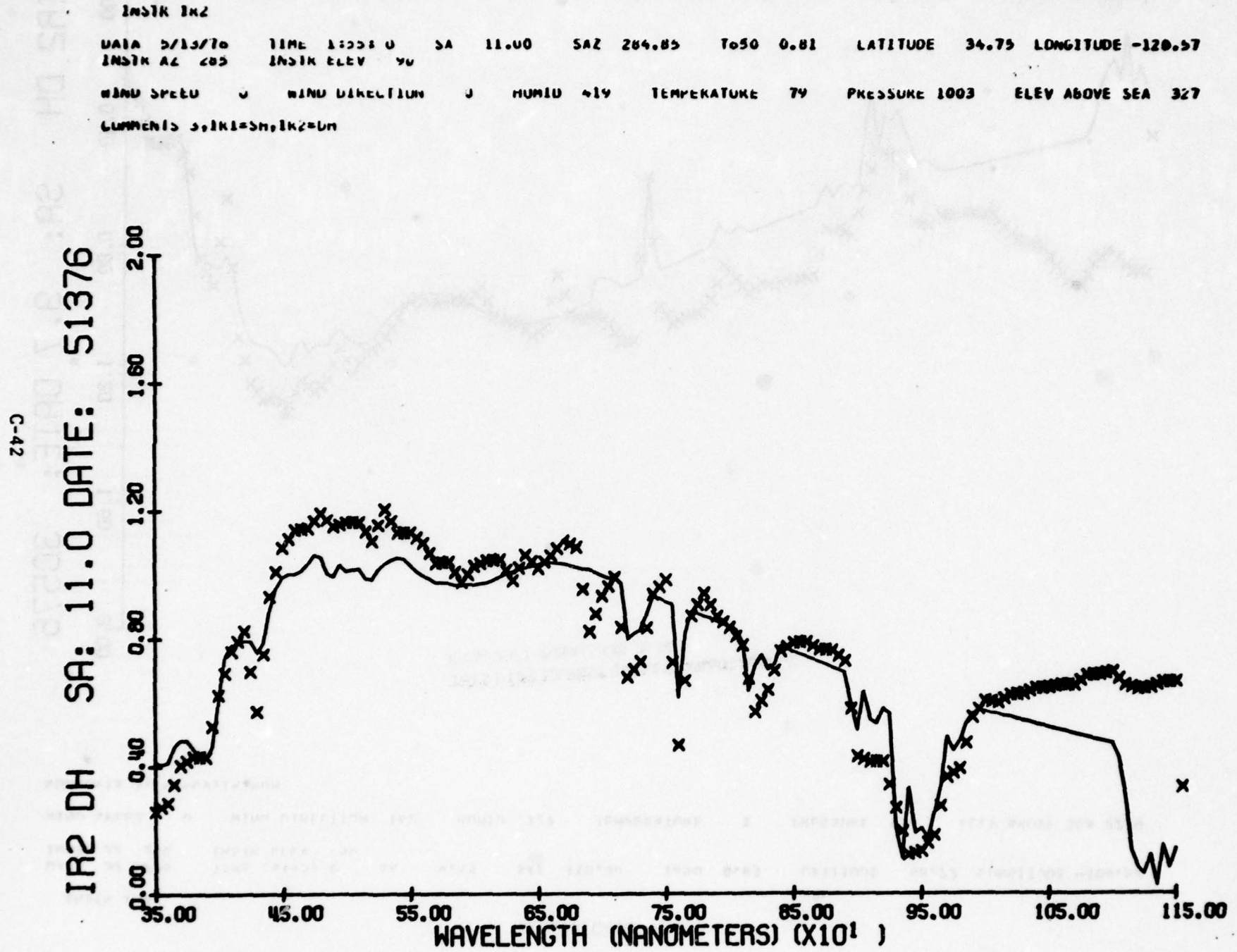
INSTR IR2
DATA 5/13/76 TIME 1:55:5 U SA 11.00 SAZ 284.85 TO50 0.81 LATITUDE 34.75 LONGITUDE -120.57
INSTR AZ 285 INSTR ELEV 90
WIND SPEED 0 WIND DIRECTION 0 HUMID 419 TEMPERATURE 79 PRESSURE 1003 ELEV ABOVE SEA 327
COMMENTS S,IR1=SM,IR2=DM
IR2 DH SA: 11.0 DATE: 51376
2.00
1.60
1.20
0.80
0.40
0.00
35.00
45.00
55.00
65.00
75.00
85.00
95.00
105.00
115.00
WAVELENGTH (NANOMETERS) (X10¹)

Figure C-42

INSTR IR2

DATA 3/ 9/80 TIME [illegible] 0 SA 4.05 SAZ 110.30 IDSU 0.83 LATITUDE 48.22 LONGITUDE -106.62
INSTR AZ 290 INSTR ELEV 90

WIND SPEED 0 WIND DIRECTION 102 HUMID 727 TEMPERATURE 1 PRESSURE 930 ELEV ABOVE SEA 2279

COMMENTS 3,IR1=DV,IR2=DH

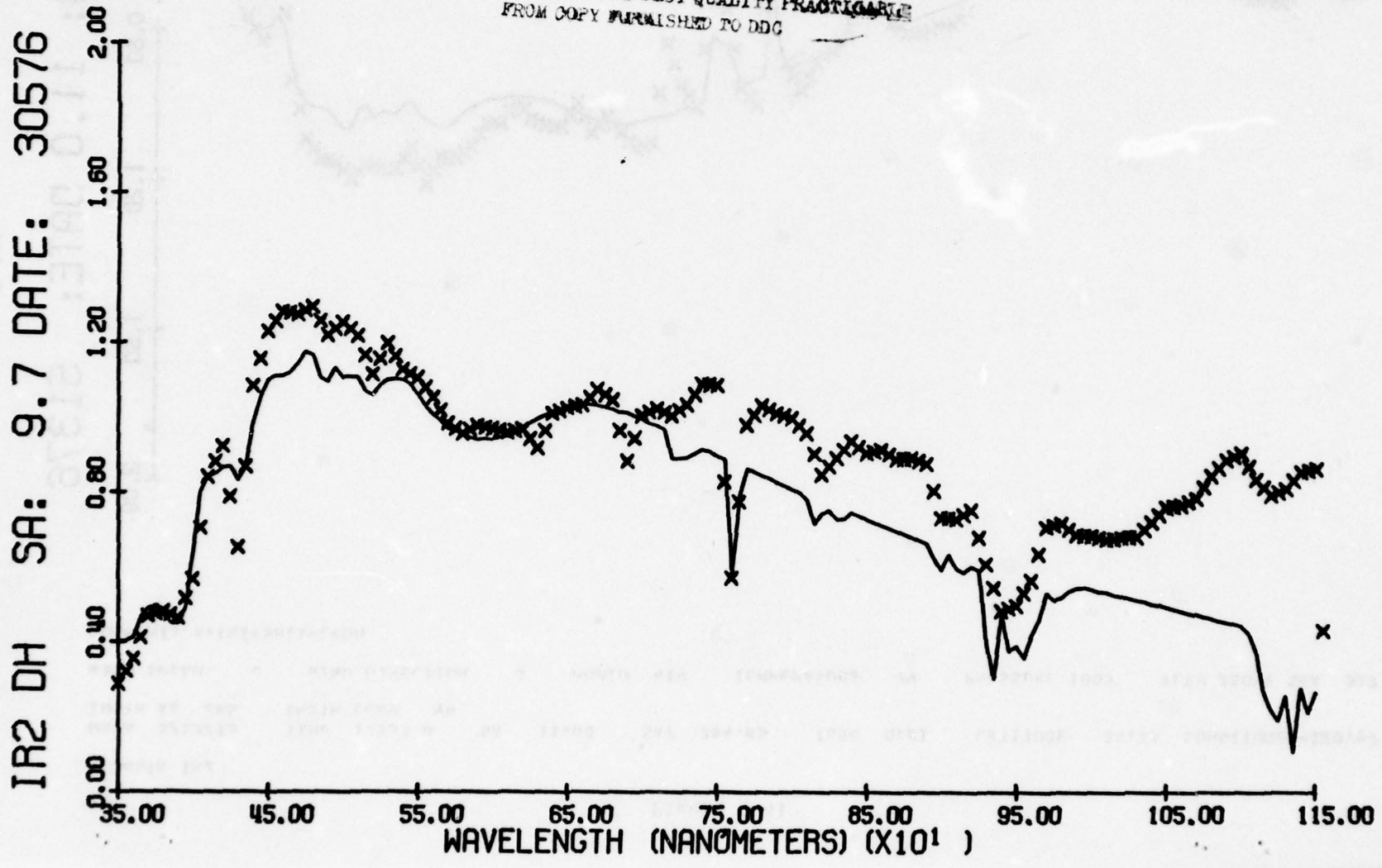

Figure C-43

INSTR IR1

DATA 5/13/76 TIME [illegible] SA 8.04 SAZ 286.84 T650 0.82 LATITUDE 34.75 LONGITUDE -120.57
INSTR AZ 167 INSTR ELEV 90

WIND SPEED 0 WIND DIRECTION 0 HUMID 434 TEMPERATURE 78 PRESSURE 1003 ELEV ABOVE SEA 327

COMMENTS 3,IR1=DH,IR2=DV

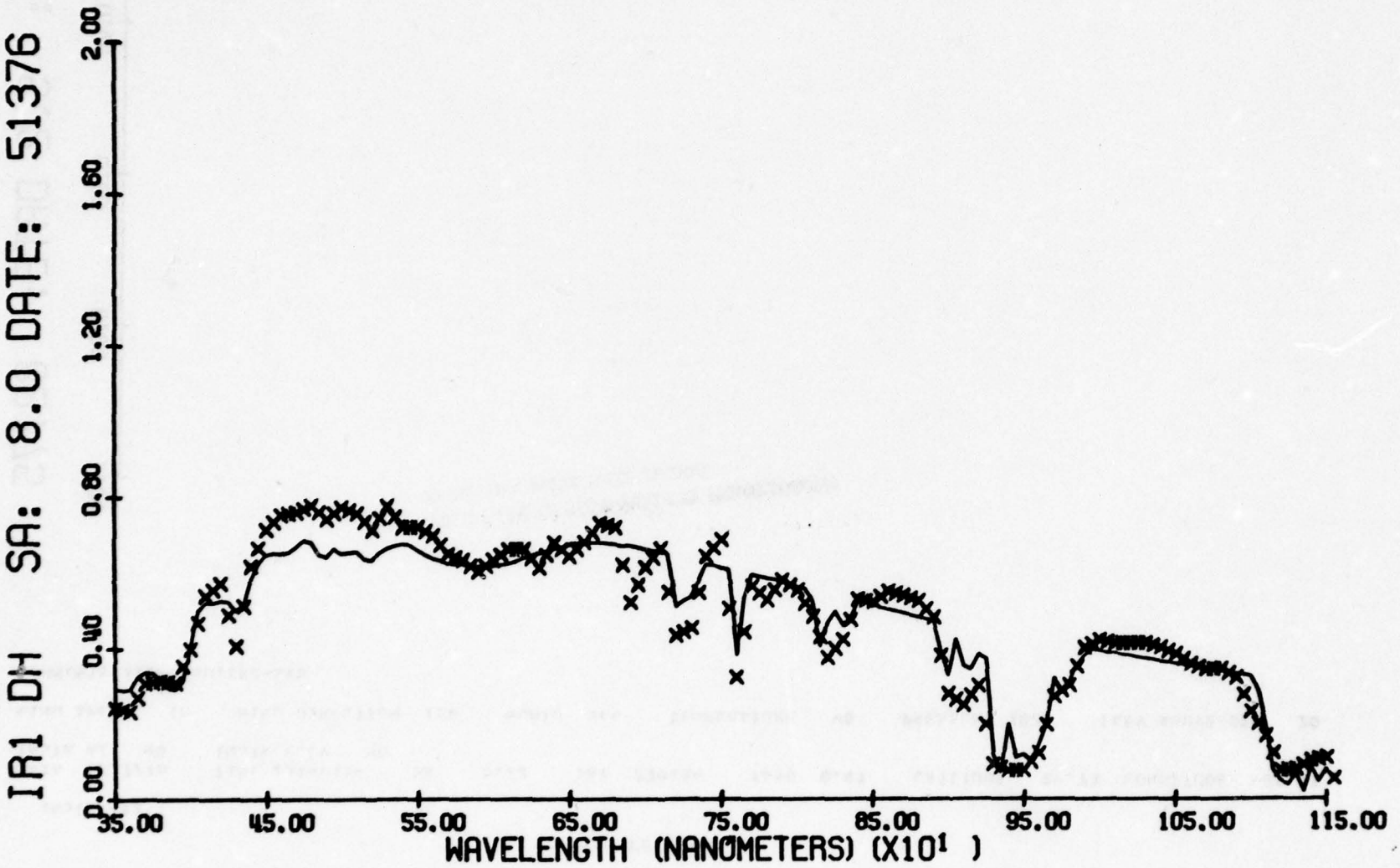

Figure C-44

INSTR IR1

DATA 8/27/75 TIME 23340154 SA 5.22 SAZ 278.54 T650 0.47 LATITUDE 29.73 LONGITUDE -85.05
INSTR AZ 98 INSTR ELEV 90

WIND SPEED 18 WIND DIRECTION 150 HUMID 564 TEMPERATURE 90 PRESSURE 1020 ELEV ABOVE SEA 20

COMMENTS S,IR1=DH,IR2=SVB

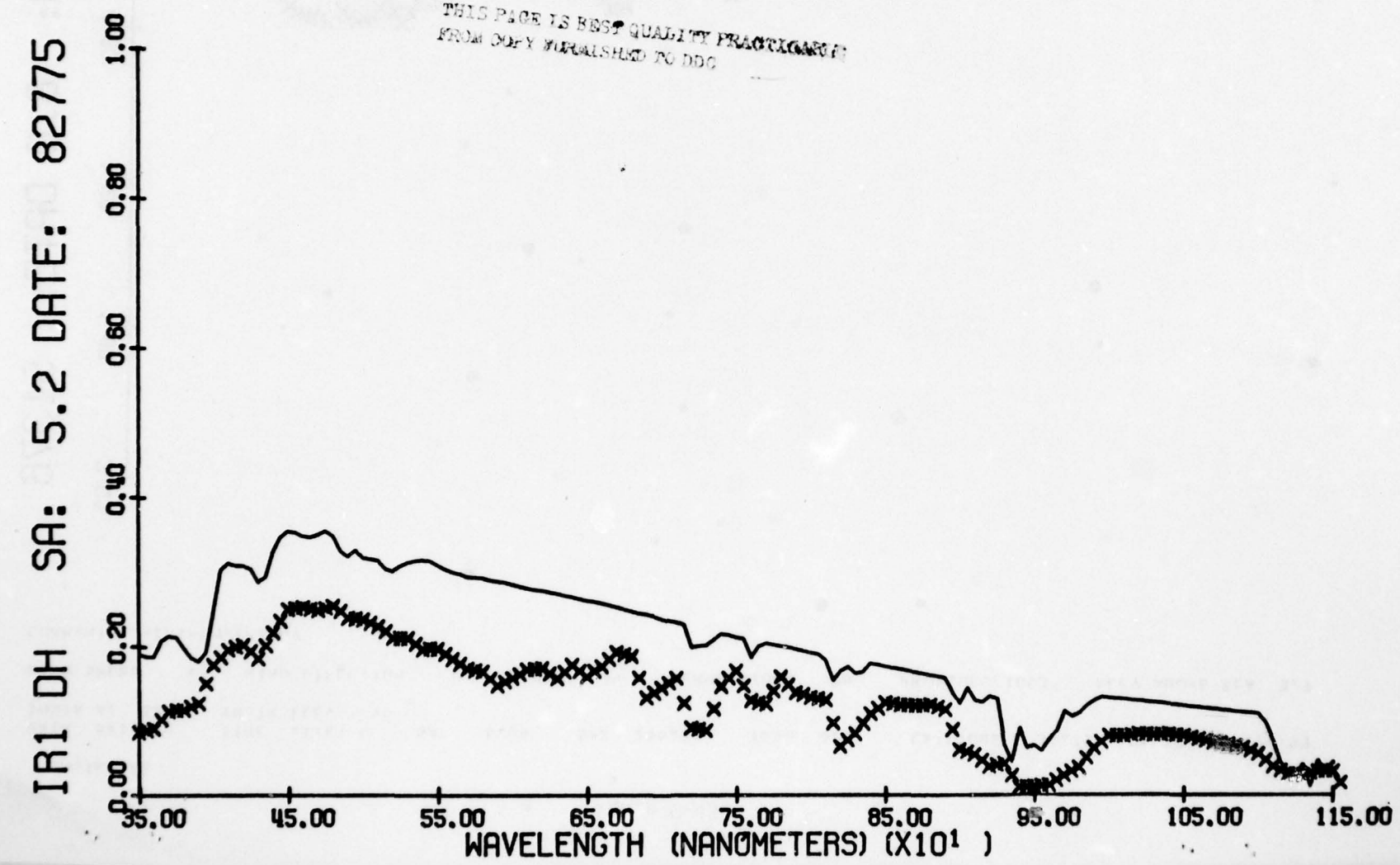

Figure C-45

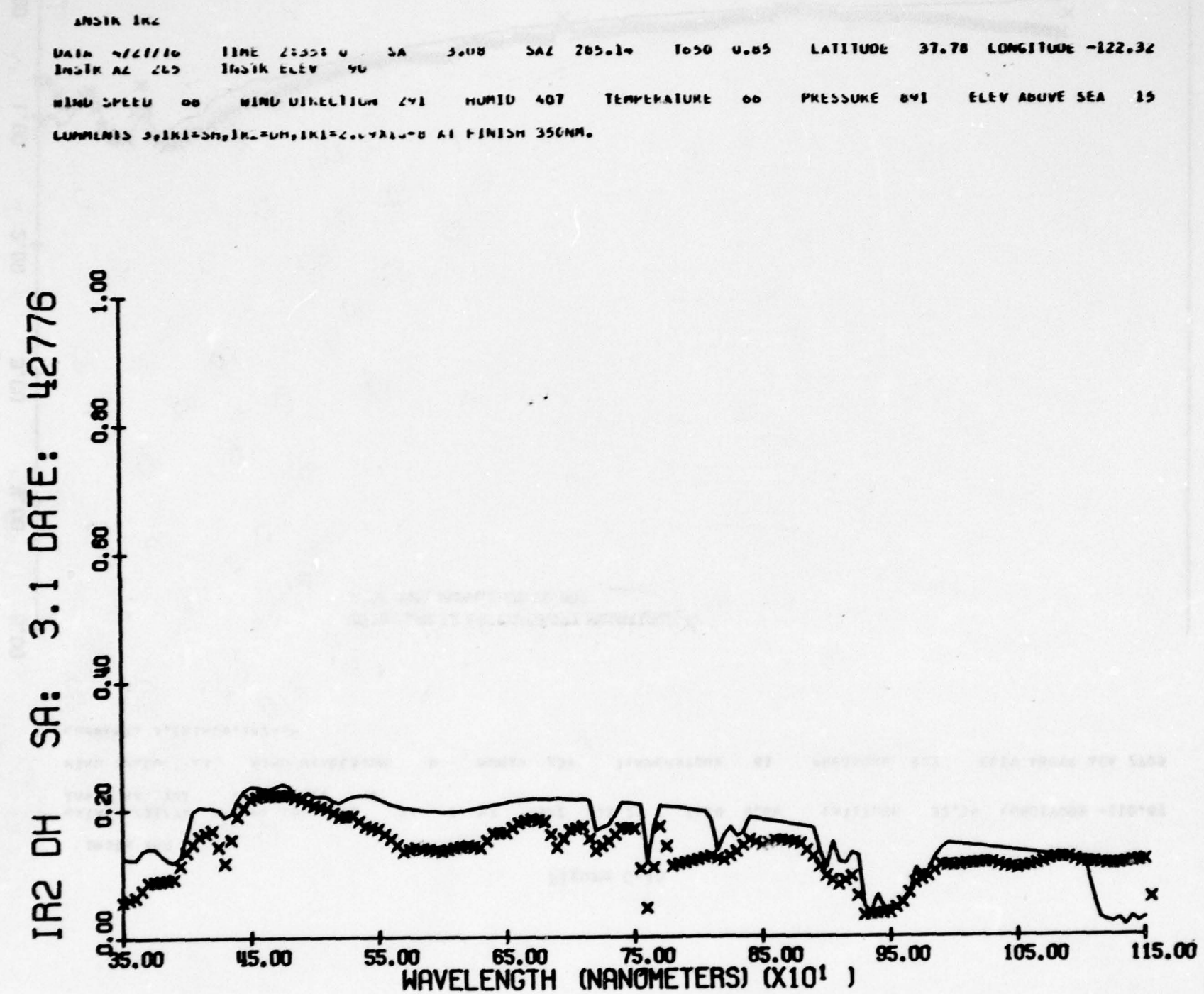
ANSIK IR2
DATA 4/27/86 TIME 2:33:3 U SA 3.08 SAZ 285.14 TO50 0.85 LATITUDE 37.78 LONGITUDE -122.32
INSIK AZ 265 INSIK ELEV 90
WIND SPEED 08 WIND DIRECTION 291 HUMID 407 TEMPERATURE 60 PRESSURE 841 ELEV ABOVE SEA 15
COMMENTS S,IR1=SA,IR2=DH,IR1=2.0 VALID=8 AT FINISH 350NM.
IR2 DH SA: 3.1 DATE: 42776
1.00
0.80
0.60
0.40
0.20
0.00
35.00
45.00
55.00
65.00
75.00
85.00
95.00
105.00
115.00
WAVELENGTH (NANOMETERS) (X10¹)

Figure C-46

INSTR IR2

DATA 6/11/76 TIME 18:40:0 GMT SA 76.97 SAZ 131.25 TOSO 0.69 LATITUDE 32.19 LONGITUDE -110.87
INSTR AZ 131 INSTR ELEV 90

WIND SPEED 23 WIND DIRECTION 0 HUMID 23% TEMPERATURE 81 PRESSURE 922 ELEV ABOVE SEA 2705

COMMENTS 3,IR1=UV,IR2=SH

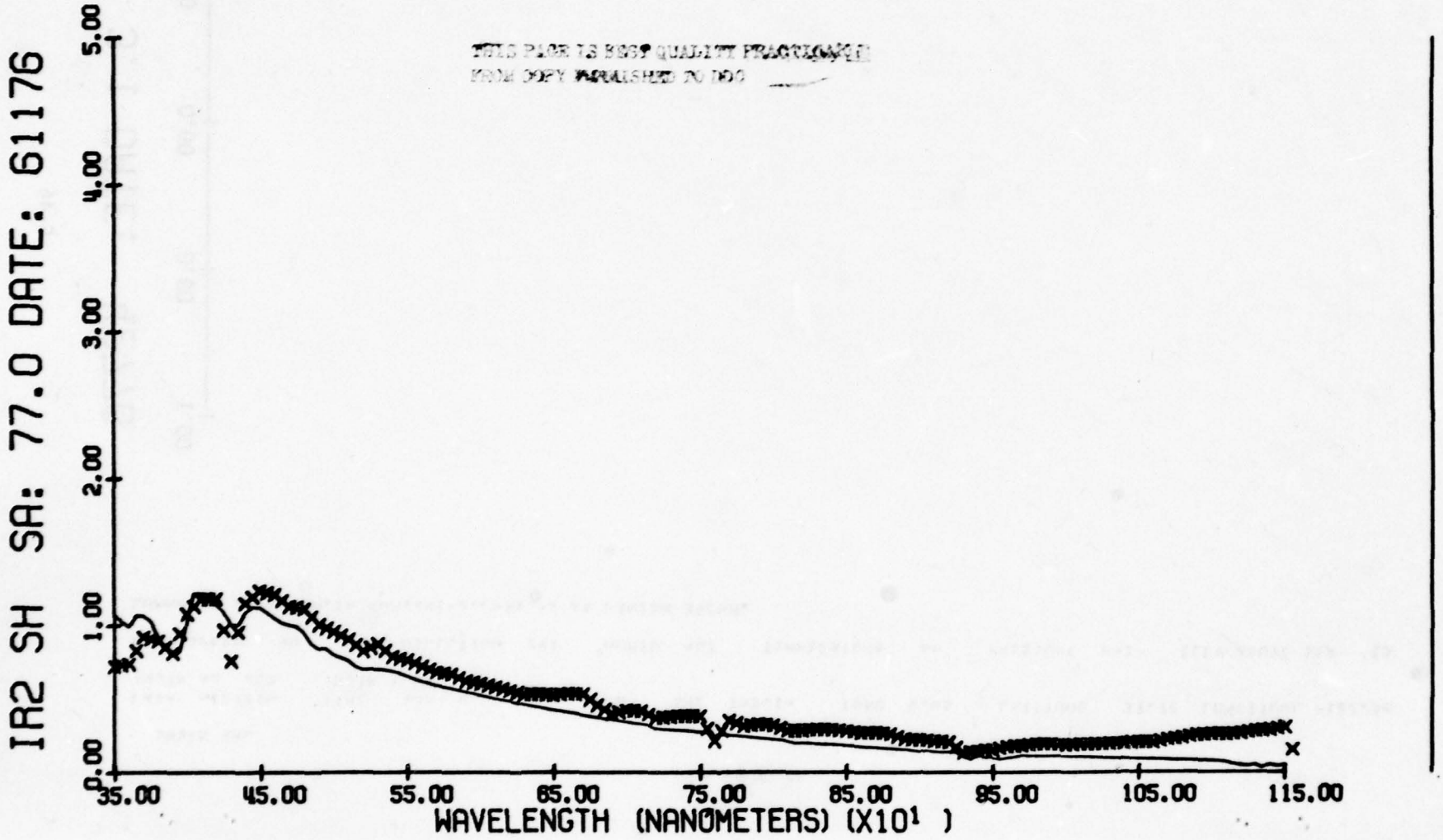

Figure C-47

INSTR IR2

DATA 5/12/78 TIME 20:25:31 U SA 72.54 SAZ 201.66 fo50 0.67 LATITUDE 34.75 LONGITUDE -120.57
INSTR AZ 202 INSTR ELEV 90

WIND SPEED 36 WIND DIRECTION 0 HUMID 424 TEMPERATURE 80 PRESSURE 1003 ELEV ABOVE SEA 327

COMMENTS 3,IR1=SVB,IR2=SH

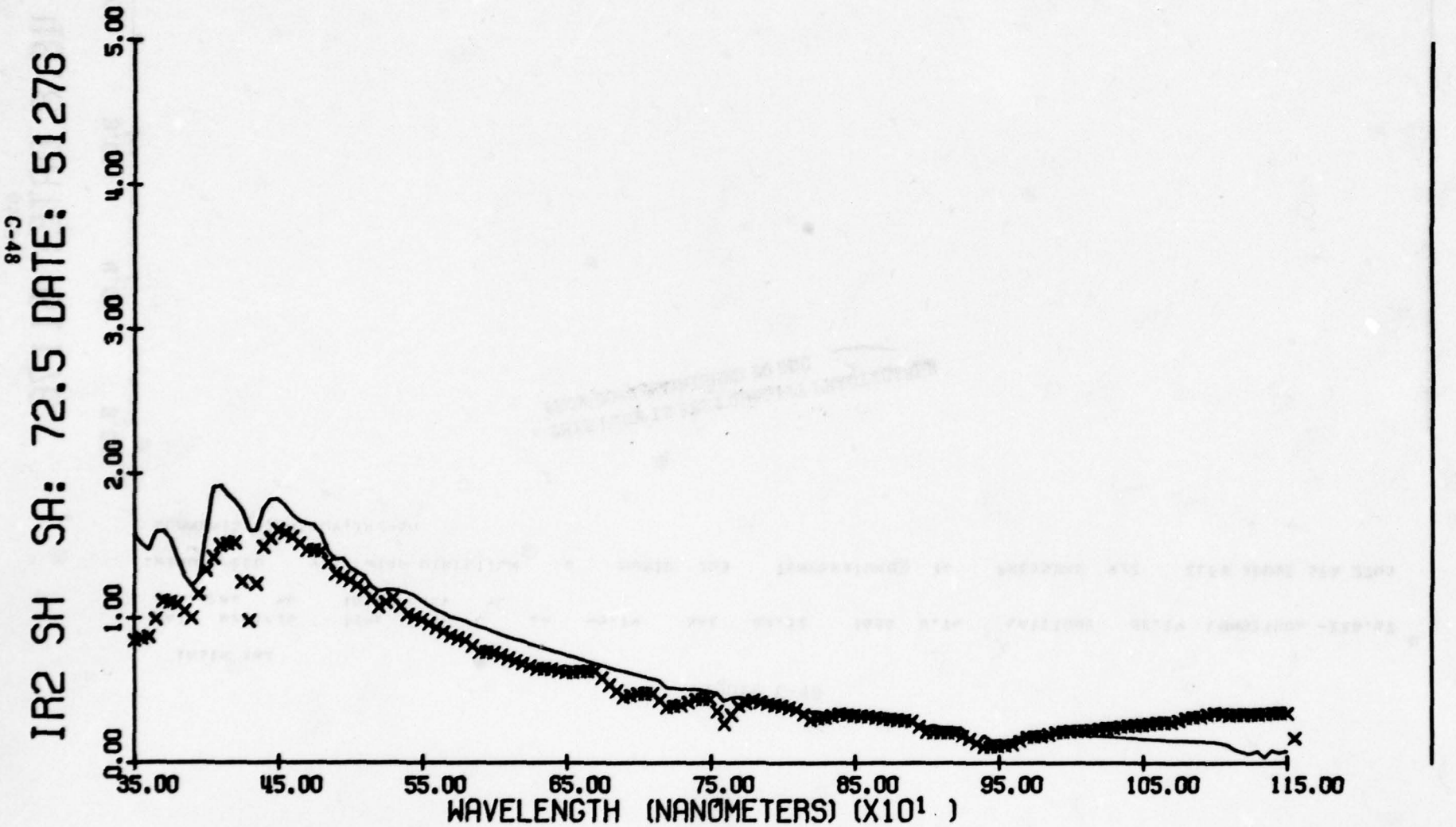

Figure C-48

INSTR IR2

DATA 6/11/76 TIME 16:10:0 G SA 46.79 SAZ 89.52 I650 0.74 LATITUDE 32.19 LONGITUDE -110.87
INSTR AZ 90 INSTR ELEV 90

WIND SPEED 9 WIND DIRECTION 0 HUMID 283 TEMPERATURE 76 PRESSURE 922 ELEV ABOVE SEA 2705

COMMENTS 3,IR1=UV,IR2=SH

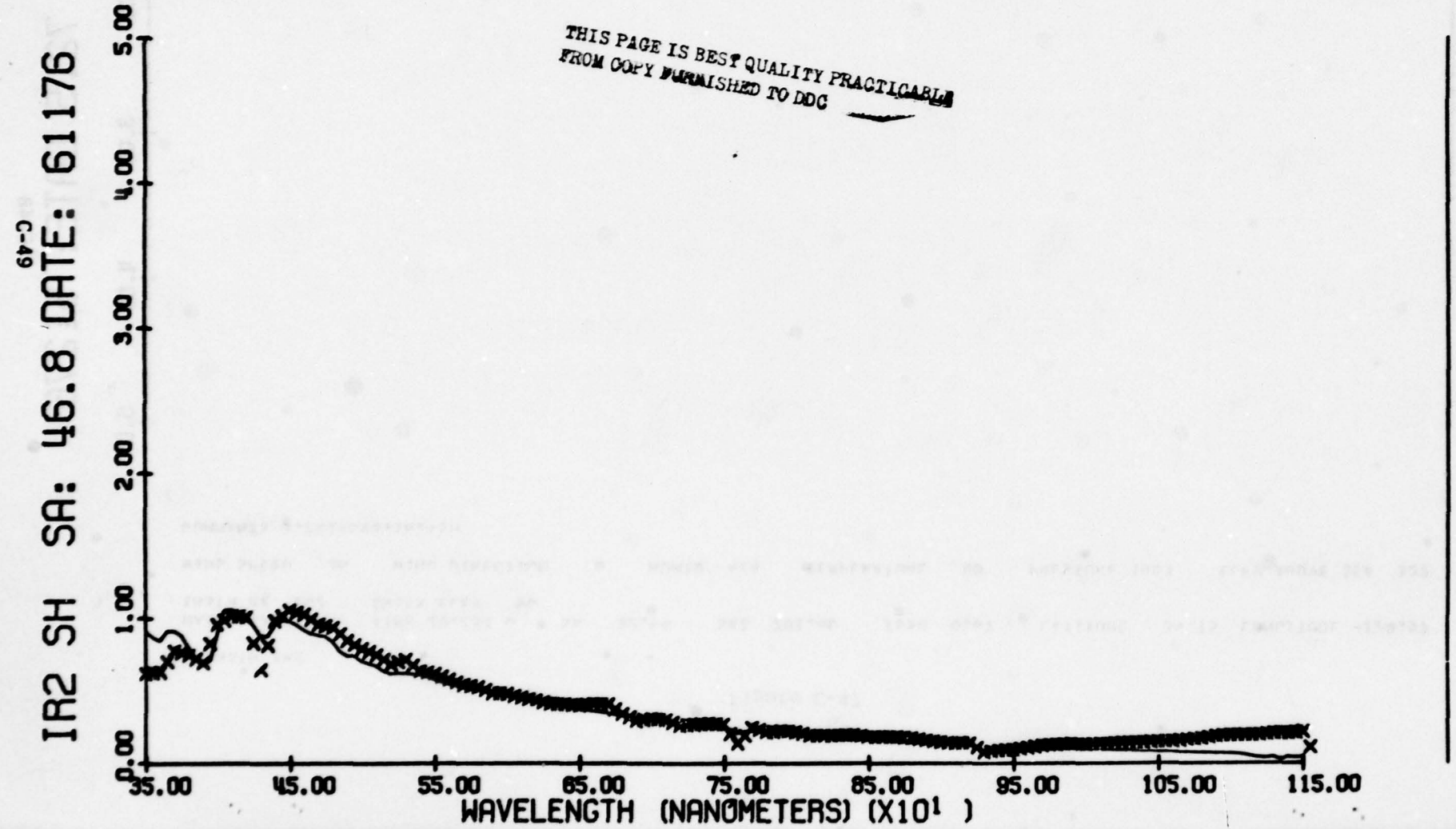

Figure C-49

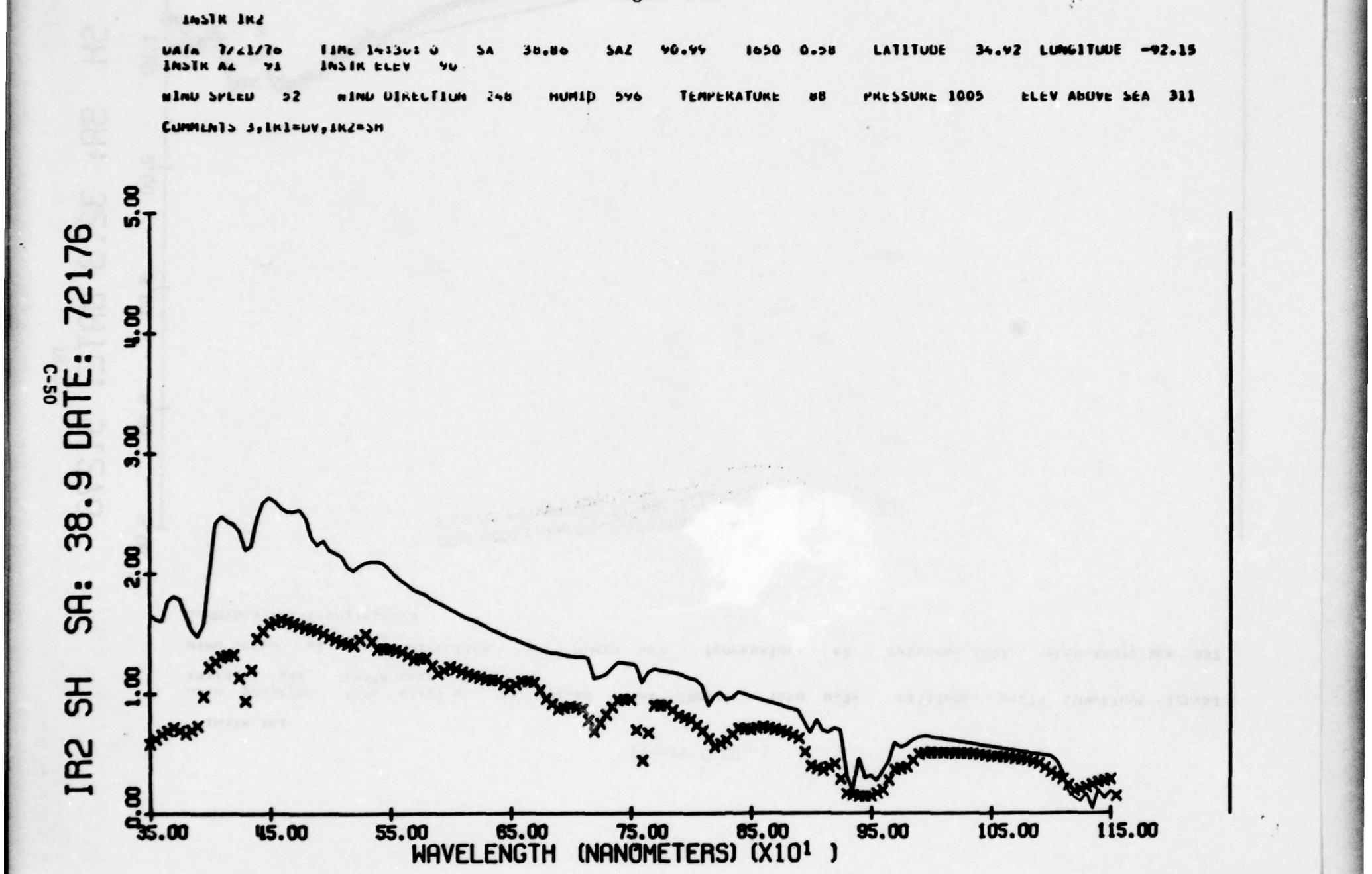
INSTR IR2
DATE 7/21/76 TIME 1433:0 0 SA 38.80 SAZ 90.99 1650 0.58 LATITUDE 34.92 LONGITUDE -92.15
INSTR AZ 91 INSTR ELEV 90
WIND SPEED 32 WIND DIRECTION 248 HUMID 596 TEMPERATURE 88 PRESSURE 1005 ELEV ABOVE SEA 311
COMMENTS 3,IR1=DV,IR2=SM
IR2 SH SA: 38.9 DATE: 72176
C-50
0.00
1.00
2.00
3.00
4.00
5.00
35.00
45.00
55.00
65.00
75.00
85.00
95.00
105.00
115.00
WAVELENGTH (NANOMETERS) (X10¹)

Figure C-50

INSTR IR1

DATA 5/13/76 TIME 6:16: 6 SA 32.30 SAZ 270.87 TOSO 0.74 LATITUDE 34.75 LONGITUDE -120.57
INSTR AZ 271 INSTR ELEV 46

WIND SPEED 42 WIND DIRECTION 0 HUMID 403 TEMPERATURE 82 PRESSURE 1003 ELEV ABOVE SEA 327

COMMENTS 3,IR1=SH,IR2=SVD

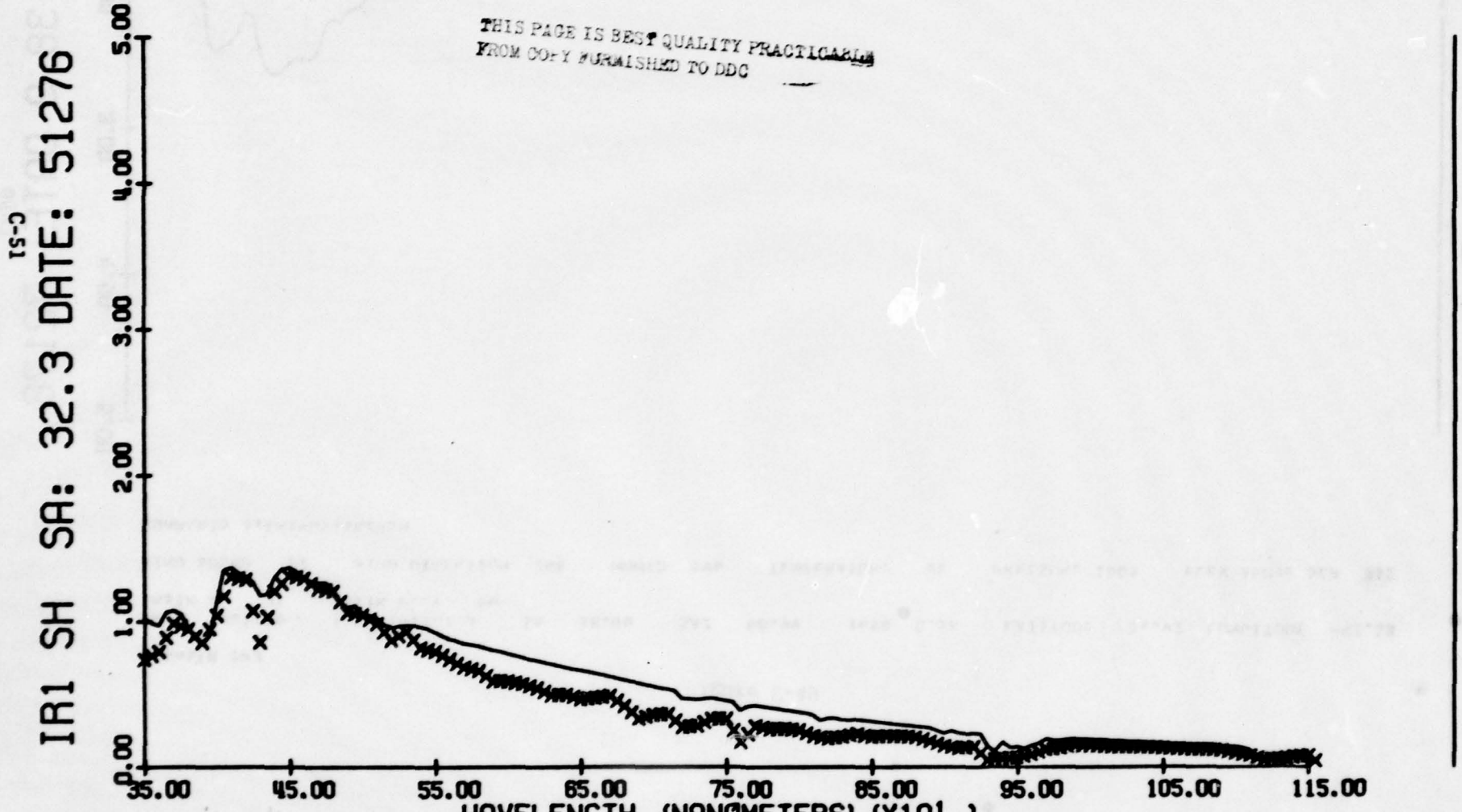

Figure C-51

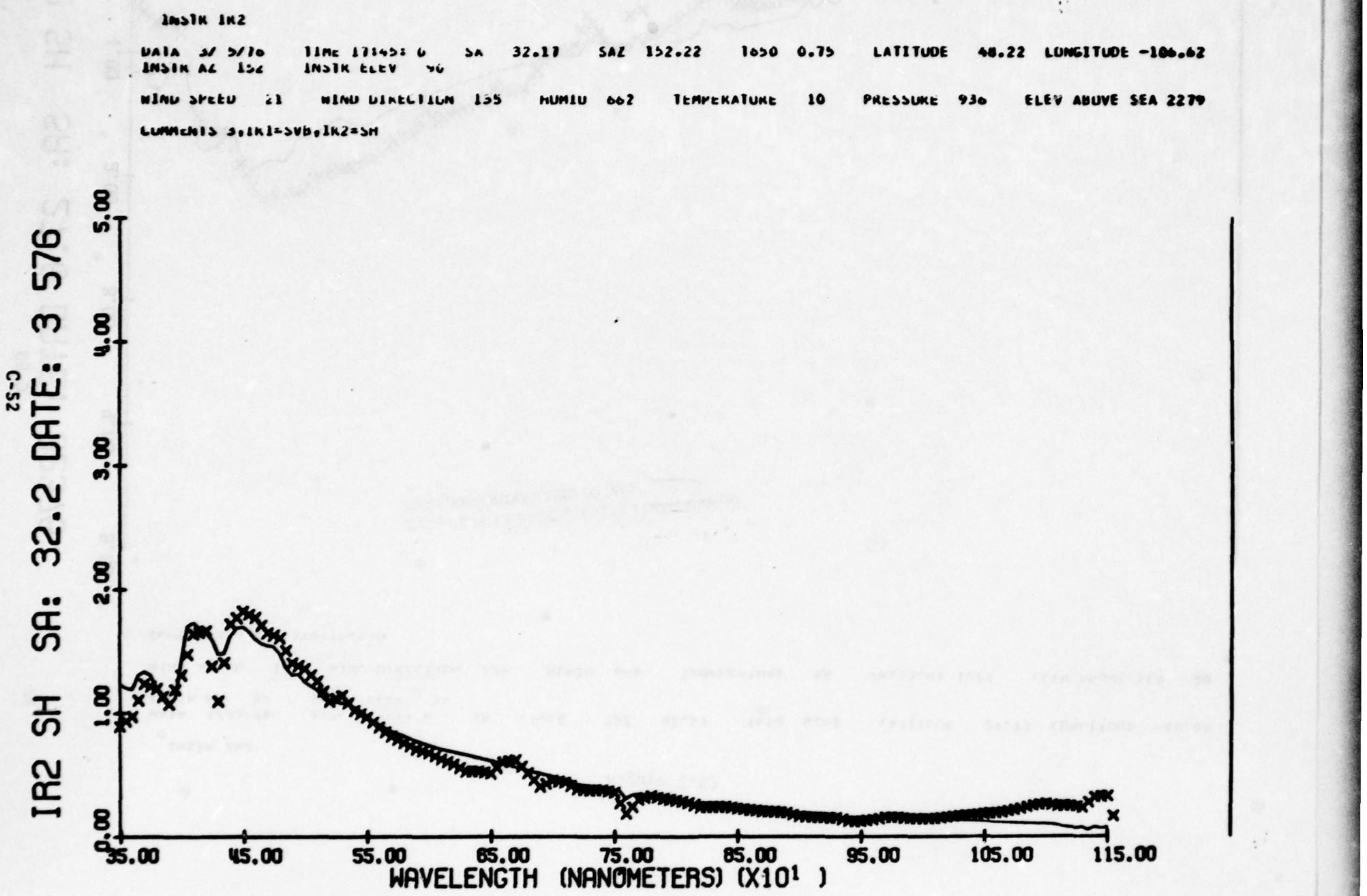
INSTR IR2
DATA 5/ 5/70 TIME 17:45: 0 SA 32.17 SAZ 152.22 1650 0.75 LATITUDE 48.22 LONGITUDE -106.62
INSTR AZ 152 INSTR ELEV 90
WIND SPEED 21 WIND DIRECTION 135 HUMID 662 TEMPERATURE 10 PRESSURE 930 ELEV ABOVE SEA 2279
COMMENTS 3,IR1=SVB,IR2=SH
IR2 SH SA: 32.2 DATE: 3 576
C-52
0.00
1.00
2.00
3.00
4.00
5.00
35.00
45.00
55.00
65.00
75.00
85.00
95.00
105.00
115.00
WAVELENGTH (NANOMETERS) (X10¹)

Figure C-52

INSTR IR2

DATA 8/23/80 TIME 13:23: 0 SA 27.58 SAZ 92.57 T650 0.01 LATITUDE 24.73 LONGITUDE -85.03
INSTR AZ 93 INSTR ELEV 90

WIND SPEED 10 WIND DIRECTION 334 HUMID 044 TEMPERATURE 84 PRESSURE 1015 ELEV ABOVE SEA 20

COMMENTS 3,IR1=SVD,IR2=SM

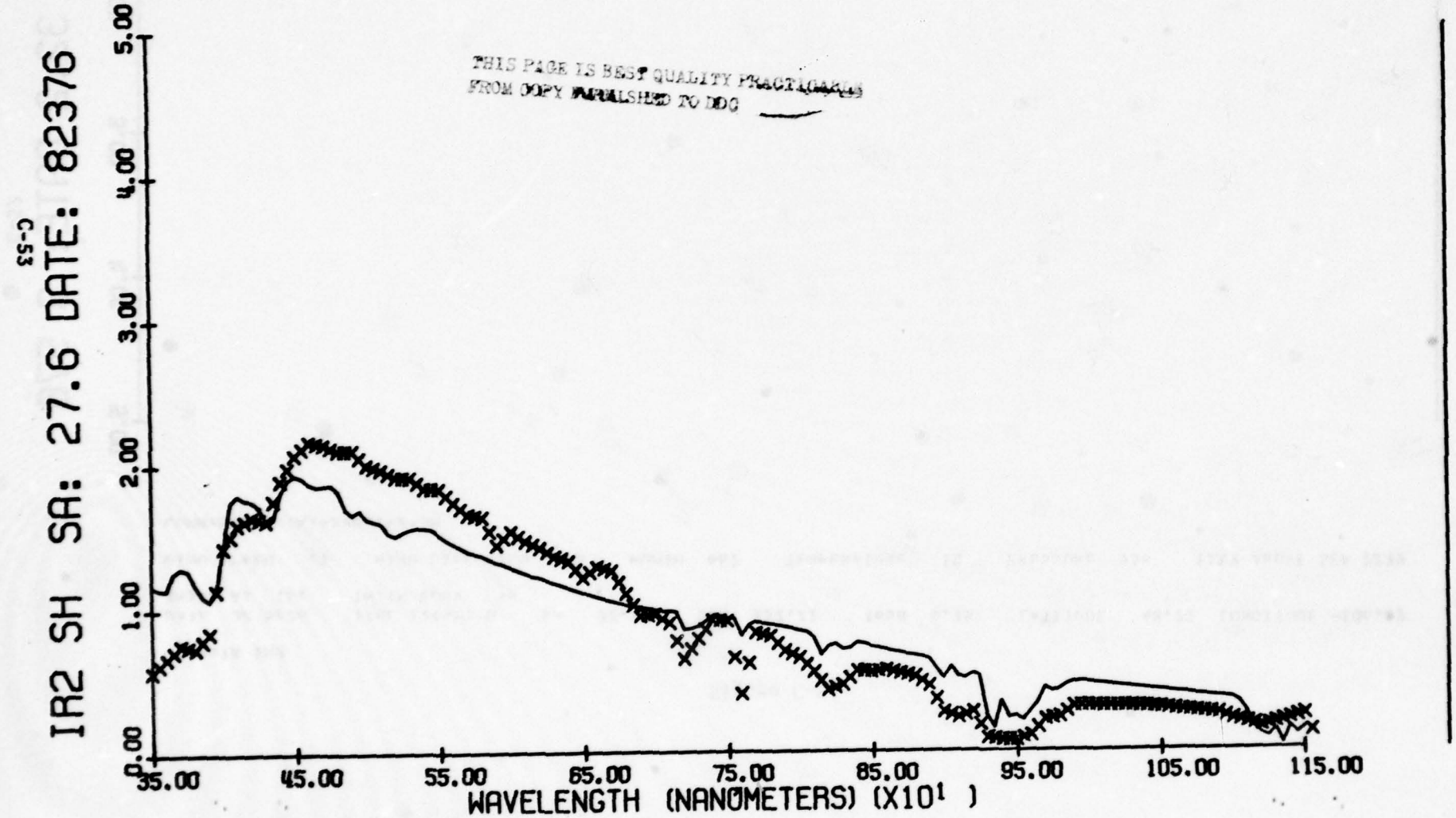

Figure C-53

INSTR IR2

DATA 6/11/76 TIME 13:55: 0 SA 18.62 SAZ 73.87 TOSG 0.82 LATITUDE 32.19 LONGITUDE -110.87
INSTR AZ 69 INSTR ELEV 90

WIND SPEED 0 WIND DIRECTION 0 HUMID 310 TEMPERATURE 69 PRESSURE 922 ELEV ABOVE SEA 2705

COMMENTS 2,IR1=SVB,IR2=SH, PHONE TRANSMITTING.

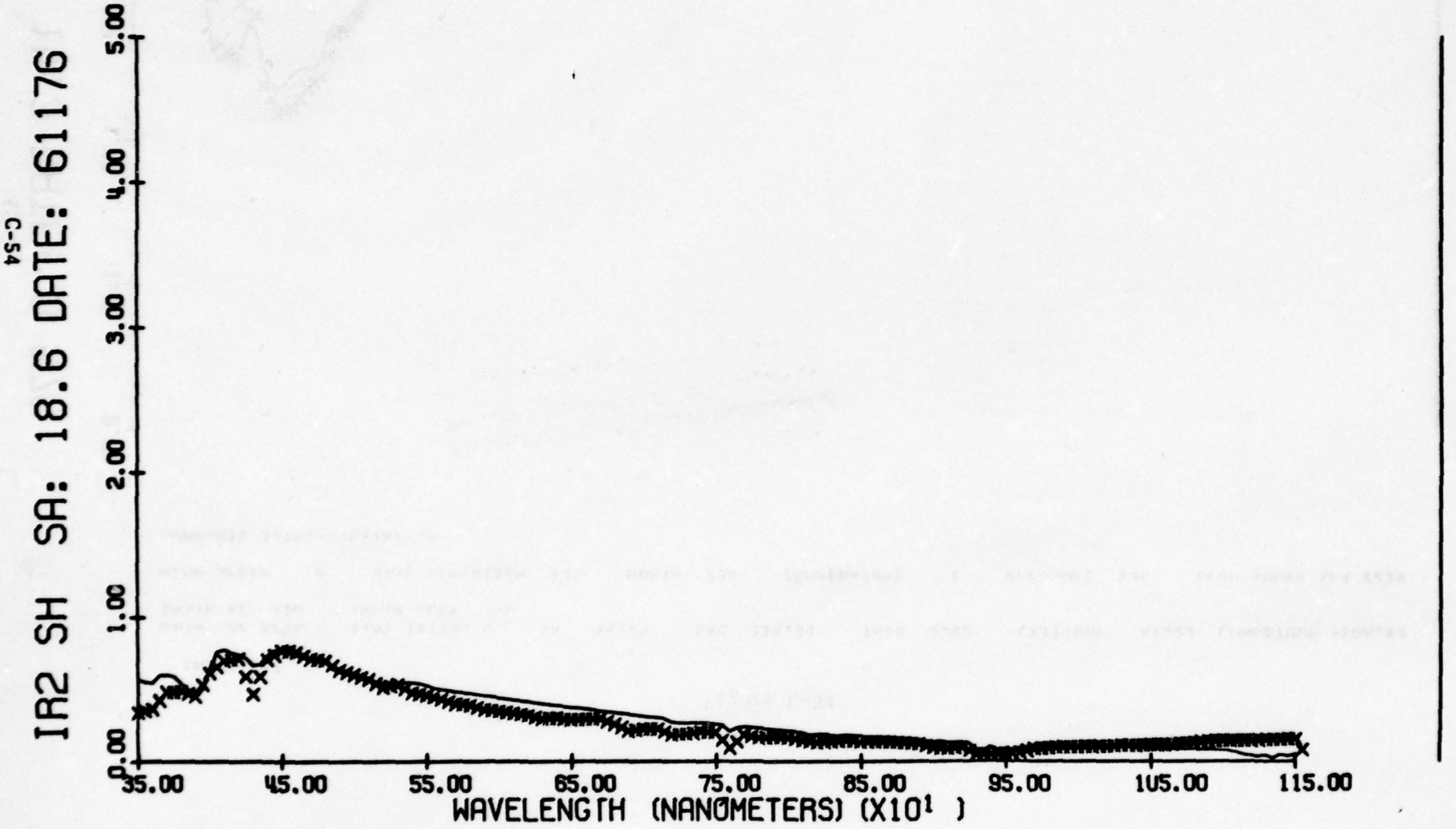

Figure C-54

INSIK IR2

DATA 3/ 5/76 TIME 15:15: 0 SA 14.25 SAZ 116.31 To50 0.82 LATITUDE 48.22 LONGITUDE -106.62
INSIK AZ 116 INSIK ELEV 90

WIND SPEED 0 WIND DIRECTION 133 HUMID 72% TEMPERATURE 1 PRESSURE 930 ELEV ABOVE SEA 2279

COMMENTS 3,IR1=SVB,IR2=SH

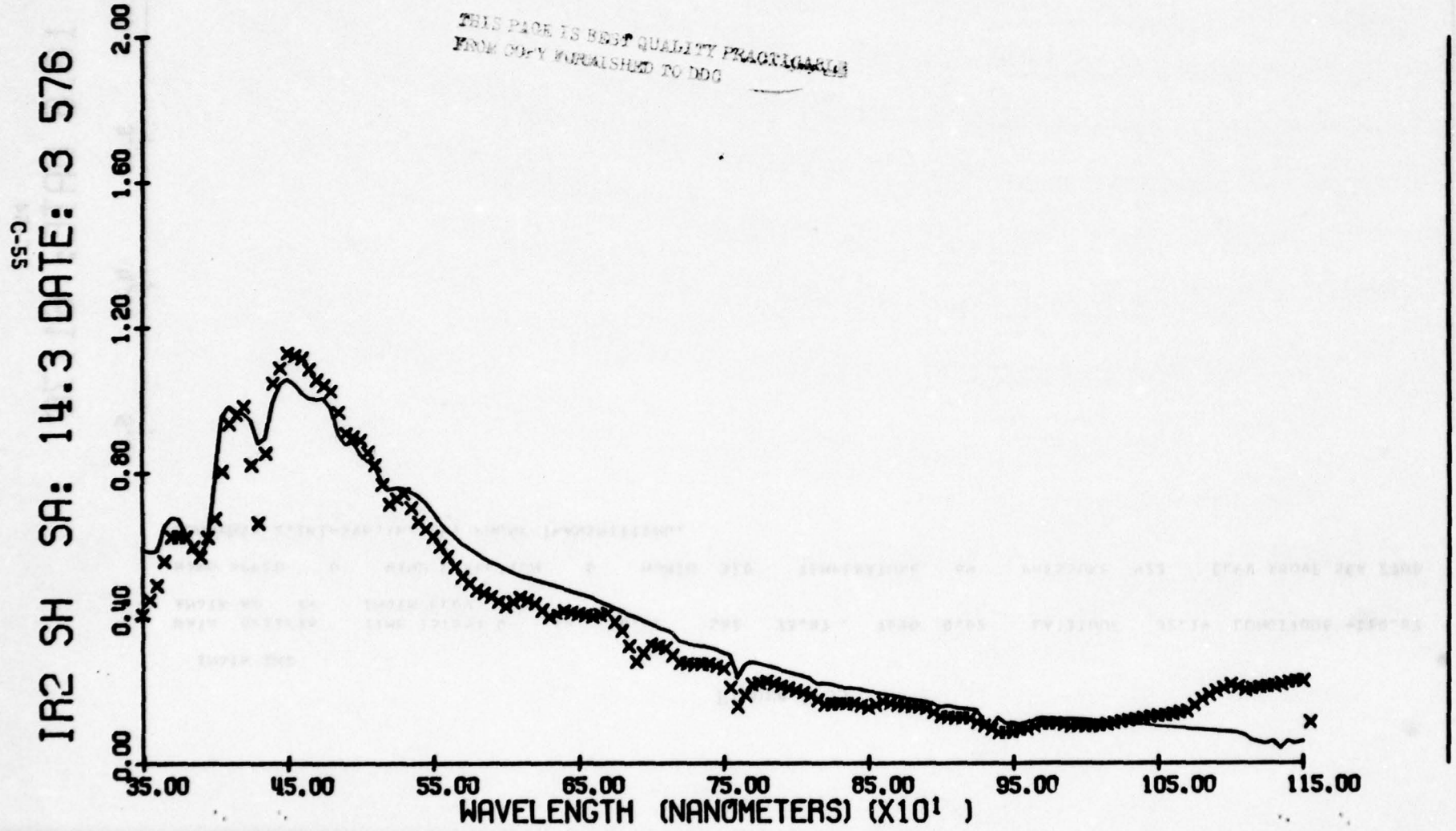

Figure C-55

INSTR IR1

DATA 5/13/76 TIME 1:55: 0 SA 11.00 SAZ 284.85 TAU50 0.81 LATITUDE 34.75 LONGITUDE -120.57
INSTR AZ 265 INSTR ELEV 90

WIND SPEED 0 WIND DIRECTION 0 HUMID 419 TEMPERATURE 79 PRESSURE 1003 ELEV ABOVE SEA 327

COMMENTS 3,IR1=SM,IR2=DM

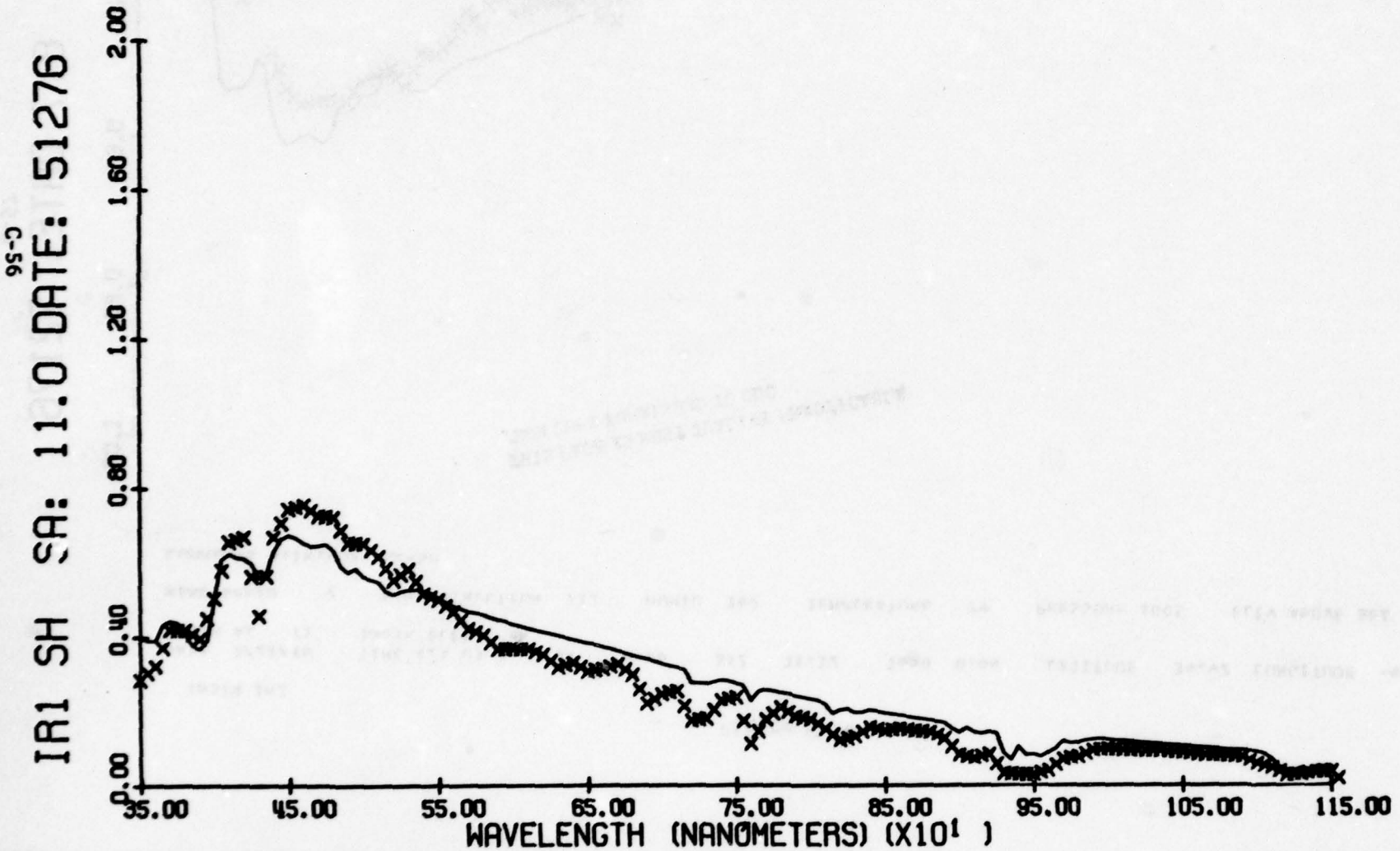

Figure C-56

INSTR IR2

DATA 7/21/76 TIME 123 03 0 SA 8.66 SAZ 71.12 TOSD 0.64 LATITUDE 34.92 LONGITUDE -92.15
INSTR AZ 71 INSTR ELEV 90

WIND SPEED 0 WIND DIRECTION 212 HUMID 762 TEMPERATURE 79 PRESSURE 1005 ELEV ABOVE SEA 311

COMMENTS 3,IR1=UV,IR2=SM

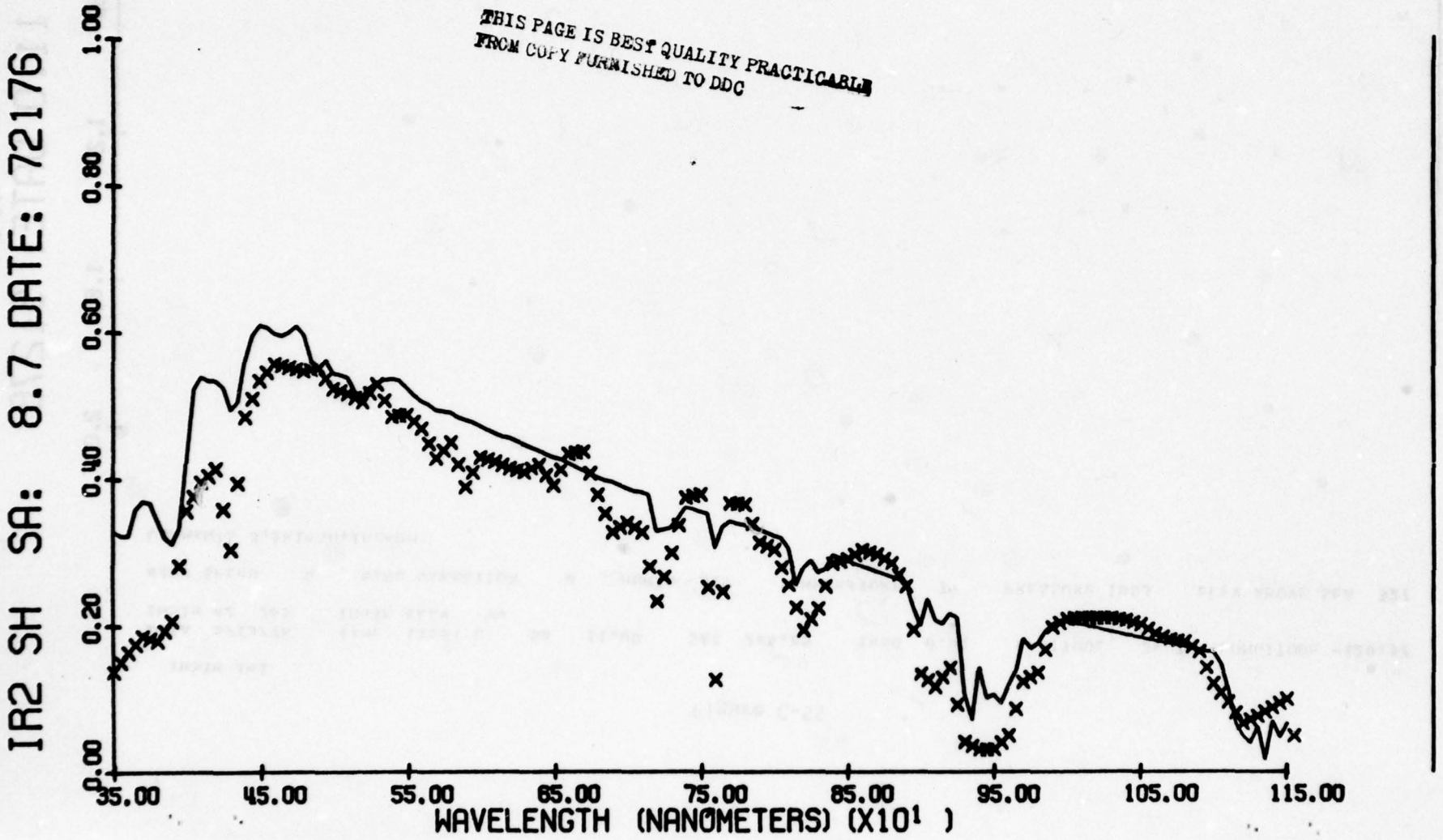

Figure C-57

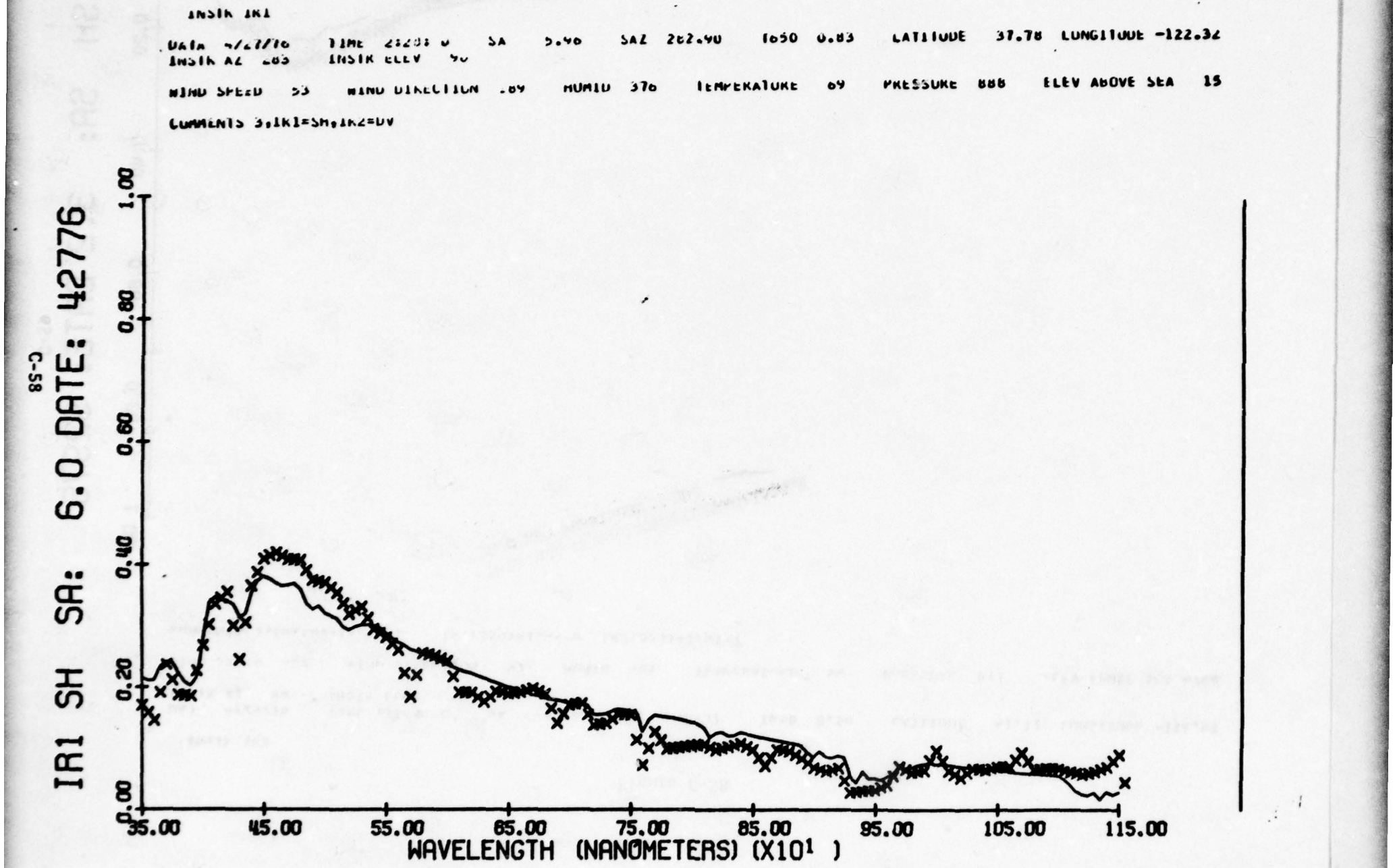
INSTR IR1
DATA 7/27/76 TIME 2320:0 SA 5.40 SAZ 282.40 I650 0.83 LATITUDE 37.78 LONGITUDE -122.32
INSTR AZ 283 INSTR ELEV 90
WIND SPEED 33 WIND DIRECTION 284 HUMID 37% TEMPERATURE 69 PRESSURE 888 ELEV ABOVE SEA 15
COMMENTS 3;IR1=SH;IR2=DV
IR1 SH SA: 6.0 DATE: 42776
1.00
0.80
0.60
0.40
0.20
0.00
35.00
45.00
55.00
65.00
75.00
85.00
95.00
105.00
115.00
WAVELENGTH (NANOMETERS) (X10¹)

Figure C-58

INSTR IR2

DATA 4/24/76 TIME 13:45:0 SA 3.10 SAZ 40.31 TOSO 0.56 LATITUDE 41.12 LONGITUDE -111.97
INSTR AZ 90 INSTR ELEV 90

WIND SPEED 12.7 WIND DIRECTION 97 HUMID 481 TEMPERATURE 54 PRESSURE 873 ELEV ABOVE SEA 4788

COMMENTS 3;IR1=DV;IR2=SH; IR1(350)=1.44-8 IR2(350)=1.07-7

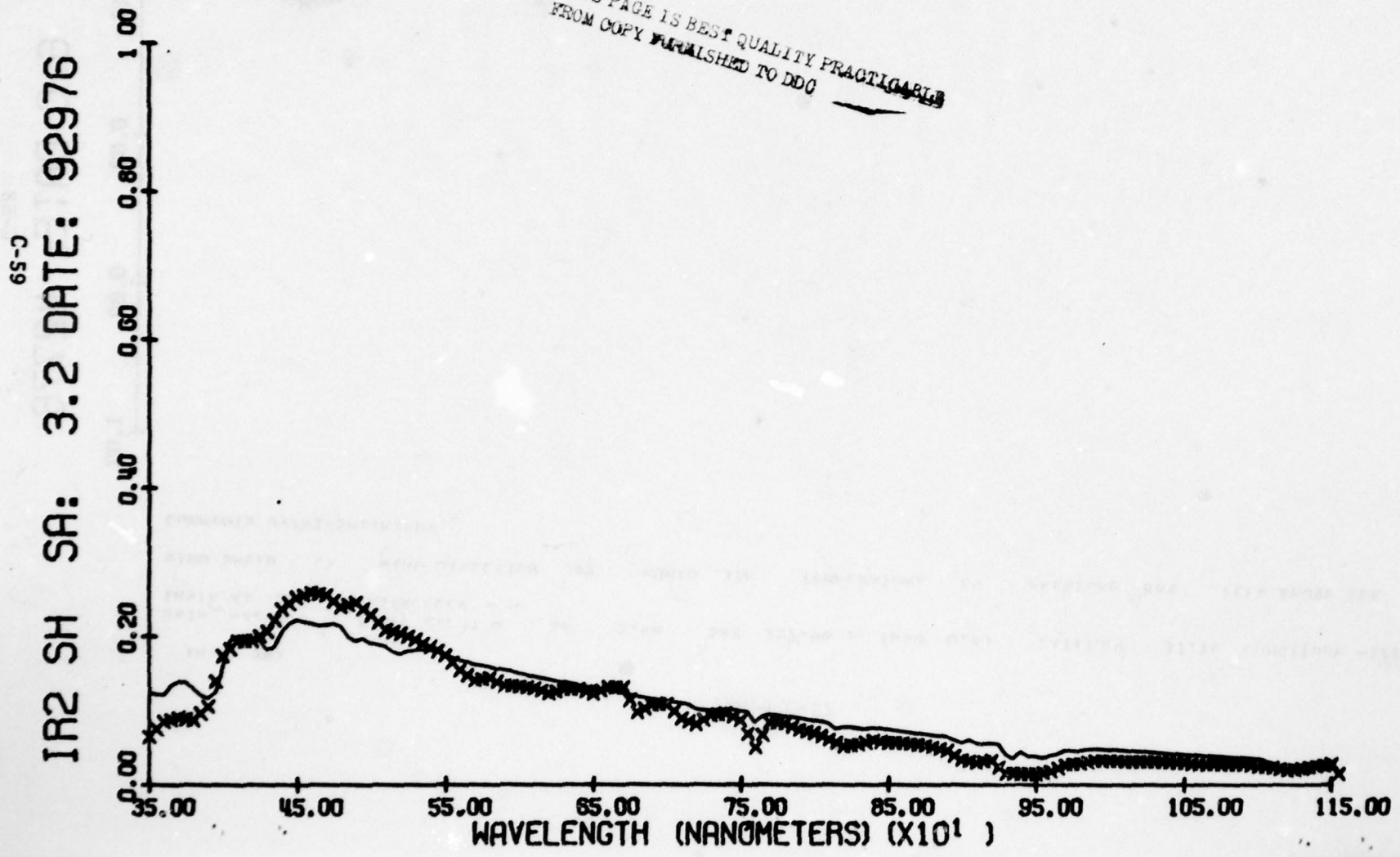

Figure C-59

INSTR IR1

DATA 4/6/76 TIME 2335: 0 SA 3.08 SAZ 285.14 TOSO 0.85 LATITUDE 37.78 LONGITUDE -122.52
INSTR AZ 285 INSTR ELEV 90

WIND SPEED 06 WIND DIRECTION 291 HUMID 407 TEMPERATURE 06 PRESSURE 841 ELEV ABOVE SEA 15

COMMENTS S,IR1-SM,IR2-DM,IR1=2.09X10-8 AT FINISH 350NM.

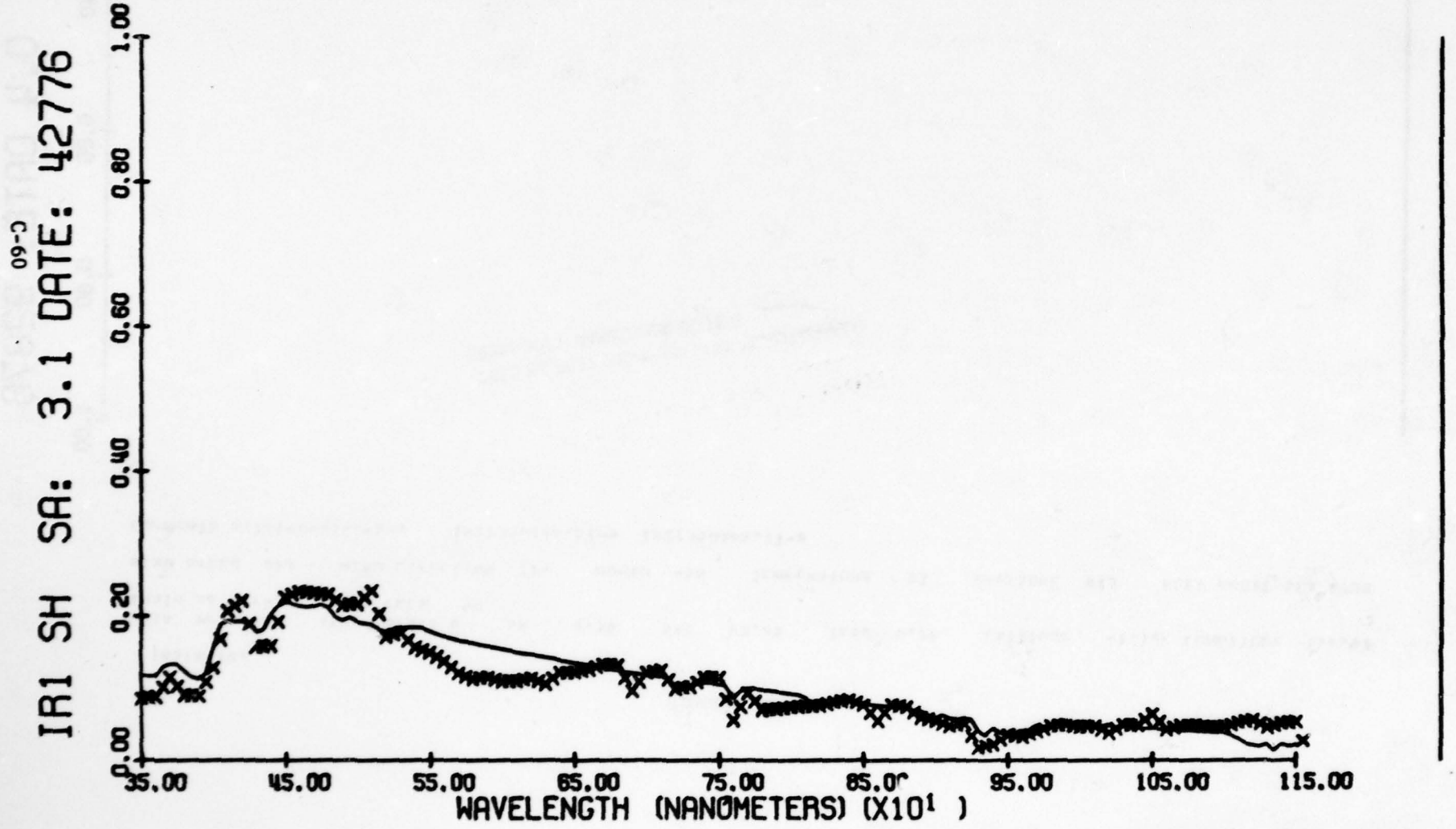

Figure C-60

INSTR IR2

DATA 9/29/80 TIME 13:30:0 0 SA 0.35 SAZ 93.83 TOD 0.78 LATITUDE 41.12 LONGITUDE -111.97
INSTR AZ 90 INSTR ELEV 90

WIND SPEED 113 WIND DIRECTION 114 HUMID 486 TEMPERATURE 53 PRESSURE 873 ELEV ABOVE SEA 4788

COMMENTS S,IR1=DV,IR2=SM, IR1(350)=6.57-9 IR2(350)=4.77-8

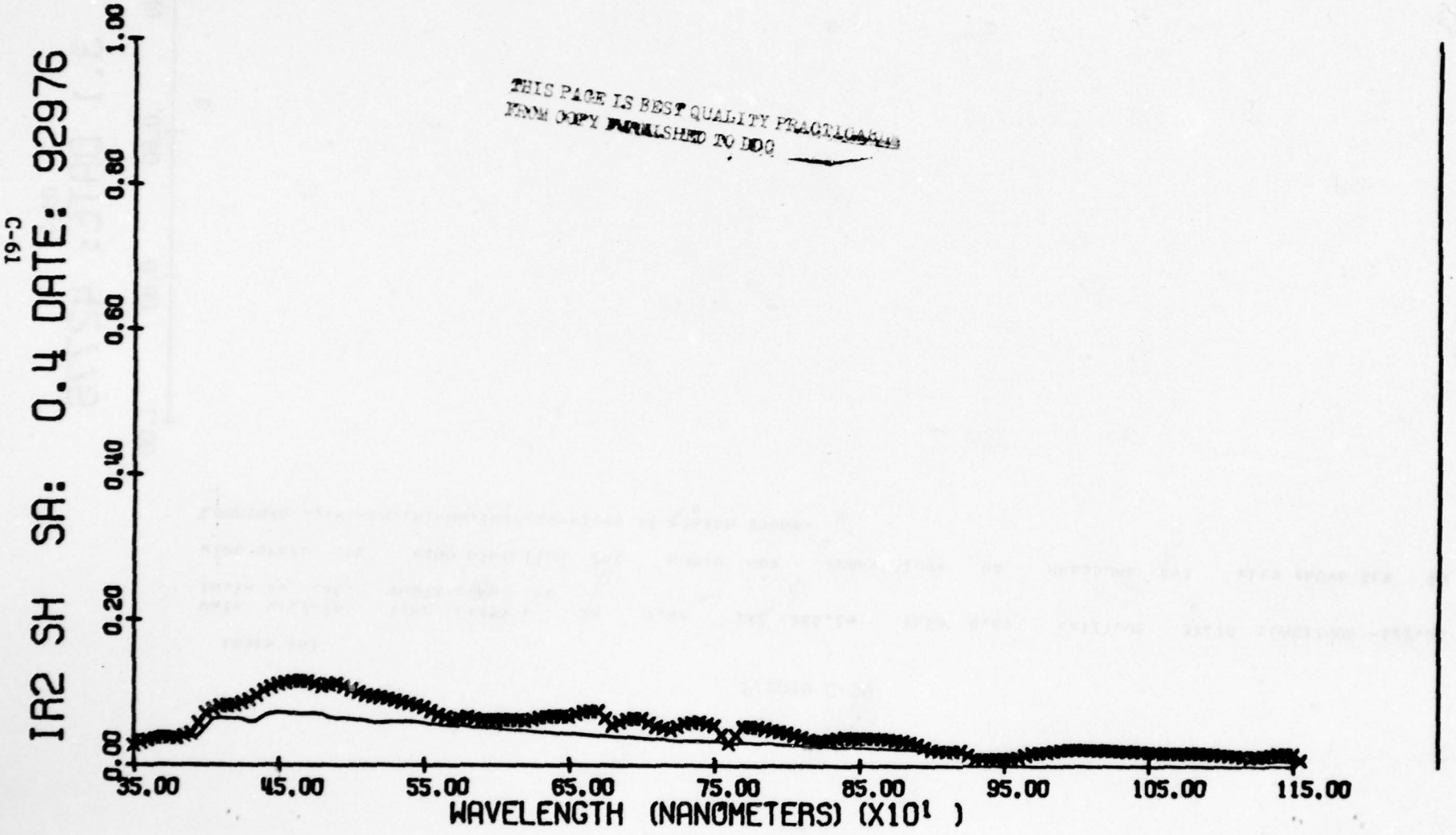

Figure C-61

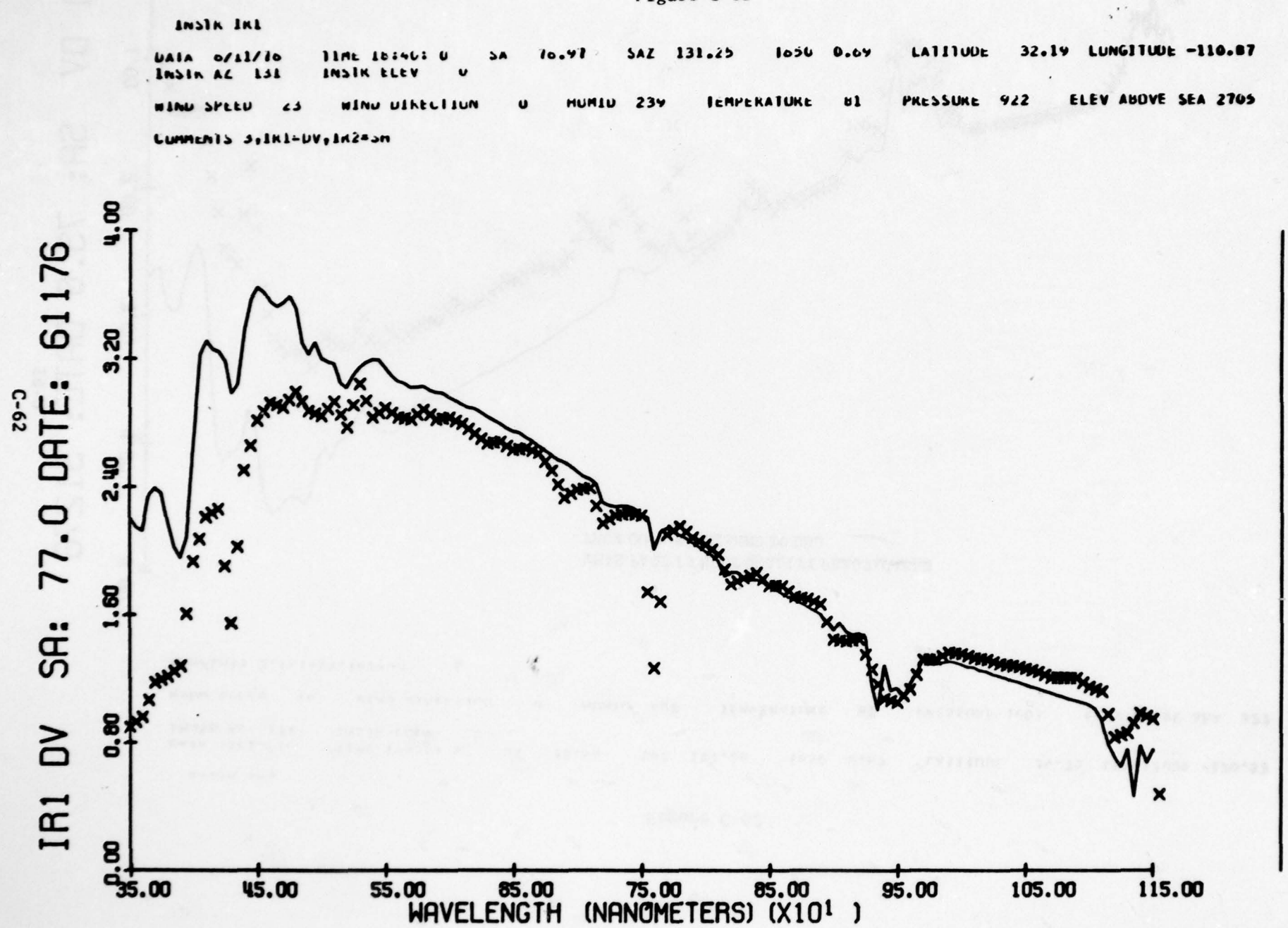
INSIK IR1
DATA 6/11/86 TIME 16:46: 0 SA 76.97 SAZ 131.25 ISO 0.69 LATITUDE 32.19 LONGITUDE -110.87
INSIK AZ 131 INSIK ELEV 0
WIND SPEED 23 WIND DIRECTION 0 HUMID 23% TEMPERATURE 81 PRESSURE 922 ELEV ABOVE SEA 2705
COMMENTS 3,IR1-DV,IR2=3M
IR1 DV SA: 77.0 DATE: 61176
0.00
0.80
1.60
2.40
3.20
4.00
35.00
45.00
55.00
65.00
75.00
85.00
95.00
105.00
115.00
WAVELENGTH (NANOMETERS) (X10¹)

Figure C-62

[illegible] ANS

DATA 5/12/76 TIME 14:55: 6 SA 73.56 SAZ 177.26 1650 0.67 LATITUDE 34.75 LONGITUDE -120.57
INSTR AZ 177 INSTR ELEV 0

WIND SPEED 26 WIND DIRECTION 0 HUMID 428 TEMPERATURE 61 PRESSURE 1003 ELEV ABOVE SEA 327

COMMENTS 3,IR1=DV,IR2=UM

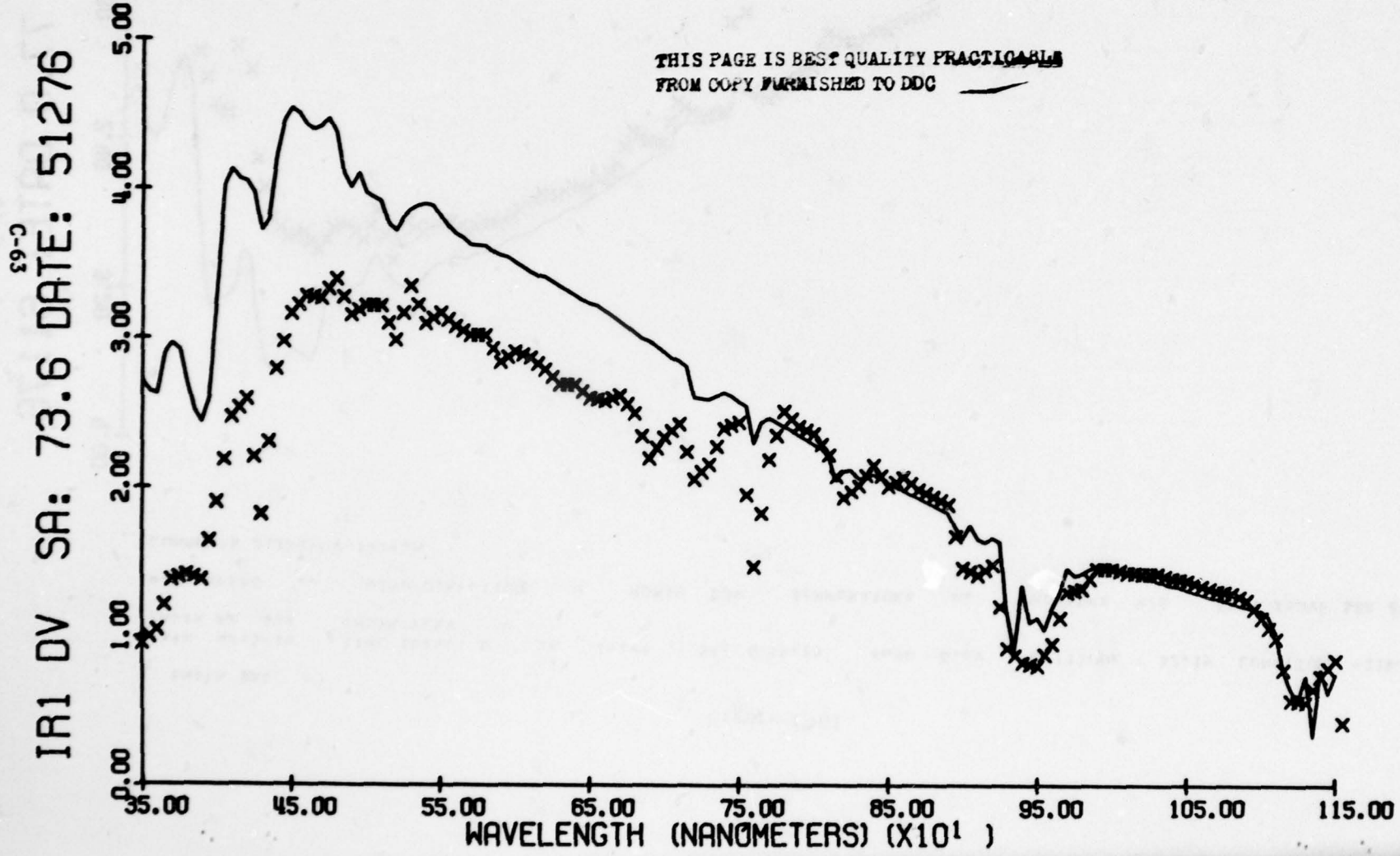

Figure C-63

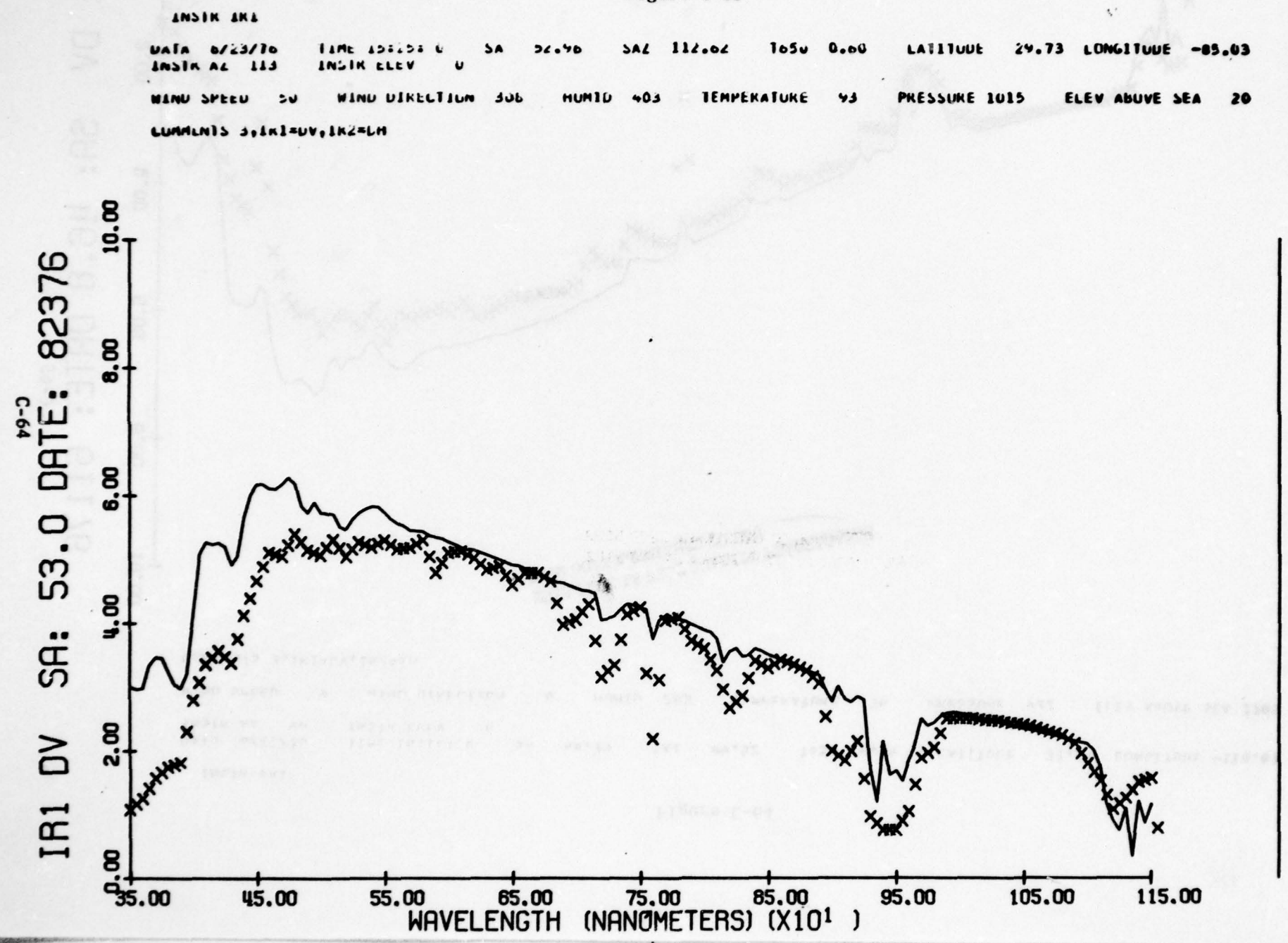
INSTR IR1
DATA 8/23/78 TIME 15:53:3 G SA 52.96 SAZ 112.02 165U 0.00 LATITUDE 29.73 LONGITUDE -85.03
INSTR AZ 113 INSTR ELEV 0
WIND SPEED 30 WIND DIRECTION 306 HUMID 403 TEMPERATURE 93 PRESSURE 1015 ELEV ABOVE SEA 20
COMMENTS 3,IR1=DV,IR2=LM
IR1 DV SA: 53.0 DATE: 82376
C-64
10.00
8.00
6.00
4.00
2.00
0.00
35.00
45.00
55.00
65.00
75.00
85.00
95.00
105.00
115.00
WAVELENGTH (NANOMETERS) (X10¹)

Figure C-64

INSTR IR1

DATA 6/11/76 TIME 16:16:0 U SA 46.79 SAZ 84.52 1650 0.74 LATITUDE 32.19 LONGITUDE -110.87
INSTR AZ 90 INSTR ELEV 0

WIND SPEED 9 WIND DIRECTION 0 HUMID 283 TEMPERATURE 76 PRESSURE 922 ELEV ABOVE SEA 2705

COMMENTS 3,IR1=DV,IR2=SM

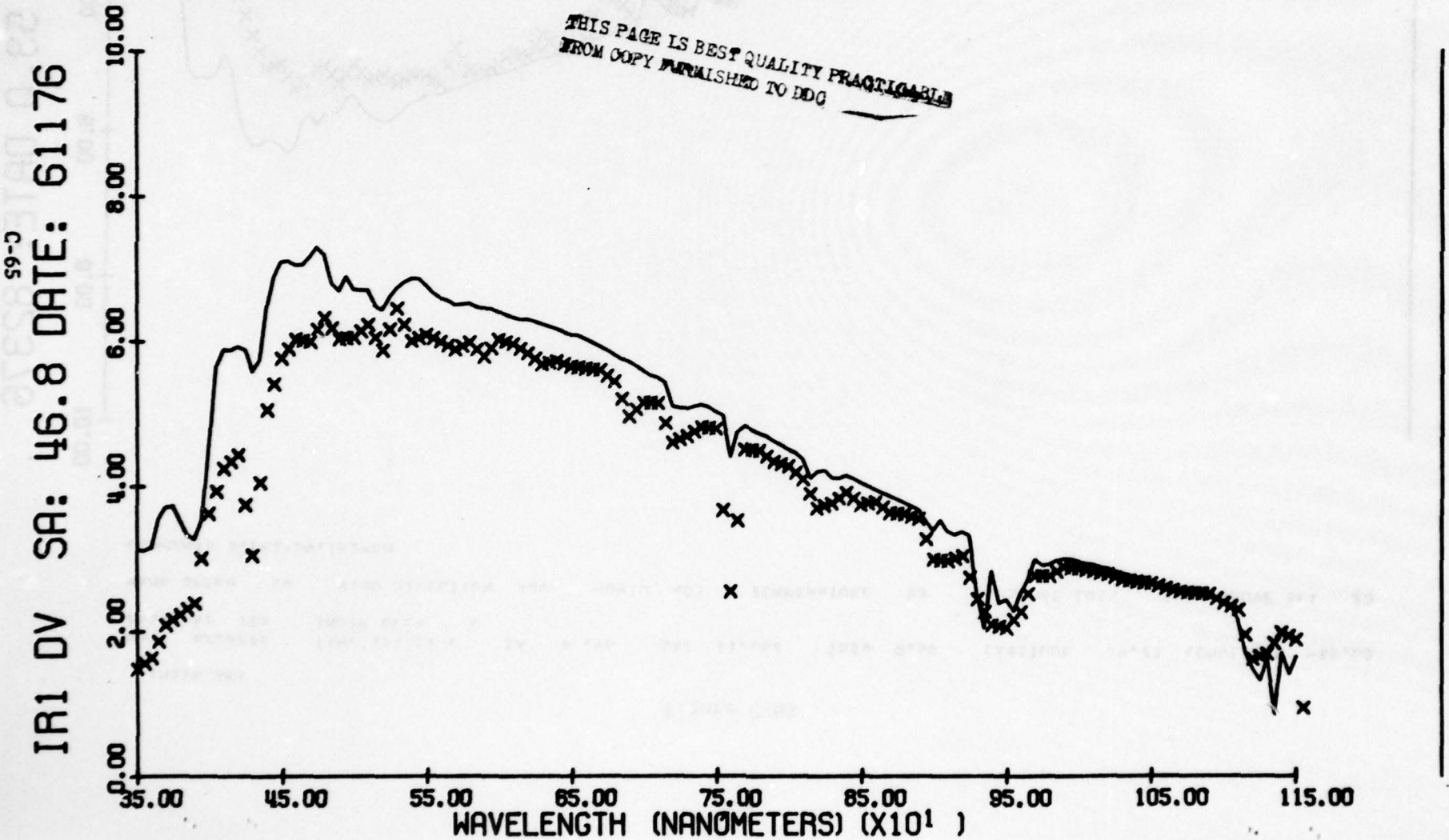

Figure C-65

INSIK IR1

DATA 7/21/76 TIME 14:30:00 G SA 38.86 SAZ 90.99 1650 0.58 LATITUDE 34.92 LONGITUDE -92.15
INSIK AZ 91 INSIK ELEV 0

WIND SPEED 52 WIND DIRECTION 248 HUMID 59% TEMPERATURE 88 PRESSURE 1005 ELEV ABOVE SEA 311

COMMENTS 3,IR1=DV,IR2=SM

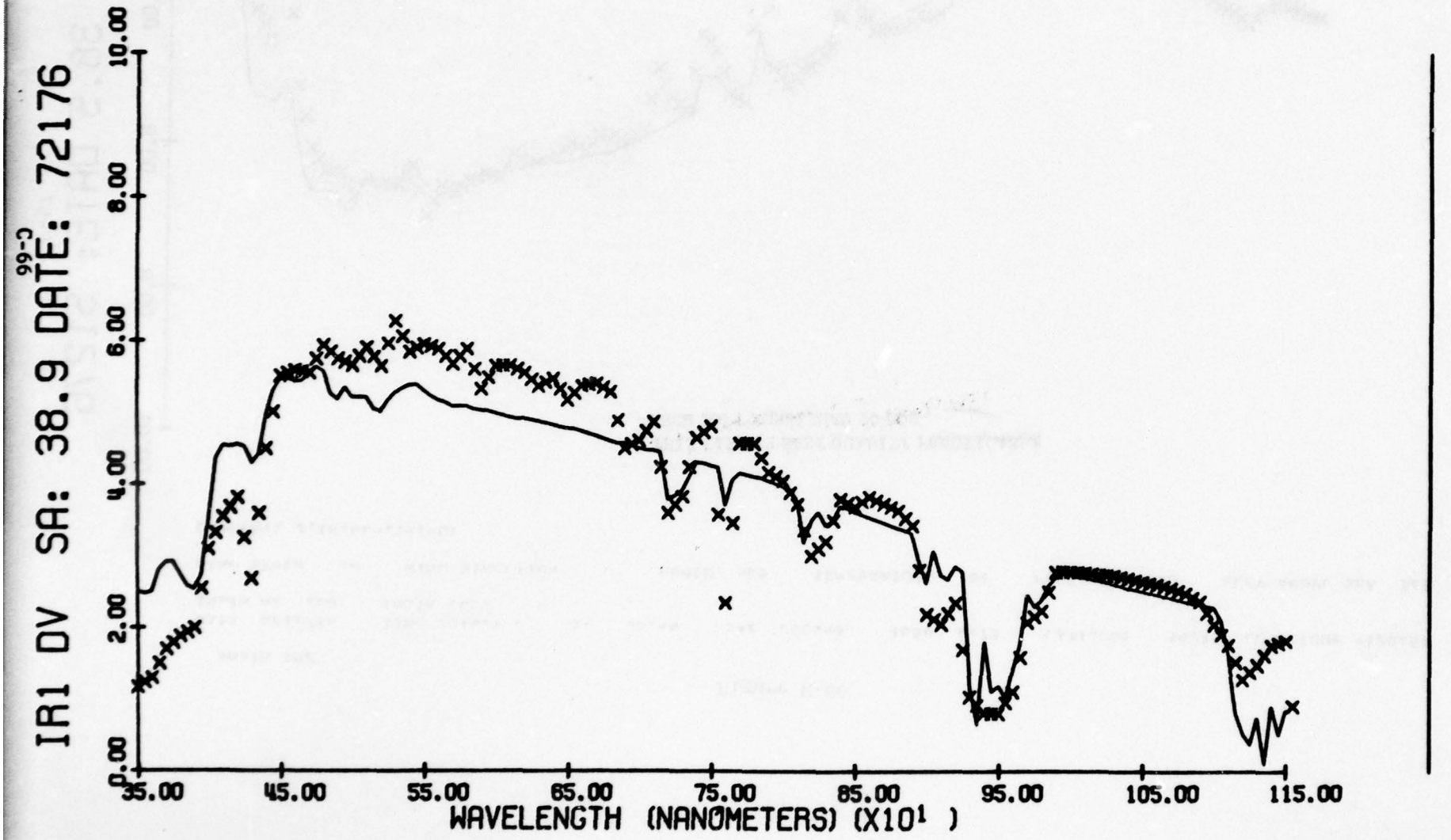

Figure C-66

INSTR IR2

DATA 5/12/76 TIME 23:46:3 U SA 38.46 SAZ 266.46 1650 0.73 LATITUDE 34.75 LONGITUDE -120.57
INSTR AZ 266 INSTR ELEV 0

WIND SPEED 20 WIND DIRECTION 0 HUMID 465 TEMPERATURE 81 PRESSURE 1003 ELEV ABOVE SEA 327

COMMENTS 3,IR1=LM,IR2=DV

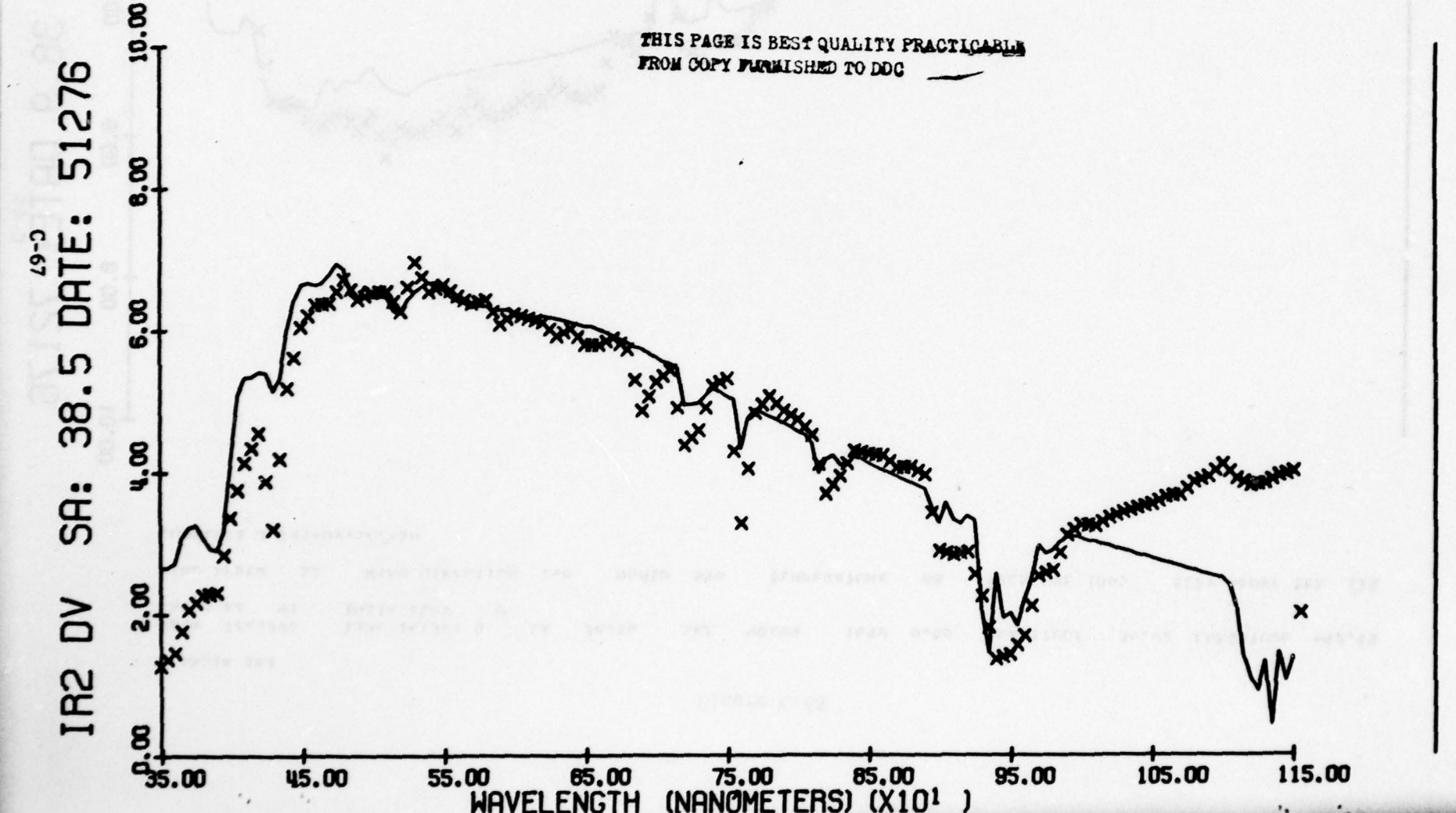

Figure C-67

INSTR IR1

DATE 3/ 5/80 TIME 17:15:5 U SA 29.55 SAZ 144.09 TESU 0.77 LATITUDE 48.22 LONGITUDE -166.62
INSTR AZ 144 INSTR ELEV 0

WIND SPEED 5 WIND DIRECTION 157 HUMID 664 TEMPERATURE 9 PRESSURE 936 ELEV ABOVE SEA 2279

COMMENTS 5,IR1=DV,IR2=DH

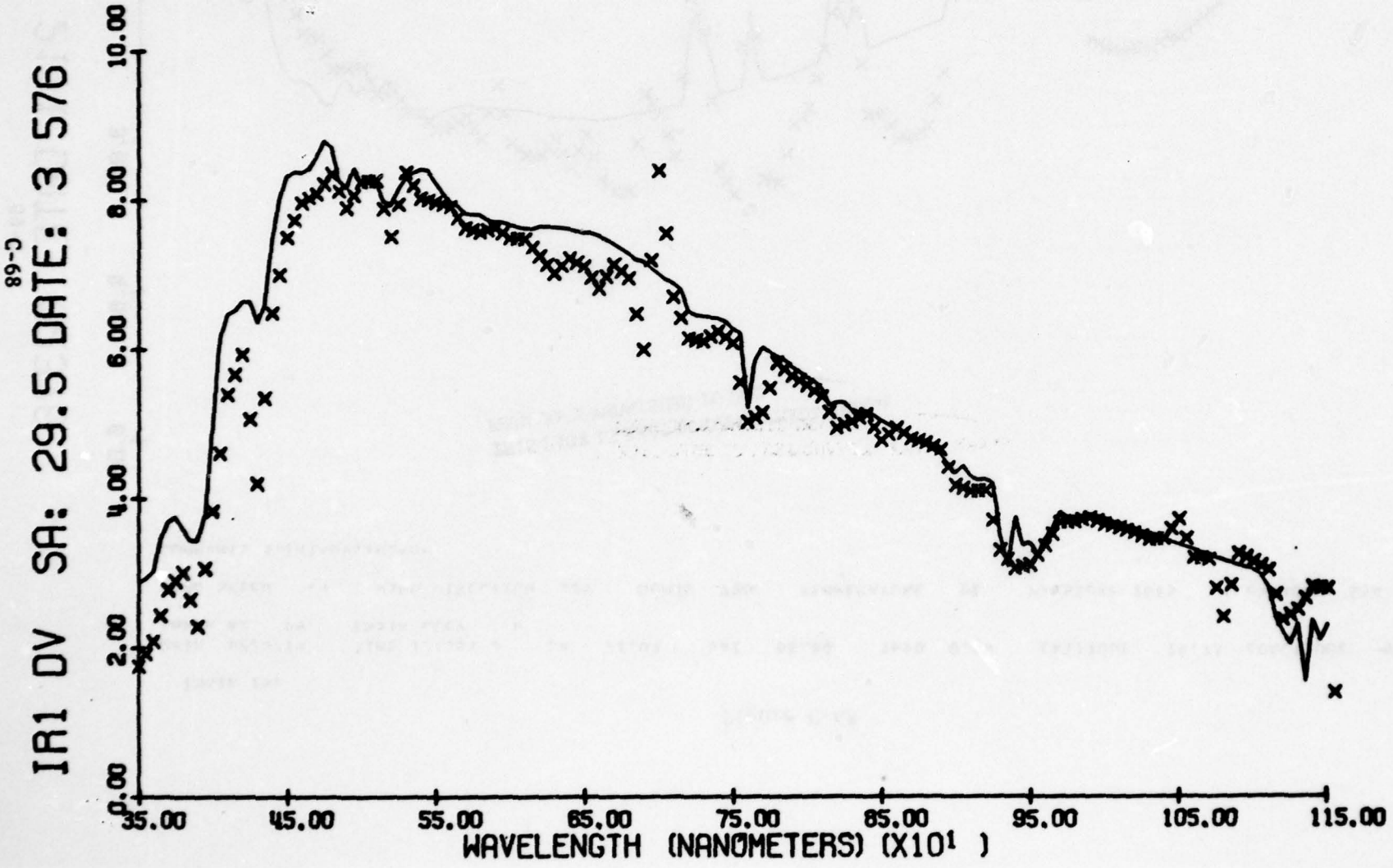

Figure C-68

INSTR IR1

DATA 8/23/76 TIME 12:55:1 U SA 21.07 SAZ 88.80 1650 0.54 LATITUDE 24.73 LONGITUDE -85.03
INSTR AZ 89 INSTR ELEV 0

WIND SPEED 24 WIND DIRECTION 339 HUMID 706 TEMPERATURE 81 PRESSURE 1015 ELEV ABOVE SEA 20

COMMENTS 3,IR1=DV,IR2=DH

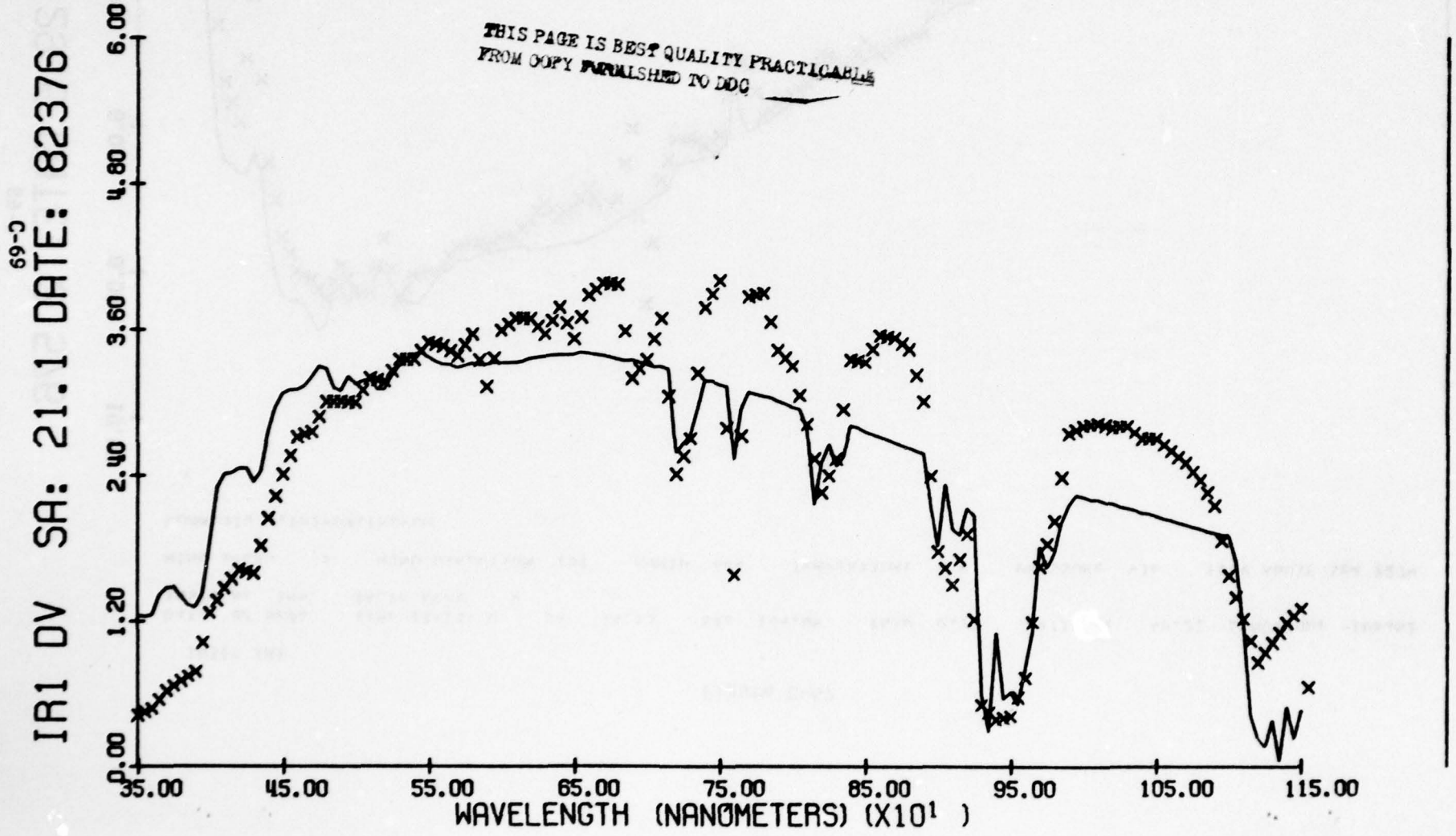

Figure C-69

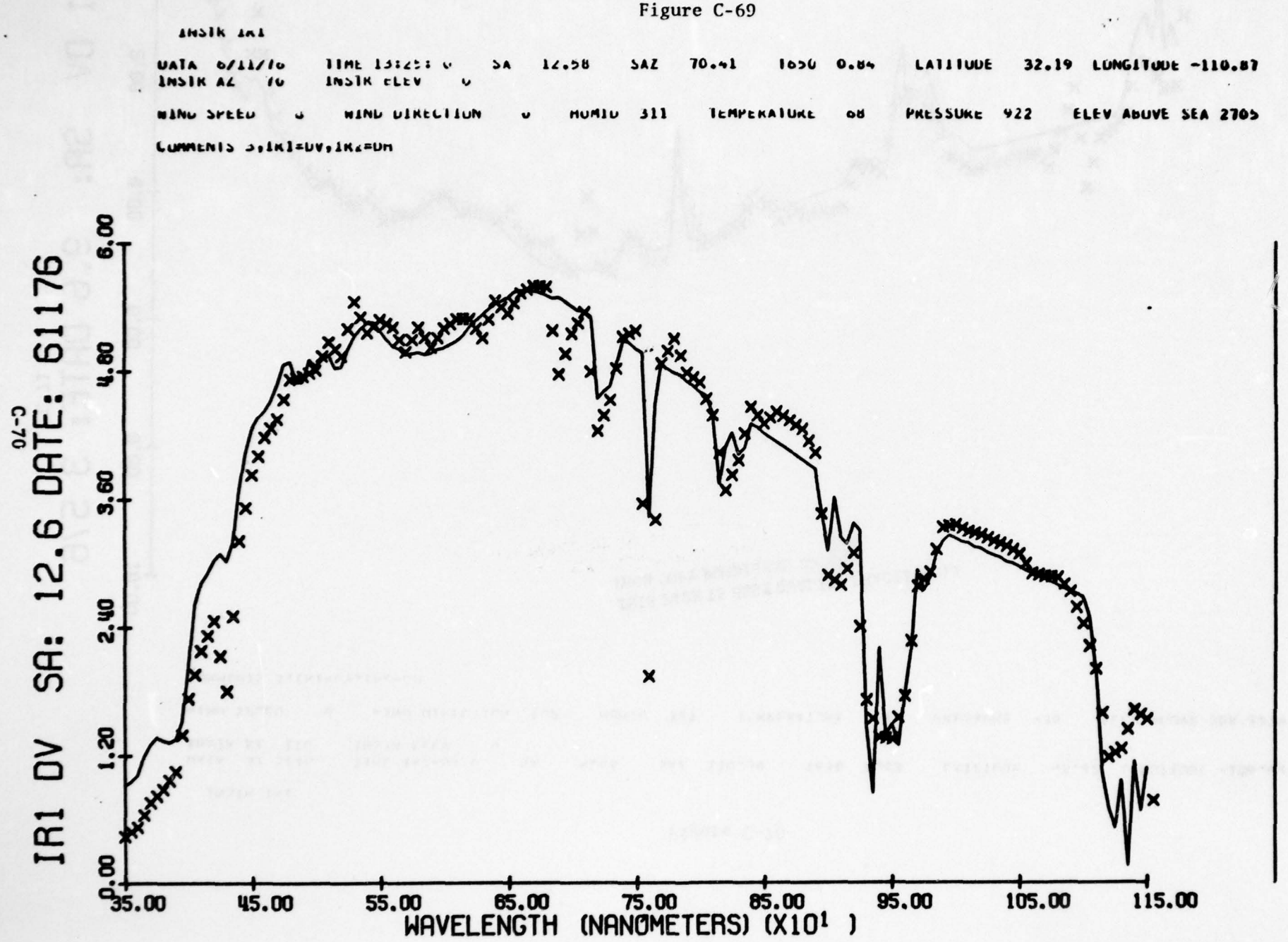
INSTR IR1
DATA 6/11/76 TIME 13:25:3 U SA 12.58 SAZ 70.41 1650 0.84 LATITUDE 32.19 LONGITUDE -110.87
INSTR AZ 76 INSTR ELEV 0
WIND SPEED 0 WIND DIRECTION 0 HUMID 311 TEMPERATURE 68 PRESSURE 922 ELEV ABOVE SEA 2705
COMMENTS S;IR1=DV;IR2=DM
IR1 DV SA: 12.6 DATE: 61176
C-70
6.00
4.80
3.60
2.40
1.20
0.00
35.00
45.00
55.00
65.00
75.00
85.00
95.00
105.00
115.00
WAVELENGTH (NANOMETERS) (X10¹)

Figure C-70

INSTR IR1

DATA 3/ 5/76 TIME 14:45: 0 SA 4.65 SAZ 110.30 T650 0.83 LATITUDE 48.22 LONGITUDE -106.62
INSTR AZ 110 INSTR ELEV 0

WIND SPEED 0 WIND DIRECTION 162 HUMID 727 TEMPERATURE 1 PRESSURE 936 ELEV ABOVE SEA 2274

COMMENTS 3,IR1=DV,IR2=DM

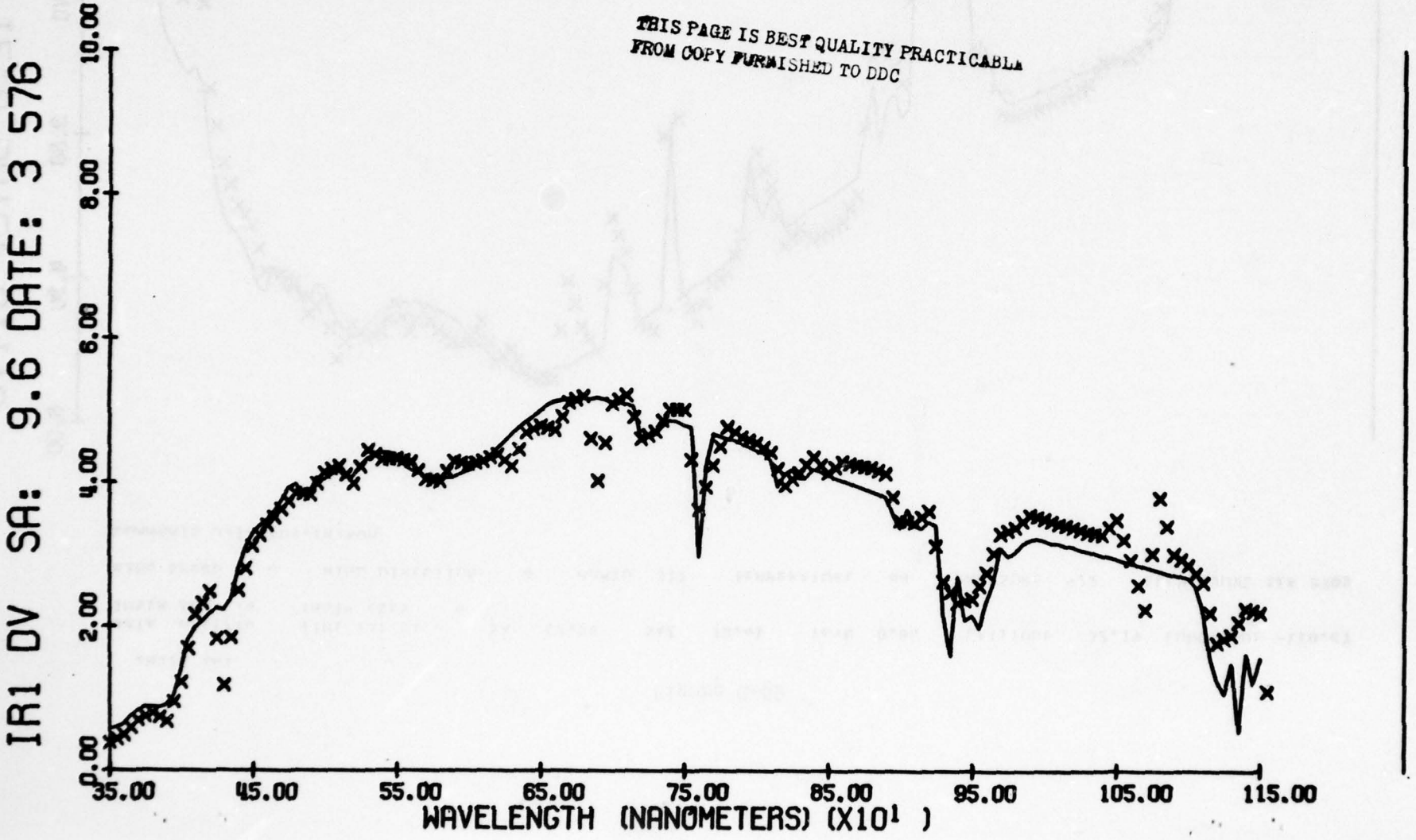

Figure C-71

INSTR IR1

DATA 7/21/76 TIME [illegible] SA 8.66 SAZ 71.12 TESU 0.04 LATITUDE 34.92 LONGITUDE -92.15
INSTR AZ 71 INSTR ELEV 0

WIND SPEED 0 WIND DIRECTION 212 HUMID 762 TEMPERATURE 79 PRESSURE 1005 ELEV ABOVE SEA 311

COMMENTS 3,IR1=DV,IR2=SM

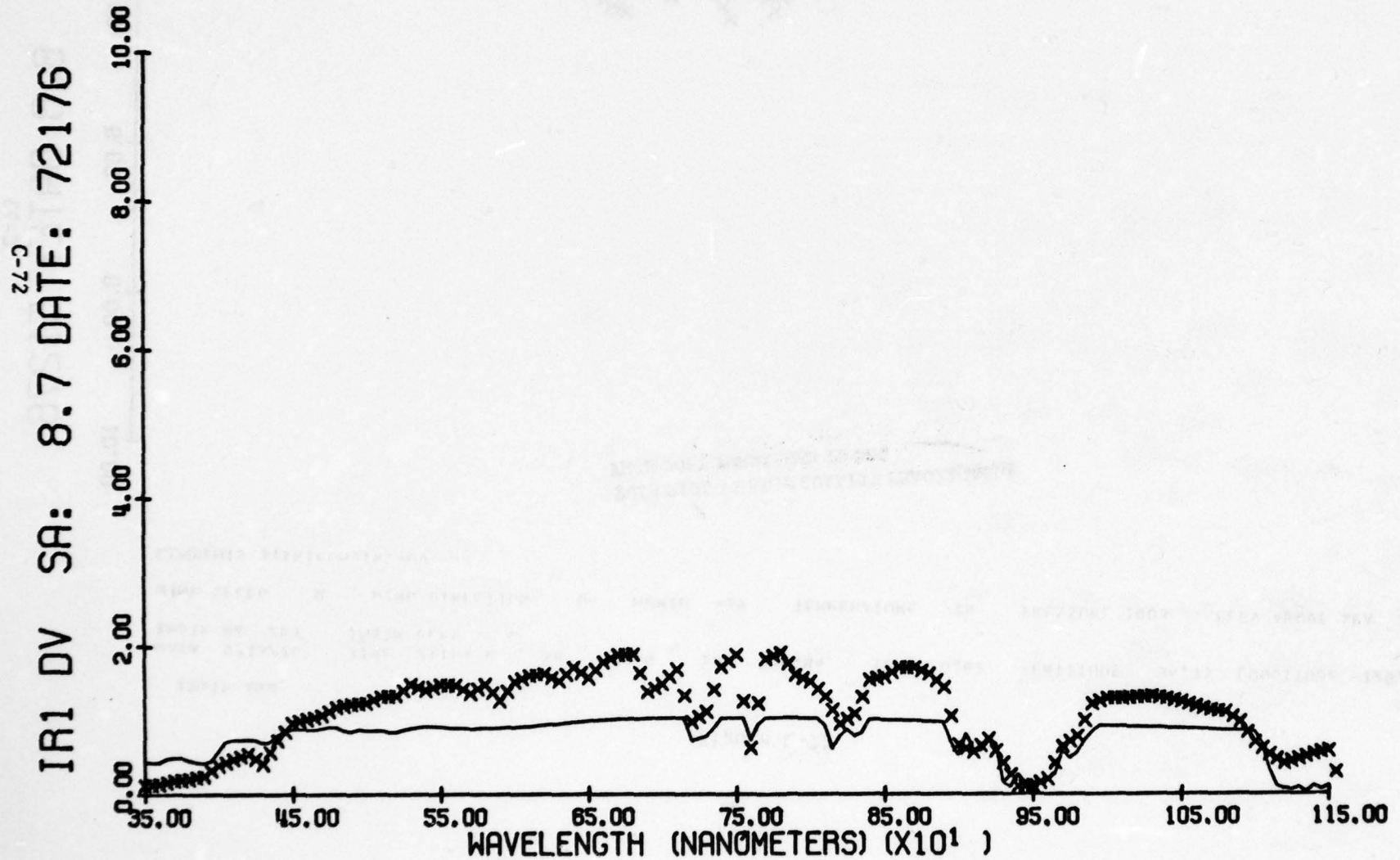

Figure C-72

INSTR IR2

DATA 5/13/76 TIME 2110: 0 SA 8.04 SAZ 286.84 T650 [illegible] LATITUDE 34.75 LONGITUDE -120.57
INSTR AZ 287 INSTR ELEV 0

WIND SPEED 0 WIND DIRECTION 0 HUMID 439 TEMPERATURE 78 PRESSURE 1003 ELEV ABOVE SEA 327

COMMENTS 3,IR1=DH,IR2=DV

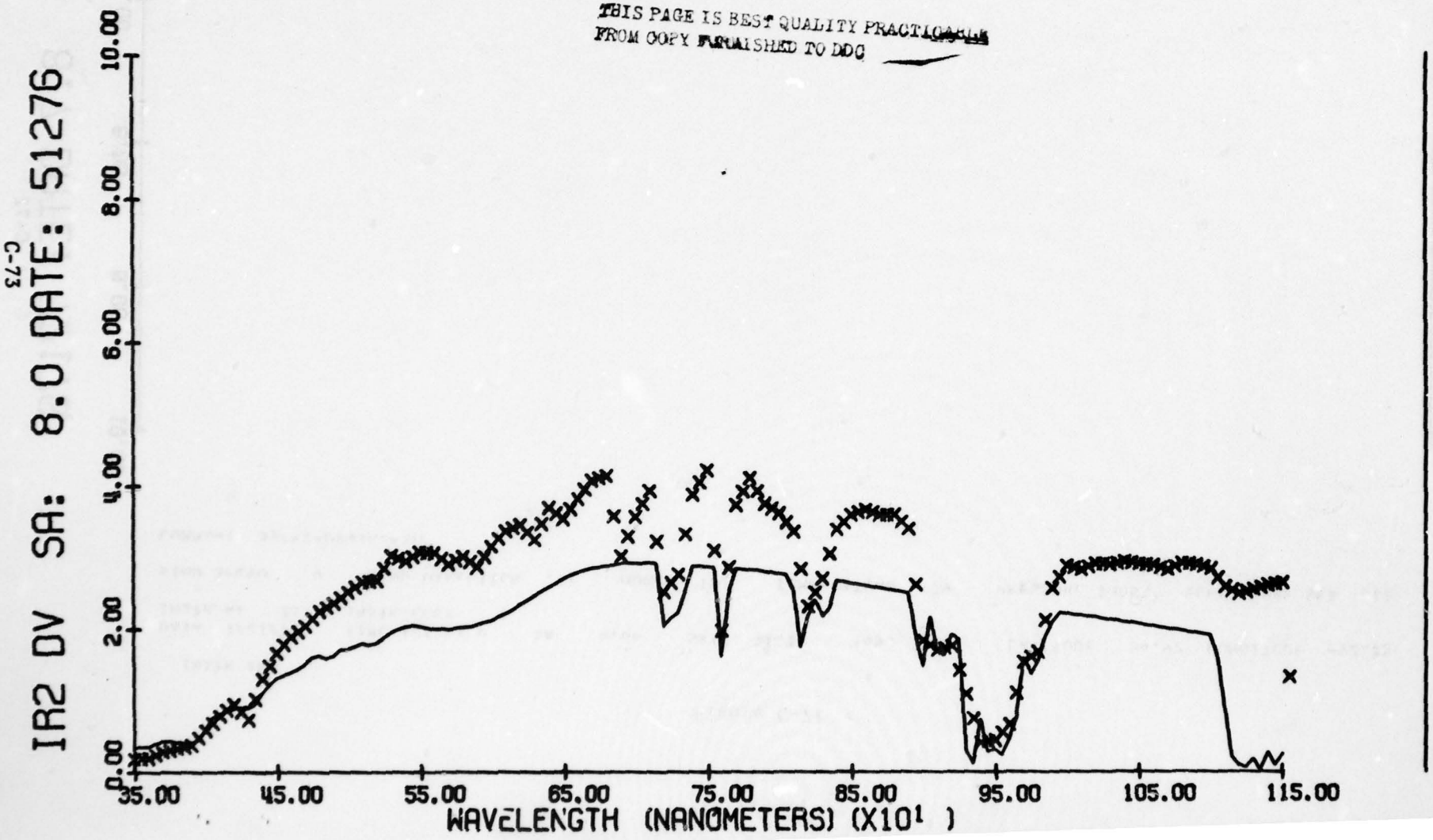

AD-A072 080 EASTMAN KODAK CO ROCHESTER N Y APPARATUS AND OPTICAL DIV F/G 14/2
SPECTRAL RADIOMETRIC MEASUREMENT AND ANALYSIS PROGRAM. VOLUME 3--ETC(U)
APR 79 L G CHRISTENSEN, R SIMMONS, G SCHAUSS

UNCLASSIFIED AWS-TN-79/001-VOL-3 NL

3 OF 3
AD
A072080

END
DATE
FILMED
9-79
DDC

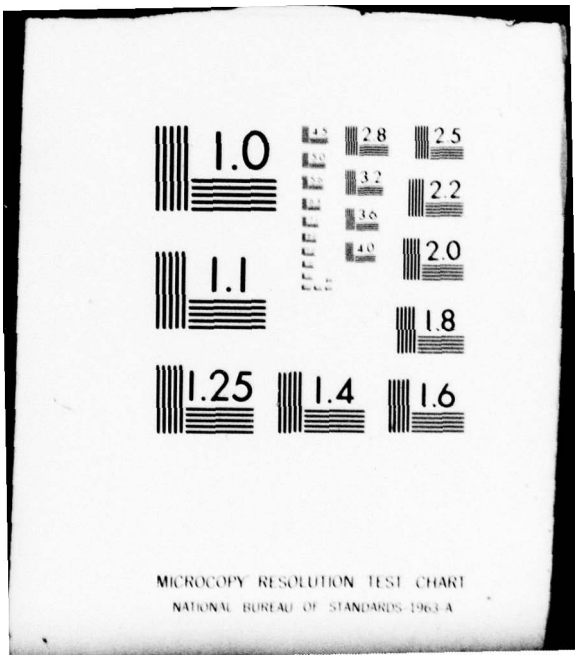
1.0
1.1
1.25
1.4
1.6
1.8
2.0
2.2
2.5
2.8
3.2
3.6
4.0
MICROCOPY RESOLUTION TEST CHART
NATIONAL BUREAU OF STANDARDS-1963-A

Figure C-73

INSTR IR2 .

DATA 4/27/76 . TIME 21:20:3 0 SA 5.96 SAZ 282.96 To50 0.83 LATITUDE 37.78 LONGITUDE -122.32
INSTR AZ 283 INSTR ELEV 0

WIND SPEED 33 WIND DIRECTION 289 HUMID 37o TEMPERATURE 69 PRESSURE 888 ELEV ABOVE SEA 15

COMMENTS S,IR1=SM,IR2=DV

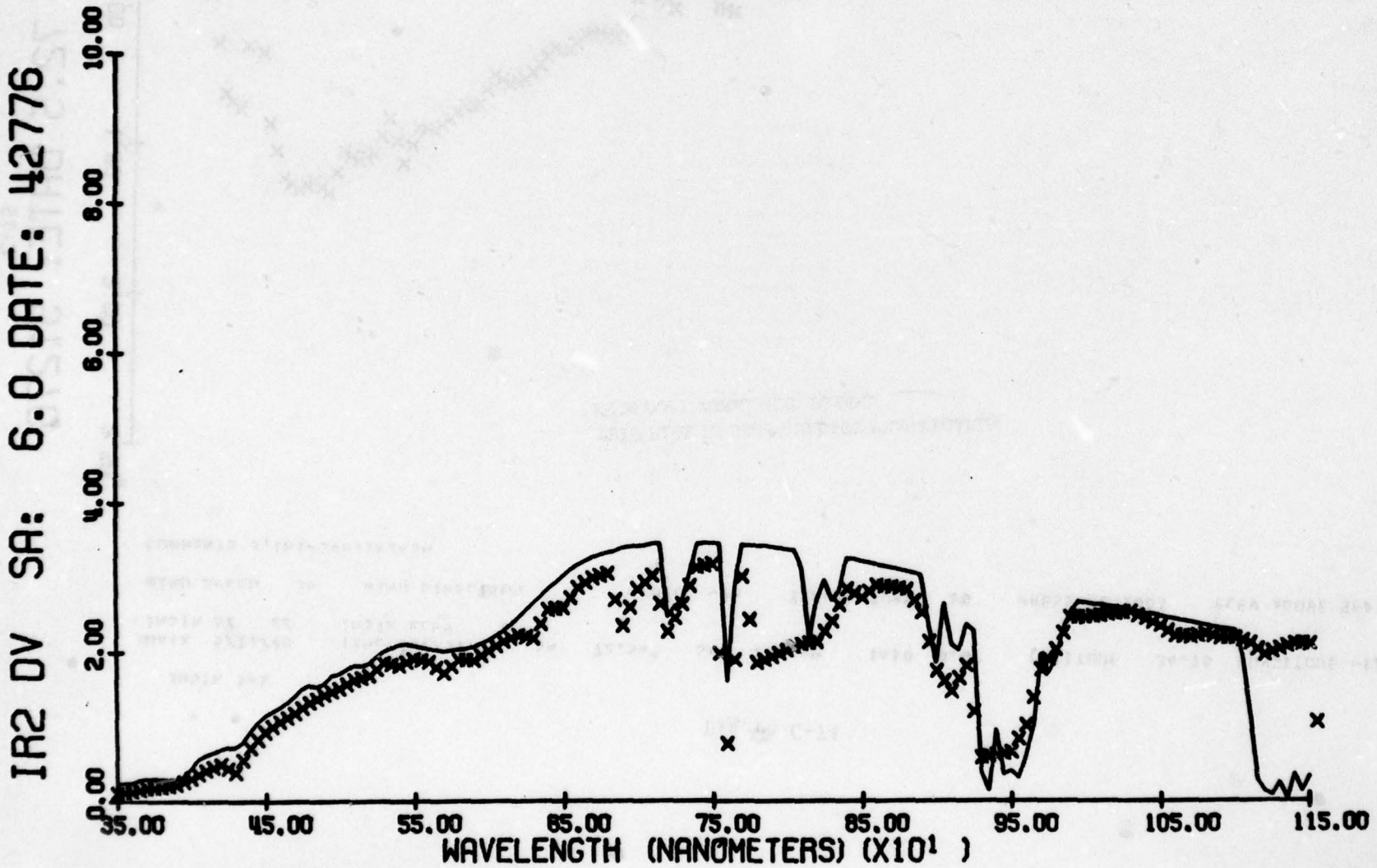

Figure C-74

INSTR IR1

DATA 5/12/80 TIME 20:25: 0 SA 72.54 SAZ 201.60 1650 0.67 LATITUDE 34.75 LONGITUDE -120.57
INSTR AZ 22 INSTR ELEV 0

WIND SPEED 30 WIND DIRECTION 0 HUMID 424 TEMPERATURE 60 PRESSURE 1003 ELEV ABOVE SEA 327

COMMENTS 3,IR1=SVB,IR2=SM

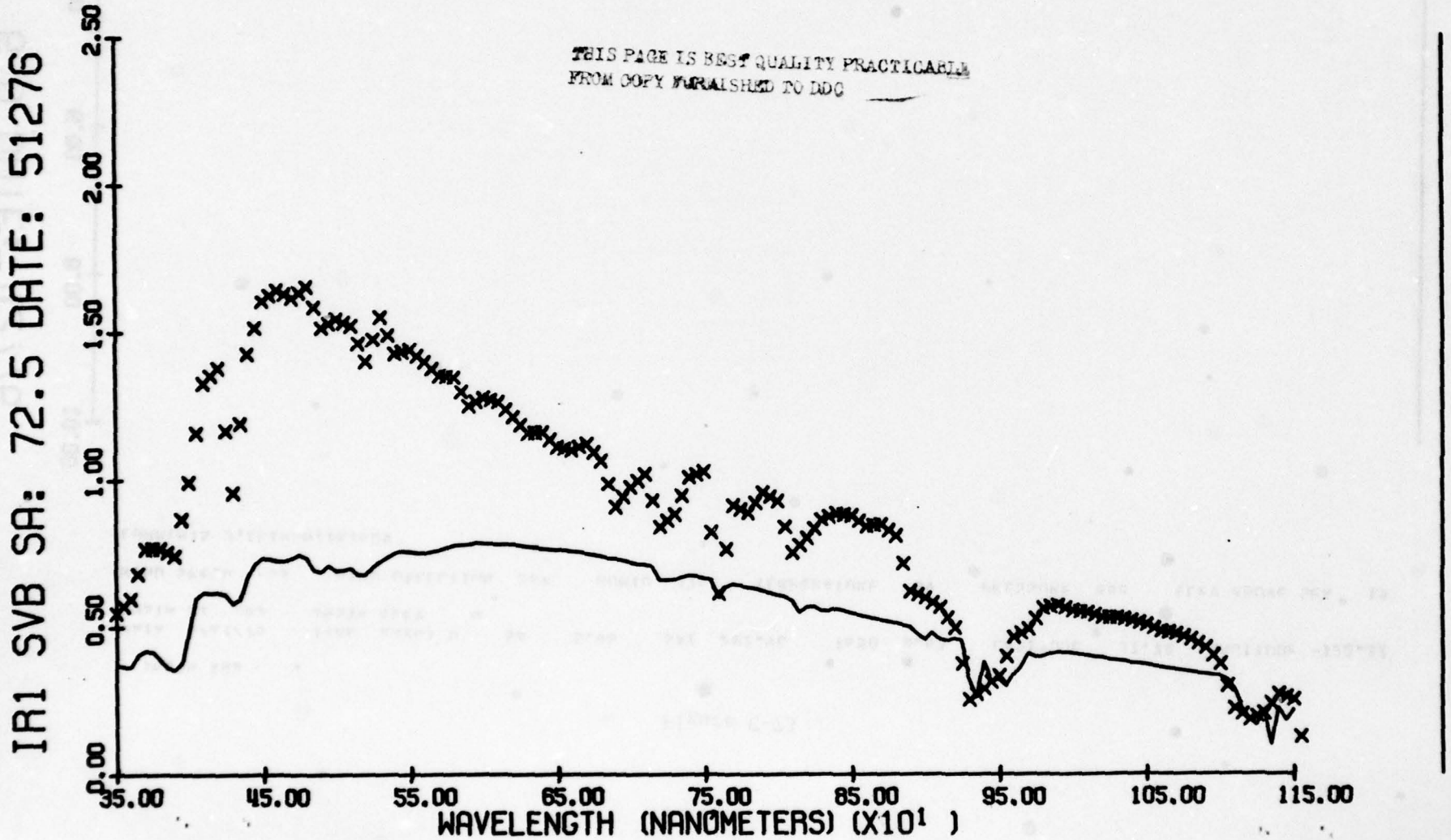

Figure C-75

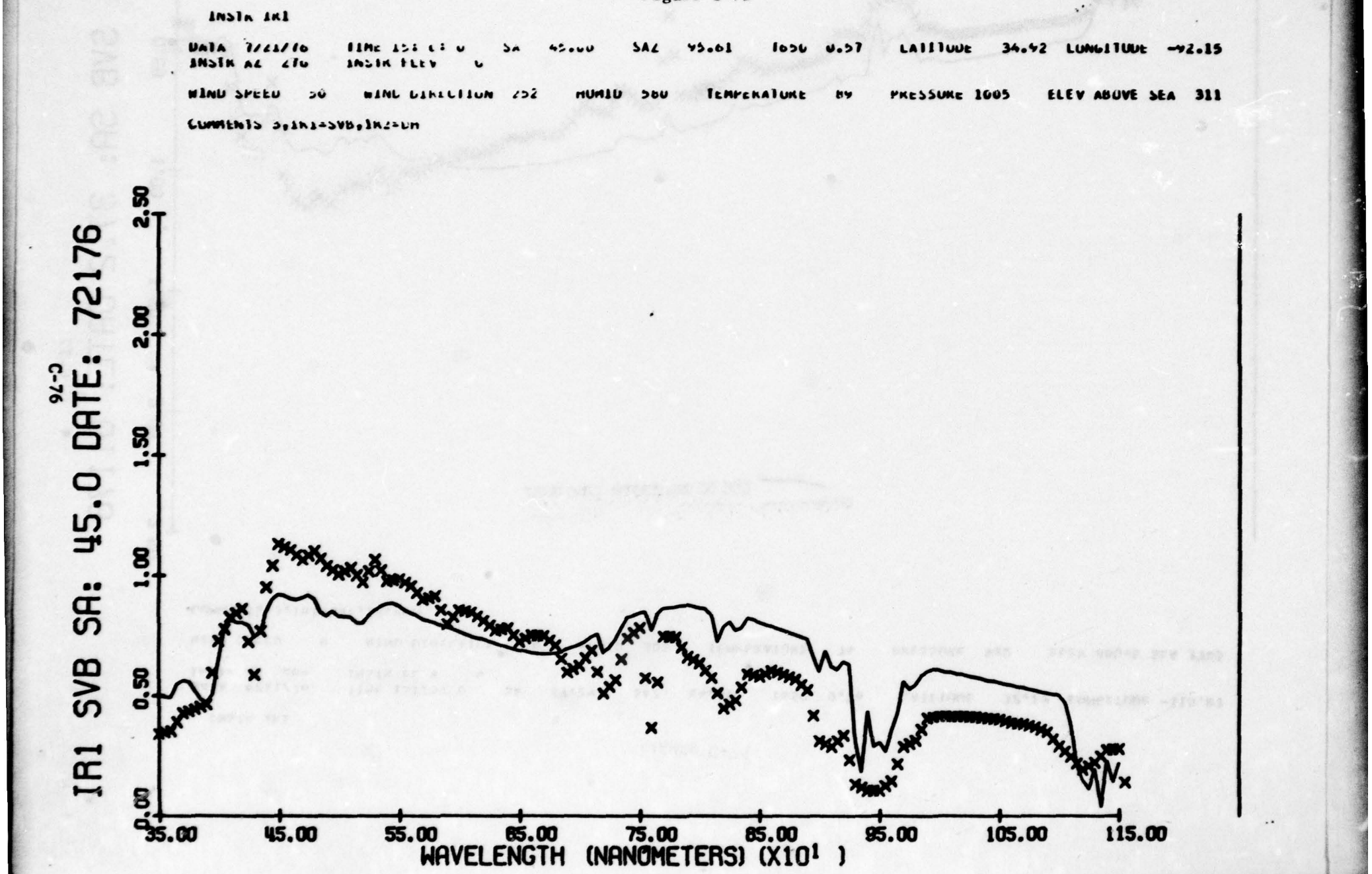
INSTR IR1
DATA 7/21/76 TIME 15:[illegible] SA 45.00 SAZ 95.01 ISOL 0.57 LATITUDE 34.42 LONGITUDE -92.15
INSTR AZ 270 INSTR ELEV 0
WIND SPEED 30 WIND DIRECTION 252 HUMID 580 TEMPERATURE 89 PRESSURE 1005 ELEV ABOVE SEA 311
COMMENTS 3,IR1=SVB,IR2=UM
IR1 SVB SA: 45.0 DATE: 72176
C-76
2.50
2.00
1.50
1.00
0.50
0.00
35.00
45.00
55.00
65.00
75.00
85.00
95.00
105.00
115.00
WAVELENGTH (NANOMETERS) (X10¹)

Figure C-76

INSTR IR1

DATA 6/11/76 TIME 15:25: 0 SA 37.24 SAZ 84.01 1650 0.76 LATITUDE 32.14 LONGITUDE -110.87
INSTR AZ 209 INSTR ELEV 0

WIND SPEED 0 WIND DIRECTION 0 HUMID 305 TEMPERATURE 74 PRESSURE 922 ELEV ABOVE SEA 2705

COMMENTS 3,IR1=SVB,IR2=UM

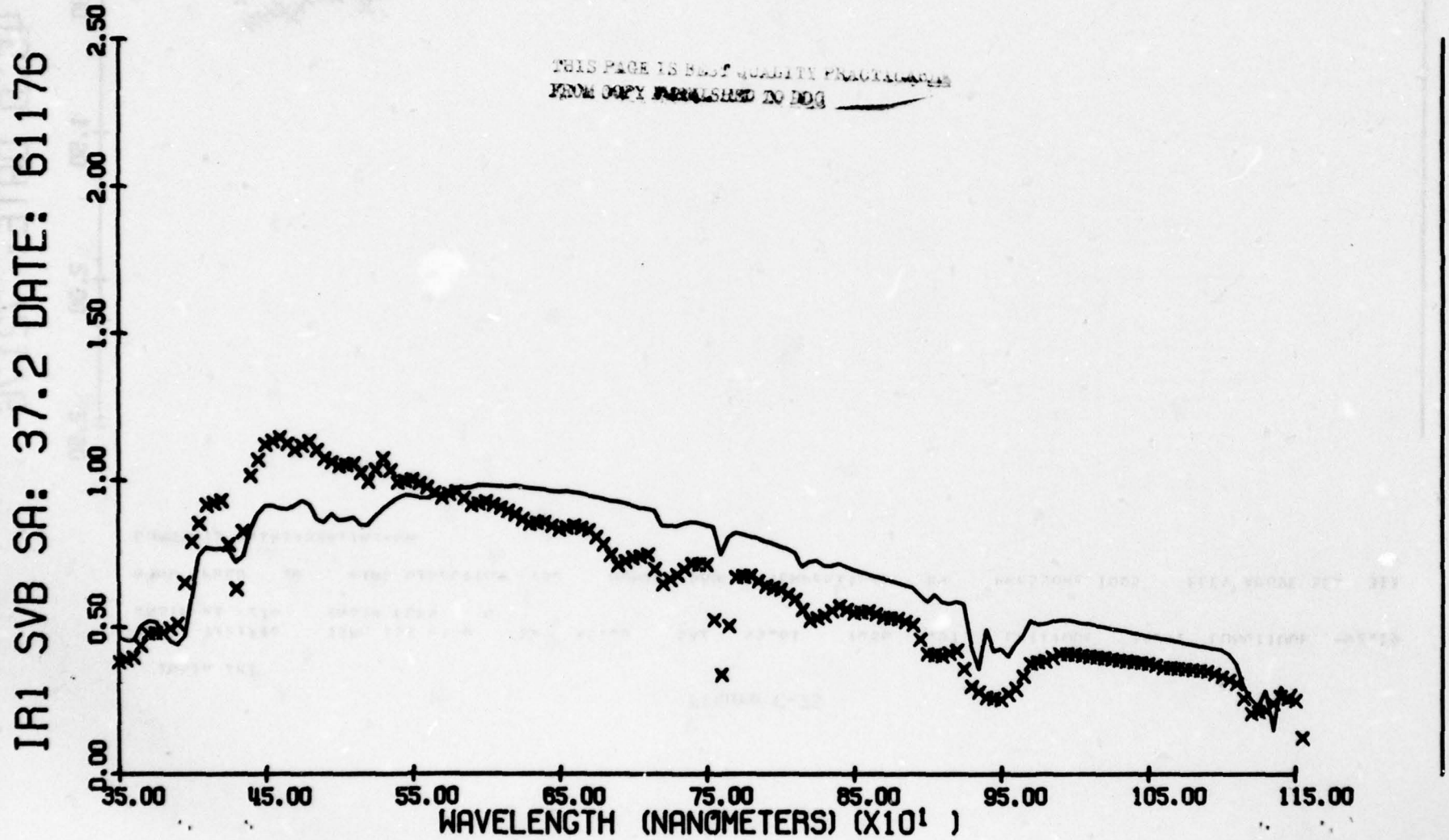

Figure C-77

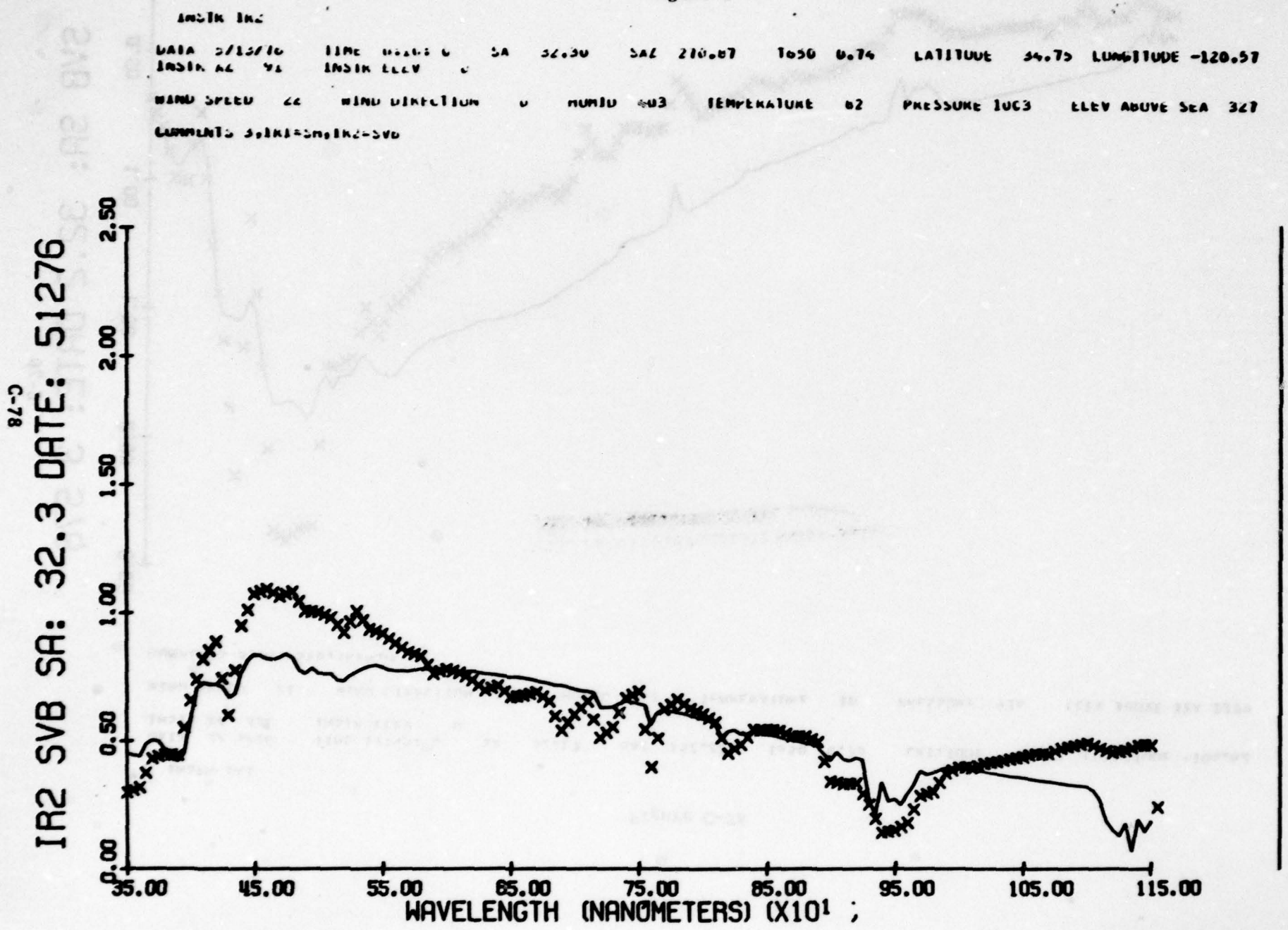
IR2 SVB SA: 32.3 DATE: 51276
0.00
0.50
1.00
1.50
2.00
2.50
35.00
45.00
55.00
65.00
75.00
85.00
95.00
105.00
115.00
WAVELENGTH (NANOMETERS) (X10¹ ;

Figure C-78

INSTR IR1

DATA 3/ 5/76 TIME 17:45: 0 SA 32.17 SAZ 152.22 TO50 0.15 LATITUDE +0.22 LONGITUDE -100.62
INSTR AZ 332 INSTR ELEV 0

WIND SPEED 21 WIND DIRECTION 135 HUMID 662 TEMPERATURE 10 PRESSURE 930 ELEV ABOVE SEA 2279

COMMENTS 3,IR1=SVB,IR2=SM

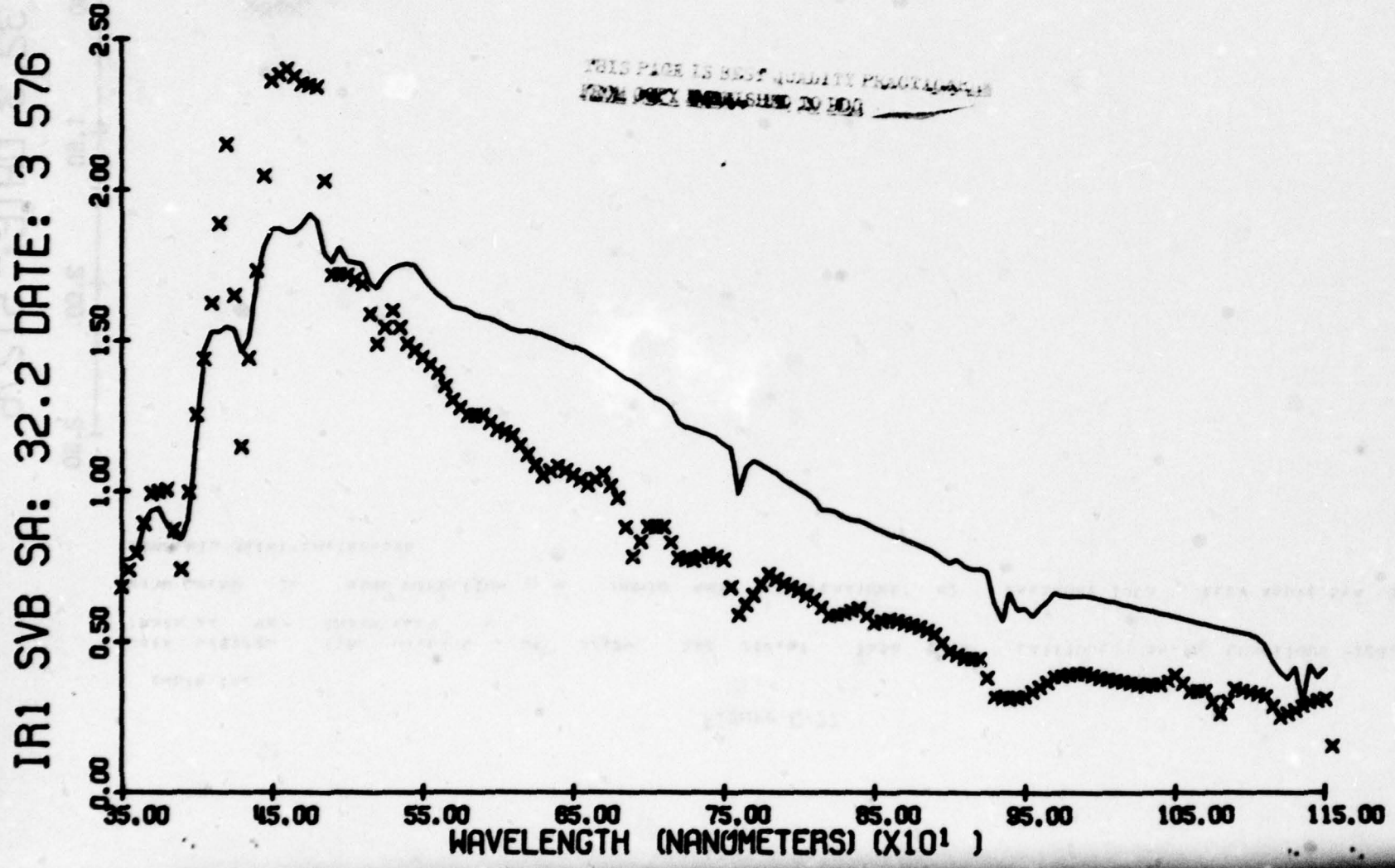

Figure C-79

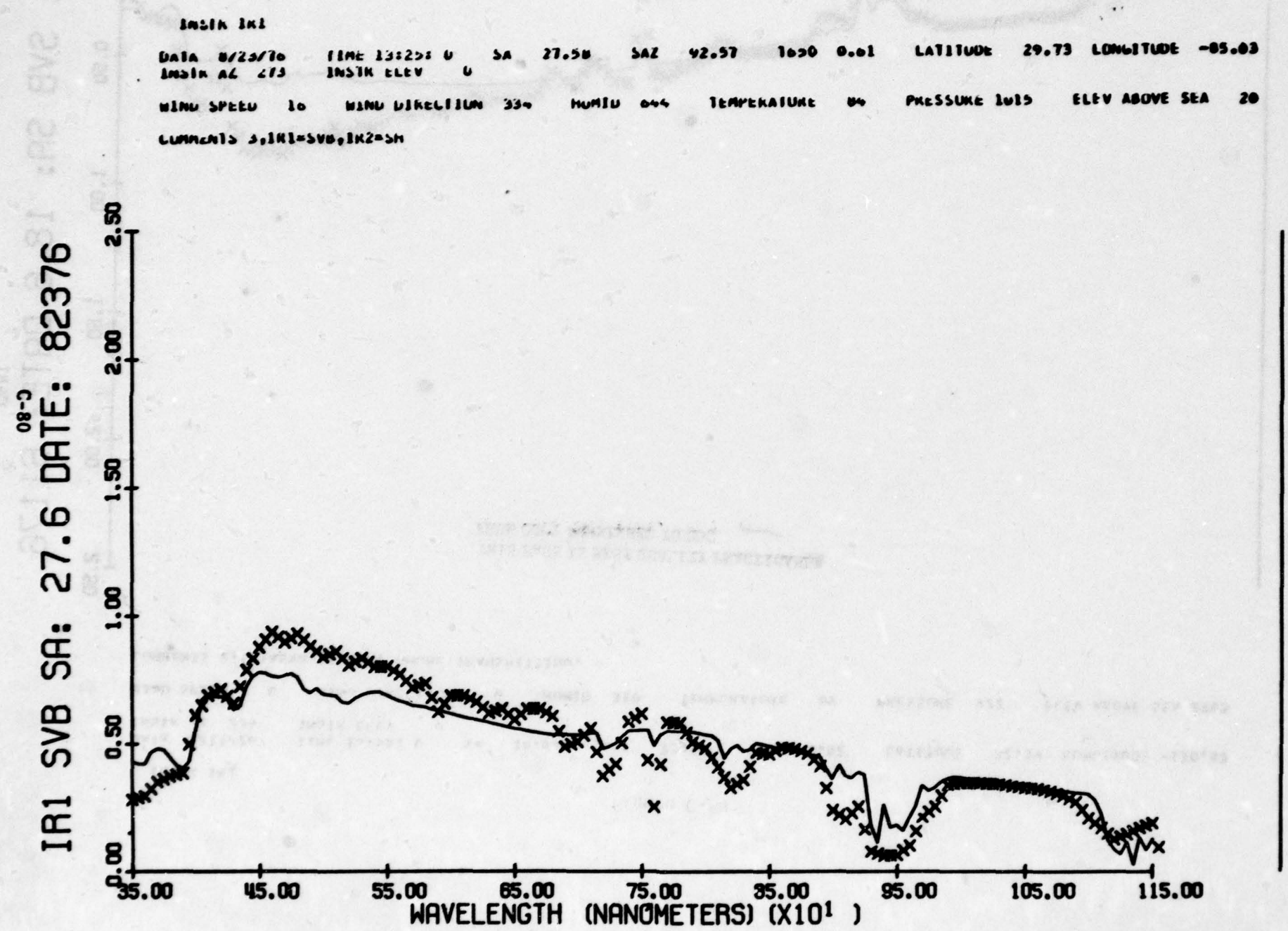
INSTR IR1
DATA 8/23/80 TIME 13:23:3 U SA 27.58 SAZ 92.57 TAU0 0.01 LATITUDE 29.73 LONGITUDE -85.03
INSTR AZ 273 INSTR ELEV 0
WIND SPEED 10 WIND DIRECTION 330 HUMID 044 TEMPERATURE 84 PRESSURE 1015 ELEV ABOVE SEA 20
COMMANDS 3,IR1=SVB,IR2=SM
IR1 SVB SA: 27.6 DATE: 82376
0.00
0.50
1.00
1.50
2.00
2.50
35.00
45.00
55.00
65.00
75.00
85.00
95.00
105.00
115.00
WAVELENGTH (NANOMETERS) (X10¹)

Figure C-80

INSTR IR1

DATA 6/11/76 TIME [illegible] SA 18.62 SAZ 73.87 1656 0.82 LATITUDE 32.14 LONGITUDE -110.87
INSTR AZ 254 INSTR ELEV 0

WIND SPEED 0 WIND DIRECTION 0 HUMID 310 TEMPERATURE 69 PRESSURE 922 ELEV ABOVE SEA 2705

COMMENTS 2,IR1=SVB,IR2=SM, MOUNT TRANSMITTING.

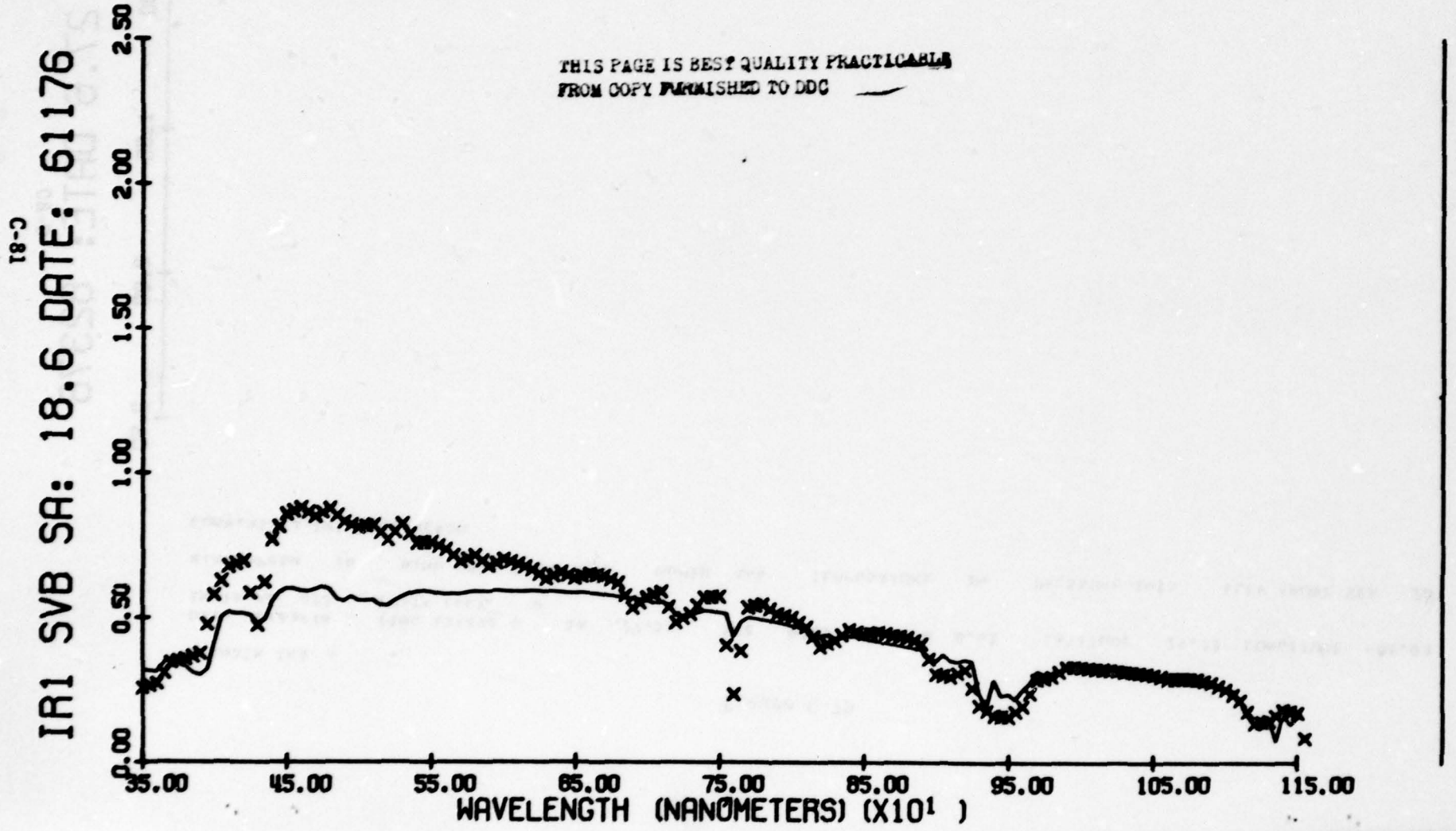

Figure C-81

INSTR IR1

DATA 7/21/76 TIME 12:30:0 U SA 14.34 SAZ 75.05 FOSO 0.02 LATITUDE 34.92 LONGITUDE -92.15
INSTR AZ 255 INSTR ELEV 0

WIND SPEED 10 WIND DIRECTION 240 HUMID 78 TEMPERATURE 81 PRESSURE 1005 ELEV ABOVE SEA 311

COMMENTS S,IR1=SVB,IR2=UM

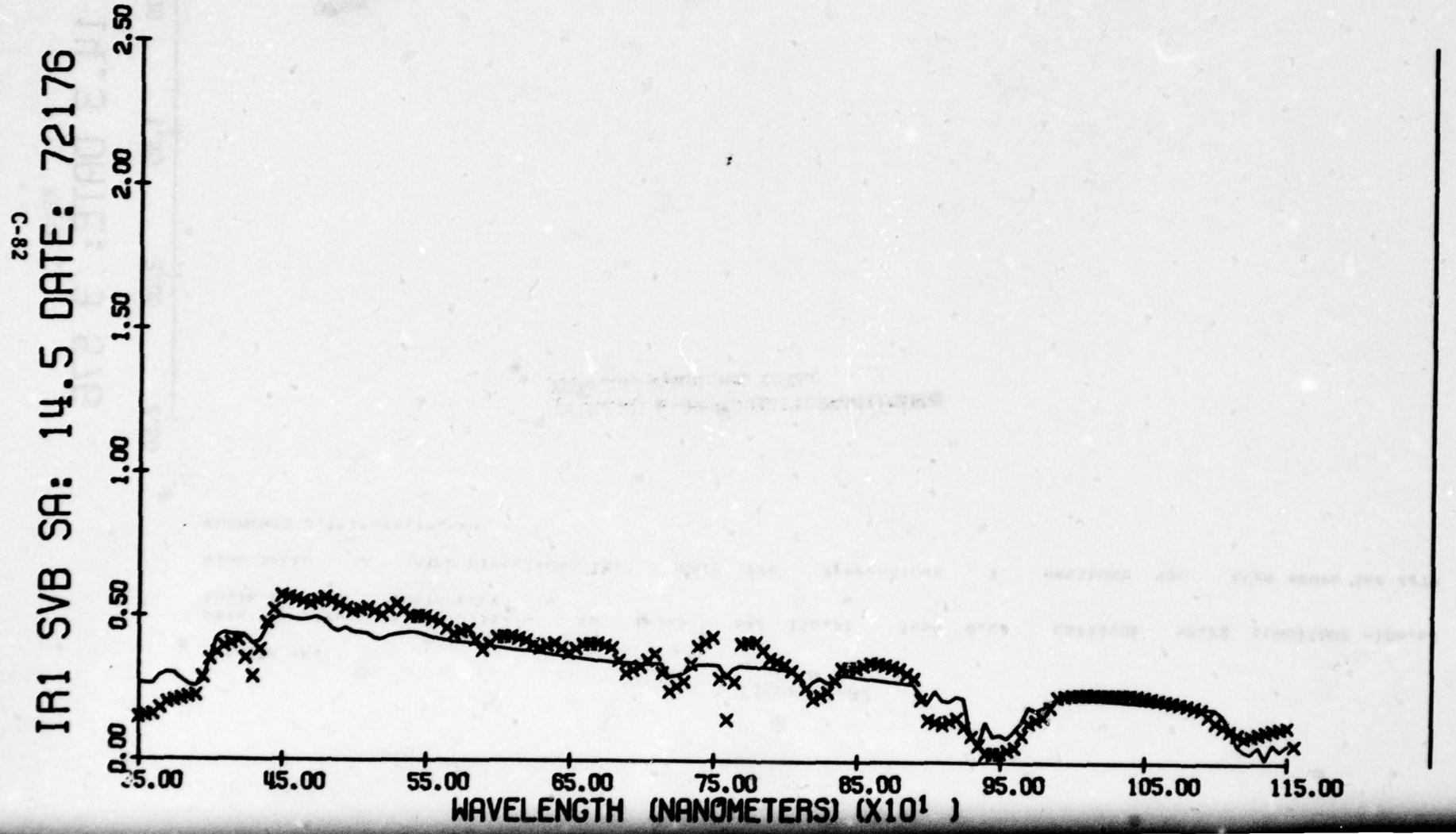

Figure C-82

INSTR IR1

DATA 3/ 3/76 TIME 15:15: 0 SA 14.25 SAZ 110.31 TOG 0.82 LATITUDE 48.22 LONGITUDE -106.62
INSTR AZ 290 INSTR ELEV 0

WIND SPEED 0 WIND DIRECTION 132 HUMID 726 TEMPERATURE 1 PRESSURE 930 ELEV ABOVE SEA 2279

COMMENTS 3,IR1=SVB,IR2=SH

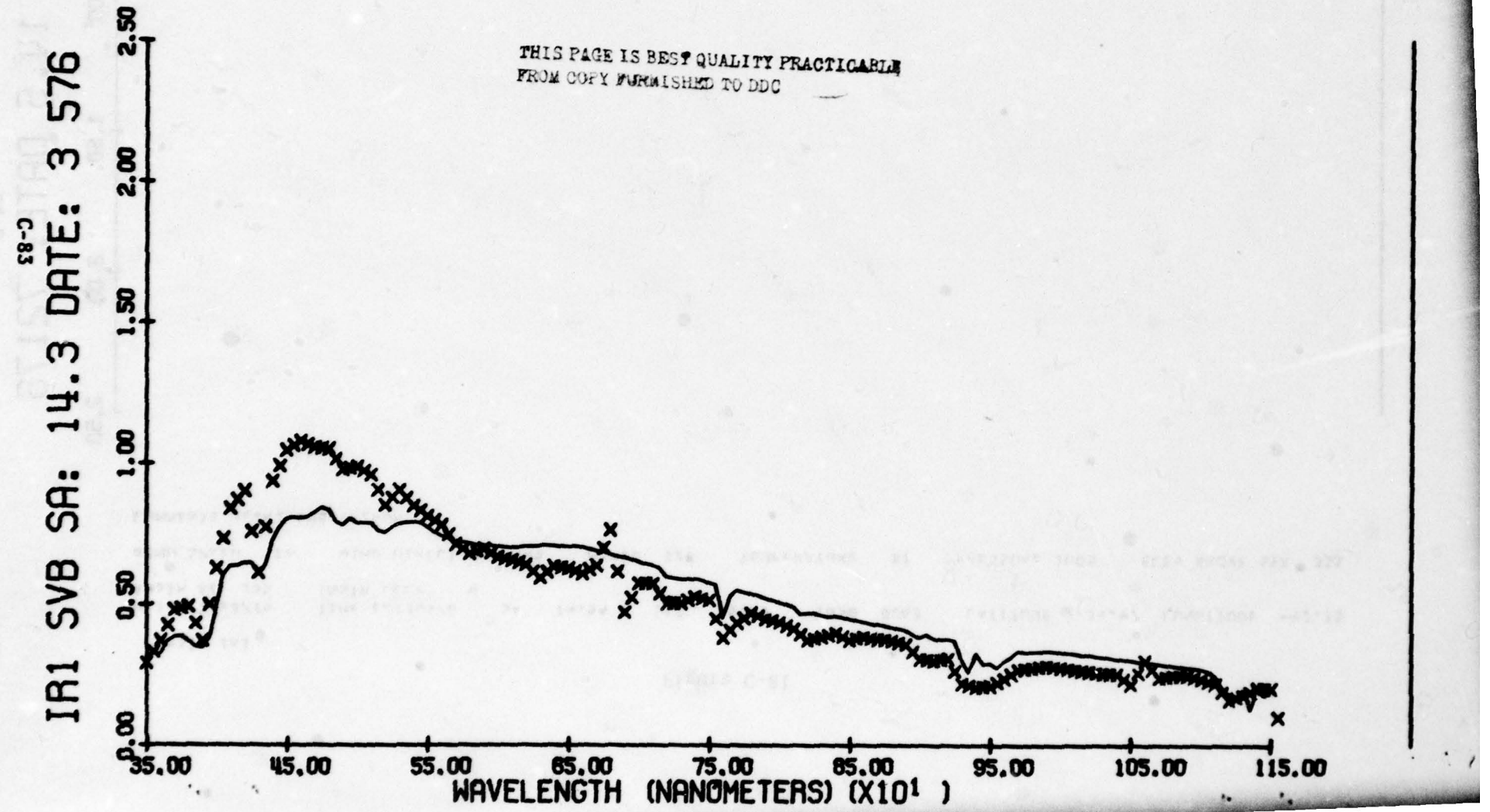

Figure C-83

INSTR IR2

DATA 5/13/16 TIME 11401 G SA 13.99 SAZ 282.87 TOSO 0.80 LATITUDE 34.75 LONGITUDE -120.57
INSTR AZ 103 INSTR ELEV 0

WIND SPEED 0 WIND DIRECTION 0 HUMID 425 TEMPERATURE 80 PRESSURE 1003 ELEV ABOVE SEA 327

COMMENTS S,IR1=LM,IR2=SVB

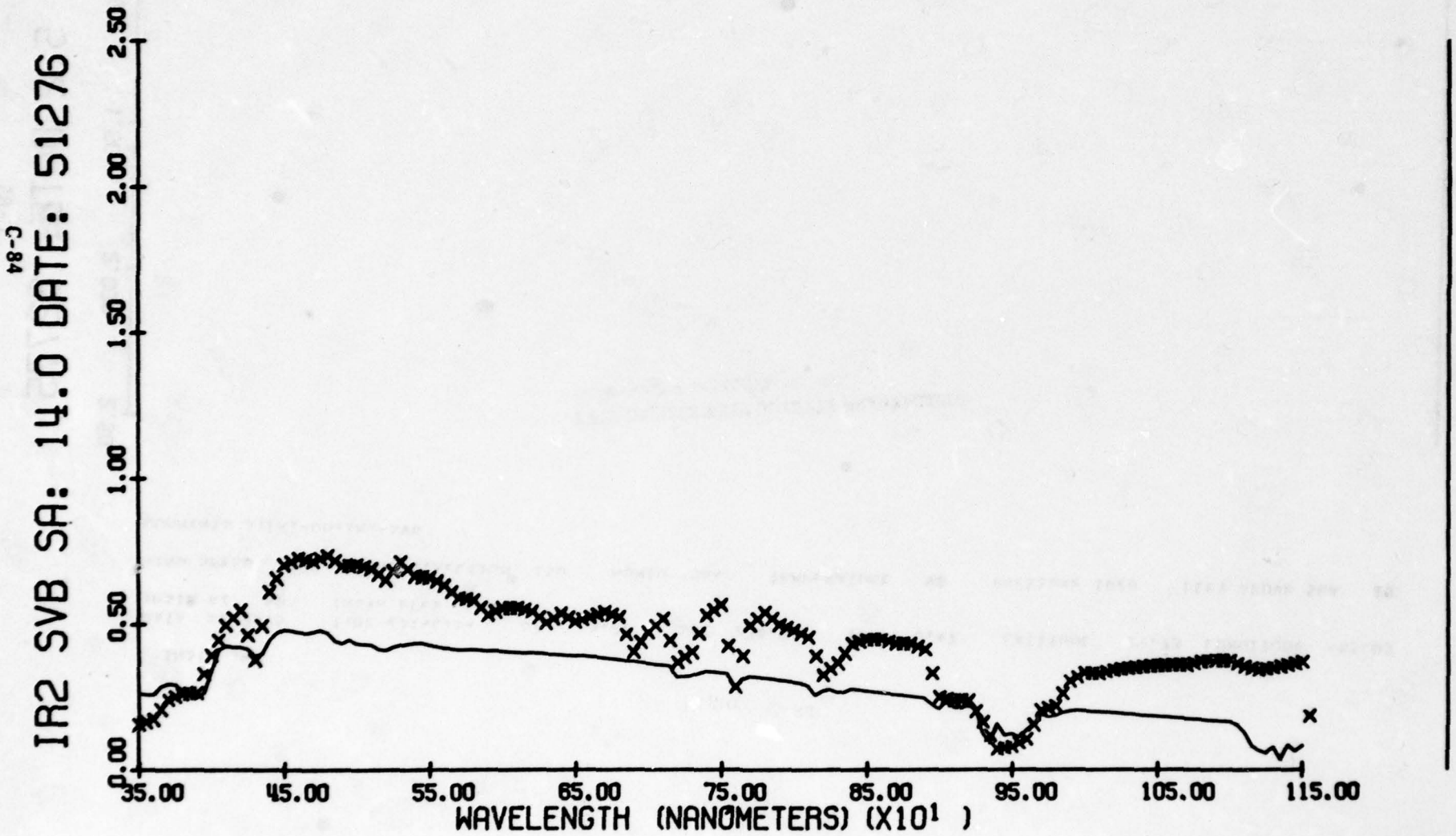

Figure C-84

INSTR IR2

DATA 8/27/75 TIME 23:46:54 SA 5.22 SAZ 278.54 1650 0.47 LATITUDE 29.73 LONGITUDE -85.05
INSTR AZ 98 INSTR ELEV 0

WIND SPEED 18 WIND DIRECTION 150 HUMID 564 TEMPERATURE 90 PRESSURE 1020 ELEV ABOVE SEA 20

COMMENTS 3,IR1=UM,IR2=SVB

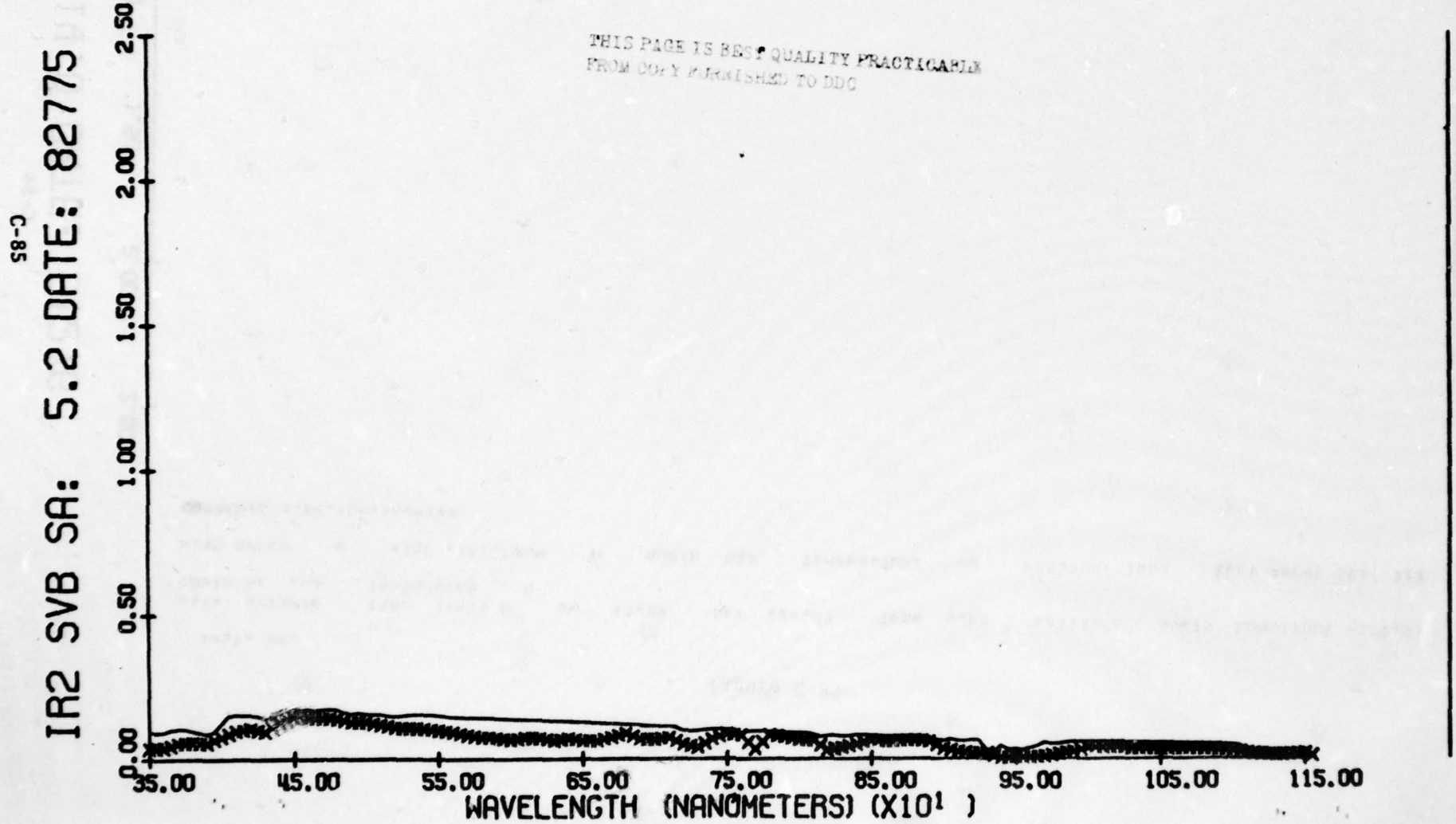

TABLE C-1

INPUT PARAMETER SUMMARY FOR SCAT3 RECONSTRUCTION EXAMPLES

Date	GMT	Solar Altitude (°)	Moisture Scale Height (cm)	Terrain Type	Terrain Reflectance	RH (%)	Temperature (°C)	Pressure (mb)	Irradiance Measurement Type	Terrain Elevation (km)	LATITUDE (°)
8/23/76	15:55	58.78	3.85	3	.055	58.	31	1015	SVB,SH	0	29.13
8/23/76	15:25	52.96	3.85	3	.055	58.	31	1015	DV,DH	0	29.13
8/23/76	12:55	21.07	3.85	3	.055	87.5	24	1014	DV,DH	0	29.13
8/23/76	13:25	27.58	3.85	3	.055	87.5	24	1014	SVB,SH	0	29.13
5/12/76	19:55	73.56	1.2	1	.181	33.	26	1003	DV,DH	.1	34.75
5/12/76	20:25	72.54	1.2	1	.181	33.	26	1003	SVB,SH	.1	34.75
5/12/76	23:40	38.46	1.2	1	.181	33.	26	1003	DH,DV	.1	34.75
5/13/76	0:10	32.30	1.2	1	.181	33.	26	1003	SH,SVB	.1	34.75
5/13/76	1:40	13.99	1.2	1	.181	33.	26	1003	DH,SVB	.1	34.75
5/13/76	1:55	11.00	1.2	1	.181	33.	26	1003	SH,DH	.1	34.75
5/13/76	2:10	8.04	1.2	1	.181	33.	26	1003	DH,DV	.1	34.75
6/11/76	13:25	12.58	.76	1	.264	29.	17	922	DV,DH	.82	32.19
6/11/76	13:55	18.62	.76	1	.264	29.	17	922	SVB,SH	.82	32.19
6/11/76	15:25	37.24	.76	1	.264	26.	22	923	SVB,DH	.82	32.19
6/11/76	16:10	46.79	.76	1	.264	26.	22	923	DV,SH	.82	32.19
6/11/76	18:40	76.97	.76	1	.264	26.	22	923	DV,SH	.82	32.19
6/11/76	19:10	80.55	.76	1	.264	26.	22	923	SVB,DH	.82	32.19
7/21/76	12:00	8.66	3.0	3	.081	79.	23	1000	DV,SH	.1	34.92
7/21/76	12:30	14.54	3.0	3	.081	70.	25	1000	SVB,DH	.1	34.92
7/21/76	14.30	38.86	3.0	3	.081	62.	27	1000	DV,SH	.1	34.92
7/21/76	15:00	45.00	3.0	3	.081	55.	29	1000	SVB,DH	.1	34.92
3/5/76	14:45	9.65	.23	2	.603	56.	-16	936	DV,DH	.69	48.22
3/5/76	15:15	14.25	.23	2	.603	56.	-16	936	SVB,SH	.69	48.22
3/5/76	17:15	29.53	.23	2	.603	56.	-16	936	DV,DH	.69	48.22
3/5/76	17:45	32.17	.23	2	.603	56.	-16	936	SVB,SH	.69	48.22

APPENDIX D

SCAT3 MODEL RECONSTRUCTED SPECTRAL TRANSMITTANCE

The following Figures D-1 through D-3 illustrate the dependency of the SCAT3 model for spectral transmittance on surface pressure, relative humidity, and temperature.

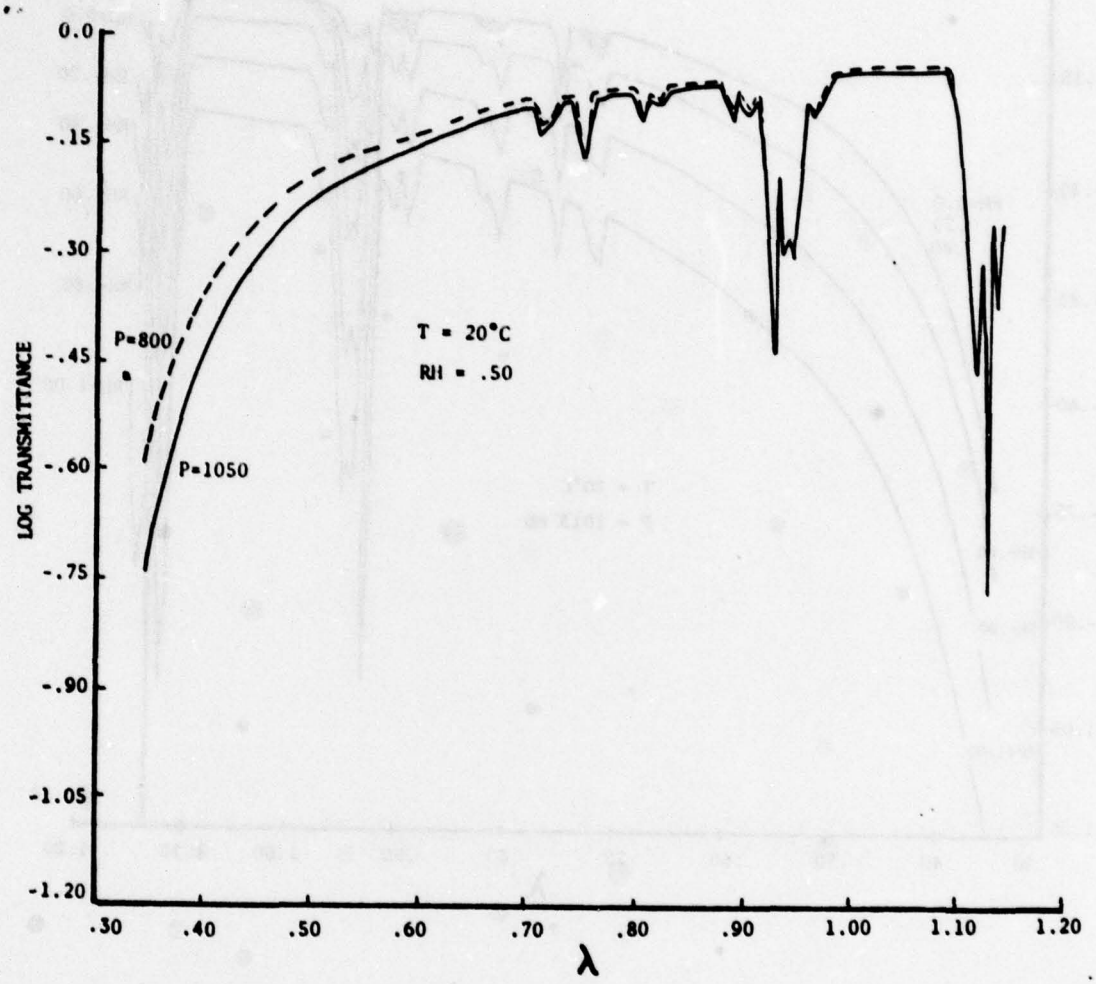

Figure D-1. Effect of Surface Pressure on Transmittance

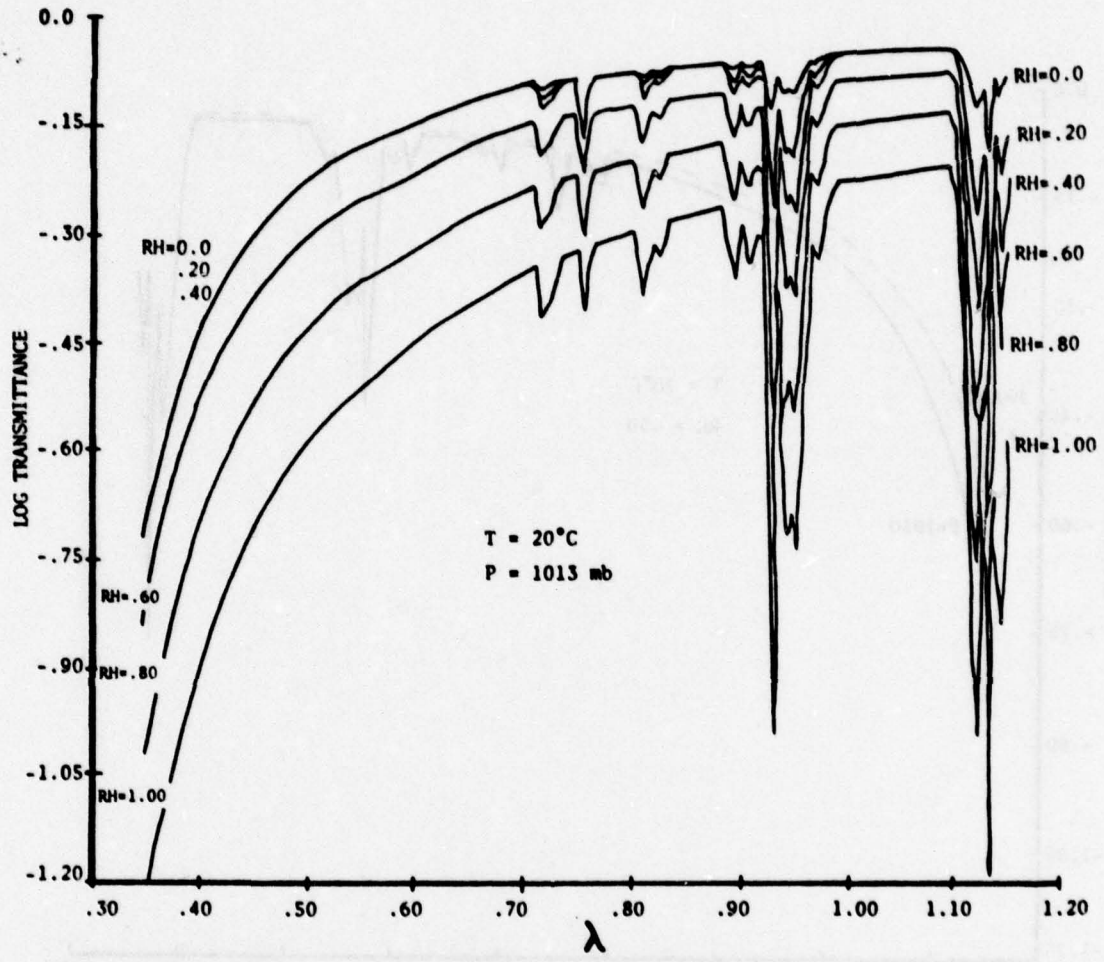

Figure D-2. Effect of Relative Humidity on Transmittance

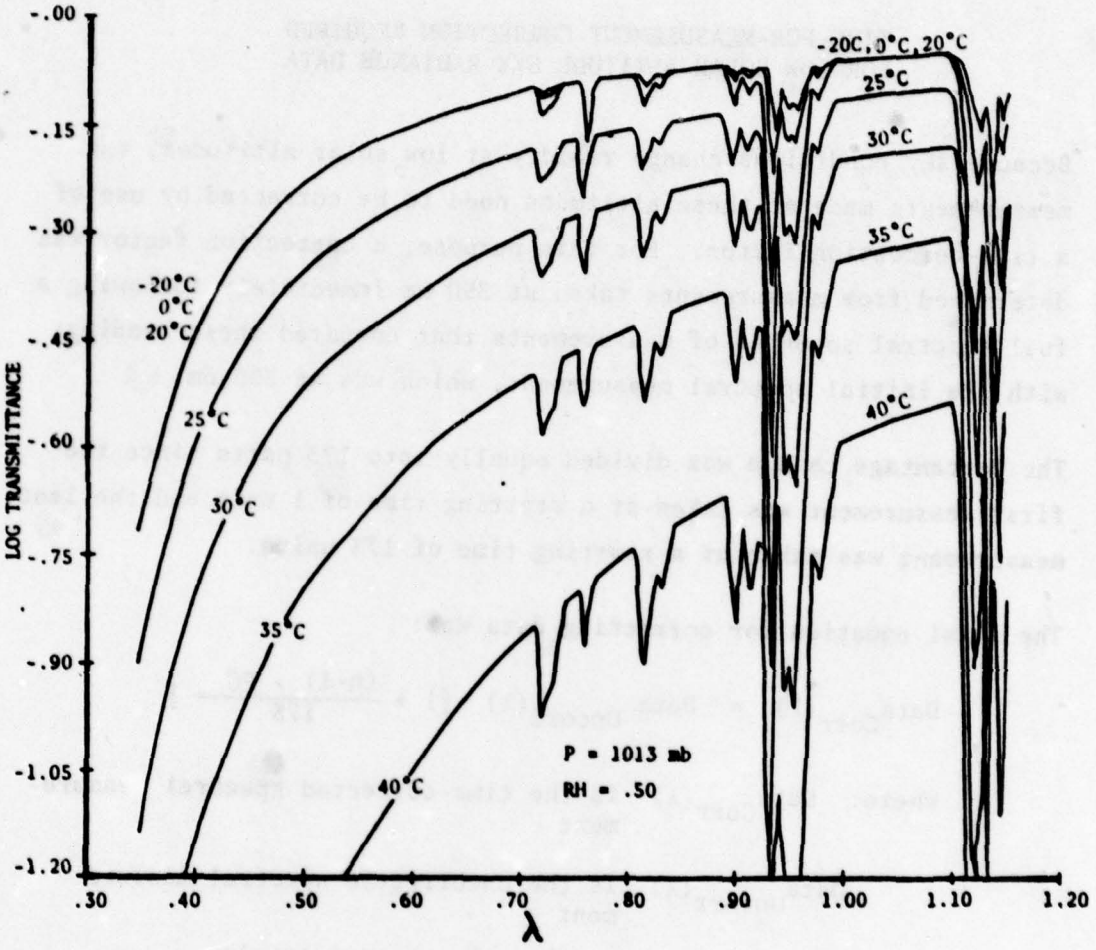

Figure D-3. Effect of Temperature on Transmittance

APPENDIX E

TIME-FOR-MEASUREMENT CORRECTION REQUIRED FOR LOW SOLAR ALTITUDE SKY RADIANCE DATA

Because sky conditions change rapidly at low solar altitudes, the measurements made at these altitudes need to be corrected by use of a time-correction factor. For this purpose, a correction factor was determined from measurements taken at 350 nm immediately following a full spectral sequence of measurements that compared these readings with the initial spectral measurement, which was at 350 nm.

The percentage change was divided equally into 173 parts since the first measurement was taken at a starting time of 1 unit and the last measurement was taken at a starting time of 173 units.

The final equation for correcting data was:

$$\text{Data}_{\text{Corr}}(\lambda) = \text{Data}_{\text{Uncorr}}(\lambda) \left[1 + \frac{(n-1) \cdot PC}{173}\right]$$

Where: $\text{Data}_{\text{Corr}}(\lambda)$ is the time-corrected spectral measurement

$\text{Data}_{\text{Uncorr}}(\lambda)$ is the uncorrected spectral measurement

n is the nth spectral sample

173 is the number of spectral samples including the first 350 nm sample and the last 350 nm spectral sample, and

$$PC = \frac{\text{Data}(1) - \text{Data}(173)}{\text{Data}(1)}$$

Not all spectral sequences at solar altitudes below 8° had a 350 nm measurement taken immediately following. In order to correct those data that did not have the extra measurement, a function for PC was formulated from the sequences that had had the extra measurement. PC was found to be a function of solar altitude.

Thus, from repeated measurements at various solar altitudes for the daylight vertical, skylight vertical, daylight horizontal, and skylight horizontal irradiances the following equation was determined for the percentage change as a function of solar altitude:

$$PC = .23784 - .041119 \cdot SA + .0025274 \cdot SA^2$$

where SA is between -1° and 8°.

APPENDIX F

VERY LOW SOLAR ALTITUDE SCALING OF SPECTRAL QUANTITIES

At solar altitudes of eight degrees or below, either sufficient data was not always available to test the model or the model was not adequately describing the data, whether it was radiance or irradiance data. At lower solar altitudes than those thought to be the minimum solar altitude (MSA) for an accurate fit, the model was extrapolated down to -5 degrees by multiplying the model results at the MSA by a scaling coefficient. This scaling coefficient is solar-altitude-dependent and is based on horizontal daylight irradiance. The scaling coefficient (SC) is considered valid down to -5 degrees solar altitude. This coefficient is:

$$SC = \frac{10^{f_1(SA)}}{10^{f_1(MSA)}} \qquad \text{Equation F-1}$$

The factors $f_1(SA)$ and $f_1(MSA)$ are computed using the following polynomial:

$$f_1(SA \text{ or } MSA) = 2.112 + .1575\ SA - .00721\ SA^2 \qquad \text{Equation F-2}$$

where SA is the solar altitude between -5° and 90°, and MSA is the lowest, valid solar altitude between -5° and 90°.

Application of the coefficient to haze radiance or irradiance gives the following equation:

$$H(\lambda, SA) = SC \cdot H(\lambda, MSA) \qquad \text{Equation F-3}$$

Each irradiance type and the haze radiance have a different minimum valid solar altitude (MSA). For this reason, when the MSA is involved, reference should be made to the different sections of this report to find the MSA associated with each irradiance or radiance.

APPENDIX G

CALCULATION OF APPARENT SOLAR ALTITUDE

The continuous change in the index of refraction of the atmosphere as a function of altitude causes the apparent position of the sun to be higher than its actual geocentric position. For a typical atmospheric density profile, this solar altitude error was computed by McClatchey et al* for solar zenith angles in excess of 75°. These data are reproduced below.

Apparent Solar Zenith Angle (In Degrees)	Geocentric Solar Zenith Angle (In Degrees)
75	75.061
80	80.090
83	83.124
85	85.167
86	86.199
87	87.248
88	88.311
88.5	88.858
89	89.417
89.5	89.997
90	90.570

Since the SCAT3 atmospheric model uses trigonometric functions to compute the parametric spectral vectors for several radiometric quantities, it was necessary to substitute apparent solar altitude in the equations rather than true, geocentric solar altitude. The conversion between geocentric and apparent solar altitude is done in the program by using the following polynomial equation:

$$SA_a = SA_g + .544 - .1572 \cdot SA_g + .01764 \cdot SA^2_g$$

---

* McClatchey et al, "Optical Properties of the Atmosphere," Air Force Cambridge Research Labs 71-0279, May 1971, Table 6, p 41.

Where: SA_g is the geocentric solar altitude in degrees, and

SA_a is the apparent solar altitude in degrees.

This equation was derived from the above table data by first converting the data from zenith to altitude angles (90° - solar zenith angle) and then regressing the apparent solar altitudes, SA_a, against the geocentric solar altitudes, SA_g.

No correction is applied to solar altitudes higher than 5°. Below 0° apparent solar altitude, corrected values are computed, but they have no significance for the SCAT3 equations.

APPENDIX H

PATH-LENGTH CORRECTION FOR THE POLAR SCATTER FUNCTION

Each particular volume of air in the sky that is observed by the sky radiometer receives a different amount of light depending on the extinction coefficient of the atmosphere, and the atmospheric distance each point is away from the sun. In addition, the sky spectroradiometer receives an amount of light from this volume of air along its line-of-sight that is diminished by the air path length to the radiometer. As a result, the total relative amount of light reaching the radiometer can be expressed in terms of the following quantities:

a. The amount of light reaching a particular volume of air whose position lies along the observer's line-of-sight,

b. The amount of light reaching the observer from that volume of air, and

c. The scattering of light by the volume of air toward the observer.

The geometry involved in the above is shown in Figure H-1 for the volume of air at point P in the atmosphere. Two integrations are involved: (1) over the path defined by the sun-to-volume line, and (2) the volume-to-radiometer path defined by the observer's line-of-sight. The integral that expresses energy reaching the observer (or radiometer) is:

$$PL(AZ) = \int_0^{Lmax} T_{P-O} \cdot T_{E-P}(AZ) \cdot H_{SC} \cdot S \cdot dL \qquad \text{Equation H-1}$$

Where: $PL(AZ)$ is the relative amount of light reaching the observer at point O from a volume of air at point P and for an observer's azimuth AZ relative to the sun,

$T_{E-P}(AZ)$ is the transmittance of light between the edge of the atmosphere, point E, to a volume of air along the observer's line-of-sight, point P,

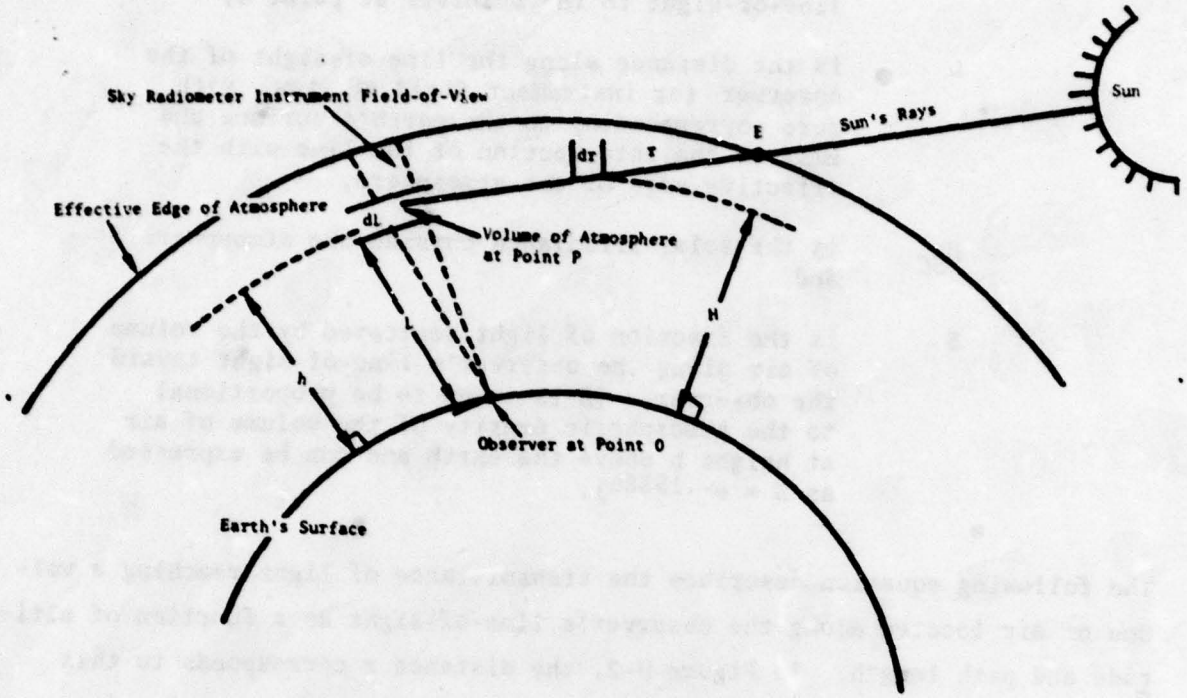

Figure H-1. Definition of Geometry Conditions of Integration of the Sampled Volume of Atmosphere

T_{P-O} is the transmittance of light between the volume of air at point P along the observer's line-of-sight to the observer at point O,

L is the distance along the line-of-sight of the observer (or instrument field of view) with zero corresponding to the earth's surface and Lmax to the intersection of the line with the effective edge of the atmosphere,

H_{SC} is the solar irradiance outside the atmosphere, and

S is the fraction of light scattered by the volume of air along the observer's line-of-sight toward the observer. (S is taken to be proportional to the atmospheric density of the volume of air at height h above the earth and can be expressed as $S = e^{-.1535h}$).

The following equation describes the transmittance of light reaching a volume of air located along the observer's line-of-sight as a function of altitude and path length. In Figure H-2, the distance r corresponds to this transmittance.

$$T_{E-P} = e^{\int_0^{rmax} \alpha_o e^{-.1535H} dr} \qquad \text{Equation H-2}$$

Where: r is the distance along a line between the sun and the volume of atmosphere under consideration as measured from the edge of the atmosphere,

α_o is the extinction coefficient of the atmosphere at the earth's surface calculated for each day,*

rmax is the distance from the outer edge of the atmosphere to the volume of atmosphere under consideration, and

H is the perpendicular height above the earth to point r.

---

* The daily calculation of atmospheric transmittance is explained in Section 2 above.

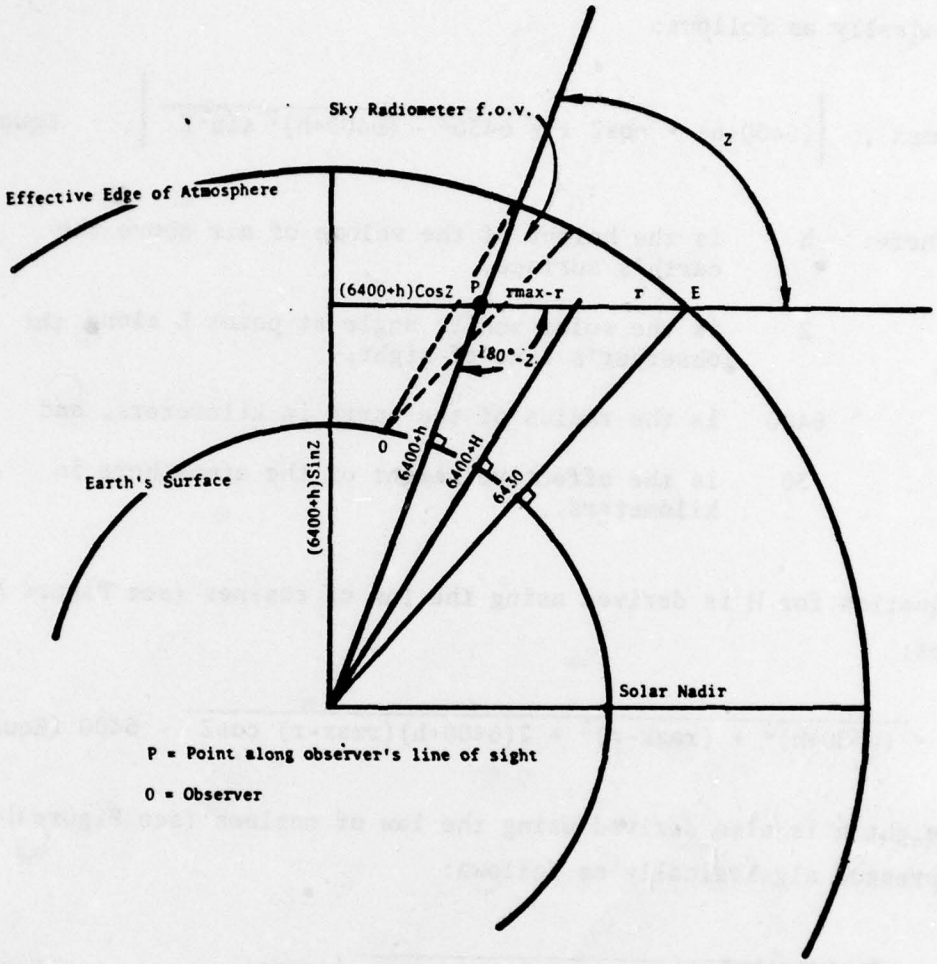

Figure H-2. Trigonometric Definitions for an Atmospheric Volume at Point P

The equation for rmax, the distance between point E and point P, is derived from the Pythogorean theorem (see Figure H-2) and is expressed algebraically as follows:

$$rmax = \left| (6400+h) \cdot \cos Z \pm \sqrt{6430^2 - (6400+h)^2 \sin^2 Z} \right| \qquad \text{Equation H-3}$$

Where: h is the height of the volume of air above the earth's surface,

Z is the solar zenith angle at point L along the observer's line-of-sight.

6400 is the radius of the earth in kilometers, and

30 is the effective height of the atmosphere in kilometers.

The equation for H is derived using the law of cosines (see Figure H-2) and becomes:

$$h = \sqrt{(6400+h)^2 + (rmax-r)^2 + 2(6400+h)(rmax-r)\cos Z} - 6400 \qquad \text{(Equation H-4)}$$

The height h is also derived using the law of cosines (see Figure H-3) and is expressed algebraically as follows:

$$h = \sqrt{6400^2 + s^2 - \cos(ALS) \cdot s \cdot 6400} - 6400 \qquad \text{Equation H-5}$$

Where: s is the distance from the observer to a point along the line-of-sight, and

ALS is 90° plus the angle between the observer's line-of-sight and the local horizon.

The cosine of the zenith angle, Z, is derived from the spherical law of cosines (see Figure H-4); it is expressed algebraically as follows:

$$\text{CosZ} = \cos Z \cdot \cos\phi + \sin Z_o \cdot \sin\phi \cdot \cos\theta \qquad \text{Equation H-6}$$

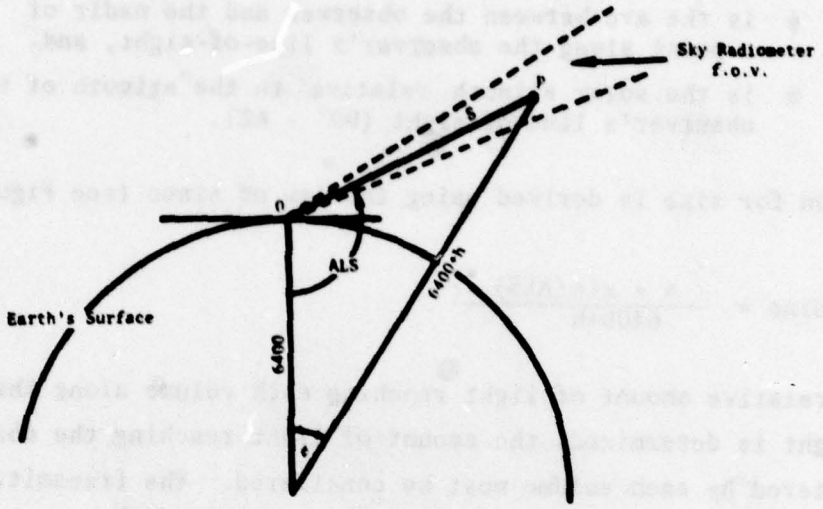

Figure H-3. Trigonometric Definition of the Angle ϕ and Altitude h

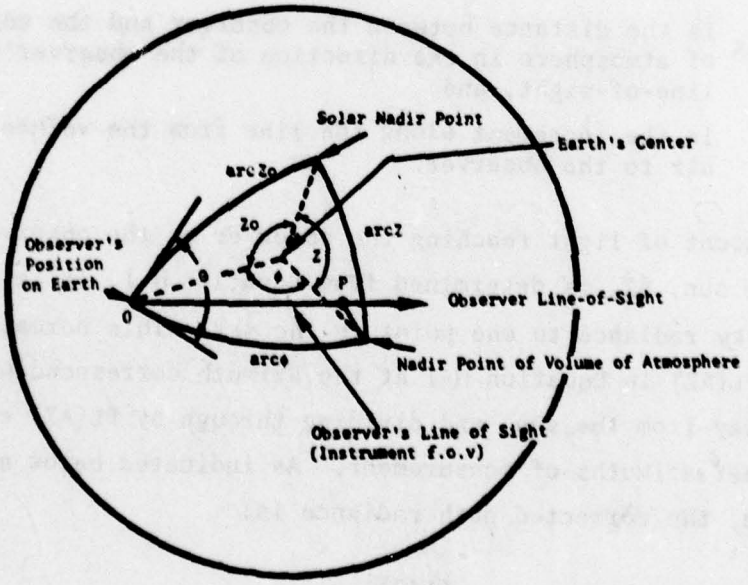

Figure H-4. Spherical Trigonometric Definition of Angle Z

Where: Z is the observer's zenith angle,

ϕ is the arc between the observer and the nadir of a point along the observer's line-of-sight, and

θ is the solar azimuth relative to the azimuth of the observer's line-of-sight (90° - AZ).

The equation for $\sin\phi$ is derived using the law of sines (see Figure H-3):

$$\sin\phi = \frac{s \cdot \sin(ALS)}{6400+h} \qquad \text{Equation H-7}$$

After the relative amount of light reaching each volume along the observer's line-of-sight is determined, the amount of light reaching the observer after it is scattered by each volume must be considered. The transmittance of light between the volume of air and the observer is defined in a manner similar to that resulting in Equation H-2, and becomes:

$$T_{P-O} = e^{\int_0^{s_{max}} \alpha_o e^{-.1535h} ds} \qquad \text{Equation H-8}$$

Where: s_{max} is the distance between the observer and the edge of atmosphere in the direction of the observer's line-of-sight, and

s is the increment along the line from the volume of air to the observer.

The relative amount of light reaching the observer at the observer's azimuth relative to the sun, AZ, is determined from Equation H-1. It is used to normalize the sky radiance to one point in the sky. This normalizing is done by evaluating PL(AZ) in Equation H-1 at the azimuth corresponding to direct backscatter (away from the sun) and dividing through by PL(AZ) evaluated at each of the other azimuths of measurement. As indicated below and in paragraph 3.4 above, the corrected path radiance is:

$$N''(AZ) = N'(AZ) \cdot \frac{PL(O)}{PL(AZ)}$$

Where: N"(AZ) is the path length and time-corrected sky radiance at azimuth angle AZ,

N'(AZ) is the sky radiance at azimuth angle AZ before path-length correction, and

AZ is the instrument's azimuth angle relative to the solar azimuth. (The direction away from the sun is 0°).

APPENDIX I

CORRECTION OF MEAN EXTRA-TERRESTRIAL IRRADIANCE BY TIME-OF-YEAR

The SCAT3 model incorporates a function to change the extra terrestrial spectral irradiance with time-of-year according to the orbital eccentricity of the earth. This correction is described below.

The values for the Solar Constant are the mean of the extraterrestrial irradiance values, and are given for the mean distance between the sun and earth (one astronomical unit distance). The annual variation in irradiance due to the cyclical variation in earth-sun distance amounts to approximately 7%, and can be determined with much greater accuracy than the Solar Constant itself.* This variation can be computed directly from an eccentricity of the earth's orbit and from the mean anomaly (the angular difference between the mean solar longitude and the mean solar longitude of perigee). The computational procedure as used in SCAT3 is outlined below.

The irradiance factor applied to the mean irradiance is given by:

$$K = (I/R)^2 \qquad \text{Equation I-1}$$

where R is the earth-sun radius vector. This radius vector (R) is computed from:

$$R = 1 + (1/2)\, e^2 - (e \cos M) - [(1/2)\, e^2 \cos^2 M]$$

where e is the eccentricity of the earth's orbit, and M is the mean anomoly.

The eccentricity, which diminishes constantly, can be computed from:

$$e = .01675 - .00004\, T$$

where T is the number of centuries elapsed from the epoch beginning noon, 1 January 1900, each century being of 36525 ephemeris days (Julian Calendar).

Therefore, $T = d/36525$.

---

* Explanatory Supplement to the Astronomical Ephemeris and the American Ephemeris and Nautical Almanac, H.M. Nautical Almanac Office, Her Majesty's Stationary Office, 1961.

The mean anomaly is computed from:

$$M = 358.475845 + 0.9858600267d - 0.0000112\ D^2 - 0.00000007\ D^3$$

Where: d is the number of ephemeris days elapsed from noon, 1 January 1900, and

D is d/10000.